Growth factors and hepatic progenitor cells in liver regeneration

translating bench to bedside

Hedwig Kruitwagen

2017

ISBN: 978-94-6332-273-7

Cover: Anjolieke Dertien, beeld via iStock

Lay-out and printing: GVO drukkers & vormgevers, Ede, the Netherlands

Publication of this thesis was made possible by the generous support of the Department of Clinical Sciences of Companion Animals, Faculty of Veterinary Medicine, Boehringer Ingelheim B.V., Greiner Bio-One B.V., Merck Chemicals B.V., de Nederlandse Vereniging voor Hepatologie, Royal Canin Nederland B.V.

Growth factors and hepatic progenitor cells in liver regeneration

translating bench to bedside

Groeifactoren en lever progenitor cellen bij leverregeneratie

translatie van laboratorium naar patiënt

(met een samenvatting in het Nederlands)

Proefschrift

ter verkrijging van de graad van doctor aan de Universiteit Utrecht
op gezag van de rector magnificus, prof.dr. G.J. van der Zwaan,
ingevolge het besluit van het college voor promoties
in het openbaar te verdedigen op donderdag
14 december 2017 des middags te 12.45 uur

door

Hedwig Suzanne Kruitwagen

geboren op 23 november 1983 te Nijmegen

Promotoren:	Prof.dr. J. Rothuizen
	Prof.dr. J.W. Hesselink
Copromotoren:	Dr. B. Spee
	Dr. L.C. Penning

Opgedragen aan mijn gezin

Contents

Aims and scope

Both in veterinary and human medicine new therapies for liver diseases are urgently needed. Although knowledge of the liver's regenerative potential dates back to ancient Greece, clinical liver disease will develop upon a severe loss of hepatocytes, hepatic inflammation, architectural disturbances due to excessive fibrosis, vascular anomalies, or a combination of these factors. In such circumstances the regenerative capacity of the healthy liver decreases and may even fail completely. Due to the high reserve capacity of the liver, symptoms often only become apparent in an advanced stage of the disease. Regenerative medicine is aimed at targeting intrinsic repair mechanisms within an organ or tissue by using stem cells, growth factors, and gene therapy. Fundamental knowledge of the cells and pathways involved in repair of damaged liver tissue may contribute to the development of new regenerative therapies for liver disease.

Stem cells are defined by having the capacity for self-renewal and the ability to differentiate into one or more mature cell types. While embryonic stem cells can give rise to all tissue types within an organism, adult tissue-specific stem or progenitor cells are more committed in their fate and generate only a limited number of mature cell types. First discovered in rodents and later also in humans, dogs, and cats, the liver contains adult liver stem cells also known as hepatic progenitor cells (HPCs). HPCs are normally quiescent, but start to proliferate during severe liver disease and can differentiate into new hepatocytes or cholangiocytes depending on the type of injury. Hence, stimulating HPC-mediated liver regeneration during disease is a prime focus in liver regenerative medicine research. In **chapter 1**, we review the existing literature on HPCs in different species. We compare experimental rodent data with human, canine, and feline *ex vivo* pathology studies and discuss the characteristics of HPCs and their micro-environment (or niche) in health and disease.

Part I of this thesis is aimed at gaining more insight into HPC activation mechanisms in different species. Insight into pathways involved in HPC proliferation and differentiation can result in new targets for exogenous HPC manipulation. For example, drugs could be developed in order to stimulate HPC proliferation *in vivo* to enhance HPC-mediated liver regeneration during liver disease, or *in vitro* to expand HPCs in culture.

In **chapter 2**, we investigate canine HPCs and their niche in normal liver and in liver samples from diagnostic biopsies or pathology cases from dogs with acute hepatitis, chronic hepatitis, lobular dissecting hepatitis and biliary disease. We describe their marker expression, and the cells and extracellular matrix components that are associated with their activation.

The Wnt/β-catenin and Notch signaling pathways have been implicated in driving the proliferation and differentiation of HPCs in rodent and human liver. In **chapter 3**, we perform transcriptional analysis of quiescent and activated HPC niches in canine liver and measure Wnt/β-catenin and Notch target gene expression. We confirm our findings on protein level by immunohistochemical and –fluorescent stainings of Wnt/β-catenin and Notch pathway components in normal and diseased liver sections.

Although several external activation mechanisms have been described, little is known about which key intracellular signals govern the switch between HPC quiescence and proliferation. In **chapter 4**, we screen a kinase RNAi library in a human HPC-like cell line and investigate the effects on S phase and proliferation. After hit selection, we validate our findings in primary HPCs cultured as liver

organoids and also study the effects on proliferation in an overexpression model.

Part II of this thesis is aimed at the application of regenerative medicine strategies in models of liver disease. We investigate growth factor therapy and stem cell transplantations *in vivo* in dogs with naturally occurring liver disease and we establish an *in vitro* feline stem cell culture model for hepatic steatosis.

In **chapter 5**, we describe the clinical course and outcome of Hepatocyte Growth Factor (HGF) therapy in six dogs with liver hypoplasia due to a congenital portosystemic shunt. Effects on liver size, hepatocyte proliferation, HGF pathway activation, and portal perfusion are studied before, during and after HGF treatment.

In **chapter 6**, we evaluate the transplantation potential of HPCs cultured as liver organoids in COMMD1 deficient dogs. These dogs develop hepatic copper storage disease similar to human Wilson's disease. As canine HPCs can be isolated from a liver biopsy, we explored the possibility to culture autologous liver organoids, perform a gene correction, expand the corrected cells and use them as cell source for transplantation.

Another possible use for HPCs cultured as liver organoids is *in vitro* modeling of liver diseases by mimicking pathophysiological processes or responses to drugs. In **chapter 7**, we develop a long-term culture of feline liver organoids and extensively characterize it. As cats are predisposed to hepatic steatosis, we test whether also feline liver organoids can accumulate lipids *in vitro*. We compare feline liver organoid lipid accumulation capacity with liver organoids from mouse, human, and dog and test possible drug interference.

This thesis aims to translate 1. fundamental findings to (pre)clinical application, 2. *in vivo* disease to *in vitro* disease models, and 3. disease mechanisms and therapeutic options between different species. The overall objective is to advance liver regenerative medicine for both the veterinary and human hepatology patient.

Chapter 1

General introduction

Hepatic progenitor cells in canine and feline medicine: potential for regenerative strategies.

H.S. Kruitwagen, B. Spee, B.A. Schotanus

BMC Vet Res. 2014;10:137

Abstract

New curative therapies for severe liver disease are urgently needed in both the human and veterinary clinic. It is important to find new treatment modalities which aim to compensate for the loss of parenchymal tissue and to repopulate the liver with healthy hepatocytes. A prime focus in regenerative medicine of the liver is the use of adult liver stem cells, or hepatic progenitor cells (HPCs), for functional recovery of liver disease. This review describes recent developments in HPC research in dog and cat and compares these findings to experimental rodent studies and human pathology. Specifically, the role of HPCs in liver regeneration, key components of the HPC niche, and HPC activation in specific types of canine and feline liver disease will be reviewed. Finally, the potential applications of HPCs in regenerative medicine of the liver are discussed and a potential role is suggested for dogs as first target species for HPC-based trials.

Introduction

Regenerative medicine is a rapidly developing field in which diseased tissues are restored or regenerated. This interdisciplinary field converges biomedical research, technology and clinical care, and is based on the concept of employing intrinsic repair mechanisms within the tissue itself. A hallmark of regenerative medicine is the clinical use of stem cells, either by manipulation of endogenous progenitor populations *in situ*, or by transplantation of stem cells (autologous or allogeneic). Recent developments in human stem cell therapy are highly visible and it appears that this phenomenon is now also entering the veterinary clinic. In April 2013, *Nature* published a report in its news section on the growing use of stem cells in veterinary medicine. Although popularity has increased, the efficacy of many stem cell therapies is often unproven. New FDA regulations in the USA are pending and if stem cells are defined as a drug, application as a new treatment modality requires evidence-based veterinary medicine [1].

Regenerative strategies in the liver seem redundant, as adult hepatocytes are widely known for their large regenerative capacity. However, developments in the field of hepatology make clear that in severe or chronic ongoing liver disease, regeneration by hepatocyte replication is failing or absent [2]. In these specific circumstances liver-specific stem cells, or hepatic progenitor cells (HPCs), become activated and attempt to repopulate the liver. HPCs are a reserve compartment of adult stem /progenitor cells that reside within the liver and are found in rodents, humans, dogs and cats [3-7]. HPC activation in a diseased liver section is described as 'ductular reaction' or 'bile duct proliferation' in a histology report [8,9]. Diagnostically, it indicates severe liver disease. In addition, the presence of progenitor cell markers in hepatocellular carcinoma (HCC) is an indicator of malignancy in humans as well as dogs [10-12]. Conversely, HPCs hold potential as a therapeutic target since they are committed liver stem cells, show self-renewal capacity and can differentiate into hepatocytes and cholangiocytes (Figure 1) [13]. Literature on HPCs focuses on mouse, rat, and human. There are few publications on canine HPCs and even fewer on cat or other species and it is clear that the HPC response is often referred to as 'bile duct proliferation' when observed in liver histological sections [8,14]. In this terminology there is no suggestion of the presence and activation of stem cells, implying that the presence of HPCs in the liver of dogs and cats is not widely recognized and that there is no consensus on terminology in veterinary pathology. An attempt to achieve this consensus in clinical and histological diagnosis of liver disease has been made by the WSAVA Liver Standardization Group.

In this review, we will provide an overview of the role of HPCs in liver regeneration and will address the most important cellular and stromal players in HPC biology. Although current knowledge about HPCs stems primarily from experimental rodent and clinical human studies, we will review available literature on HPCs in canine and feline liver regeneration, and support these with recent data from our own research. To conclude, we will discuss the possible use of HPCs for clinical purposes in veterinary regenerative medicine and for future research needs.

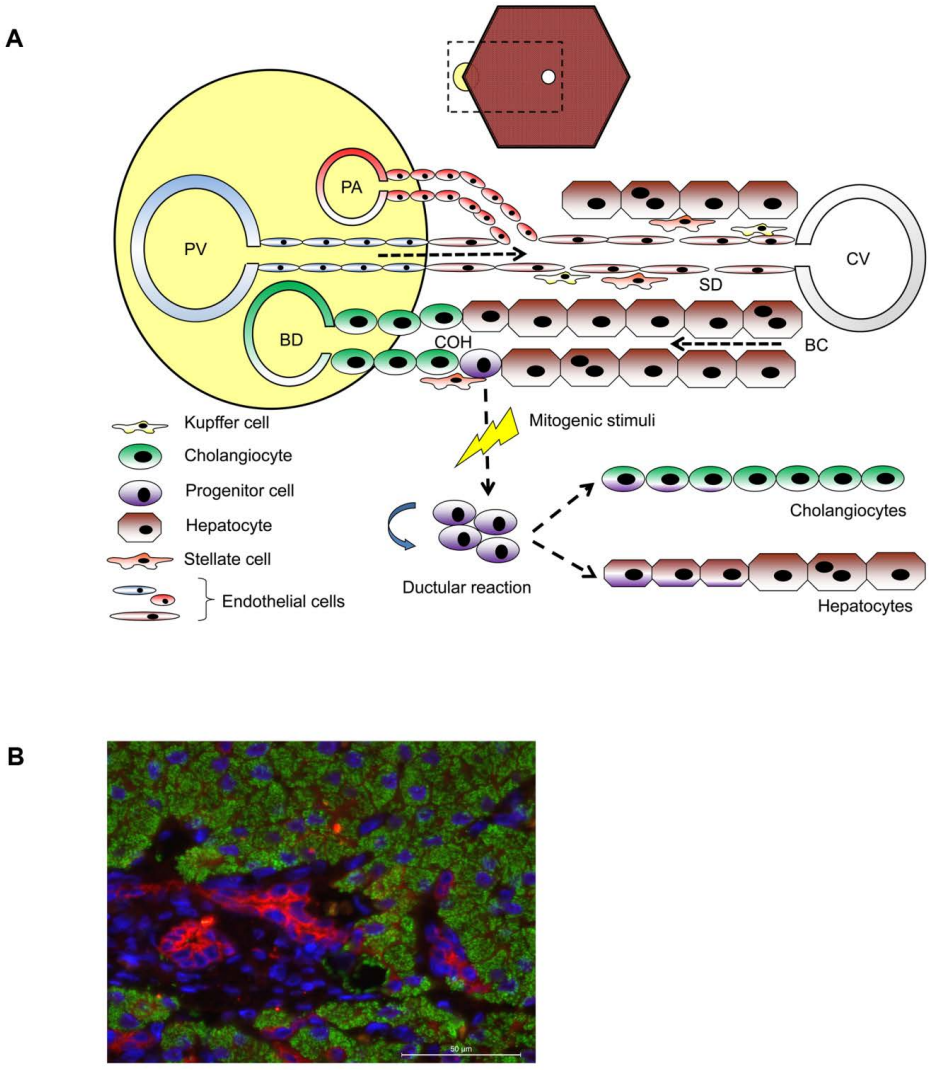

Figure 1 Anatomical location and differentiation capability of hepatic progenitor cells. A. Schematic representation of the anatomical location of the hepatic progenitor cell (HPC) in the canal of Hering. Upon activation the normally quiescent HPCs will proliferate. Depending on the disease and the concurrent changes in microenvironment HPCs will differentiate into either hepatocytes or cholangiocytes. PV: portal vein; BD; bile duct; PA: portal artery; COH: canal of Hering; SD: space of Disse; BC: bile canaliculus; CV: central vein **B**. Immunofluorescent double staining of panCK (red) and HepPar-1 (green) with a nuclear counterstaining (DAPI, blue) of a liver section of canine chronic hepatitis. Differentiation into hepatocytes can be observed where the ductular reaction enters the parenchyma as the intermediate hepatocytes lose panCK immunoreactivity and become positive for HepPar-1. [7].

The role of HPCs in liver regeneration

Seventy percent of the liver consists of mature hepatocytes located in the parenchyma. These adult hepatocytes are normally quiescent, but enter the cell cycle when the liver is damaged. They can

restore liver function by compensatory hyperplasia, an efficient and well-orchestrated physiological response [15]. The large replicative potential has designated hepatocytes as a stem cell of the liver in the past [16], but their lack of differentiation potential does not render them true stem cells [17]. This process of liver regeneration has been thoroughly investigated by using the partial hepatectomy (PHx) model in rodents as well as in dogs, and has revealed the involvement of a plethora of growth factors and cytokines [2,18-21]. Previous work by our group demonstrates that in canine liver disease the primary molecular pathways associated with liver regeneration (e.g. the hepatocyte growth factor (HGF) signaling pathway) are highly comparable with those in rodents and humans [22-24]. For the cat, the underlying molecular mechanisms of disease and regeneration have not been described.

Upon acute severe or chronic hepatic injury, hepatocyte replication is impaired or exhausted. This impairment in hepatocyte replication is linked to an increase in HPC activation [2]. For example, in biopsies of human patients with severe acute liver damage it was shown that more than 50 percent hepatocyte loss results in a lower proliferative activity of the remaining hepatocytes, when compared with less severe hepatic injuries. This was associated with a pronounced HPC response, and positively correlated with symptoms of liver failure [25]. Hepatocyte senescence occurs in chronic liver disease, which is characterized by increased p21 expression (cell cycle inhibitor) and shortened telomeres in the hepatocytes [26,27]. A report from Liu et al. showed that when hepatocytes from a cirrhotic donor rat were transplanted into a non-cirrhotic host liver, the cells engrafted but showed decreased metabolic function and delayed proliferation due to replicative senescence [28]. This phenomenon of hepatocyte senescence was also observed in a mouse model of fatty liver disease and a marked progenitor cell response was observed in the affected animals when compared to their wild type controls [29].

Hepatocyte senescence in chronic liver disease has not been investigated in the dog and cat. However, immunohistochemical stainings for PCNA or Ki67 in various canine liver diseases show prominent proliferation of hepatocytes after experimental PHx and mild acute hepatitis, with moderate proliferation in chronic hepatitis. Conversely, HPC response was pronounced in chronic hepatitis, moderate in mild acute hepatitis and non-existent after PHx (Figure 2) [6,30]. The response pattern of HPCs to various types of liver disease in the dog appears to be comparable to human pathology and rodent experimental findings, and recent studies suggest a similar comparison for feline HPC response [6,7,31, Unpublished observations section: Valtolina et al.]. In all species, HPC response correlates with the severity of disease and is localized at the site of disease activity [6,25,32,33]. The current consensus is that the HPC pool is a reserve compartment in the liver that contributes to regeneration when hepatocytes do not replicate sufficiently to restore liver mass and function.

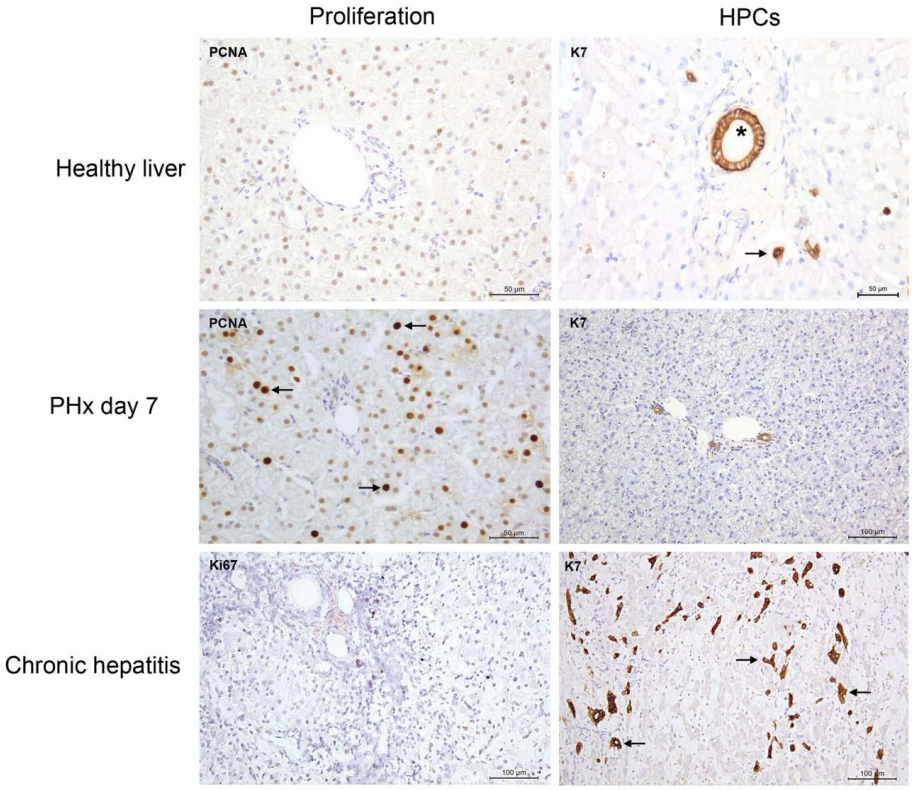

Figure 2 The first and second line of defense in canine liver regeneration. In liver sections proliferation is visualized by PCNA or Ki67 immunohistochemistry. K7 was used as a marker for hepatic progenitor cells. In healthy liver, both hepatocytes and HPCs are quiescent, indicated by a few hepatocytes that stain for PCNA and only a few K7 positive cells close to the portal area (indicated with arrow, asterisk indicates bile duct). After partial hepatectomy (PHx), liver regeneration occurs through hepatocyte proliferation (many PCNA positive hepatocytes indicated by arrows) but the HPC remains quiescent (few K7 positive cells). In chronic hepatitis the proliferative capacity of hepatocytes is exhausted indicated by a few Ki67 positive hepatocytes and a prominent ductular reaction (K7 positive, indicated by arrows). [6,30].

The hepatic progenitor cell

HPCs are present in healthy adult liver tissue and can be found in small numbers in the Canal of Hering, the smallest ramifications of the intrahepatic biliary tree, which connect to the intralobular canaliculi. These structures are located close to the portal area and are lined by both cholangiocytes and hepatocytes [34]. This is the most commonly described HPC niche, although there is still debate about the exact origin of the HPC. A number of studies state a possible biliary origin of HPCs [35-37]; other studies in humans describe extrahepatic peribiliary glands as the prime location for HPCs [38,39]; and a few publications even speculate on a hematopoietic origin of HPCs, which is also highly debated [40-44]. For this review we assume an HPC niche within the Canal of Hering, as described in mouse, rat, human, and dog [3,4,7,45]. HPCs can be histologically characterized by a

combination of their specific morphology upon activation (ductular reaction, DR) and by marker expression. Many classic HPC-markers, such as keratin (K)7 and K19, have a shared expression with cholangiocytes, which underlines the significance of combining the interpretation of marker expression with histological evaluation. Other reported markers include CD133 and EpCAM, which are also expressed in other stem cells such as hematopoietic or embryonic stem cells (for a review, see [46]). HPCs are epithelial cells that can display mesenchymal characteristics, depending on their activation status (e.g. need for migration capacity). This is reflected in the expression of CD29 (integrin β1) and CD44 (hyaluronic acid receptor and co-receptor for hepatocyte growth factor), proteins involved in cell-matrix interactions and potentially critical for cell migration. When reviewing HPC marker expression, interspecies differences emerge. Therefore, it is necessary to evaluate appropriate markers in the species of interest and, in rodents, to consider the model used [47]. In Table 1 we provide an overview of available literature on HPC markers in mouse, rat, human, dog, and cat. It is important to take into account that the HPC niche can be dynamic during its various states of quiescence, proliferation and differentiation, which is reflected by marker expression. Some markers (such as CD133 and Lgr5) are expressed by only a subset of cells or only upon activation [48,49].

Table 1 Comparison of HPC marker expression across species

Marker	Mouse	Rat	Cat	Dog	Human
A6	[3,50]				
ABCG2/BCRP1	[47]	[47]		[7]	[7,48]
AFP		[47,51,52]		[53]	[48,54-56]
Alb	[57]				[54,55,58]
Dlk/Pref-1	[59]	[47]			
c-kit		[60]			[48,56]
CD24	[50]				
CD29		[51]		[53]	[54]
CD34		[60]			
CD44	[49]	[51]		[53]	[48,54,55]
CD45		[60]			
CD73					[54]
CD90		[52,60]			[54]
CD133/PROM1	[49,57,59,61]	[51]		[53]	[48]
CLDN3					[55]
chrom-A					[32,33]
EpCAM	[50,57,59]	[45,51]			[55,62]
FN14	[59]	[51]		[53]	
GPC3		[52]			
Hedgehog proteins				Schotanus (unpublished data)	[55]
HNF4α		[45]		[53]	
ICAM1					[55]
K7	[36,57]	[32,63]	[31]	[6,7,53]	[6,7,25,32,33,48,64,65]
K8					[33,54]
K18					[33,54]
K19	[3,37,57,59]	[32,45,51,52,63,66]		[6,53]	[6,25,32,33,48,55,56,58,64,67]
Lgr5	[49]				
MPK		[47]			
NCAM					[32,48,55]
NES					[54]
Nope	[50]				
OPN	[37]			[53]	
OV6		[32,45,66]			[32,33]
Sca1	[59]				
SOX9	[36,37,49,59,61]			[53]	
vimentin					[54]

References are indicated per marker per species. Expression was measured at mRNA and/or protein level and was reported for adult liver.

Cells, signals and stroma in the HPC niche

An essential feature of stem cell biology is the niche, or micro-environment, in which stem cells reside. It consists of neighboring cells, extracellular matrix (ECM) components and soluble and bound growth factors and cytokines that govern self-renewal and maturation/differentiation status [68]. The composition of the HPC niche is well defined and adapts during specific types of liver disease [44,69]. A number of cellular niche components have been described, and below we discuss the hepatic stellate cell, the macrophage and the ECM.

Hepatic stellate cells

Hepatic stellate cells (HSCs, or previously called Ito cells) are found in the space of Disse and can transform into myofibroblasts upon injury-induced activation. Quiescent HSCs are important in vitamin A storage (mainly as retinol-containing lipid droplets) and function as liver resident antigen presenting cells [70,71]. Activated HSCs produce ECM components such as collagen and are the main contributors to fibrosis development in chronic liver disease [72]. Interestingly, HSCs are also an essential mediator of the HPC response and the primary source of HGF, which stimulates hepatocyte and HPC proliferation and liver regeneration [73,74]. HSCs may also play a role in directing the differentiation of HPCs, and co-culture studies of HSCs and HPC-like cells indicate that this is probably mediated by both soluble and membrane-bound factors or matrix components [75].

Macrophages

Macrophages in the liver are a second important niche component. Macrophages are activated upon hepatocyte damage and are integral to the local immune response [76]. Cytokines (e.g. TWEAK) produced by this inflammatory cell can modulate HPC behavior over large distances in the tissue [77,78]. HPC migration through the parenchyma was significantly decreased in mice depleted for macrophages with clodronate and subsequently subjected to liver injury [79]. Boulter et al. corroborated this finding by reporting a pivotal role of both activated myofibroblasts and macrophages in murine HPC differentiation. Mediated by Wnt and Notch signaling, respectively, macrophages are involved in the specification of hepatocyte differentiation upon hepatocellular injury and myofibroblasts promote biliary differentiation of HPCs [80]. These data support previous studies on the involvement of Wnt and Notch signaling in human clinical HPC activation. In human samples of acute hepatitis, a parenchymal liver disease, the activated HPC niche showed increased Wnt signaling. Active Notch signaling in the activated HPC niche was mainly observed in biliary-type diseases [48].

Extracellular matrix

A third critical component of the HPC niche is the extracellular matrix (ECM) and its specific composition. In particular, laminin has been shown in both mouse models and human fibrotic liver disease to play an important role in HPC biology. A laminin matrix develops in many liver diseases and consistently surrounds the ductular reaction. The deposition and remodeling of laminin is required for HPC proliferation and migration and it maintains the undifferentiated state of the HPCs. It is only when the HPCs 'escape' from the laminin matrix and enter the parenchyma that differentiation occurs [44,81,82]. HPCs express markers such as CD29 and CD44, clearly indicating that they have the molecular make-up to communicate with their ECM [59,83]. Interestingly, ECM remodeling is modified by HSCs and macrophages through expression of matrix metalloproteinases (MMPs) and tissue inhibitors of metalloproteinases (TIMPs), and is associated with the extent of ductular reaction and fibrosis [76,84]. Several studies suggest a direct relation of HPCs with increased fibrosis development and remodeling [85,86].

To date, there are only a few publications on HPC niche components in dog. An immunohistochemistry study evaluated the inflammatory infiltrate and fibrosis in samples of canine chronic hepatitis, and recorded an increased amount of 'bile duct proliferation' in cases with marked inflammation and more advanced stages of fibrosis. A positive correlation was found between the stage of fibrosis and the number of myofibroblasts and bile duct proliferation [87]. The location and characteristics of quiescent canine HSCs and portal myofibroblasts were characterized in healthy liver. HSCs were found in the space of Disse as previously described for other species [88]. A subsequent study focused on samples of canine chronic hepatitis and lobular dissecting hepatitis and reported a positive correlation between the presence of tenascin-C, a specific component of ECM, and stage of fibrosis, degree of inflammation and the number of K7 positive cells [89]. These findings confirm HPC activation upon severe liver disease in the dog and suggest an association with stellate cells and/or myofibroblasts, but do not exactly specify the HPC niche components.

A publication on the relation between HPCs, HSCs, fibrosis and disease severity in healthy and diseased liver samples describes the presence of activated HSCs in close vicinity to the ductular reaction in all types of liver disease studied. In liver disease with fibrosis, HPC activation was most pronounced and both HPCs and HSCs localized to the primary site of injury [6]. This was substantiated by a second study, using immunofluorescent double stainings to evaluate HPCs and their niche in different types of liver disease (Figure 3). Activated stellate cells, characterized by positive alpha-smooth muscle actin (αSMA), were predominantly present in fibrotic liver diseases, such as lobular dissecting hepatitis and chronic hepatitis. HSCs colocalized with the prominent ductular reaction and this colocalization was also seen for laminin at the site of disease activity where it consistently surrounded the ductular reaction. Total macrophage numbers were significantly increased in chronic hepatitis and lobular dissecting hepatitis. Although macrophages were identified throughout the parenchyma, they appeared to cluster at the injury site; periportal in acute hepatitis and in the fibrotic septa in chronic hepatitis [53].

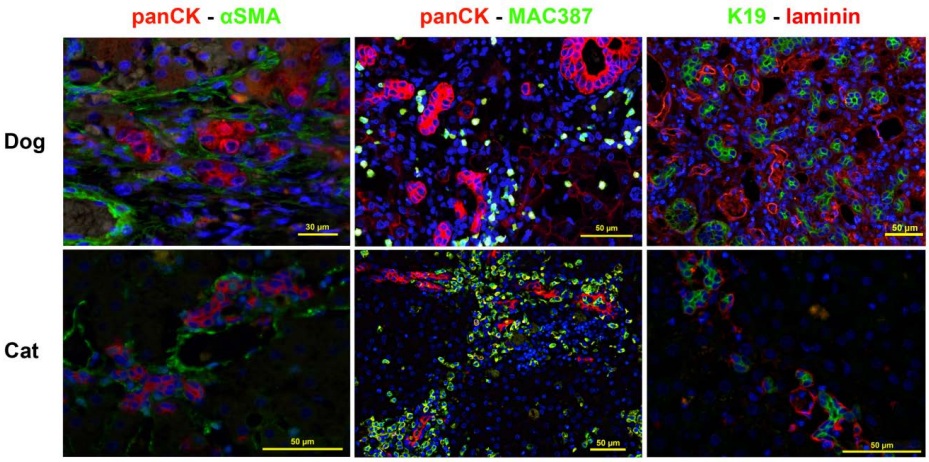

Figure 3 Cellular and stromal components of an activated hepatic progenitor cell niche in dog and cat. Immunofluorescent double stainings of liver sections of canine chronic hepatitis and feline chronic neutrophilic cholangitis. PanCK or K19 was used as a marker for HPCs, activated stellate cells are visualized using αSMA staining and macrophages using MAC387 staining. Nuclei were counterstained with DAPI (blue). In canine and feline liver disease there is clear colocalization of activated HPCs with hepatic stellate cells, macrophages and laminin. [53, Unpublished observations section: Valtolina et al.].

To our knowledge no literature available for cats on the interaction or co-occurrence of HPCs, HSCs, macrophages and/or ECM. In light of the similar presence of HPCs in liver disease in cats, one would also expect a highly activated and comparable HPC niche in these animals [14,31]. Recent unpublished data indeed show similar involvement of HSCs, macrophages and laminin in the feline HPC niche (Figure 3) [Unpublished observations section: Valtolina et al.].

HPC activation in different types of liver disease in man, dog and cat

In the following section, the HPC response is described as it occurs in various forms of hepatitis, biliary disease and liver tumors. Figure 4 shows a representative selection of diseased canine and feline liver sections stained for K19.

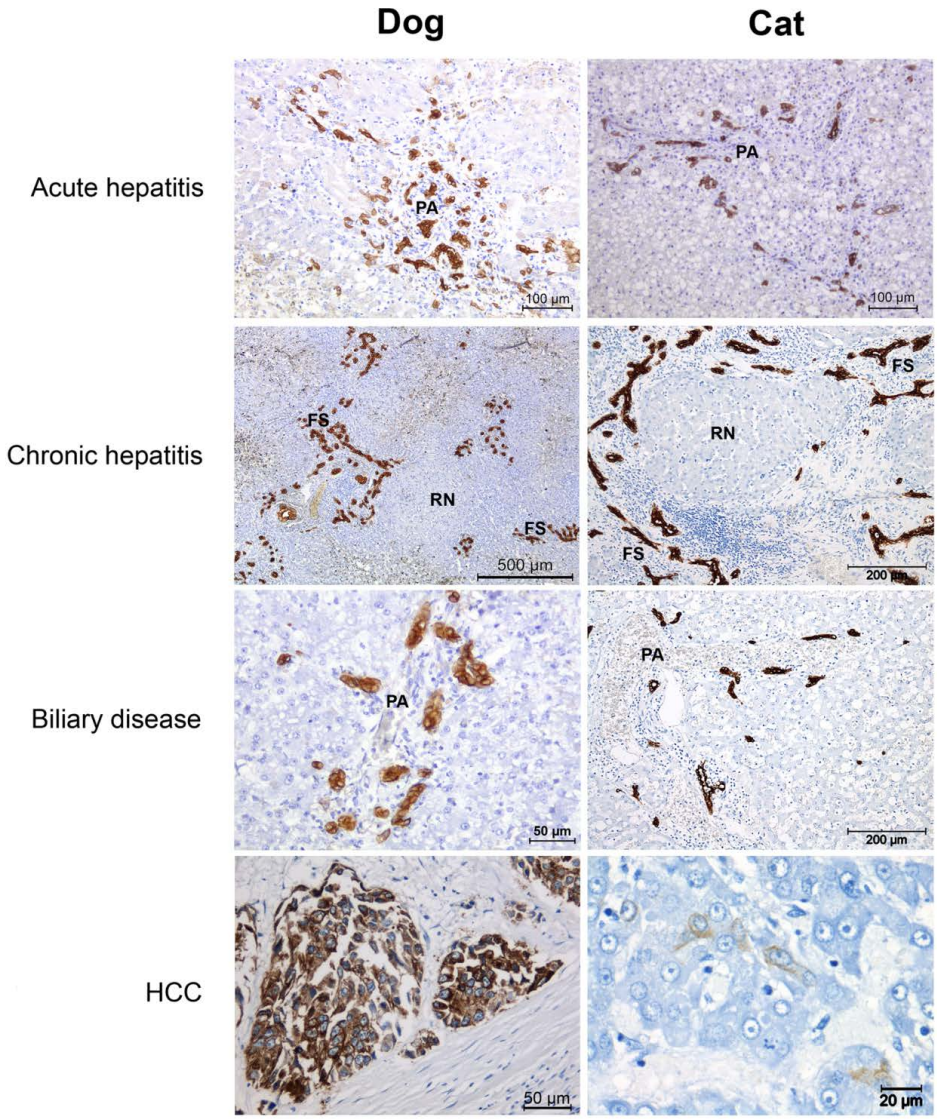

Figure 4 Hepatic progenitor cell activation in liver disease in dog and cat. K19 immunohistochemistry of liver sections from different types of liver disease in dog and cat. HPCs are activated in acute and chronic hepatitis and in biliary disease. The extent and location of the ductular reaction depends on type and severity of disease. Canine extrahepatic cholestasis and feline neutrophilic cholangitis were selected as representative biliary diseases. The lower panel shows K19 positive hepatocellular carcinoma in dog and cat. [6,11, Unpublished observations section: Valtolina et al., Van Sprundel et al.].

Acute hepatitis

In human hepatology, severe acute parenchymal liver failure is most often caused by viral infections (e.g. hepatitis A, B, E) and ingestion of toxic substances (e.g. acetaminophen, Amanitum mushrooms) [90,91]. Massive hepatocyte loss triggers an HPC response, and is most apparent in human subjects suffering from acute submassive necrosis [25,64]. This response will rapidly develop and already after 24 hours a prominent ductular reaction can be observed. Proliferation is followed by differentiation, during which the ductular reactions give rise to 'hepatocyte-like cells' (also identified as intermediate hepatocytes) that spread into the parenchyma [32].
In the dog and cat, acute liver injury most often presents as (mild) acute hepatitis and is characterized by inflammation and apoptosis/necrosis. Fulminant hepatitis is rarely diagnosed in the veterinary clinic. Etiology is not always known but numerous causative agents have been described. Similar to human hepatology, viral infections can cause acute hepatitis (e.g. canine adenovirus I, canine or feline herpesvirus) and ingestion of toxic substances (iatrogenic or accidental) can result in considerable hepatocellular damage (e.g. Amanitum mushrooms, Cyanophyceae algae, acetaminophen, and benzodiazepines) [9]. The involvement of the HPC compartment in canine and feline acute hepatitis has been described in only very few studies. For canines, a ductular reaction has been observed localized to the site of injury (primarily periportal in acute hepatitis), accompanied by intermediate cells (recognized among others by submembranous K7 staining), suggesting early differentiation [7]. In addition, colocalization of activated HPCs and HSCs has been observed [6]. Ijzer et al. published the only paper specifically describing HPC behavior in liver disease of six cats with acute or fulminant hepatitis. In the periportal areas, there was evidence of an extensive ductular reaction, branching into the parenchyma, containing mitotic figures [31].

Chronic hepatitis

In humans, chronic hepatitis results in morbidity and mortality world-wide. Important causes are viral infections (e.g. hepatitis C), alcohol abuse, and autoimmune disease [92]. In human chronic hepatitis, the HPC compartment is activated when hepatocyte replication becomes exhausted. A ductular reaction develops and expands with disease severity [33,65,67].
In veterinary medicine, chronic hepatitis is seen predominantly in dogs and infrequently in cats [93,94]. Fibrosis is the histological hallmark and is accompanied by inflammation and hepatocyte apoptosis/necrosis. Regeneration will occur to some extent; in cirrhosis this is represented by hyperplastic nodules of newly formed hepatocytes which emerge between the fibrotic septa [9]. HPCs and their niche are activated and a clear ductular reaction develops at the site of disease activity, which is usually in and adjacent to the fibrotic septa. HSCs are also strongly activated, differentiate into myofibroblasts, and are found at the site of fibrosis surrounding the activated HPCs [6,7]. Chronic hepatitis in dogs is perhaps best characterized as a degenerative process with unsuccessful regenerative attempts in most cases.

Fatty liver disease

Human non-alcoholic steatohepatitis (NASH) and fatty liver disease ((NA)FLD) are increasingly common hepatic disorders associated with obesity and insulin-resistance [95]. Storage of large quantities of fat and subsequent inflammation can ultimately result in liver fibrosis, cirrhosis and HCC. Human FLD is associated with increased oxidative stress and inhibition of hepatocyte replication. A strong HPC response is observed, which correlates with disease severity and fibrosis [96]. A recent study by Nobili et al. showed similar results in pediatric NASH and NAFLD and revealed adipokine signaling in activated HPCs, suggesting an active (or reactive) role in the steatosis process [97].

In cats, one of the most common hepatic parenchymal diseases is hepatic lipidosis, a fat storage disease. Hepatocytes accumulate fat vacuoles, microscopically appreciated as micro- or macrovesicular steatosis [98,99]. In sections of feline hepatic lipidosis a ductular reaction was observed, which extended into the periportal parenchyma and was associated with intermediate hepatocytes [31]. Awareness about the existence of feline HPCs during hepatic lipidosis and the appropriate terminology describing their histological appearance are currently lacking [98]. Since they possibly share a common etiology of metabolic dysfunction, the histological similarity of feline lipidosis to human NASH and NAFLD at the tissue level is currently under investigation. It appears that these fat-storing hepatic diseases have a comparable histopathological reaction pattern to inflammation and fibrosis [Unpublished observations section: Valtolina et al.].

Canine lobular dissecting hepatitis

Lobular dissecting hepatitis (LDH) is unique only to dogs, and displays extraordinary clinical behavior and histology. LDH has an acute disease progression but is histologically characterized as a chronic hepatitis, due to the occurrence of extensive fibrosis. Interestingly, in LDH a massive and unrivalled expansion of the HPC pool is seen dispersed throughout the parenchyma [6,9,89]. When the HPC niche was studied in detail using laser-microdissection, expression of self-renewal and progenitor markers was present, but markers of hepatocyte differentiation were absent. This is indicative of a strong proliferative response that is not followed by appropriate differentiation. Recent work showed that pre-existent liver fibrosis impaired liver regeneration upon partial hepatectomy in mice. Impaired liver regeneration was associated with increased HPC proliferation and *de novo* fibrogenesis. Interestingly, suppression of the HPC response attenuated fibrogenesis and restored regeneration by mature hepatocytes [100]. Perhaps in LDH the high amount of fibrosis somehow interferes with the maturation/differentiation of the cells in the ductular reaction, suggesting a disturbed niche biology [53]. Further research is needed to clarify the potential contribution of HPCs to fibrosis progression and their potential negative contribution to liver regeneration. LDH could be a very interesting disease to investigate this phenomenon [85,86].

Biliary disease

In human biliary disease, a local regenerative response results in bile duct proliferation, most probably comprising of both HPC activation and proliferation of pre-existing bile duct cells [32]. As markers for HPCs often overlap with cholangiocyte markers, it can be challenging to ascertain the

specific origin of newly formed bile ducts. However, in the case of biliary cirrhosis specific stainings suggested HPCs to be the cell of origin to repopulate and regenerate injured bile ducts [101]. Canine biliary diseases include extrahepatic cholestasis and destructive cholangitis. These diseases present with an activated HPC niche but are not often diagnosed [53,102]. In felines, biliary disease is frequently seen, most commonly lymphocytic and neutrophilic cholangitis, and are associated with inflammatory cell infiltrates [94,103,104]. Lymphocytic cholangitis is a chronic disease that results in portal fibrosis and bile duct proliferation [14,102]. In a large cohort of feline liver biopsies Gagne et al. observed bile duct proliferation in 26 out of 27 cats with lymphocytic cholangitis. Both the extent of bile duct proliferation and the degree of fibrosis were positively correlated with the severity of the inflammatory infiltrate. In 10 out of 11 cats with neutrophilic cholangitis, an acute biliary disease, bile duct proliferation was observed [94]. Similar to humans and dogs it is likely that bile duct proliferation in cats involves both cholangiocytes and HPCs.

Liver tumors

An emerging research area focuses on the association between HPCs and liver tumors, both in man and dog. This association is plausible, as HPCs have self-renewal capacity and migratory potential, which is required for invasion and metastasis [105]. However, the presence of HPC features within a liver tumor can be explained by more than one theory. First, HPCs are described as a possible cell of origin for hepatocellular carcinoma (HCC) and cholangiolocellular carcinoma (CLC, a specific type of cholangiocarcinoma), although no one has yet directly shown this lineage relationship [10,106-109]. Second, the presence of HPC markers in HCC is compatible with the possible dedifferentiation of resident hepatocytes that undergo malignant transformation, resulting in the expression of immature markers like K19 on HCCs [106,110].
There is clinical evidence that expression of HPC markers in human HCC is a negative prognostic indicator, as these tumors show a higher recurrence rate and shortened patient survival [10,111]. In dogs, the presence of progenitor (K19) and malignancy (glypican-3) markers was evaluated immunohistochemically, and related to a histological grade and a staging score (including local or distant metastasis). The occurrence of K19 positive HCCs was 12%, which resembles the prevalence in humans. This K19 positive subset was poorly differentiated and more likely to metastasize, suggesting that K19 may be a malignancy marker in canine HCC [11]. However, for both dog and human it is still unclear whether HPCs are the cell of origin in these types of liver cancer. For liver tumors in cats, an association with HPC characteristics is under investigation by our group [Unpublished observations section: Van Sprundel et al.]. Patnaik et al. demonstrated in a retrospective study of 47 feline liver tumors that the majority of neoplasms were epithelial and primarily of biliary origin [112]. Further research is required to understand whether HPC markers are a prognostic indicator in feline liver tumors.
Ultimately, while further studies are required to reach a definitive answer on the cellular origin of liver tumors, the association between HPC markers and malignancy is now widely acknowledged.

HPCs in regenerative medicine

For severe parenchymal or biliary liver diseases, definitive and curative treatment options are currently lacking in both human and veterinary medicine. In humans, the final treatment option is a

liver transplantation, but many patients die while on the waiting list (for actual data on US organ transplants see UNOS website [113]). Moreover, not all grafts remain viable after transplantation (e.g. due to rejection), warranting extensive immunosuppression or a second transplantation if possible. In dog and cat, liver transplantation is not performed. Since the etiology of liver disease is often not known, current therapy in veterinary medicine is restricted to symptomatic treatment and the use of corticoids [114-117]. To be able to improve patient survival and disease outcome, new curative therapies for advanced liver disease are required. Hepatocyte transplantations have been studied most extensively and have been performed in human patients with metabolic liver disease [118-120]. The use of hepatocytes does, however, not solve the problem of donor-shortage. Additionally, hepatocytes cannot be expanded to reach sufficient numbers for transplantation [121] which also inhibits the establishment of cell banks. The development of 'humanized livers', where murine or porcine host livers are used as an *in vivo* bioreactor to grow (human) hepatocytes, are potential ways to bypass this problem [122-124], but further research is needed to explore its potential for therapeutic use. Especially for veterinary medicine this approach could raise ethical questions. HPC-based treatment modalities could avoid the problems encountered when using hepatocytes for transplantation. HPCs can self-renew, generating a stable pool of progenitors, and can differentiate into newly generated hepatocytes or cholangiocytes which restore liver function [13,125]. There are two regenerative strategies that could be employed in the (veterinary) clinical use of HPCs and we will briefly discuss them in the light of previous studies (Figure 5).

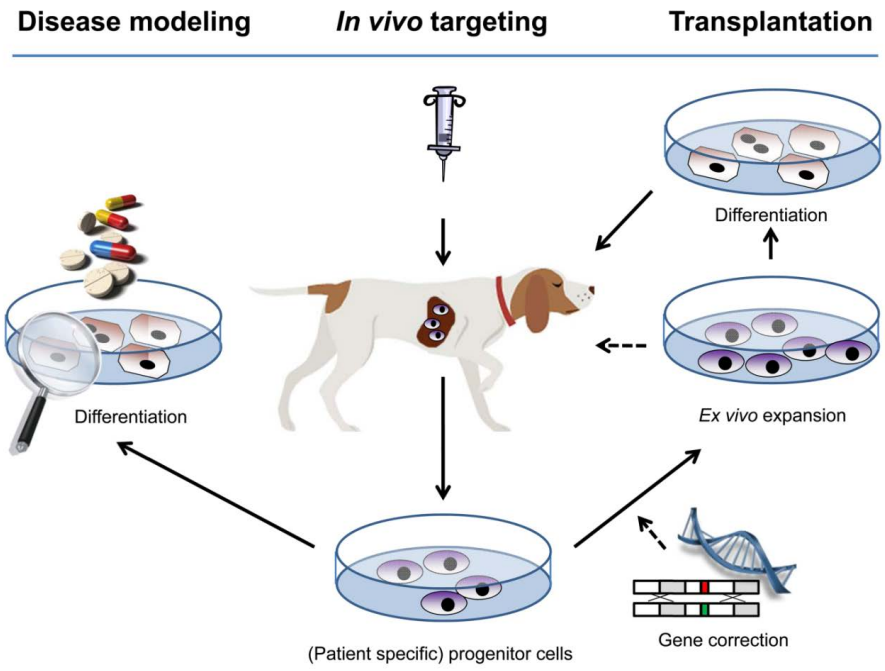

Figure 5 Application of hepatic progenitor cells in regenerative medicine. Schematic representation of the potential use of hepatic progenitor cells in veterinary medicine. *In vivo* targeting of a patient's endogenous HPC population with small molecules would be the most elegant approach. Another option is *ex vivo* expansion of HPCs in culture, potential differentiation into hepatocytes and subsequent use in clinical cell transplantation. Upon differentiation HPCs can also be used for disease modeling. For example, by culturing HPCs from a patient with an inborn error of metabolism it is possible to study mechanisms of disease and to perform drug discovery screens.

The first option would be to target a patient's own HPC population *in vivo* by specific drugs or small molecules. This elegant approach is quick, minimally invasive, does not carry risk of rejection, and has the potential to be relatively cost-effective. The goal would be to activate a patient's own HPC pool and to boost proliferation and/or differentiation depending on the type of liver disease. A prerequisite is that the essential signals required to mount an HPC response are known, and that these signals are specific to HPCs and do not, for example, activate HSCs and cause excessive fibrosis. Additionally, one needs to consider that overstimulation of the HPC pool might have unexpected and undesirable side effects. HPCs have the capacity of regenerating the liver but in many diseases this is too little and too late. Possibly in these cases specific pathological or molecular characteristics somehow interfere with HPC proliferation or differentiation. Therefore, any signal that is found to benefit the HPC response must be reviewed in a clinical and disease-specific perspective. This highly promising but very challenging approach is currently unexplored in all species. Once these signals are unraveled this approach may become a primary focus for the development of new hepatic regenerative treatments.

The second option is to use differentiated HPCs as a cell source for transplantation, either autologous or allogeneic. Technically it is possible to harvest autologous HPCs from a liver biopsy, expand them in culture and differentiate them into hepatocytes for transplantation purposes. In case of inherited metabolic disease, gene correction could be applied before transplantation. HPCs can be cultured *in vitro* upon isolation from primary canine liver tissue as shown by Arends et al. [126]. Using a plate-and-wait method, they were able to grow colonies of canine HPCs from the non-parenchymal fraction of a digested liver sample within a few weeks. Unfortunately, in cases of urgent clinical needs, this culture method as an autologous source for transplantation would not be feasible. In chronic cases, however, this would be an option and would circumvent rejection issues. Optimization of culture conditions of primary HPCs is needed in addition to characterization of cells in culture, most importantly, self-renewal and differentiation capacity and stability. A promising recent development is the discovery of Lgr5 positive cells in injured mouse livers that can be FACS sorted or isolated as 'ducts' and form organoids upon 3D culturing [49,127]. These cells rapidly expand, have the capacity to differentiate into hepatocytes, and can be kept in culture for more than a year, while maintaining their genomic integrity. An important caveat in clinical HPC transplantation are the costs associated with the expansion of HPCs in culture. In veterinary medicine this must be balanced against the amount a pet owner is willing to pay for treatment. The costs will be highly influenced by the number of patients that could benefit from a new therapy [128]. In a UK study, the prevalence of chronic hepatitis in a dog population from first opinion practices was 12% [129], supporting an economical niche to develop new therapeutics for veterinary liver disease. The fact that treatment of dogs may serve as pre-clinical studies for human drug development could provide an economically interesting approach for pharmaceutical industries. The predicted doubling frequency of end stage liver disease in man worldwide shows the medical and economic relevance to design new therapies for human liver disease [113]. As stem cell-based therapies are being developed for multiple organs and diseases, advances are likely to be made in the near future [128].

When planning the use of HPCs for cell transplantation, three variables are essential: cell number, engraftment potential and differentiation state. The cell number administered may be critical for functional recovery of a damaged liver. An indication of the number necessary can be derived from hepatocyte transplantation studies. Jorns et al. provided a concise literature overview of hepatocyte

transplantations in various species, including human, which may be most relevant for application in veterinary medicine [130]. The number of transplanted cells depends on the infusion rate and injection route, and can be divided over multiple sessions. It is accepted that for correction of a genetic metabolic disease, 2-5% repopulation is sufficient to correct the phenotype [13]. Generally, billions of hepatocytes are used for intraportal delivery in human. Engraftment potential of hepatocytes may be very different than that of stem cells. In addition, the host environment of the diseased liver, and thus the type of disease, determines successful engraftment and therefore the number of cells needed for functional recovery. Finally, the differentiation status of the HPCs is important for the success of transplantation. The stage of maturation may determine homing and engraftment ability of HPCs. For example, undifferentiated HPCs have the capacity to migrate [33,79]. On the other hand, a cell in a more differentiated state with developing hepatocyte characteristics might pose an attractive clinical application in cases of acute liver failure.
With respect to HPC transplantation, metabolic diseases will probably be the first to be addressed in both dog and human. In dogs, transplantation of hepatocytes has been reported in a number of studies, mostly in Dalmatians as a model for metabolic disease (hyperuricosuria) [131-133]. In these types of diseases, improvement of the phenotype can be accomplished by providing a relatively low number of cells from a healthy donor, or upon genetic correction of autologous cells. The COMMD1 deficient dog presenting with copper storage disease resulting in chronic hepatitis, provides an excellent model for clinical HPC transplantation trials [134,135]. Such studies will reveal important information on efficacy and safety of HPC transplantation and will facilitate translation of this therapeutic strategy to the veterinary and human clinic. Diseases with a more complex pathophysiology, such as chronic hepatitis involving fibrosis and remodeling of tissue architecture, will be more challenging. These types of diseases will require a multimodal approach targeting not only hepatocyte regeneration but also fibrosis resolution and modulation of inflammation. Current developments in anti-fibrotic therapies and the co-transplantation of mesenchymal stem cells or macrophages to modulate inflammatory responses may aid the development of new regenerative therapies for chronic and severe liver diseases in man and dog [136,137].

Conclusions

There is much promise in the use of HPCs in regenerative therapies for both human and veterinary medicine. Fundamental studies in toxic and genetic rodent models, together with (comparative) histo-pathological studies in humans have determined HPCs to be clinically relevant. In canines, important molecular and cellular reaction patterns in particular liver diseases are reported, and characterize HPCs and their niche. Overall, HPC marker expression in dogs is comparable to that of humans, as is response to injury and the cell types involved in modulating HPC response. This suggests that the therapeutic potential of these cells is similar in dog when compared to man, and opens up the potential for developing new strategies for currently untreatable canine liver diseases (Figure 6).

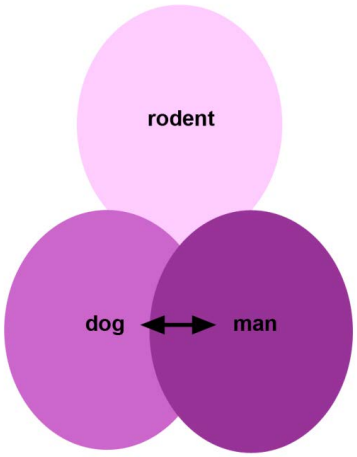

Figure 6 Translational medicine in veterinary and human hepatology. In HPC biology inter-species differences and similarities can be found. When reviewing HPC markers, niche characteristics and HPC response in health and disease, dogs share many similarities with man. Furthermore, dogs can bridge the gap between experimental rodent studies and human clinical application. Human medicine could benefit from its canine counterpart by appreciating the dog as a target species as well as a large animal model for the development of new therapies.

On the other hand, there is still much to be conducted in feline hepatology. As with canine investigations, studies on cat liver disease and pathology would benefit from focusing on the molecular mechanisms of disease and regeneration in comparison to human and canine models, including the presence and characteristics of feline HPCs. In addition, feline lipidosis and cholangitis, diseases that are rare in dogs, may provide important models for human steatohepatitis and biliary disease.

We conclude that humans and dogs share many similarities with respect to liver disease and HPC biology, especially since dogs have spontaneous liver disease that equally requires treatment. With the emergence of regenerative medicine, veterinary and human medicine have the unique opportunity to advance potential therapies and technologies together. In particular, human medicine could greatly benefit from HPC-based trials in dogs.

Unpublished observations

Valtolina C, Muys J, Penning LC, Grinwis GG, Schotanus BA: Characterization of the feline hepatic progenitor cell niche in health and disease, manuscript in preparation.

Van Sprundel RGHM, Van Den Ingh TSGAM, Guscetti F, Kershaw O, Kanemoto H, Van Gils HM, Rothuizen J, Spee B: Classification of primary hepatic tumours in the cat, manuscript in preparation.

Abbreviations

HPC, Hepatic progenitor cell; HCC, Hepatocellular carcinoma; PHx, Partial hepatectomy; HGF, Hepatocyte growth factor; PCNA, Proliferating cell nuclear antigen; DR, Ductular reaction; K (7), Keratin (7); ECM, Extracellular matrix; HSC, Hepatic stellate cell; MMP, Matrix metalloproteinase; TIMP, Tissue inhibitor of matrix metalloproteinase; αSMA, Alpha smooth muscle actin; NASH, Non-alcoholic steatohepatitis; NAFLD, Non-alcoholic fatty liver disease; LDH, Lobular dissecting hepatitis; CLC, Cholangiolocellular carcinoma

Competing interests

The authors declare that they have no competing interests.

Authors' contributions

Authors HS Kruitwagen, B Spee and BA Schotanus contributed equally to the writing of this manuscript and preparation of the figures. All authors read and approved the final manuscript.

Acknowledgements

The authors would like to thank Sarah Opitz for editing the manuscript. HS Kruitwagen and BA Schotanus receive funding from ZonMW for translational research on hepatic progenitor cells.

References

1. Cyranoski D: **Stem cells boom in vet clinics.** *Nature* 2013, **496**(7444)**:**148–149.

2. Riehle KJ, Dan YY, Campbell JS, Fausto N: **New concepts in liver regeneration.** *J Gastroenterol Hepatol* 2011, **26**(Suppl 1)**:**203–212.

3. Wang X, Foster M, Al-Dhalimy M, Lagasse E, Finegold M, Grompe M: **The origin and liver repopulating capacity of murine oval cells.** *Proc Natl Acad Sci U S A* 2003, **100**(Suppl 1)**:**11881–11888.

4. Roskams TA, Libbrecht L, Desmet VJ: **Progenitor cells in diseased human liver.** *Semin Liver Dis* 2003, **23**(4)**:**385–396.

5. Arends B, Vankelecom H, Vander Borght S, Roskams T, Penning LC, Rothuizen J, Spee B: **The dog liver contains a "side population" of cells with hepatic progenitor-like characteristics.** *Stem Cells Dev* 2009, **18**(2)**:**343–350.

6. Schotanus BA, van den Ingh TS, Penning LC, Rothuizen J, Roskams TA, Spee B: **Cross-species immunohistochemical investigation of the activation of the liver progenitor cell niche in different types of liver disease.** *Liver Int* 2009, **29**(8)**:**1241–1252.

7. Ijzer J, Schotanus BA, Vander Borght S, Roskams TA, Kisjes R, Penning LC, Rothuizen J, van den Ingh TS: **Characterisation of the hepatic progenitor cell compartment in normal liver and in hepatitis: an immunohistochemical comparison between dog and man.** *Vet J* 2010, **184**(3)**:**308–314.

8. Yoshioka K, Enaga S, Taniguchi K, Fukushima U, Uechi M, Mutoh K: **Morphological characterization of ductular reactions in canine liver disease.** *J Comp Pathol* 2004, **130**(2–3)**:**92–98.

9. Van Den Ingh TSGAM, Van Winkle T, Cullen JM, Charles JA, Desmet VJ, *et al*: **Morphological classification of parenchymal disorders of the canine and feline liver: 2. Hepatocellular death, hepatitis and cirrhosis**. In *WSAVA Standards for clinical and histological diagnosis of canine and feline liver disease.* Edited by Rothuizen J, Bunch SE, Charles JA. Edinburgh, Great Britain: Saunders-Elsevier; 2006:85–102.

10. Durnez A, Verslype C, Nevens F, Fevery J, Aerts R, Pirenne J, Lesaffre E, Libbrecht L, Desmet V, Roskams T: **The clinicopathological and prognostic relevance of cytokeratin 7 and 19 expression in hepatocellular carcinoma Histopathology.** *Histopathology* 2006, **49**(2)**:**138–151.

11. van Sprundel RGHM, van den Ingh TS, Desmet VJ, Katoonizadeh A, Penning LC, Rothuizen J, Roskams T, Spee B: **Keratin 19 marks poor differentiation and a more aggressive behaviour in canine and human hepatocellular tumours.** *Comp Hepatol* 2010, **9**(1)**:**4.

12. Van Sprundel RGHM, van den Ingh TSGAM, Guscetti F, Kershaw O, Kanemoto H, Van Gils HM, Rothuizen J, Roskams T, Spee B: **Classification of primary hepatic tumours in the dog.** *Vet J* 2013, **197**(3)**:**596-606.

13. Sancho-Bru P, Najimi M, Caruso M, Pauwelyn K, Cantz T, Forbes S, Roskams T, Ott M, Gehling U, Sokal E, Verfaillie CM, Muraca M: **Stem and progenitor cells for liver repopulation: can we standardise the process from bench to bedside?** *Gut* 2009, **58**(4)**:**594–603.

14. Warren A, Center S, McDonough S, Chiotti R, Goldstein R, Meseck E, Jacobsen M, Rowland P, Simpson K: **Histopathologic features, immunophenotyping, clonality, and eubacterial fluorescence in situ hybridization in cats with lymphocytic cholangitis/cholangiohepatitis.** *Vet Pathol* 2011, **48**(3)**:**627–641.

15. Taub R: **Liver regeneration: from myth to mechanism.** *Nat Rev Mol Cell Biol* 2004, **5**(10)**:**836–847.

16. Overturf K, A-Dhalimy M, Ou CN, Finegold M, Grompe M: **Serial transplantation reveals the stem-cell-like regenerative potential of adult mouse hepatocytes.** *Am J Pathol* 1997, **15**(5)**:**1273–1280.

17. Fuchs E, Chen T: **A matter of life and death: self-renewal in stem cells.** *EMBO Rep* 2013, **14**(1)**:**39–48.

18. Higgins GM, Anderson RM: **Experimental pathology of the liver. I. Restoration of the liver of the white rat following partial surgical removal.** *Arch Pathol* 1931, **12:**186–202.

19. Francavilla A, Porter KA, Benichou J, Jones AF, Starzl TE: **Liver regeneration in dogs: morphologic and chemical changes.** *J Surg Res* 1978, **25**(5)**:**409–419.

20. Szawlowski AW, Saint-Aubert B, Gouttebel MC, Astre C, Joyeux H: **Experimental model of extended repeated partial hepatectomy in the dog.** *Eur Surg Res* 1987, **19**(6)**:**375–380.

21. Michalopoulos GK: **Liver regeneration.** *J Cell Physiol* 2007, **213**(2)**:**286–300.

22. Spee B, Penning LC, van den Ingh TS, Arends B, Ijzer J, van Sluijs FJ, Rothuizen J: **Regenerative and fibrotic pathways in canine hepatic portosystemic shunt and portal vein hypoplasia, new models for clinical hepatocyte growth factor treatment.** *Comp Hepatol* 2005, **4:**7.

23. Spee B, Arends B, van den Ingh TS, Brinkhof B, Nederbragt H, Ijzer J, Roskams T, Penning LC, Rothuizen J: **Transforming growth factor beta-1 signalling in canine hepatic diseases: new models for human fibrotic liver pathologies.** *Liver Int* 2006, **26**(6)**:**716–725.

24. Spee B, Arends B, van den Ingh TS, Roskams T, Rothuizen J, Penning LC: **Major HGF-mediated regenerative pathways are similarly affected in human and canine cirrhosis.** *Comp Hepatol* 2007, **6:**8.

25. Katoonizadeh A, Nevens F, Verslype C, Pirenne J, Roskams T: **Liver regeneration in acute severe liver impairment: A clinicopathological correlation study.** *Liver Int* 2006, **26**(10)**:**1225–1233.

26. Aravinthan A, Scarpini C, Tachtatzis P, Verma S, Penrhyn-Lowe S, Harvey R, Davies SE, Allison M, Coleman N, Alexander G: **Hepatocyte senescence predicts progression in non-alcohol-related fatty liver disease.** *J Hepatol* 2013, **58**(3)**:**549–556.

27. Lunz JG 3rd, Tsuji H, Nozaki I, Murase N, Demetris AJ: **An inhibitor of cyclin-dependent kinase, stress-induced p21Waf-1/Cip-1, mediates hepatocyte mito-inhibition during the evolution of cirrhosis.** *Hepatology* 2005, **41**(6)**:**1262–1271.

28. Liu L, Yannam GR, Nishikawa T, Yamamoto T, Basma H, Ito R, Nagaya M, Dutta-Moscato J, Stolz DB, Duan F, Kaestner KH, Vodovotz Y, Soto-Gutierrez A, Fox IJ: **The microenvironment in hepatocyte regeneration and function in rats with advanced cirrhosis.** *Hepatology* 2012, **55**(5)**:**1529–1539.

29. Yang S, Koteish A, Lin H, Huang J, Roskams T, Dawson V, Diehl AM: **Oval cells compensate for damage and replicative senescence of mature hepatocytes in mice with fatty liver disease.** *Hepatology* 2004, **39**(2)**:**403–411.

30. Arends B, Spee B, Hoffmann G, Jansen GE, Slump E, Auriemma E, Ijzer J, Hemrika W, Romijn RA, van der Heijden-Liefkens KH, Sondermeijer PJ, van den Ingh TS, Penning LC, Rothuizen J: **In vitro and in vivo bioactivity of recombinant canine hepatocyte growth factor.** *Vet J* 2008, **178**(1)**:**70–77.

31. Ijzer J, Kisjes JR, Penning LC, Rothuizen J, van den Ingh TS: **The progenitor cell compartment in the feline liver: an (immuno) histochemical investigation.** *Vet Pathol* 2009, **46**(4)**:**614–621.

32. Roskams T, De Vos R, Van Eyken P, Myazaki H, Van Damme B, Desmet V: **Hepatic OV-6 expression in human liver disease and rat experiments: evidence for hepatic progenitor cells in man.** *J Hepatol* 1998, **29**(3)**:**455–463.

33. Libbrecht L, Desmet V, Van Damme B, Roskams T: **Deep intralobular extension of human hepatic 'progenitor cells' correlates with parenchymal inflammation in chronic viral hepatitis: can 'progenitor cells' migrate?** *J Pathol* 2000, **192**(3)**:**373–378.

34. Roskams TA, Theise ND, Balabaud C, Bhagat G, Bhathal PS, Bioulac-Sage P, Brunt EM, Crawford JM, Crosby HA, Desmet V, Finegold MJ, Geller SA, Gouw AS, Hytiroglou P, Knisely AS, Kojiro M, Lefkowitch JH, Nakanuma Y, Olynyk JK, Park YN, Portmann B, Saxena R, Scheuer PJ, Strain AJ, Thung SN, Wanless IR, West AB: **Nomenclature of the finer branches of the biliary tree: canals, ductules, and ductular reactions in human livers.** *Hepatology* 2004, **39**(6)**:**1739–1745.

35. Kuwahara R, Kofman AV, Landis CS, Swenson ES, Barendswaard E, Theise ND: **The hepatic stem cell niche: identification by label-retaining cell assay.** *Hepatology* 2008, **47**(6)**:**1994–2002.

36. Furuyama K, Kawaguchi Y, Akiyama H, Horiguchi M, Kodama S, Kuhara T, Hosokawa S, Elbahrawy A, Soeda T, Koizumi M, Masui T, Kawaguchi M, Takaori K, Doi R, Nishi E, Kakinoki R, Deng JM, Behringer RR, Nakamura T, Uemoto S: **Continuous cell supply from a Sox9-expressing progenitor zone in adult liver, exocrine pancreas and intestine.** *Nat Genet* 2011, **43**(1)**:**34–41.

37. Espanol-Suner R, Carpentier R, Van Hul N, Legry V, Achouri Y, Cordi S, Jacquemin P, Lemaigre F, Leclercq IA: **Liver progenitor cells yield functional hepatocytes in response to chronic liver injury in mice.** *Gastroenterology* 2012, **143**(6)**:**1564–1575. e7.

38. Turner R, Lozoya O, Wang Y, Cardinale V, Gaudio E, Alpini G, Mendel G, Wauthier E, Barbier C, Alvaro D, Reid LM: **Human hepatic stem cell and maturational liver lineage biology.** *Hepatology* 2011, **53**(3)**:**1035–1045.

39. Semeraro R, Carpino G, Cardinale V, Onori P, Gentile R, Cantafora A, Franchitto A, Napoli C, Anceschi M, Brunelli R, Bosco D, Torrice A, Reid L, Gaudio E, Alvaro D: **Multipotent stem/progenitor cells in the human foetal biliary tree.** *J Hepatol* 2012, **57**(5)**:**987–994.

40. Petersen BE, Bowen WC, Patrene KD, Mars WM, Sullivan AK, Murase N, Boggs SS, Greenberger JS, Goff JP: **Bone marrow as a potential source of hepatic oval cells.** *Science* 1999, **284**(5417)**:**1168–1170.

41. Oh SH, Witek RP, Bae SH, Zheng D, Jung Y, Piscaglia AC, Petersen BE: **Bone marrow-derived hepatic oval cells differentiate into hepatocytes in 2-acetylaminofluorene/partial hepatectomy-induced liver regeneration.** *Gastroenterology* 2007, **132**(3)**:**1077–1087.

42. Alison MR, Vig P, Russo F, Bigger BW, Amofah E, Themis M, Forbes S: **Hepatic stem cells: from inside and outside the liver?** *Cell Prolif* 2004, **37**(1)**:**1–21.

43. Vig P, Russo FP, Edwards RJ, Tadrous PJ, Wright NA, Thomas HC, Alison MR, Forbes SJ: **The sources of parenchymal regeneration after chronic hepatocellular liver injury in mice.** *Hepatology* 2006, **43**(2)**:**316–324.

44. Lorenzini S, Bird TG, Boulter L, Bellamy C, Samuel K, Aucott R, Clayton E, Andreone P, Bernardi M, Golding M, Alison MR, Iredale JP, Forbes SJ: **Characterisation of a stereotypical cellular and extracellular adult liver progenitor cell niche in rodents and diseased human liver.** *Gut* 2010, **59**(5)**:**645–654.

45. Chen YH, Chang MH, Chien CS, Wu SH, Yu CH, Chen HL: **Contribution of mature hepatocytes to small hepatocyte-like progenitor cells in retrorsine-exposed rats with chimeric livers.** *Hepatology* 2013, **57**(3)**:**1215–1224.

46. Calloni R, Cordero EA, Henriques JA, Bonatto D: **Reviewing and updating the major molecular markers for stem cells.** *Stem Cells Dev* 2013, **22**(9)**:**1455–1476.

47. Jelnes P, Santoni-Rugiu E, Rasmussen M, Friis SL, Nielsen JH, Tygstrup N, Bisgaard HC: **Remarkable heterogeneity displayed by oval cells in rat and mouse models of stem cell-mediated liver regeneration.** *Hepatology* 2007, **45**(6)**:**1462–1470.

48. Spee B, Carpino G, Schotanus BA, Katoonizadeh A, Vander Borght S, Gaudio E, Roskams T: **Characterisation of the liver progenitor cell niche in liver diseases: potential involvement of Wnt and Notch signalling.** *Gut* 2010, **59**(2)**:**247–257.

49. Huch M, Dorrell C, Boj SF, van Es JH, Li VS, van de Wetering M, Sato T, Hamer K, Sasaki N, Finegold MJ, Haft A, Vries RG, Grompe M, Clevers H: **In vitro expansion of single Lgr5+ liver stem cells induced by Wnt-driven regeneration.** *Nature* 2013, **494**(7436)**:**247–250.

50. Schievenbusch S, Sauer E, Curth HM, Schulte S, Demir M, Toex U, Goeser T, Nierhoff D: **Neighbor of Punc E 11: expression pattern of the new hepatic stem/progenitor cell marker during murine liver development.** *Stem Cells Dev* 2012, **21**(14)**:**2656–2666.

51. Yovchev MI, Grozdanov PN, Zhou H, Racherla H, Guha C, Dabeva MD: **Identification of adult hepatic progenitor cells capable of repopulating injured rat liver.** *Hepatology* 2008, **47**(2)**:**636–647.

52. Grozdanov PN, Yovchev MI, Dabeva MD: **The oncofetal protein glypican-3 is a novel marker of hepatic progenitor/oval cells.** *Lab Invest* 2006, **86**(12)**:**1272–1284.

53. Kruitwagen HS, Spee B, Viebahn CS, Venema HB, Penning LC, Grinwis GG, Favier RP, Van Den Ingh TSGAM, Rothuizen J, Schotanus BA: **The canine hepatic progenitor cell niche: Molecular characterisation in health and disease.** *in press in The Veterinary Journal* (doi: 10.1016/j.tvjl.2014.05.024).

54. Herrera MB, Bruno S, Buttiglieri S, Tetta C, Gatti S, Deregibus MC, Bussolati B, Camussi G: **Isolation and characterization of a stem cell population from adult human liver.** *Stem Cells* 2006, **24**(12)**:**2840–2850.

55. Zhang L, Theise N, Chua M, Reid LM: **The stem cell niche of human livers: symmetry between development and regeneration.** *Hepatology* 2008, **48**(5)**:**1598–1607.

56. Theise ND, Saxena R, Portmann BC, Thung SN, Yee H, Chiriboga L, Kumar A, Crawford JM: **The canals of Hering and hepatic stem cells in humans.** *Hepatology* 1999, **30**(6)**:**1425–1433.

57. Okabe M, Tsukahara Y, Tanaka M, Suzuki K, Saito S, Kamiya Y, Tsujimura T, Nakamura K, Miyajima A: **Potential hepatic stem cells reside in EpCAM + cells of normal and injured mouse liver.** *Development* 2009, **136**(11)**:**1951–1960.

58. Demetris AJ, Seaberg EC, Wennerberg A, Ionellie J, Michalopoulos G: **Ductular reaction after submassive necrosis in humans.** *Special emphasis on analysis of ductular hepatocytes. Am J Pathol* 1996, **149**(2)**:**439–448.

59. Qiu Q, Hernandez JC, Dean AM, Rao P, Darlington G: **CD24 positive cells from normal adult mouse liver are hepatocyte progenitor cells.** *Stem Cells Dev* 2011, **20**(12)**:**2177-2188.

60. Sahin MB, Schwartz RE, Buckley SM, Heremans Y, Chase L, Hu WS, Verfaillie CM: **Isolation and characterization of a novel population of progenitor cells from unmanipulated rat liver.** *Liver Transpl* 2008, **14**(3)**:**333–345.

61. Dorrell C, Erker L, Lanxon-Cookson KM, Abraham SL, Victoroff T, Ro S, Canaday PS, Streeter PR, Grompe M: **Surface markers for the murine oval cell response.** *Hepatology* 2008, **48**(4)**:**1282–1291.

62. de Boer CJ, van Krieken JH, Janssen-van Rhijn CM, Litvinov SV: **Expression of Ep-CAM in normal, regenerating, metaplastic, and neoplastic liver.** *J Pathol* 1999, **188**(2)**:**201–206.

63. Paku S, Dezso K, Kopper L, Nagy P: **Immunohistochemical analysis of cytokeratin 7 expression in resting and proliferating biliary structures of rat liver.** *Hepatology* 2005, **42**(4)**:**863–870.

64. Tan J, Hytiroglou P, Wieczorek R, Park YN, Thung SN, Arias B, Theise ND: **Immunohistochemical evidence for hepatic progenitor cells in liver diseases.** *Liver* 2002, **22**(5)**:**365–373.

65. Fotiadu A, Tzioufa V, Vrettou E, Koufogiannis D, Papadimitriou CS, Hytiroglou P: **Progenitor cell activation in chronic viral hepatitis.** *Liver Int* 2004, **24**(3)**:**268–274.

66. Corcelle V, Stieger B, Gjinovci A, Wollheim CB, Gauthier BR: **Characterization of two distinct liver progenitor cell subpopulations of hematopoietic and hepatic origins.** *Exp Cell Res* 2006, **312**(15)**:**2826–2836.

67. Lowes KN, Brennan BA, Yeoh GC, Olynyk JK: **Oval cell numbers in human chronic liver diseases are directly related to disease severity.** *Am J Pathol* 1999, **154**(2)**:**537–541.

68. Fuchs E, Tumbar T, Guasch G: **Socializing with the neighbors: stem cells and their niche.** *Cell* 2004, **116**(6)**:**769–778.

69. Roskams T: **Different types of liver progenitor cells and their niches.** *J Hepatol* 2006, **45**(1)**:**1–4.

70. Geerts A: **History, heterogeneity, developmental biology, and functions of quiescent hepatic stellate cells.** *Semin Liver Dis* 2001, **21**(3)**:**311–335.

71. Winau F, Hegasy G, Weiskirchen R, Weber S, Cassan C, Sieling PA, Modlin RL, Liblau RS, Gressner AM, Kaufmann SH: **Ito cells are liver-resident antigen-presenting cells for activating T cell responses.** *Immunity* 2007, **26**(1)**:**117–129.

72. Friedman SL: **Mechanisms of hepatic fibrogenesis.** *Gastroenterology* 2008, **134**(6)**:**1655–1669.

73. Pintilie DG, Shupe TD, Oh SH, Salganik SV, Darwiche H, Petersen BE: **Hepatic stellate cells' involvement in progenitor-mediated liver regeneration.** *Lab Invest* 2010, **90**(8)**:**1199–1208.

74. Ishikawa T, Factor VM, Marquardt JU, Raggi C, Seo D, Kitade M, Conner EA, Thorgeirsson SS: **Hepatocyte growth factor/c-met signaling is required for stem-cell-mediated liver regeneration in mice.** *Hepatology* 2012, **55**(4)**:**1215–1226.

75. Nagai H, Terada K, Watanabe G, Ueno Y, Aiba N, Shibuya T, Kawagoe M, Kameda T, Sato M, Senoo H, Sugiyama T: **Differentiation of liver epithelial (stem-like) cells into hepatocytes induced by coculture with hepatic stellate cells.** *Biochem Biophys Res Commun* 2002, **293**(5)**:**1420–1425.

76. Gadd VL, Melino M, Roy S, Horsfall L, O'Rourke P, Williams MR, Irvine KM, Sweet MJ, Jonsson JR, Clouston AD, Powell EE: **Portal, but not lobular, macrophages express matrix metalloproteinase-9: association with the ductular reaction and fibrosis in chronic hepatitis C.** *Liver Int* 2013, **33**(4)**:**569–579.

77. Tirnitz-Parker JE, Viebahn CS, Jakubowski A, Klopcic BR, Olynyk JK, Yeoh GC, Knight B: **Tumor necrosis factor-like weak inducer of apoptosis is a mitogen for liver progenitor cells.** *Hepatology* 2010, **52**(1)**:**291–302.

78. Viebahn CS, Benseler V, Holz LE, Elsegood CL, Vo M, Bertolino P, Ganss R, Yeoh GC: **Invading macrophages play a major role in the liver progenitor cell response to chronic liver injury.** *J Hepatol* 2010, **53**(3)**:**500–507.

79. Van Hul N, Lanthier N, Espaol Suer R, Abarca Quinones J, Van Rooijen N, Leclercq I: **Kupffer cells influence parenchymal invasion and phenotypic orientation, but not the proliferation, of liver progenitor cells in a murine model of liver injury.** *Am J Pathol* 2011, **179**(4)**:**1839–1850.

80. Boulter L, Govaere O, Bird TG, Radulescu S, Ramachandran P, Pellicoro A, Ridgway RA, Seo SS, Spee B, Van Rooijen N, Sansom OJ, Iredale JP, Lowell S, Roskams T, Forbes SJ: **Macrophage-derived Wnt opposes Notch signaling to specify hepatic progenitor cell fate in chronic liver disease.** *Nat Med* 2012, **18**(4)**:**572–579.

81. Kallis YN, Robson AJ, Fallowfield JA, Thomas HC, Alison MR, Wright NA, Goldin RD, Iredale JP, Forbes SJ: **Remodelling of extracellular matrix is a requirement for the hepatic progenitor cell response.** *Gut* 2011, **60**(4)**:**525–533.

82. Van Hul NK, Abarca-Quinones J, Sempoux C, Horsmans Y, Leclercq IA: **Relation between liver progenitor cell expansion and extracellular matrix deposition in a CDE-induced murine model of chronic liver injury.** *Hepatology* 2009, **49**(5)**:**1625–1635.

83. Ichinohe N, Tanimizu N, Ooe H, Nakamura Y, Mizuguchi T, Kon J, Hirata K, Mitaka T: **Differentiation capacity of hepatic stem/progenitor cells isolated from D-galactosamine-treated rat livers.** *Hepatology* 2013, **57**(3)**:**1192–1202.

84. Bedossa P, Paradis V: **Liver extracellular matrix in health and disease.** *J Pathol* 2003, **200**(4)**:**504–515.

85. Clouston AD, Powell EE, Walsh MJ, Richardson MM, Demetris AJ, Jonsson JR: **Fibrosis correlates with a ductular reaction in hepatitis C: roles of impaired replication, progenitor cells and steatosis.** *Hepatology* 2005, **41**(4)**:**809–818.

86. Knight B, Lim R, Yeoh GC, Olynyk JK: **Interferon-gamma exacerbates liver damage, the hepatic progenitor cell response and fibrosis in a mouse model of chronic liver injury.** *J Hepatol* 2007, **47**(6)**:**826–833.

87. Boisclair J, Dore M, Beauchamp G, Chouinard L, Girard C: **Characterization of the inflammatory infiltrate in canine chronic hepatitis.** *Vet Pathol* 2001, **38**(6)**:**628–635.

88. Ijzer J, Roskams T, Molenbeek RF, Ultee T, Penning LC, Rothuizen J, van den Ingh TS: **Morphological characterisation of portal myofibroblasts and hepatic stellate cells in the normal dog liver.** *Comp Hepatol* 2006, **5:**7.

89. Mekonnen GA, Ijzer J, Nederbragt H: **Tenascin-C in chronic canine hepatitis: immunohistochemical localization and correlation with necro-inflammatory activity, fibrotic stage, and expression of alpha-smooth muscle actin, cytokeratin 7, and CD3+ cells.** *Vet Pathol* 2007, **44**(6)**:**803–813.

90. Bernal W, Auzinger G, Dhawan A, Wendon J: **Acute liver failure.** *Lancet* 2010, **376**(9736)**:**190–201.

91. Larsen FS, Bjerring PN: **Acute liver failure.** *Curr Opin Crit Care* 2011, **17**(2)**:**160–164.

92. Kuntz E, Kuntz HD: **Chronic hepatitis**. In *Hepatology Textbook and Atlas.* 3rd edition. Edited by Kuntz E, Kuntz HD. Heidelberg, Germany: Springer; 2008:712–736.

93. Poldervaart JH, Favier RP, Penning LC, Van Den Ingh TSGAM, Rothuizen J: **Primary hepatitis in dogs: A retrospective review (2002–2006).** *J Vet Intern Med* 2009, **23**(1)**:**72–80.

94. Gagne JM, Armstrong PJ, Weiss DJ, Lund EM, Feeney DA, King VL: **Clinical features of inflammatory liver disease in cats: 41 cases (1983–1993).** *J Am Vet Med Assoc* 1999, **214**(4)**:**513–516.

95. Cohen JC, Horton JD, Hobbs HH: **Human fatty liver disease: old questions and new insights.** *Science* 2011, **332**(6037)**:**1519–1523.

96. Roskams T, Yang SQ, Koteish A, Durnez A, DeVos R, Huang X, Achten R, Verslype C, Diehl AM: **Oxidative stress and oval cell accumulation in mice and humans with alcoholic and nonalcoholic fatty liver disease.** *Am J Pathol* 2003, **163**(4)**:**1301–1311.

97. Nobili V, Carpino G, Alisi A, Franchitto A, Alpini G, De Vito R, Onori P, Alvaro D, Gaudio E: **Hepatic progenitor cells activation, fibrosis, and adipokines production in pediatric nonalcoholic fatty liver disease.** *Hepatology* 2012, **56**(6)**:**2142–2153.

98. Armstrong PJ, Blanchard G: **Hepatic lipidosis in cats.** *Vet Clin North Am Small Anim Pract* 2009, **39**(3)**:**599–616.

99. Cullen JM, Van den Ingh TSGAM, Van Winkle T, Charles JA, Desmet VJ, *et al*: **Morphological classification of parenchymal disorders of the canine and feline liver: 1. Normal histology, reversible hepatocytic injury and hepatic amyloidosis**. In *WSAVA Standards for clinical and histological diagnosis of canine and feline liver disease.* Edited by Rothuizen J, Bunch SE, Charles JA. Edinburgh, Great Britain: Saunders-Elsevier; 2006:77–83.

100. Kuramitsu K, Sverdlov DY, Liu SB, Csizmadia E, Burkly L, Schuppan D, Hanto DW, Otterbein LE, Popov Y: **Failure of fibrotic liver regeneration in mice is linked to a severe fibrogenic response driven by hepatic progenitor cell activation.** *Am J Pathol* 2013, **183**(1)**:**182–194.

101. Libbrecht L, Cassiman D, Desmet V, Roskams T: **Expression of neural cell adhesion molecule in human liver development and in congenital and acquired liver diseases.** *Histochem Cell Biol* 2001, **116**(3)**:**233–239.

102. Van Den Ingh TSGAM, Cullen JM, Twedt DC, Van Winkle T, Desmet VJ, Rothuizen J, *et al*: **Morphological classification of biliary disorders of the canine and feline liver**. In *WSAVA Standards for clinical and histological diagnosis of canine and feline liver disease.* Edited by Rothuizen J, Bunch SE, Charles JA. Edinburgh, Great Britain: Saunders-Elsevier; 2006:61–76.

103. Weiss DJ, Gagne JM, Armstrong PJ: **Characterization of portal lymphocytic infiltrates in feline liver.** *Vet Clin Pathol* 1995, **24**(3)**:**91–95.

104. Callahan Clark JE, Haddad JL, Brown DC, Morgan MJ, Van Winkle TJ, Rondeau MP: **Feline cholangitis: a necropsy study of 44 cats (1986–2008).** *J Feline Med Surg* 2011, **13**(8)**:**570–576.

105. Nguyen LV, Vanner R, Dirks P, Eaves CJ: **Cancer stem cells: an evolving concept.** *Nat Rev Cancer* 2012, **12**(2)**:**133–143.

106. Lee JS, Heo J, Libbrecht L, Chu IS, Kaposi-Novak P, Calvisi DF, Mikaelyan A, Roberts LR, Demetris AJ, Sun Z, Nevens F, Roskams T, Thorgeirsson SS: **A novel prognostic subtype of human hepatocellular carcinoma derived from hepatic progenitor cells.** *Nat Med* 2006, **12**(4)**:**410–416.

107. Komuta M, Spee B, Vander Borght S, De Vos R, Verslype C, Aerts R, Yano H, Suzuki T, Matsuda M, Fujii H, Desmet VJ, Kojiro M, Roskams T: **Clinicopathological study on cholangiolocellular carcinoma suggesting hepatic progenitor cell origin.** *Hepatology* 2008, **47**(5)**:**1544–1556.

108. Mishra L, Banker T, Murray J, Byers S, Thenappan A, He AR, Shetty K, Johnson L, Reddy EP: **Liver stem cells and hepatocellular carcinoma.** *Hepatology* 2009, **49**(1)**:**318–329.

109. Kim H, Choi GH, Na DC, Ahn EY, Kim GI, Lee JE, Cho JY, Yoo JE, Choi JS, Park YN: **Human hepatocellular carcinomas with "Stemness"-related marker expression: keratin 19 expression and a poor prognosis.** *Hepatology* 2011, **54**(5)**:**1707–1717.

110. Sell S, Leffert HL: **Liver cancer stem cells.** *J Clin Oncol* 2008, **26**(17)**:**2800–2805.

111. Uenishi T, Kubo S, Yamamoto T, Shuto T, Ogawa M, Tanaka H, Tanaka S, Kaneda K, Hirohashi K: **Cytokeratin 19 expression in hepatocellular carcinoma predicts early postoperative recurrence.** *Cancer Sci* 2003, **94**(10)**:**851–857.

112. Patnaik AK: **A morphologic and immunocytochemical study of hepatic neoplasms in cats.** *Vet Pathol* 1992, **29**(5)**:**405–415.

113. United Network for Organ Sharing website [http://www.unos.org/index.php].

114. Strombeck DR, Miller LM, Harrold D: **Effects of corticosteroid treatment on survival time in dogs with chronic hepatitis: 151 cases (1977–1985).** *J Am Vet Med Assoc* 1988, **193**(9)**:**1109–1113.

115. Rothuizen J: **General principles in the treatment of liver disease**. In *Textbook of Veterinary Internal Medicine.* 6th edition. Edited by Ettinger SJ, Feldman E. St. Louis, USA: Elsevier; 2005:1435–1442.

116. Favier RP: **Idiopathic hepatitis and cirrhosis in dogs.** *Vet Clin North Am Small Anim Pract* 2009, **39**(3)**:**481–488.

117. Favier RP, Poldervaart JH, Van Den Ingh TS, Penning LC, Rothuizen J: **A retrospective study of oral prednisolone treatment in canine chronic hepatitis.** *Vet Q* 2013, **33**(3)**:**113-120.

118. Fox IJ, Chowdhury JR, Kaufman SS, Goertzen TC, Chowdhury NR, Warkentin PI, Dorko K, Sauter BV, Strom SC: **Treatment of the Crigler-Najjar syndrome type I with hepatocyte transplantation.** *N Engl J Med* 1998, **338**(20)**:**1422–1426.

119. Stephenne X, Najimi M, Sibille C, Nassogne MC, Smets F, Sokal EM: **Sustained engraftment and tissue enzyme activity after liver cell transplantation for argininosuccinate lyase deficiency.** *Gastroenterology* 2006, **130**(4)**:**1317–1323.

120. Puppi J, Tan N, Mitry RR, Hughes RD, Lehec S, Mieli-Vergani G, Karani J, Champion MP, Heaton N, Mohamed R, Dhawan A: **Hepatocyte transplantation followed by auxiliary liver transplantation–a novel treatment for ornithine transcarbamylase deficiency.** *Am J Transplant* 2008, **8**(2)**:**452–457.

121. Soltys KA, Soto-Gutierrez A, Nagaya M, Baskin KM, Deutsch M, Ito R, Shneider BL, Squires R, Vockley J, Guha C, Roy-Chowdhury J, Strom SC, Platt JL, Fox IJ: **Barriers to the successful treatment of liver disease by hepatocyte transplantation.** *J Hepatol* 2010, **53**(4)**:**769–774.

122. Azuma H, Paulk N, Ranade A, Dorrell C, Al-Dhalimy M, Ellis E, Strom S, Kay MA, Finegold M, Grompe M: **Robust expansion of human hepatocytes in Fah−/−/Rag2−/−/Il2rg−/− mice.** *Nat Biotechnol* 2007, **25**(8)**:**903–910.

123. Hickey RD, Lillegard JB, Fisher JE, McKenzie TJ, Hofherr SE, Finegold MJ, Nyberg SL, Grompe M: **Efficient production of Fah-null heterozygote pigs by chimeric adeno-associated virus-mediated gene knockout and somatic cell nuclear transfer.** *Hepatology* 2011, **54**(4)**:**1351–1359.

124. Grompe M, Strom S: **Mice with human livers.** *Gastroenterology* 2013, **145**(6)**:**1209–1214.

125. Forbes SJ, Newsome PN: **New horizons for stem cell therapy in liver disease.** *J Hepatol* 2012, **56**(2)**:**496–499.

126. Arends B, Spee B, Schotanus BA, Roskams T, van den Ingh TS, Penning LC, Rothuizen J: **In vitro differentiation of liver progenitor cells derived from healthy dog livers.** *Stem Cells Dev* 2009, **18**(2)**:**351–358.

127. Huch M, Boj SF, Clevers H: **Lgr5(+) liver stem cells, hepatic organoids and regenerative medicine.** *Regen Med* 2013, **8**(4)**:**385–387.

128. Liras A: **Future research and therapeutic applications of human stem cells: general, regulatory, and bioethical aspects.** *J Transl Med* 2010, **8:**131–5876. 8-131.

129. Watson PJ, Roulois AJ, Scase TJ, Irvine R, Herrtage ME: **Prevalence of hepatic lesions at post-mortem examination in dogs and association with pancreatitis.** *J Small Anim Pract* 2010, **51**(11)**:**566–572.

130. Jorns C, Ellis EC, Nowak G, Fischler B, Nemeth A, Strom SC, Ericzon BG: **Hepatocyte transplantation for inherited metabolic diseases of the liver.** *J Intern Med* 2012, **272**(3)**:**201–223.

131. Dunn TB, Kumins NH, Raofi V, Holman DM, Mihalov M, Blanchard J, Law WR, Rastellini C, Benedetti E: **Multiple intrasplenic hepatocyte transplantations in the dalmatian dog.** *Surgery* 2000, **127**(2)**:**193–199.

132. Benedetti E, Kirby JP, Asolati M, Blanchard J, Ward MG, Williams R, Hewett TA, Fontaine M, Pollak R: **Intrasplenic hepatocyte allotransplantation in dalmation dogs with and without cyclosporine immunosuppression.** *Transplantation* 1997, **63**(9)**:**1206–1209.

133. Kocken JM, Borel Rinkes IH, Bijma AM, de Roos WK, Bouwman E, Terpstra OT, Sinaasappel M: **Correction of an inborn error of metabolism by intraportal hepatocyte transplantation in a dog model.** *Transplantation* 1996, **62**(3)**:**358–364.

134. Favier RP, Spee B, Penning LC, Rothuizen J: **Copper-induced hepatitis: the COMMD1 deficient dog as a translational animal model for human chronic hepatitis.** *Vet Q* 2011, **31**(1)**:**49–60.

135. Favier RP, Spee B, Schotanus BA, van den Ingh TS, Fieten H, Brinkhof B, Viebahn CS, Penning LC, Rothuizen J: **COMMD1-deficient dogs accumulate copper in hepatocytes and provide a good model for chronic hepatitis and fibrosis.** *PLoS One* 2012, **7**(8)**:**e42158.

136. Thomas JA, Pope C, Wojtacha D, Robson AJ, Gordon-Walker TT, Hartland S, Ramachandran P, Van Deemter M, Hume DA, Iredale JP, Forbes SJ: **Macrophage therapy for murine liver fibrosis recruits host effector cells improving fibrosis, regeneration, and function.** *Hepatology* 2011, **53**(6)**:**2003–2015.

137. Fouraschen SM, Pan Q, de Ruiter PE, Farid WR, Kazemier G, Kwekkeboom J, Ijzermans JN, Metselaar HJ, Tilanus HW, de Jonge J, van der Laan LJ: **Secreted factors of human liver-derived mesenchymal stem cells promote liver regeneration early after partial hepatectomy.** *Stem Cells Dev* 2012, **21**(13)**:**2410–2419.

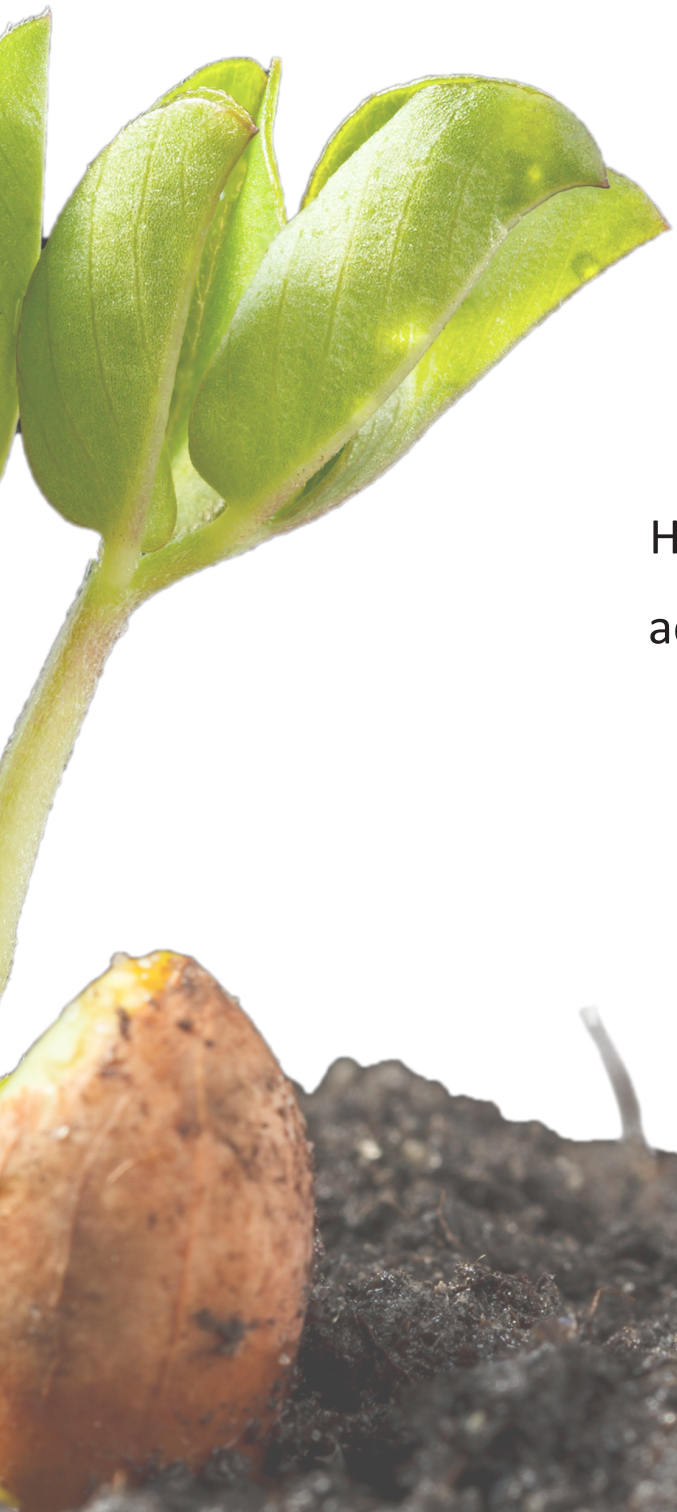

Part I

Hepatic progenitor cell activation mechanisms

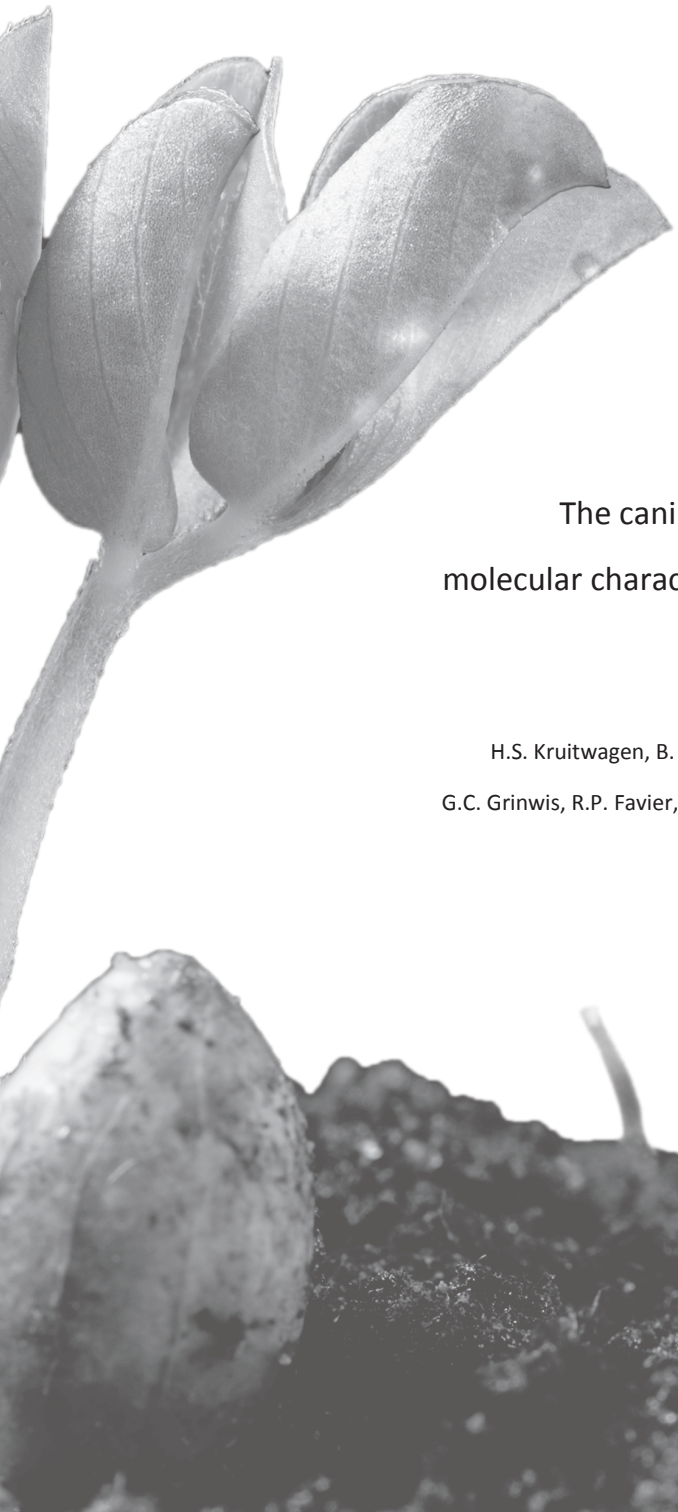

Chapter 2

The canine hepatic progenitor cell niche: molecular characterisation in health and disease.

H.S. Kruitwagen, B. Spee, C.S. Viebahn, H.B. Venema, L.C. Penning, G.C. Grinwis, R.P. Favier, T.S. van den Ingh, J. Rothuizen, B.A. Schotanus

Vet J. 2014 Sep;201(3):345-52

Abstract

Hepatic progenitor cells (HPCs) are an adult stem cell compartment in the liver that contribute to liver regeneration when replication of mature hepatocytes is insufficient. In this study, laser microdissection was used to isolate HPC niches from the livers of healthy dogs and dogs with lobular dissecting hepatitis (LDH), in which HPCs are massively activated. Gene expression of HPC, hepatocyte and biliary markers was determined by quantitative reverse transcriptase PCR. Expression and localisation of selected markers were further studied at the protein level by immunohistochemistry and immunofluorescent double staining in samples of normal liver and liver from dogs with LDH, acute and chronic hepatitis, and extrahepatic cholestasis. Activated HPC niches had higher mRNA expression of the hepatic progenitor markers *OPN*, *FN14*, *CD29*, *CD44*, *CD133*, *LIF*, *LIFR* and *BMI1* compared to HPCs from normal liver. There was lower expression of albumin, but activated HPC niches were positive for the biliary markers SOX9, HNF1β and KRT19 by immunohistochemistry and immunofluorescence. Laminin, activated stellate cells and macrophages are abundant extracellular matrix and cellular components of the canine HPC niche. This study demonstrates that the molecular and cellular characteristics of canine HPCs are similar to rodent and human HPCs and that canine HPCs are distinctively activated in different types of liver disease.

Introduction

In dogs and other species, chronic liver disease frequently leads to progressive fibrosis, loss of regenerative capacity and reduced functional liver mass. Replication of mature hepatocytes can compensate for a substantial reduction in parenchymal mass (Fausto et al., 2006). However, the proliferative capacity of hepatocytes is insufficient in fulminant and chronic hepatopathies (Lunz et al., 2005). In these cases, hepatic progenitor cells (HPCs) become activated (Evarts et al., 1987; Katoonizadeh et al., 2006).

HPCs are a reserve population of adult stem cells located in the canals of Hering. Upon activation, HPCs can proliferate, migrate and differentiate into cholangiocytes or hepatocytes, depending on the type of injury and the microenvironment (Fausto, 2004; Duncan et al., 2009). Histologically, proliferating HPCs are often referred to as a 'ductular reaction' (DR), since they form structures resembling small ductules. HPCs differentiating into hepatocytes are described as 'intermediate hepatocytes'. These cells are found in anatomic relation with the DR and can be recognised by a larger cell size and lower nucleus/cytoplasm ratio (Roskams et al., 2004). HPCs hold potential as therapeutic target in regenerative medicine. They could either be used for cell transplantation or the resident progenitor pool could be stimulated with specific drugs (Sancho-Bru et al., 2009; Forbes and Newsome, 2012).

Most of the knowledge of HPC biology originates from experimental rodent studies, in which HPC responses are induced in specific liver injury models. In addition, the pattern of reaction of HPCs in response to liver pathology in human beings has been described extensively (Libbrecht and Roskams, 2002; Corcelle et al., 2006; Herrera et al., 2006; Yovchev et al., 2007; Yovchev et al., 2008; Zhang et al., 2008; Furuyama et al., 2011; Espanol-Suner et al., 2012). Numerous markers (e.g. keratin 7 and 19, EpCAM, CD133) have been shown to be expressed in rodent and human (activated) HPCs at the mRNA and/or protein level, most of which are also expressed in biliary cells.

Adult stem cells reside in a specific stem cell niche. This niche is the immediate microenvironment of the cells, and is composed of other cell types, signals and extracellular matrix components (Ohlstein et al., 2004). Dynamic cell signalling in this niche controls self-renewal and differentiation of stem cells (Fuchs et al., 2004). Activation of hepatic stellate cells and macrophages, which play a pivotal role in hepatitis, are involved in the activation of the HPC compartment (Roskams, 2008; Viebahn et al., 2010; Boulter et al., 2012).

HPCs have been identified in the canine liver, but HPCs and the HPC niche have not been characterised in detail (Yoshioka et al., 2004; Mekonnen et al., 2007; Arends et al., 2009a and b; Schotanus et al., 2009; Ijzer et al., 2010). The aim of the present study was to characterise canine HPCs and the HPC niche using a large marker set selected from studies in rodents and human beings. The markers were validated by gene expression analysis in activated and quiescent HPCs. Samples of canine liver were collected by laser microdissection (LMD) from cryosections of cases of lobular dissecting hepatitis (LDH), representing an activated niche characterised by a pronounced ductular reaction, and normal liver, representing a quiescent niche (van den Ingh and Rothuizen, 1994; Schotanus et al., 2009; Spee et al., 2010). Selected markers with increased mRNA expression in the activated HPC niche were investigated at the protein level using immunohistochemical and immunofluorescent double staining on sections of normal liver, along with liver from cases of LDH, acute hepatitis (AH), chronic hepatitis (CH) and extrahepatic cholestasis (EHC), the latter representative of biliary injury.

Materials and methods

Liver samples

Liver tissues were obtained from healthy dogs (*n* = 7) used in non-liver related research projects (surplus material, University 3R policy) and from dogs (patients) presented to the University Clinic for Companion Animals of Utrecht University with LDH (*n* = 9), AH (*n* = 5), CH (*n* = 5), and EHC (*n* = 5). Informed consent was obtained from owners to collect post-mortem liver samples for scientific use. No animals were harmed or killed for the purpose of this study. Diagnoses were confirmed histologically by a board-certified veterinary pathologist (TvdI) according to World Small Animal Veterinary Association standards (Rothuizen et al., 2006). For immunohistochemistry and immunofluorescence, obtained tissue samples were fixed in 10% neutral buffered formalin for 24 hours and then transferred to 70% ethanol until paraffin-embedding. From paraffin blocks, 4 µm thick sections were cut. For LMD, samples were frozen in liquid nitrogen. Ten µm thick cryosections were cut in an RNAse free environment and stored at -70°C until further processing.

Immunohistochemistry, double-immunofluorescence and cell quantification

Immunohistochemistry was performed on paraffin-embedded normal liver and liver samples from dogs with LDH, AH, CH and EHC (*n* = 4-5). For each antibody, the antigen retrieval method, antibody dilution and incubation times are summarised in Table 1. Sections were stained for K19, CD29, CD44, BMI1, HNF4α, SOX9 and HNF1β essentially as described previously (van Steenbeek et al., 2013). For CD44 staining, an additional rabbit anti-rat secondary antibody labelling was performed for 45 min at room temperature (1:2,000). For laser microdissection, rapid immunohistochemistry for K7 was performed on cryosections essentially as described previously (Spee et al., 2010). For immunohistochemistry on frozen sections, we could not use the K19 antibody and opted for the K7 antibody (an HPC marker, listed in Table 1).

Immunofluorescent double staining for pancytokeratin (panCK)-α smooth muscle actin (αSMA), panCK-MAC387 and K19-laminin were performed in a parallel approach on paraffin-embedded liver sections. Based on immunohistochemical staining, 2-7 representative samples per disease were selected for immunofluorescence. After antigen retrieval, primary antibodies were incubated overnight at 4 °C, secondary antibodies were incubated at room temperature for 60 min and nuclei were counterstained with To-Pro-3 or 4',6-diamidino-2-phenylindole (DAPI) (Life Technologies) at room temperature for 10 min. For negative controls, the primary antibody was omitted. Slides were analysed using a Leica DMRE fluorescent microscope with Photometrics Coolsnap CCD digital photo camera and CellB software (AnalySIS, Olympus). Cell counts were performed for panCK and MAC387 and expressed relative to total cell number (To-Pro-3 positive). For each sample, five fields were counted at 200x magnification using ImageJ 1.44 software. Statistical analysis was performed using Mann-Whitney *U* post hoc tests to assess differences in cell counts between diseases. $P < 0.05$ was considered to be significant.

Table 1. Antibodies used in this study.

Antibody	Antibody source/type	Clone	Company	Application	Dilution	Incubation	Antigen retrieval
K7	Mu/Mo	OV-TL 12/30	Dako	IHC/LMDC	1:50	1 h RT	-
K19	Mu/Mo	K4.62	Sigma	IHC	1:100	O/N 4 ºC	Proteinase K RT

CD29	Mu/Mo	18/CD29	BD Biosciences	IHC	1:100	O/N 4 ºC	Citrate 98 ºC
CD44	Rat		Hubrecht Institute	IHC	1:200	O/N 4 ºC	Citrate 98 ºC
BMI1	Mu/Mo	F6	Millipore	IHC	1:150	O/N 4 ºC	TE 98 ºC
HNF4α	Rb/Po		Santa Cruz	IHC	1:300	O/N 4 ºC	TE 98 ºC
SOX9	Rb/Po		LS Biosciences	IHC	1:250	O/N 4 ºC	Citrate 98 ºC
HNF1β	Rb/Po		Sigma	IHC	1:400	O/N 4 ºC	Citrate 98 ºC
PanCK	Rb/Po		Dako	IF	1:400	O/N 4 ºC	Proteinase K RT
αSMA	Mu/Mo	1A4	BioGenex	IF	1:200	O/N 4 ºC	Citrate 98 ºC
MAC387	Mu/Mo	MAC387	Abcam	IF	1:500	O/N 4 ºC	Proteinase K RT
Laminin	Rb/Po		Abcam	IF	1:100	O/N 4 ºC	Proteinase K RT

Mu Mo, mouse monoclonal; Rb Po, rabbit polyclonal; IHC, immunohistochemistry; IF, immunofluorescence; LMD, laser microdissection cryosections; RT, room temperature; O/N, overnight; TE, Tris EDTA.

Laser microdissection of keratin 7 positive cells

K7 positive cells were dissected together with neighbouring cells and stroma (total of 2-3.5 x 10^6 μm^2 tissue per sample), representing their anatomically defined niche. LMD was performed with a Nikon Eclipse TE300 inverted microscope connected to a Sony 3-CCD Microscope Colour Video Camera, using MMI CellTools software (Molecular Machines & Industries). Dissected cell niches were collected with adhesive lid tubes (MMI), lysed in 50 µL Extraction Buffer (PicoPure RNA isolation kit, Molecular Devices, MDS Analytical Technologies), processed according to the manufacturer's protocol and stored at -70°C until further use.

RNA isolation and amplification

Total RNA was extracted from LMD samples using the PicoPure RNA isolation kit (MDS Analytical Technologies) with an on-column DNase treatment (0.1 U/µL; Qiagen). RNA integrity was moderate to good and comparable between samples (Bioanalyzer 2100, Agilent Technologies). RNA was stored at -70 °C. RNA was reverse transcribed to cDNA and amplified using the WT-Ovation RNA amplification system (NuGEN Technologies) as described previously (Spee et al., 2010).

Quantitative reverse transcriptase PCR and relative expression analysis

For gene expression analysis, a SYBR Green-based quantitative PCR (qPCR) was performed using a Bio-Rad My-IQ detection system as described previously (van Steenbeek et al., 2013). Primer details and PCR conditions are listed in Table 2. Gene products measured were *keratin 7 (KRT7)*, *osteopontin (OPN)*, *tumour necrosis factor receptor superfamily member 12A (FN14)*, *integrin β1 (CD29)*, *CD44*, *prominin1 (CD133)*, *leukaemia inhibitory factor (LIF)*, *LIF receptor (LIFR), BMI1 polycomb ring finger oncogene (BMI1), α feto-protein (AFP), hepatocyte nuclear factor 4α (HNF4α), albumin (ALB), sex-determining-region-Y-box 9 (SOX9), HNF1β, KRT19* and *neural cell adhesion molecule (NCAM)*. Sequencing reactions confirmed specificity of the amplified products. Accurate normalisation was secured by using four reference genes (*B2M, HPRT, RPS5* and *RPS19*) selected upon stability determination. Relative expression of each gene product ($^{\Delta}$Cq method) was used to

compare normal liver with liver from cases of LDH. Expression levels that were undetectable were arbitrarily set to Cq 45. For statistical analysis SPSS20 was used (SPSS20 Benelux). The non-parametric Mann-Whitney *U* test was used to compare gene expression levels from normal and diseased HPC niches. *P* values <0.05 were considered to be significant.

Table 2. Primers and qPCR conditions.

Gene	Direction	Sequence (5'- 3')	Tm (°C)	Product size (base pairs)	Ensembl TranscriptID
B2M[a]	Forward	TCCTCATCCTCCTCGCT	61.2	85	ENSCAFT00000038092
	Reverse	TTCTCTGCTGGGTGTCG			
HPRT[a]	Forward	AGCTTGCTGGTGAAAAGGAC	58	104	ENSCAFT00000029948
	Reverse	TTATAGTCAAGGGCATATCC			
RPS5[a]	Forward	TCACTGGTGAGAACCCCCT	62.5	141	ENSCAFT00000003710
	Reverse	CCTGATTCACACGGCGTAG			
RPS19[a]	Forward	CCTTCCTCAAAAAGTCTGGG	61	95	ENSCAFT00000008009
	Reverse	GTTCTCATCGTAGGGAGCAAG			
KRT7	Forward	GCGTGGGAGCCGTGAACATC	56	112	ENSCAFT00000011720
	Reverse	CCGCCGCCGCTGGAGAA			
OPN	Forward	GAATGCTGTGCTGACTGAGG	66	113	ENSCAFT00000039667
	Reverse	TGGCTATCCACATCGTCTCC			
FN14	Forward	AACACCAGGCCCCACCCACTC	65.7	190	ENSCAFT00000030714
	Reverse	TTCTCCCTCCCCTCCAAACTCTCC			
CD29	Forward	GATGCCTACAACTCCCTTTCCTCA	58.3	118	ENSCAFT00000006178
	Reverse	CATTTTCCCCTGTTCCATTCACC			
CD44	Forward	CGCTCCTGGCCTTGGCTTTGATT	65.7	110	ENSCAFT00000011067
	Reverse	CCCCACTGCTCCATTGCCATTGT			
CD133	Forward	CTGGGGCTGCTCTTTGTGAT	60.3	115	ENSCAFT00000044445
	Reverse	AGGCCCCATTTTTCTTCTGTC			
LIF	Forward	GAGCCCCCTTCCTATCAC	63	242	ENSCAFT00000045345
	Reverse	CCAGCCGGGTCTTCTCC			
LIFR	Forward	ACTGGAGTTGGACCTCAGAC	62	149	ENSCAFT00000029624
	Reverse	CTGAGAATCAGGTGACCAAG			
BMI1	Forward	TGGACTGACAAATGCTGGAGAACT	68	116	ENSCAFT00000006682
	Reverse	AGGGAACTGAGGATGAGGAGACTG			
AFP	Forward	GCTGCTCCGCCATCCATCC	65.1	123	ENSCAFT00000004849
	Reverse	GGGGTGCCTTCTTGCTATCTCAT			
HNF4α	Forward	GACCGGGCCACAGGGAAACACTAC	65	122	ENSCAFT00000014977
	Reverse	TCCACGACGCATTGCCGACTAAAC			
ALB	Forward	TGTTCCTGGGCACGTTTTTGTA	63.7	92	ENSCAFT00000004843
	Reverse	GGCTTCATATTCCTTGGCGAGTCT			

SOX9	Forward	CGCTCGCAGTACGACTACAC	63	105	ENSCAFT00000007033
	Reverse	GGGGTTCATGTAGGTGAAGG			
HNF1β	Forward	GCCACAATCTCCTCTCACC	62	175	ENSCAFT00000028830
	Reverse	GTTGAGGCTTTGTGCAATGG			
KRT19	Forward	GCCCAGCTGAGCGATGTGC	63.7	86	ENSCAFT00000025270
	Reverse	TGCTCCAGCCGTGACTTGATGT			
NCAM	Forward	GCTCATGTGCATCGCTGTCAACCT	67.2	137	ENSCAFT00000022012
	Reverse	CTCCTCCTCAGTCCGCACCTCCAC			

[a] Reference genes.

Results

Selection of activated HPC niches from lobular dissecting hepatitis

The presence and location of HPCs in different types of liver disease was evaluated with immunohistochemical staining for K19 (Fig. 1a). In the normal liver K19 stained the bile duct epithelium and in addition one or a few K19 positive cells were present near the portal area, indicative of quiescent HPCs. In samples of liver from dogs with liver disease, the DR was positive for K19. K19 positive cells were mainly localised in periportal hepatic parenchyma in AH, within portal areas in EHC (i.e. within the boundaries of the portal stroma), and mainly in and around fibrotic septa in CH. The highest density of K19 positive cells was found in LDH, extensively distributed throughout the parenchyma. In normal liver the median proportion of cells positive for panCK on immunofluorescence was 2.2% (range: 1.2-3.3%), 20% in LDH (range: 12-27%), 11% in AH (range: 1.6-19%), and 14% in CH (range: 5.3-20%) (Fig. 1b). Based on the density and parenchymal distribution of the HPCs, LDH was chosen for laser microdissection and further gene expression analysis of activated HPC niches. Successful selection of HPC niches using laser microdissection was confirmed by increased *KRT7* gene expression in activated compared to quiescent HPC niches (Fig. 1c).

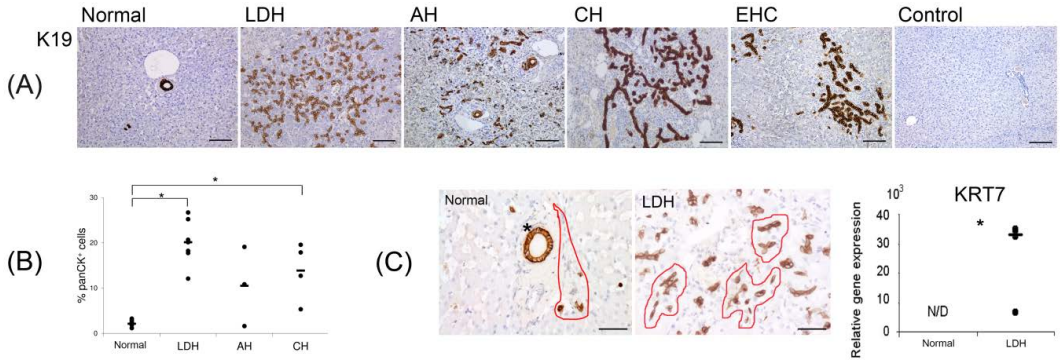

Fig. 1. **Enrichment of activated hepatic progenitor cell (HPC) niches.** (A) Immunohistochemistry of K19 in normal liver, lobular dissecting hepatitis (LDH), acute hepatitis (AH), chronic hepatitis (CH) and extrahepatic cholestasis (EHC). Control, omission of primary antibody (normal liver). Scale bar = 100 µm. (B) Quantification of the number of panCK positive cells in normal liver (n = 7), LDH (n = 9), AH (n = 3) and CH (n = 4). (C) Example of selected microdissected areas (indicated by red lines) after K7 immunohistochemistry in normal liver and LDH sections and relative gene expression measurements of KRT7 in the microdissected HPC niches from normal liver and LDH. Scale bar = 50 µm. * $P < 0.05$.

Expression of HPC markers in the activated canine HPC niche

Gene expression levels of *OPN, FN14, CD29, CD44, CD133, LIF, LIFR* and *BMI1* were significantly higher in activated HPC niches in LDH compared to quiescent HPC niches in normal liver (Fig. 2a). To investigate protein expression and determine the cells that specifically express the protein, immunohistochemistry for CD29, CD44 and BMI1 was performed (Fig. 2b). In normal liver, CD29 was moderately expressed by sinusoidal endothelium and weakly on hepatocyte membranes; bile duct epithelium and vascular smooth muscle in the portal areas were strongly positive. In LDH, AH and CH, there was a strong membranous staining of the DR. Hepatocytes in close vicinity of the DR showed more intense membranous staining for CD29 than hepatocytes in areas where no DR were present. In EHC, only some of the ductules in the portal area were immunoreactive for CD29 and the staining intensity varied. CD44 staining showed strong immunoreactivity of sinusoidal endothelium in normal liver and bile duct epithelium and endothelium in the portal areas of normal and diseased livers. In LDH, AH, CH and EHC, strong CD44 staining could additionally be observed in cells of the DR and in macrophages. In AH, some of the hepatocytes in close vicinity to the DR also showed staining for CD44. Immunohistochemical staining for BMI1 in normal liver showed nuclear positivity in bile duct epithelium and occasionally some endothelial cells in portal areas. In addition, in the samples from dogs with liver disease, the DR showed strong nuclear staining for BMI1 and a somewhat less intense staining in intermediate hepatocytes.

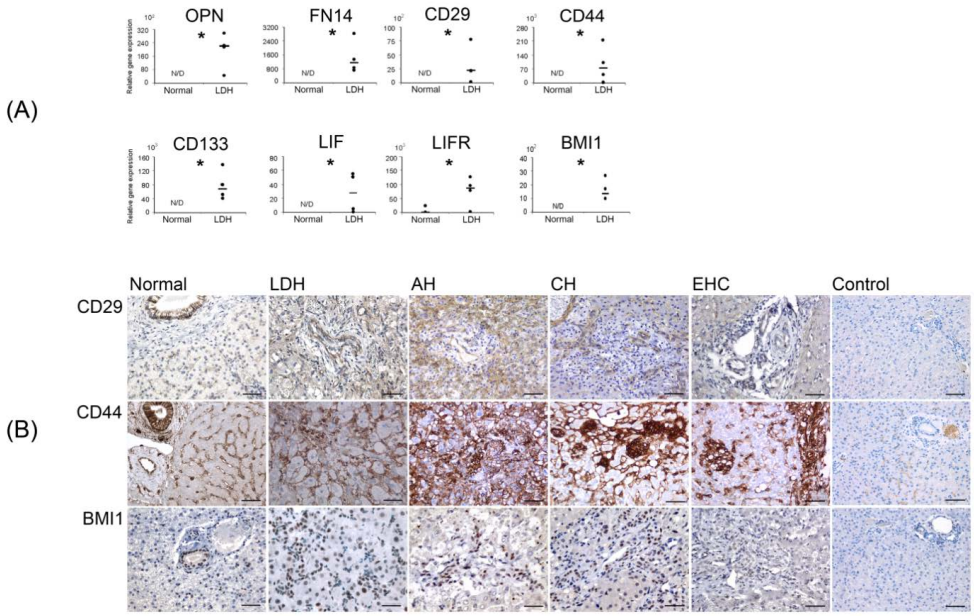

Fig. 2. Expression of hepatic progenitor cell (HPC) markers in the canine HPC niche. (A) Relative gene expression of HPC markers in the quiescent (normal liver) vs. the activated (LDH) HPC niche. (B) Immunohistochemistry for CD29, CD44 and BMI1 in normal liver, lobular dissecting hepatitis (LDH), acute hepatitis (AH), chronic hepatitis (CH) and extrahepatic cholestasis (EHC). Control, omission of primary antibody (normal liver); OPN, osteopontin; FN14, tumour necrosis factor receptor superfamily member 12A; CD29, integrin β1; CD133, prominin1; LIF, leukaemia inhibitory factor (LIF); LIFR, LIF receptor; BMI1, BMI1 polycomb ring finger oncogene; N/D, not detectable. * $P < 0.05$. Scale bar = 50 µm.

Expression of maturation/differentiation markers in the activated canine HPC niche

qPCR results for maturation/differentiation markers in microdissected HPC niches are shown in Fig. 3a. mRNA levels of *AFP*, a gene expressed during early embryonic hepatic development, were higher in activated HPC niches than in their quiescent counterpart. *HNF4α* was not differentially expressed. *ALB* expression was lower in the activated HPC niches. Gene expression of biliary markers *KRT19* and *SOX9* was higher in the activated HPC niches. *HNF1β* and *NCAM* were not differentially expressed. To assess protein expression and cell specificity of these markers, immunohistochemical staining for K19 (Fig. 1a), HNF4α, SOX9 and HNF1β was performed on sections of normal liver and liver from cases of LDH, AH, CH and EHC (Fig. 3b). Immunohistochemistry for HNF4α in normal liver samples showed strong expression in all hepatocyte and cholangiocyte nuclei. In samples from dogs with liver disease, all cells of the DR showed moderate to strong nuclear HNF4α staining. In normal liver, bile duct nuclei were immunoreactive for SOX9 and some of the hepatocytes had a very weak staining in the cytoplasm, whereas the nuclei of the DR showed moderate to strong protein expression of SOX9 in LDH and AH and very strong SOX9 protein expression in CH and EHC samples. Immunohistochemistry for HNF1β showed strong nuclear expression by cholangiocytes in normal liver. In samples from dogs with liver disease, the DR expressed nuclear HNF1β. In AH the staining intensity within the DR was weak to moderate and in some cells strong, in LDH, CH and EHC the staining was moderate to strong.

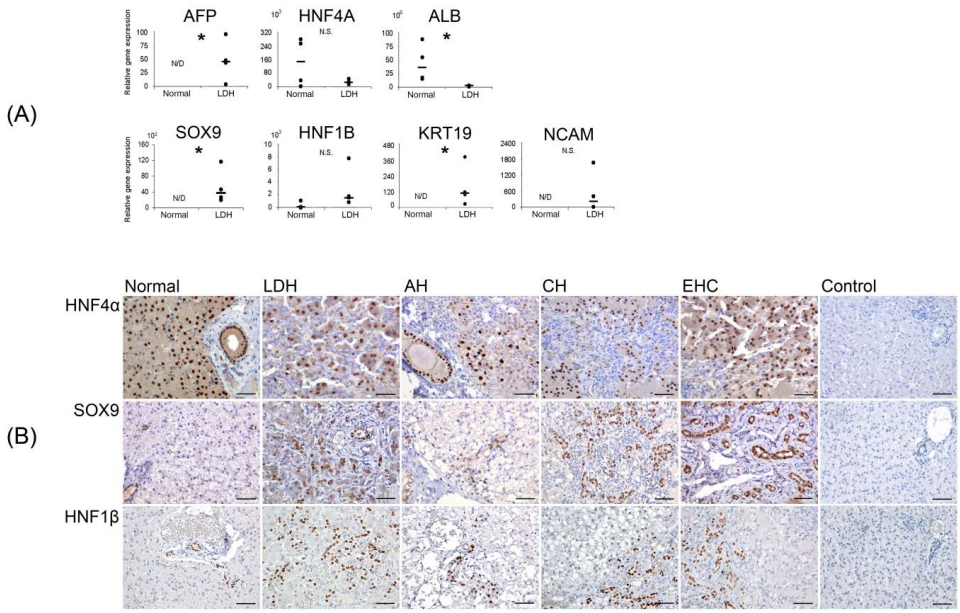

Fig. 3. Expression of maturation/differentiation markers in the canine hepatic progenitor cell (HPC) niche. (A) Relative gene expression of maturation/differentiation markers in the quiescent (normal liver) vs. the activated (LDH) HPC niche. (B) Immunohistochemistry of HNF4α, SOX9 and HNF1β in normal liver (H), lobular dissecting hepatitis (LDH), acute hepatitis (AH), chronic hepatitis (CH) and extrahepatic cholestasis (EHC). Control, omission of primary antibody (normal liver); AFP, α feto-protein; HNF, hepatocyte nuclear factor; ALB, albumin; SOX9, SRY-box 9; KRT, keratin; NCAM, neural cell adhesion molecule; N/D, not detectable; NS, not significant. * $P < 0.05$. Scale bar = 50 μm.

Components of the activated canine HPC niche

Immunofluorescent double staining was used to evaluate the anatomical relationship between the HPC and the cellular and extracellular matrix (ECM) components of the HPC niche. In addition to HPCs, we performed immunostaining for αSMA, a marker of activated hepatic stellate cells, and MAC387, a marker for invading macrophages that also stains resident macrophages and sometimes neutrophils (McGuinness et al., 2000; Schotanus et al., 2009). The ECM constituent of the HPC niche investigated was laminin, which is the ligand for CD29.

Double immunofluorescence in normal liver for panCK and αSMA stained bile ducts and individual HPCs (panCK) and vascular smooth muscle (αSMA), respectively. In samples from dogs with liver disease, αSMA immunoreactivity was mostly increased in LDH and chronic hepatitis, both characterised by excessive fibrosis. In AH, where fibrosis is absent, a small increase in αSMA immunoreactivity was found but only in close proximity to the DR. In EHC, an increased number of αSMA positive cells was present mainly in the portal areas surrounding the DR. In all dogs with liver disease, the DR was panCK positive and was consistently surrounded by αSMA positive cells (Fig. 4a).

Double immunofluorescence in normal liver for panCK and MAC387 showed small numbers of macrophages scattered throughout the parenchyma. In samples from dogs with diseased livers, the number of macrophages was increased predominantly at the site of disease activity, where also the DR was located; mainly in the periportal parenchyma in AH, within the portal areas in EHC and mainly in the fibrotic septa in CH (Fig. 4b). The percentage of parenchymal MAC387 positive cells was significantly increased in LDH and CH compared to normal liver (Fig. 4c) and significantly higher in CH compared to LDH.

Double immunofluorescence in normal liver for K19 and laminin showed protein expression of laminin within portal areas by vascular smooth muscle cells and around bile ducts. Additionally, a weak sinusoidal staining was seen which was moderate near the portal areas. In samples of liver from cases of LDH, laminin immunoreactivity was increased and laminin was extensively distributed throughout the tissue, particularly surrounding the DR. In AH and EHC, the expression of laminin was the highest in the periportal and portal areas, respectively, and most pronounced around the DR. In CH, the strongest laminin staining was apparent in the fibrotic septa where the activated HPCs are located (Fig. 4d).

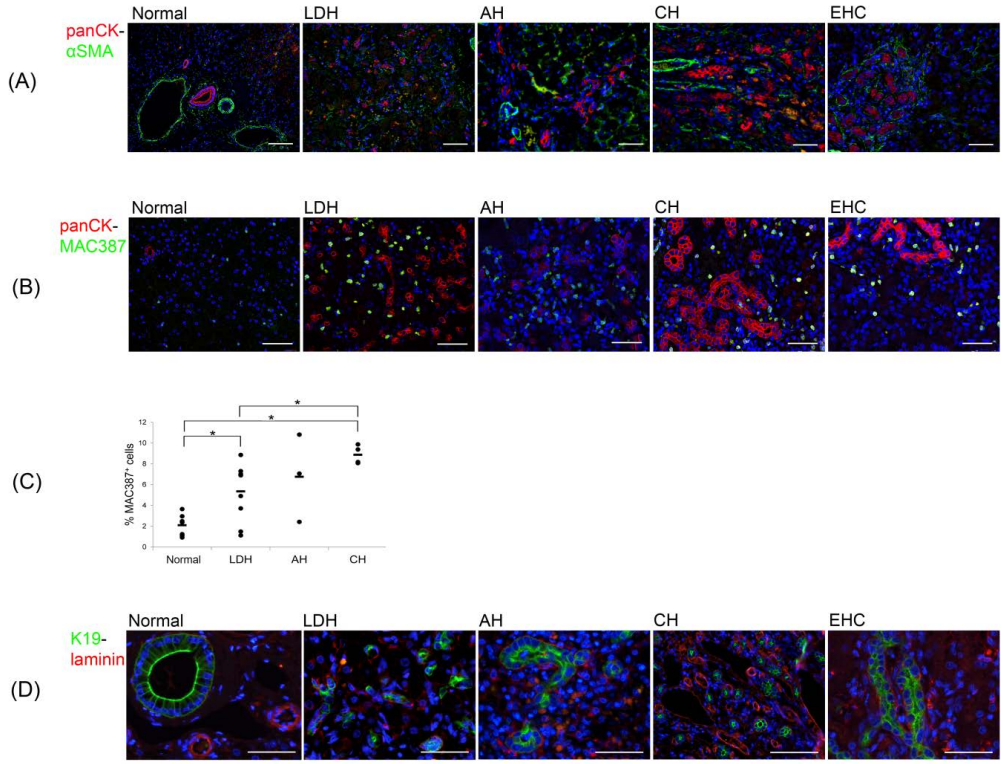

Fig. 4. Components of the canine hepatic progenitor cell (HPC) niche. (A) Double immunofluorescence of panCK (red) and α-smooth muscle actin (αSMA, green) with DAPI counterstaining (blue) in normal liver, lobular dissecting hepatitis (LDH), acute hepatitis (AH), chronic hepatitis (CH) and extrahepatic cholestasis (EHC). (B) Double immunofluorescent staining of panCK (red) and MAC387 (green) with To-Pro-3 counterstaining (blue) in normal liver, LDH, AH, CH and EHC. (C) Quantification of the number of MAC387 positive cells relative to the total number of cells in normal liver (n = 7), LDH (n = 9), AH (n = 3) and CH (n = 4). (D) Double immunofluorescence of K19 (green) and laminin (red) with DAPI counterstaining (blue) in normal liver, LDH, AH, CH and EHC. * $P < 0.02$. Scale bar = 50 µm.

Discussion

In the present study, the canine HPC and its niche were investigated in normal liver and in different types of spontaneous liver disease. LDH, in particular, showed a massive HPC response incomparable to other canine spontaneous liver diseases and experimental toxin-induced hepatopathies (Tirnitz-Parker et al., 2010; Weng et al., 2013). Therefore LDH was used for LMD to compare the activated HPC niche with the quiescent HPC niche in normal canine liver. Together with subsequent immunohistochemical and immunofluorescent staining in different types of liver disease the canine HPC niche was characterised at the molecular level. This showed that HPC marker expression, the presence of laminin around the ductular reaction and the co-localisation of HPCs with hepatic stellate cells and macrophages are conserved between species (Pintilie et al., 2010; Van Hul et al., 2011; Schotanus et al., 2009; Gadd et al., 2013).

The canine HPC niche expressed *OPN*, *FN14*, *CD133*, *LIF*, *LIFR* and *BMI1*, which are markers of progenitor cells associated with stemness and self-renewal capacity in the rodent and human liver

(Corcelle et al., 2006; Espanol-Suner et al., 2012; Furuyama et al., 2011; Herrera et al., 2006; Roskams, 2006; Yovchev et al., 2007; Yovchev et al., 2008; Zhang et al., 2008). In vitro studies on primary canine HPCs already suggested an immature and bipotential phenotype of these cells (Arends et al., 2009a). The capacity to asymmetrically self-renew and differentiate into mature cell types is a hallmark of (adult) stem cells. In continuously renewing organs like gut and skin, the adult stem cells sustain a stable pool while generating progeny that differentiates to mature functional cells (Fuchs and Chen, 2013). Whether the HPCs contribute to homeostasis is still under debate (Furuyama et al., 2011; Espanol-Suner et al., 2012).

HPC differentiation is determined by the surrounding microenvironment, providing cues to specify either hepatocyte or biliary differentiation (Boulter et al., 2012). In LDH, *HNF4α*, a transcription factor involved in differentiation towards the hepatocytic lineage was expressed and expression of *AFP*, a fetal liver marker, was increased in the activated HPC niche. These markers indicate an immature phenotype and are also expressed by rat and human HPCs (Yovchev et al., 2007; Zhang et al., 2008). However, expression of albumin, a marker for mature hepatocytes, was not detected by immunohistochemistry in canine HPCs, consistent with findings by Ijzer et al. (2010), where the ductular reaction was deemed negative for HepPar-1 staining, another adult hepatocyte marker. We therefore conclude that activated HPCs in LDH do not show mature hepatocyte characteristics. In contrast, the HPCs in LDH show strong expression of HPC/biliary markers *SOX9*, *HNF1β* and *KRT19*. This suggests the HPCs have an undifferentiated or biliary phenotype. Restoration of liver function upon parenchymal damage requires not only proliferation of HPCs and migration to the site of disease activity, but also differentiation into mature, functional hepatocytes. This differentiation seems to lack in LDH, in an otherwise highly expanded HPC population. This might account for the poor clinical outcome of LDH in dogs. In a fibrotic, non-remodelling environment the differentiation of mouse HPCs was hampered (Lorenzini et al., 2010) but the mechanism remains unknown. In AH, where no fibrosis is present, some HPCs showed intermediate expression of the biliary markers SOX9 and HNF1β. HPCs differentiating to mature hepatocytes loose the expression of biliary markers (Furuyama et al., 2011; Espanol-Suner et al., 2012). Therefore the decreased expression of these proteins by HPCs during AH could potentially indicate a less pronounced biliary phenotype.

CD29 (integrin β1), the receptor for fibronectin and laminin, and CD44, the hyaluronic acid receptor and co-receptor for HGF, are important for the interaction of cells with the ECM (Hynes, 2002). The presence of CD29 and CD44 on HPCs during disease suggests potential interaction between canine HPCs and their surrounding ECM. Laminin, which is a ligand for CD29, very closely surrounded the DR in all samples from dogs with liver disease, further supporting this close interaction. Laminin deposition and ECM remodelling (collagen degradation) were shown to be prerequisite for HPC proliferation and migration in mice treated with carbon tetrachloride, but the presence of laminin inhibited hepatocyte differentiation (Kallis et al., 2011). In samples from dogs with liver disease, activated HPCs were localised to the main site of injury, as was reported by Schotanus et al. (2009) indicating that HPCs migrate to the site of injury where regeneration is needed the most. The close anatomical relationship of CD29 and laminin was seen in all different diseases studied, but to a lower extent in EHC where some ductules were CD29 negative. This could be explained by the fact that in biliary disease HPCs do not need to migrate, as newly formed bile ducts are required in close vicinity to the native HPC niche.

Migration requires interaction of the HPC with ECM components and matrix remodelling. The main cell types involved in HPC activation are hepatic stellate cells and macrophages (Gadd et al., 2013; Roskams, 2008), which are also responsible for the deposition of ECM components and remodelling

of ECM. In addition, these cells secrete growth factors (e.g. hepatocyte growth factor, fibroblast growth factor) and cytokines (e.g. TNF-like weak inducer of apoptosis, transforming growth factor β) and are involved in the proliferation, migration and differentiation of HPCs during disease (Boulter et al., 2012; Ishikawa et al., 2012; Lorenzini et al., 2010; Nagai et al., 2002; Schotanus et al., 2009; Tirnitz-Parker et al., 2010; Van Hul et al., 2011). Double immunofluorescence for panCK-αSMA and for panCK-MAC387 in samples from dogs with liver disease demonstrated a close proximity between HPCs, and activated hepatic stellate cells and macrophages. Their co-localisation was extensively described in other species (Lorenzini et al., 2010; Schotanus et al., 2009; Gadd et al., 2013). The finding of their close co-localisation during canine liver disease suggests that the composition of the HPC niche is conserved between species. In AH, αSMA positive cells surrounded the DR but expression of αSMA throughout the tissue was only minimally increased. αSMA specifically marks the hepatic stellate cells transformed into myofibroblasts (Schotanus et al., 2009). The absence of a strong αSMA increase during AH shows that in the investigated stage of the disease, no extensive HSC transformation into myofibroblasts and subsequent fibrosis has occurred (Schotanus et al., 2009). As such, the minimal presence of activated HSCs during AH may be important to allow hepatocytic differentiation of HPCs. This would explain their less pronounced biliary phenotype in AH. Macrophage derived signals have also been reported to be important in differentiation of HPCs (Boulter et al., 2012). In CH the number of macrophages was significantly higher compared to LDH. This is another potential association with the observed undifferentiated phenotype of HPCs in LDH. Although, inter-species differences do exist and markers used for mouse, rat and human beings do not always overlap (Jelnes et al., 2007), this study shows that the canine HPC and its niche are highly comparable to their human and rodent counterparts in their molecular characteristics. In addition, the general molecular and histopathological response pattern in different types of liver disease is highly similar in dog and man (Spee et al., 2006, 2007). This comparative nature between canine and human liver disease and regeneration suggests that dogs could be an important translational animal model to study new therapeutic strategies for both species.

Conclusions

This study characterised the hepatic progenitor cell niche in the normal canine liver and in samples from dogs with liver disease, and defined important cells in canine HPC activation. The canine HPC niche is comparable to that of rodents and humans with respect to marker expression, niche composition and pattern of reaction to disease. Knowledge that is gained from HPCs in liver regeneration in man can contribute to canine liver research and vice versa, and particularly to novel HPC-based therapies.

Conflict of interest statement

None of the authors of this paper has a financial or personal relationship with other people or organisations that could inappropriately influence or bias the content of the paper. The authors declare that sponsors (ZonMW Agiko Baukje Schotanus en ZonMW TASO Hedwig Kruitwagen provided by the Netherlands Organisation for Scientific Research) did not have any influence in the study design, in the collection, analysis and interpretation of data, in the writing of the manuscript and in the decision to submit the manuscript for publication.

Acknowledgements

The authors wish to thank Joop Fama for technical assistance with the figures and Monique van Wolferen for her technical assistance with immunohistochemistry. Preliminary results have been presented at the International symposium of the Belgian Society for Cell and Developmental Biology, Brussels, Belgium (March 2008), Spring meeting Dutch Hepatology Association, Veldhoven, the Netherlands (March 2008), ECVIM conference, Toulouse, France (September 2009) ,World Conference on Regenerative Medicine, Leipzig, Germany (November 2011).

References

Arends, B., Spee, B., Schotanus, B.A., Roskams, T., van den Ingh, T.S., Penning, L.C., Rothuizen, J., 2009a. In vitro differentiation of liver progenitor cells derived from healthy dog livers. Stem Cells and Development 18, 351-358.

Arends, B., Vankelecom, H., Vander Borght, S., Roskams, T., Penning, L.C., Rothuizen, J., Spee, B., 2009b. The dog liver contains a "side population" of cells with hepatic progenitor-like characteristics. Stem Cells and Development 18, 343-350.

Boulter, L., Govaere, O., Bird, T.G., Radulescu, S., Ramachandran, P., Pellicoro, A., Ridgway, R.A., Seo, S.S., Spee, B., Van Rooijen, N., et al., 2012. Macrophage-derived Wnt opposes Notch signaling to specify hepatic progenitor cell fate in chronic liver disease. Nature Medicine 18, 572-579.

Corcelle, V., Stieger, B., Gjinovci, A., Wollheim, C.B., Gauthier, B.R., 2006. Characterization of two distinct liver progenitor cell subpopulations of hematopoietic and hepatic origins. Experimental Cell Research 312, 2826-2836.

Duncan, A.W., Dorrell, C., Grompe, M., 2009. Stem cells and liver regeneration. Gastroenterology 137, 466-481.

Espanol-Suner, R., Carpentier, R., Van Hul, N., Legry, V., Achouri, Y., Cordi, S., Jacquemin, P., Lemaigre, F., Leclercq, I.A., 2012. Liver progenitor cells yield functional hepatocytes in response to chronic liver injury in mice. Gastroenterology 143, 1564-1575.

Evarts, R.P., Nagy, P., Marsden, E., Thorgeirsson, S.S., 1987. A precursor-product relationship exists between oval cells and hepatocytes in rat liver. Carcinogenesis 8, 1737-1740.

Fausto, N., 2004. Liver regeneration and repair: Hepatocytes, progenitor cells, and stem cells. Hepatology 39, 1477-1487.

Fausto, N., Campbell, J.S., Riehle, K.J., 2006. Liver regeneration. Hepatology 43, S45-S53.

Forbes, S.J., Newsome, P.N., 2012. New horizons for stem cell therapy in liver disease. Journal of Hepatology 56, 496-499.

Fuchs, E., Tumbar, T., Guasch, G., 2004. Socializing with the neighbors: Stem cells and their niche. Cell 116, 769-778.

Fuchs, E., Chen, T., 2013. A matter of life and death: Self-renewal in stem cells. EMBO Reports 14, 39-48.

Furuyama, K., Kawaguchi, Y., Akiyama, H., Horiguchi, M., Kodama, S., Kuhara, T., Hosokawa, S., Elbahrawy, A., Soeda, T., Koizumi, M., et al., 2011. Continuous cell supply from a Sox9-expressing

progenitor zone in adult liver, exocrine pancreas and intestine. Nature Genetics 43, 34-41.

Gadd, V.L., Melino, M., Roy, S., Horsfall, L., O'Rourke, P., Williams, M.R., Irvine, K.M., Sweet, M.J., Jonsson, J.R., Clouston, A.D., et al., 2013. Portal, but not lobular, macrophages express matrix metalloproteinase-9: association with the ductular reaction and fibrosis in chronic hepatitis C. Liver International 33, 569-579.

Herrera, M.B., Bruno, S., Buttiglieri, S., Tetta, C., Gatti, S., Deregibus, M.C., Bussolati, B., Camussi, G., 2006. Isolation and characterization of a stem cell population from adult human liver. Stem cells 24, 2840-50.

Hynes, R.O., 2002. Integrins: Bidirectional, allosteric signaling machines. Cell 110, 673-687.

Ijzer, J., Schotanus, B.A., Vander Borght, S., Roskams, T.A., Kisjes, R., Penning, L.C., Rothuizen, J., van den Ingh, T.S., 2010. Characterisation of the hepatic progenitor cell compartment in normal liver and in hepatitis: An immunohistochemical comparison between dog and man. The Veterinary journal 184, 308-314.

Ishikawa, T., Factor, V.M., Marquardt, J.U., Raggi, C., Seo, D., Kitade, M., Conner, E.A., Thorgeirsson, S.S., 2012. Hepatocyte growth factor/c-Met signaling is required for stem-cell-mediated liver regeneration in mice. Hepatology 55, 1215-1226.

Jelnes, P., Santoni-Rugiu, E., Rasmussen, M., Friis, S.L., Nielsen, J.H., Tygstrup, N., Bisgaard, H.C., 2007. Remarkable heterogeneity displayed by oval cells in rat and mouse models of stem cell-mediated liver regeneration. Hepatology 45, 1462-1470.

Kallis, Y.N., Robson, A.J., Fallowfield, J.A., Thomas, H.C., Alison, M.R., Wright, N.A., Goldin, R.D., Iredale, J.P., Forbes, S.J., 2011. Remodelling of extracellular matrix is a requirement for the hepatic progenitor cell response. Gut 60, 525-533.

Katoonizadeh, A., Nevens, F., Verslype, C., Pirenne, J., Roskams, T., 2006. Liver regeneration in acute severe liver impairment: A clinicopathological correlation study. Liver International 26, 1225-1233.

Libbrecht, L., Roskams, T., 2002. Hepatic progenitor cells in human liver diseases. Seminars in Cell Development and Biology 13, 389-396.

Lorenzini, S., Bird, T.G., Boulter, L., Bellamy, C., Samuel, K., Aucott, R., Clayton, E., Andreone, P., Bernardi, M., Golding, M., et al., 2010. Characterisation of a stereotypical cellular and extracellular adult liver progenitor cell niche in rodents and diseased human liver. Gut 59, 645-654.

Lunz, J.G., 3rd, Tsuji, H., Nozaki, I., Murase, N., Demetris, A.J., 2005. An inhibitor of cyclin-dependent kinase, stress-induced p21Waf-1/Cip-1, mediates hepatocyte mito-inhibition during the evolution of cirrhosis. Hepatology 41, 1262-1271.

McGuinness, P.H., Painter, D., Davies, S., McCaughan, G.W., 2000. Increases in intrahepatic CD68 positive cells, MAC387 positive cells, and proinflammatory cytokines (particularly interleukin 18) in chronic hepatitis C infection. Gut 46, 260-269.

Mekonnen, G.A., Ijzer, J., Nederbragt, H., 2007. Tenascin-C in chronic canine hepatitis: immunohistochemical localization and correlation with necro-inflammatory activity, fibrotic stage, and expression of alpha-smooth muscle actin, cytokeratin 7, and $CD3^+$ cells. Veterinary Pathology 44, 803-813.

Nagai, H., Terada, K., Watanabe, G., Ueno, Y., Aiba, N., Shibuya, T., Kawagoe, M., Kameda, T., Sato, M., Senoo, H., et al., 2002. Differentiation of liver epithelial (stem-like) cells into hepatocytes

induced by coculture with hepatic stellate cells. Biochemical and Biophysical Research Communications 293, 1420-1425.

Ohlstein, B., Kai, T., Decotto, E., Spradling, A., 2004. The stem cell niche: Theme and variations. Current Opinion in Cell Biology 16, 693-699.

Pintilie, D.G., Shupe, T.D., Oh, S., Salganik, S.V., Darwiche, H., Petersen, B.E., 2010. Hepatic stellate cells' involvement in progenitor-mediated liver regeneration. Laboratory Investigation 90, 1199-1208.

Roskams, T., 2006. Different types of liver progenitor cells and their niches. Journal of Hepatology 45, 1-4.

Roskams, T., 2008. Relationships among stellate cell activation, progenitor cells, and hepatic regeneration. Clinics in Liver Disease 12, 853-860.

Roskams, T.A., Theise, N.D., Balabaud, C., Bhagat, G., Bhathal, P.S., Bioulac-Sage, P., Brunt, E.M., Crawford, J.M., Crosby, H.A., Desmet, V., et al., 2004. Nomenclature of the finer branches of the biliary tree: Canals, ductules, and ductular reactions in human livers. Hepatology 39, 1739-1745.

Rothuizen, J., Bunch, S.E., Charles, J.A., Cullen, J.M., Desmet, V.J., Szatmari, V., Twedt, D.C., Van Den Ingh, T.S.G.A.M., Van Winkle, T., Washabau, R.J. (Eds), 2006. WSAVA Standards for Clinical and Histological Diagnosis of Canine and Feline Liver Disease. Saunders-Elsevier, Edinburgh, UK.

Sancho-Bru, P., Najimi, M., Caruso, M., Pauwelyn, K., Cantz, T., Forbes, S., Roskams, T., Ott, M., Gehling, U., Sokal, E., et al., 2009. Stem and progenitor cells for liver repopulation: Can we standardise the process from bench to bedside? Gut 58, 594-603.

Schotanus, B.A., van den Ingh, T.S., Penning, L.C., Rothuizen, J., Roskams, T.A., Spee, B., 2009. Cross-species immunohistochemical investigation of the activation of the liver progenitor cell niche in different types of liver disease. Liver International 29, 1241-1252.

Spee, B., Arends, B., van den Ingh, T.S., Brinkhof, B., Nederbragt, H., Ijzer, J., Roskams, T., Penning, L.C., Rothuizen, J., 2006. Transforming growth factor beta-1 signalling in canine hepatic diseases: New models for human fibrotic liver pathologies. Liver International 26, 716-25.

Spee, B., Arends, B., van den Ingh, T.S., Roskams, T., Rothuizen, J., Penning, L.C., 2007. Major HGF-mediated regenerative pathways are similarly affected in human and canine cirrhosis. Comparative Hepatology 6, 8.

Spee, B., Carpino, G., Schotanus, B.A., Katoonizadeh, A., Vander Borght, S., Gaudio, E., Roskams, T., 2010. Characterisation of the liver progenitor cell niche in liver diseases: Potential involvement of Wnt and Notch signalling. Gut 59, 247-257.

Tirnitz-Parker, J.E., Viebahn, C.S., Jakubowski, A., Klopcic, B.R., Olynyk, J.K., Yeoh, G.C., Knight, B., 2010. Tumor necrosis factor-like weak inducer of apoptosis is a mitogen for liver progenitor cells. Hepatology 52, 291-302.

van den Ingh, T.S.G.A.M., Rothuizen, J., 1994. Lobular dissecting hepatitis in juvenile and young adult dogs. Journal of Veterinary Internal Medicine 8, 217-220.

Van Hul, N., Lanthier, N., Espaol Suer, R., Abarca Quinones, J., Van Rooijen, N., Leclercq, I., 2011. Kupffer cells influence parenchymal invasion and phenotypic orientation, but not the proliferation, of liver progenitor cells in a murine model of liver injury. American Journal of Pathology 179, 1839-1850.

van Steenbeek, F.G., Van den Bossche, L., Grinwis, G.C., Kummeling, A., van Gils, I.H., Koerkamp, M.J., van Leenen, D., Holstege, F.C., Penning, L.C., Rothuizen, J., et al., 2013. Aberrant gene expression in dogs with portosystemic shunts. PloS One 8, e57662.

Viebahn, C.S., Benseler, V., Holz, L.E., Elsegood, C.L., Vo, M., Bertolino, P., Ganss, R., Yeoh, G.C., 2010. Invading macrophages play a major role in the liver progenitor cell response to chronic liver injury. Journal of Hepatology 53, 500-507.

Weng, H., Feng, D., Radaeva, S., Kong, X., Wang, L., Liu, Y., Li, Q., Shen, H., Gao, Y., Müllenbach, R., et al., 2013. IFN-c inhibits liver progenitor cell proliferation in HBV-infected patients and in 3,5-diethoxycarbonyl-1,4-dihydrocollidine diet-fed mice. Journal of Hepatology 59, 738-745.

Yoshioka, K., Enaga, S., Taniguchi, K., Fukushima, U., Uechi, M., Mutoh, K., 2004. Morphological characterization of ductular reactions in canine liver disease. Journal of Comparative Pathology 130, 92-98.

Yovchev, M.I., Grozdanov, P.N., Joseph, B., Gupta, S., Dabeva, M.D., 2007. Novel hepatic progenitor cell surface markers in the adult rat liver. Hepatology 45, 139-149.

Yovchev, M.I., Grozdanov, P.N., Zhou, H., Racherla, H., Guha, C., Dabeva, M.D., 2008. Identification of adult hepatic progenitor cells capable of repopulating injured rat liver. Hepatology 47, 636-647.

Zhang, L., Theise, N., Chua, M., Reid, L.M., 2008. The stem cell niche of human livers: Symmetry between development and regeneration. Hepatology 48, 1598-1607.

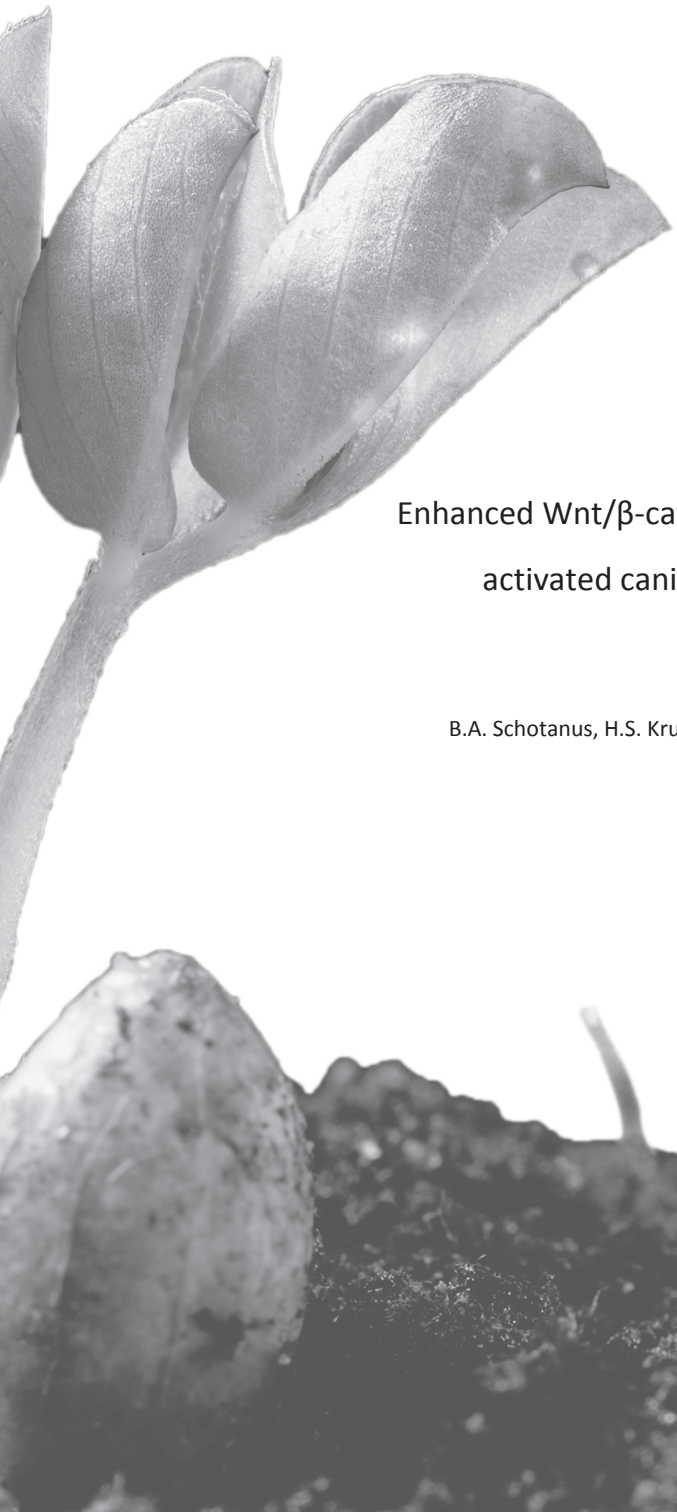

Chapter 3

Enhanced Wnt/β-catenin and Notch signalling in the activated canine hepatic progenitor cell niche.

B.A. Schotanus, H.S. Kruitwagen, T.S. van den Ingh, M.E. van Wolferen, J. Rothuizen, L.C. Penning, B. Spee

BMC Vet Res. 2014;10:309

Abstract

The liver has a large regenerative capacity. Hepatocytes can replicate and regenerate a diseased liver. However, as is the case in severe liver diseases, this replication may become insufficient or exhausted and hepatic progenitor cells (HPCs) can be activated in an attempt to restore liver function. Due to their bi-potent differentiation capacity, these HPCs have great potential for regenerative approaches yet over-activation does pose potential health risks. Therefore the mechanisms leading to activation must be elucidated prior to safe implementation into the veterinary clinic. Wnt/β-catenin and Notch signalling have been implicated in the activation of HPCs in mouse models and in humans. Here we assessed the involvement in canine HPC activation. Gene-expression profiles were derived from laser microdissected HPCs niches from lobular dissecting hepatitis (LDH) and normal liver tissue, with a focus on Wnt/β-catenin and Notch signalling. Immunohistochemical and immunofluorescent studies were combined to assess the role of the pathways in HPCs during LDH.

Gene-expression confirmed higher expression of Wnt/β-catenin and Notch pathway components and target genes in activated HPC niches in diseased liver compared to quiescent HPC niches from normal liver. Immunofluorescence confirmed the activation of these pathways in the HPCs during disease. Immunohistochemistry showed proliferating HPCs during LDH, and double immunofluorescence showed downregulation of Wnt/β-catenin and Notch in differentiating HPCs. Vimentin, a mesenchymal marker, was expressed on a subset of undifferentiated HPCs.

Together these studies clearly revealed that both Wnt/β-catenin and Notch signalling pathways are enhanced in undifferentiated, proliferating and potentially migrating HPCs during severe progressive canine liver disease (LDH).

Background

Liver diseases occur frequently in the canine pet population. Around 12% of the dogs in first opinion practices have liver disease [1,2] and they account for 1-2% of a university veterinary clinical population [3]. It is conceivable that these numbers, based on the Cambridge region (UK) and the Utrecht University Clinics (the Netherlands) respectively are exemplary for the West-European dog pet population. One third of chronic hepatitis cases are caused by copper accumulation, in addition, microorganisms, toxins and drugs have been reported to cause hepatitis in dogs. In more than 60% of cases, however, hepatitis remains idiopathic [3,4]. The recently discovered canine hepacivirus is unlikely to cause canine hepatitis [5-7].

Irrespective of the cause of hepatocyte damage, the liver can recover from such insults due to replication of fully differentiated hepatocytes [8]. In case this replication is exhausted or otherwise hampered, hepatic progenitor cells (HPCs) are reported to have the potential to take over regeneration. These stem cells are believed to be bi-potential and to have the capacity to differentiate into either hepatocytes or cholangiocytes, depending on cellular demand [9]. HPCs are located in the terminal branches of the biliary tree, called the Canal of Hering [10]. Several papers describe the cellular and molecular constituents of the canine or feline HPC niche [11-15]. The niche is not just an anatomical region in the liver but it has a biological function as it provides the cell- and matrix derived signals to instruct the HPC's cellular fate.

In order to safely use HPCs for liver regeneration in a clinical setting where hepatocyte replication is insufficient, detailed knowledge of crucial signalling cascades for HPC activation is essential. Two signalling pathways, Wnt/β-catenin and Notch, are involved in proliferation and differentiation of progenitor cells including HPCs in other mammals [16-20]. This prompted us to focus on these two transmembrane signalling pathways in the activation of HPCs in canine liver diseases. Since lobular dissecting hepatitis (LDH) was previously observed to contain the highest number of activated HPCs, we microdissected the activated HPC niche from LDH and performed molecular analyses in comparison with quiescent HPC niches harboured adjacent to portal areas of normal canine liver [13].

Our data show that both Wnt/β-catenin and Notch signalling are enhanced in activated HPC niches in dogs with LDH. The previous descriptions of the cellular constituents of the canine HPC niche and the current investigation on specific signalling cascades clearly show the similarities with other mammals, including human [12,13]. It is therefore conceivable that results of clinical approaches in human medicine will be applicable and beneficial in veterinary health care.

Results

Gene-expression profiling of laser microdissected HPC niches indicate activation of Wnt and Notch pathways

Representative pictures of laser microdissected HPC niches in normal liver and lobular dissecting hepatitis (LDH) stained with Keratin(K)7 (marker of HPCs) are depicted in Figure 1A. Expression levels of the Wnt receptor *FZD1* and the Wnt-induced transcription factor *TCF3* were significantly higher in LDH cases compared to normal controls, as measured in LMD samples (Figure 1B). Of the various Notch-receptor proteins, only *NOTCH1* and *NOTCH3* expression levels were significantly higher in diseased material (Figure 1C). In line is the observation that only ligand *JAG1* is upregulated whereas *JAG2* is not (Figure 1C). Based on these expression levels of ligand and receptors it was anticipated that an activated Wnt/β-catenin and Notch signalling cascade were present in activated HPC niches

(Figure 1B,C). Importantly the expression levels of classical target genes for Wnt/β-catenin, *AXIN2,* and Notch signalling, *HEY1*, were indeed elevated in LDH, confirming active downstream signalling (Figure 1B,C).

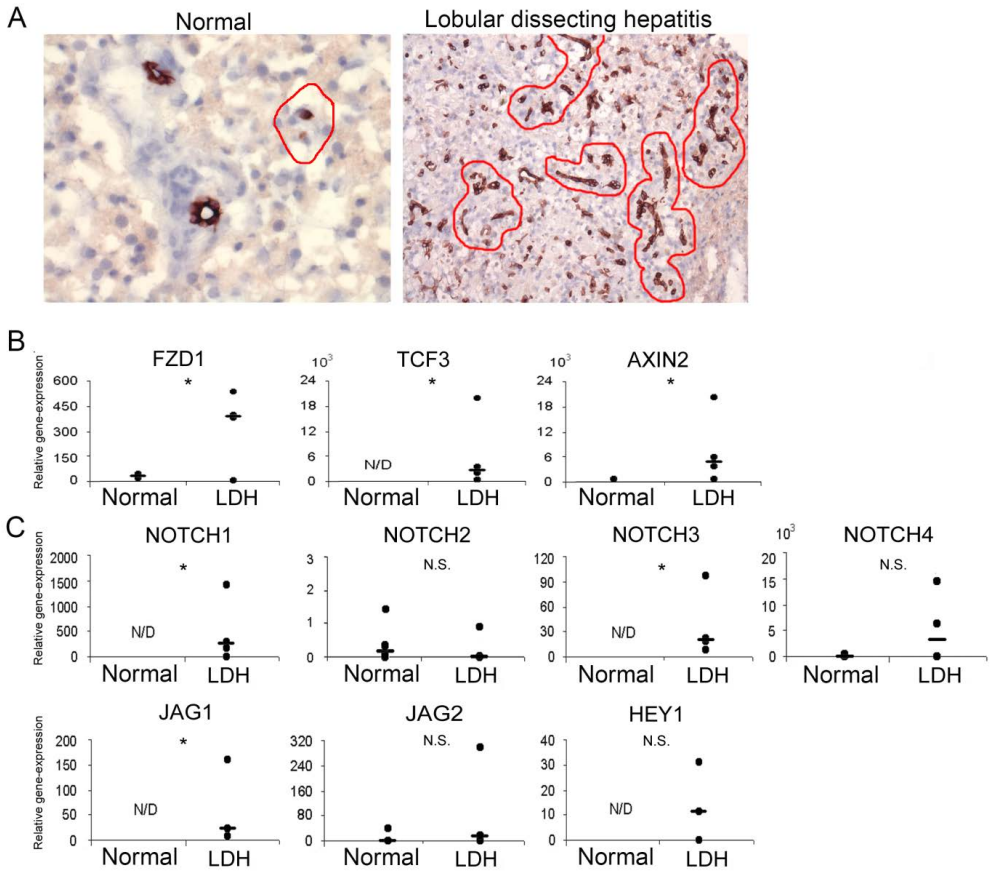

Figure 1. Gene expression of Wnt and Notch signalling components is enhanced in HPC niches during disease. Examples of cryosections (6 µm) of normal liver and lobular dissecting hepatitis immunostained for Keratin 7 (A), a marker of HPCs and cholangiocytes. The red lines indicate the quiescent HPC niche in the periportal area of normal tissue, and the activated HPC niche throughout the parenchyma of diseased tissue (A). These areas were specifically selected by means of laser microdissection for RNA isolation and gene expression analysis. Relative gene-expression for components of Wnt (B), and Notch (C) signalling pathways show upregulation of these pathways in HPC niches during disease. FZD1, Frizzled 1; TCF3, transcription factor 3; AXIN2, axis inhibitor 2; JAG, jagged; HEY1, hairy/enhancer of split-related with YRPW motif; N.S., not significant; N/D, not detectable.

Immunofluorescence confirm activated Wnt/β-catenin and Notch signalling in HPC during disease

To specify the cellular origin of the upregulated gene expression levels, we performed double immunofluorescence for β-catenin/K7 (Figure 2A) and Notch1/Notch Intra Cellular Domain (NICD)/K7 (Figure 2B). This revealed that β-catenin and Notch1/NICD were strongly expressed in the cytoplasm and/or nucleus of the cells of the ductular reaction in LDH. Expression of β-catenin in

hepatocytes and cholangiocytes was membranous, indicative for a low activation status of the Wnt/β-catenin signalling cascade. Similarly Notch1/NICD was expressed canalicular and less pronounced in basolateral membranes in hepatocytes in normal tissues.

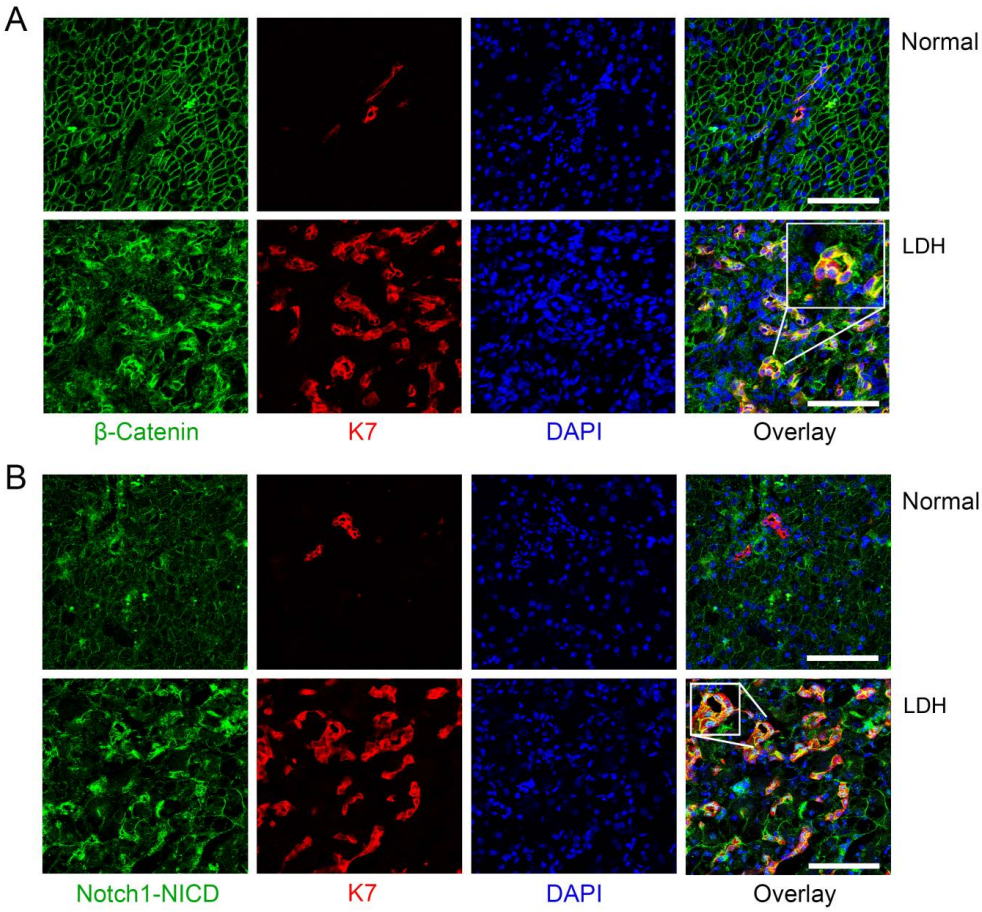

Figure 2. Wnt and Notch signalling are active in HPCs during disease. Example of immunofluorescent double staining on cryosections (15 µm) against β-catenin (green) and Keratin(K)7 (red), with ToPro3 (blue) nuclear counterstaining in normal and lobular dissecting hepatitis (LDH) liver tissue (A, size bar indicates 100 µm). In normal tissue β-catenin is present in a membranous staining pattern on hepatocytes and bile duct cells. No nuclear β-catenin is seen. In LDH β-catenin is clearly increased, and overlay shows cytoplasmic and nuclear presence of β-catenin in K7 positive cells (yellow and bright blue). Example of immunofluorescent double staining on cryosections (15 µm) against Notch/Notch Intra Cellular Domain (Notch/NICD; green) and K7 (red), with ToPro3 (blue) nuclear counterstaining in normal and diseased (LDH) liver tissue (B, size bar indicates 100 µm). In normal tissue, a canalicular staining pattern on hepatocytes and bile duct cells is found, no nuclear staining is present.

Wnt/β-catenin and Notch signalling coincide with HPC proliferation and mesenchymal characteristics, but are lost with differentiation

To investigate the functional involvement of Wnt and Notch in HPC activation immunohistochemical and immunofluorescent stainings were performed (Figure 3). With Ki67 staining we assessed the

proliferative activity in the tissues. In LDH, very few hepatocytes were found positive for Ki67, while a substantial amount of Ki67 positive cells were found in the DR (Figure 3A). To evaluate the potential of HPCs to obtain mesenchymal characteristics, immunohistochemical staining for vimentin and double immunofluorescent staining for vimentin and PanCK was performed (Figure 3B,C). This revealed strong (co-)staining of vimentin in ductular structures. Clearly showing expression of a mesenchymal marker on HPCs. To investigate the role of Wnt and Notch in HPC differentiation during liver disease, we used the mature hepatocyte marker HepPar1 in combination with β-catenin or Notch1/NICD in a double immunofluorescent staining. A clear polarisation of the ductular reaction was observed in such a way that the non-differentiated cells stained strong cytoplasmic and sometimes nuclear for both β-catenin and Notch1/NICD. This staining was lost in the intermediate and HepPar1 positive differentiated hepatocytes in continuation of the ductular reaction (Figure 3D,E). This is in line with the cytoplasmic and nuclear staining of β-catenin and Notch1/NICD in the K7-positive undifferentiated HPCs in Figure 2. In all staining procedures, negative controls remained negative, indicating the specificity of the antibodies used.

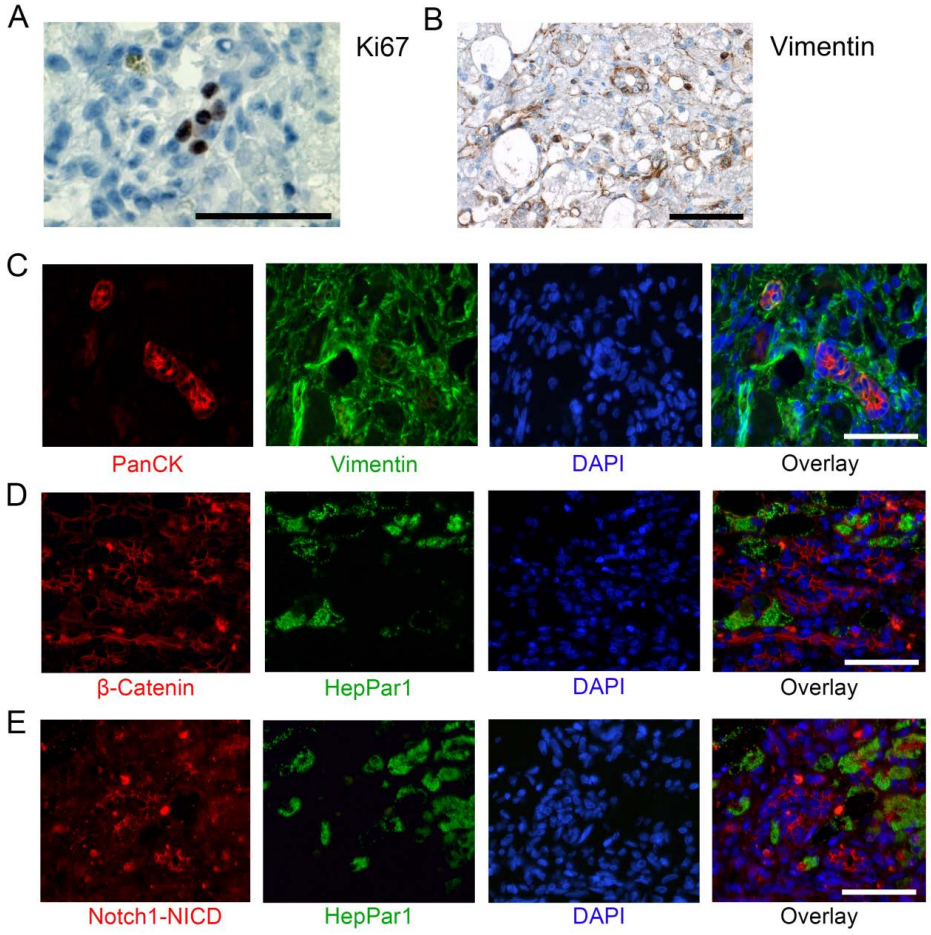

Figure 3. Proliferation and mesenchymal characteristics on HPCs and relation of differentiation with β-catenin and Notch1/NICD signalling. Immunohistochemical staining for Ki67 shows positive cells in the ductular reaction during lobular

dissecting hepatitis (LDH; A). Immunohistochemical staining for vimentin suggests positive ductular reactions (B) and an example of vimentin and PanCK double staining (C) shows clear co-localisation on HPCs in LDH. Double immunofluorescence against HepPar1 and β-catenin (D) or Notch1/Notch intracellular domain (Notch1/NICD; E) in LDH shows polarisation of the ductular reaction: clear cytoplasmic staining of β-catenin or Notch/NICD is present in non-differentiated cells of the ductular reaction and only membranous staining is present in differentiating and fully differentiated, HepPar1 positive, hepatocytes. Size bars indicate 50 µm.

Discussion

In the present study we investigated the involvement of the Wnt/β-catenin and Notch pathways in canine hepatic progenitor cell activation in LDH, a highly fibrotic and progressive liver disease. The combination of laser-microdissection, gene expression studies (Q-PCR) and immunofluorescence showed the enhanced signalling of the Wnt/β-catenin and Notch pathways in activated HPC niches compared to quiescent HPCs in normal liver. This extends the findings in mouse and human liver cancer and normal liver regeneration [19,21-27]. The fact that this apparent activation was insufficient to restore the liver, dogs presenting with LDH die within a year after diagnosis [4], suggests that therapeutic opportunities are present here. The reason why HPCs fail to regenerate the liver seems to vary with the type of disease and may be due to insufficient proliferation, migration or differentiation [28]. New therapeutic strategies could address the pathways involved in these phases of activation.

The effect of Wnt/β-catenin was previously specified as (induction of) proliferation in rodent models of HPC activation [16,24,29,30]. Similarly, for Notch a regulatory role in HPC proliferation is described [31,32]. In LDH, the concurrent presence of active Wnt and Notch signalling and actively proliferating, Ki67 positive, cells in the ductular reaction suggest a potential role for these pathways in proliferation of canine HPCs during disease as well. Another functional implication of Wnt and Notch signalling may relate to the acquisition of mesenchymal characteristics by HPCs. The presence of mesenchymal characteristics can relate to migratory potential, which is not equivalent to full epithelial-mesenchymal transition (EMT), a disputed phenomenon in adult liver [33-35]. From a regenerative point of view, migration is necessary for HPCs to move toward the site of disease activity, and is likely to occur in concert with proliferation [36,37]. Wnt and Notch pathways have been implicated in EMT and migratory potential of cells in different types of tissues and cancer development [38,39]. In canine LDH, we show the expression of vimentin on K19-positive HPCs that are also high in Wnt and Notch signalling, potentially indicating a causative relation in canine HPCs. It will be of interest to further functionally investigate this newly suggested role of Wnt or Notch in migration of HPCs during disease, as it may provide interesting potential for therapeutic intervention.

Besides the described role in proliferation and migration, both pathways can be involved in HPC differentiation. The influence of Wnt on cell fate determination is time and place dependent. During early embryonic development, and in pluripotent embryonic stem cells *in vitro*, Wnt activation leads to hepatic specification [40,41]. Later in foetal liver development, and *in vitro* in more committed multipotent cells, active Wnt inhibits (further) hepatocyte differentiation, but rather guides cells to the biliary phenotype [42,43]. Regarding the HPC as a committed progenitor cell, Wnt activation in LDH might stimulate bile duct differentiation, and inhibit hepatocyte differentiation. An interesting finding in this study is that small hepatocytes lying in continuation with ductular cells, and possibly representing intermediate hepatocytes [44], display a membranous β-catenin staining pattern (Figure 3), similar to that of hepatocytes in normal tissue. This supports the theory that the Wnt/β-

catenin pathway is not (longer) active during hepatocytic differentiation of ductular cells and is different from previous mouse data [21]. Unfortunately the lack of specific markers for intermediate hepatocytes limits their description to size and localization only [11,45]. The importance of Notch in liver development and hepatocyte differentiation is apparent in the mutation in the Notch ligand Jag1, which is associated with Alagille syndrome, presenting with aberrant bile duct development [25,46-51]. More recently, a distinctive role for the different Notch receptors has been explored, suggesting that Jag1-mediated Notch1 and Notch3 activation stimulates differentiation of hepatoblasts towards the biliary phenotype, and inhibits hepatocytic differentiation. Otherwise, the loss of Notch1 and Notch3 expression occurred when (liver progenitor) cells differentiated towards hepatocytes [52,53]. Converting these findings to our results, we might postulate that during LDH, where *NOTCH1* and *NOTCH3* expression is increased, HPC differentiation towards hepatocytes is inhibited, while bile duct differentiation may be enhanced. This is corroborated by the immunofluorescence stainings, where Notch1/NICD is lost with differentiation.
The activated states of the Wnt and Notch pathway in the diseased tissue were found at the same histological location, suggesting that Wnt and Notch act simultaneously. We can speculate that the Wnt and Notch pathways are intertwined in the activation of HPCs during liver disease, as occurs for example when cell-fate decisions are made during development [54]. Whether and how Wnt and Notch interact during HPC activation and in what manner this can be used for therapeutic benefit needs to be further investigated in molecular *in vivo* studies.

Conclusions

The combined Q-PCR and immunofluorescence results, extend existing literature on other species and indicate a critical role for Wnt and Notch in proliferation, differentiation and/or migration of canine HPCs during rapidly progressing fibrotic liver disease with hampered hepatocytic proliferation. The descriptive data presented here suggest a role in HPC activation; *in vitro* experiments with canine hepatic progenitor cells, at present not available, could shed light on these questions separately. These data from a non-experimental liver disease in client-owned pets confirm the previous separate reports on Wnt and Notch signalling in rat and mouse injury models of liver disease [16,23,24,29,30,50], and human data [19]. In the future, the implementation of pre-clinical experiments with e.g. Notch or Wnt inhibitors in order to enhance liver regeneration in patients could be mutually beneficial for dog and man.

Methods

Liver samples

Liver samples were obtained from dogs with lobular dissecting hepatitis (LDH, n=4; age range 1.5-2.5 years) a rapidly progressing disease characterized by diffuse inflammation, peri-cellular fibrosis and massive HPC activation [12,13]. Liver pathology of the dogs was confirmed histologically by one board-certified veterinary pathologist according to the World Small Animal Veterinary Association (WSAVA)-standards [55]. Normal livers (n=4; age range 1-3 years) were obtained from surplus animals of a non-liver related research project at the University Medical Centre Utrecht (University 3R policy).

Laser microdissection (LMD) of Keratin(K)7 positive cell patterns

Cryosections (10 µm) were cut using RNAse free blades on a cryostat at -20°C (Leica CM3050 cryostat, Leica Microsystems GmbH, Wetzlar, Germany), mounted on a pre-cooled (4°C) RNAse-free poly-ethylene naphthalene (PEN) membrane slide (P.A.L.M. MicroLaser Technologies AG, Burnried, Germany), immediately placed on dry ice, and stored at -70ºC for a maximum of one week until use. Rapid immunohistochemistry before laser microdissection (LMD) was performed with buffers and solutions prepared with DEPC-treated water (Ambion, Austin, TX). All glassware was treated with RNase Zap (Ambion), and washed with DEPC-treated water prior to use. To protect RNA from degradation during incubations at room temperature (RT), antibody and DAB solutions were prepared with 0.4 U/µl SUPERase RNase Inhibitor (Ambion). Frozen sections were taken from -70°C storage, immediately fixed in ice-cold acetone (-20^{o}C) for 5 minutes and washed briefly (3-5 seconds) in phosphate-buffered saline (PBS). Sections were incubated with K7 antibody (1:20; Dako, Glostrup, Denmark) in PBS for 7 minutes at RT, briefly washed in PBS, and subsequently incubated in EnVision goat anti-mouse peroxidase-conjugated antibody (Dako) for 7 minutes at RT. Staining was visualised using the chromogen diaminobenzidine (DAB; Dako) for 3 minutes at RT. Finally, sections were dehydrated in an EtOH series (75-95-100%, 15 seconds each). The LMD procedure was performed within a maximum of 20 minutes upon staining, with a Nikon eclipse TE300 inverted microscope (Nikon Inc. Instrument Group, Melville, NY), connected to a Sony 3-CCD Microscope ColorColour Video Camera (Sony Electronics Inc., Tokyo, Japan), using MMI CellTools software (MMI Molecular Machines & Industries AG, Glattbrugg, Switzerland). Tubes with an adhesive lid (MMI) were used to remove laser dissected cells from the whole liver tissue slide. After the LMD procedure collected cells were retrieved with 50 µl Extraction Buffer (PicoPure RNA isolation kit, Molecular Devices, MDS Analytical Technologies, Sunnyvale, CA), and a short centrifugal step for further molecular processing. The cell-suspension was then incubated at 42°C for 30 min, spun down for 2 min at 800g, snap frozen in liquid nitrogen, and stored at -70°C until further use. From each sample a total of 2-3.5x10^{6} µm^{2} tissue was laser-dissected, using four tissue sections per normal sample, and two tissue sections per diseased sample.

RNA isolation and amplification

Total RNA was extracted from the LMD samples using the PicoPure RNA isolation kit (MDS Analytical Technologies) according to the manufacturer's instructions, and included an on column DNAse treatment (0.1 U/ µl) to remove all DNA contaminations (Qiagen, Benelux BV, Venlo, The Netherlands). RNA quality after LMD was determined using a RNA 6000 Pico-LabChip with an Agilent BioAnalyzer 2100 (Agilent, Palo Alto, CA). Amplification of the RNA was performed with the WT-Ovation™ Pico RNA Amplification System according to the manufacturer's instructions (NuGEN Technologies Inc., Bemmel, The Netherlands). Making use of a DNA/RNA chimeric primer, cDNA is prepared from total RNA, and amplified by linear isothermal DNA amplification. The product consists of single-strand DNA (ssDNA). The amplified product was purified with DNA Clean & Concentrator-25 from Zymo research according to the manufacturers instruction (Baseclear Lab Products, Leiden, The Netherlands), replacing Wash Buffer by fresh 80% ethanol.

Q-PCR analysis

For gene expression analysis a SYBR Green based quantitative RT-PCR (Q-PCR) was performed on a Bio-Rad My-IQ detection system as described previously [56], up to 45 cycles. Gene expression of described markers of HPCs and hepatocytes, and of components of the Wnt/β-catenin and Notch signalling pathways was measured. Details of the primers and PCR conditions are listed in Table 1. Sequencing reactions confirmed amplification of the specific primer products in the Q-PCR reaction. Normalisation was secured due to the use of at least three independent reference genes: *B2MG*, *HPRT*, *RPS5*, and *RPS19*.

Table 1. Primers and PCR conditions

Gene	Direction	Sequence (5'- 3')	Tm (°C)	Product size (bp)	Genbank accession number
B2MG[a]	Forward	TCCTCATCCTCCTCGCT	60.3	85	XM_535458
	Reverse	TTCTCTGCTGGGTGTCG			
HPRT[a]	Forward	AGCTTGCTGGTGAAAAGGAC	58	114	NM_001003357
	Reverse	TTATAGTCAAGGGCATATCC			
RPS5[a]	Forward	TCACTGGTGAGAACCCCCT	62.5	141	XM_533568
	Reverse	CCTGATTCACACGGCGTAG			
RPS19[a]	Forward	CCTTCCTCAAAAAGTCTGGG	61	95	XM_533657
	Reverse	GTTCTCATCGTAGGGAGCAAG			
FZD1	Forward	GGCGCAGGGCACCAAGAAG	58.8	97	XM_539411
	Reverse	GAGCGACAGAATCACCCACCAGA			
TCF3	Forward	GGTGAATGAGCGGGTCCTGAACA	58.8	128	XM_849145
	Reverse	TGAGCTGGCTGGCACGGTAGTC			
AXIN2	Forward	CACCCGCTCTACAACAAGGT	60	128	XM_548025
	Reverse	AGGTGGAGATGAAGCACAGC			
NOTCH1	Forward	TACCGGCCAGAACTGTGAGGAGAA	56	108	XM_537795
	Reverse	GGAGGGCAGCGGCAGTTGTAAGTA			
NOTCH2	Forward	AGCACGCATCCTGGCATACCTC	58.3	106	XM_853135
	Reverse	TGGGGATTAGCTGGAAAGTCACAA			
NOTCH3	Forward	TCTGCCAGAGTTCCGTGGTG	66.8	117	XM_847948
	Reverse	ATGGGGTACAAGGGCTGCTG			
NOTCH4	Forward	GGAAGGGAGCCAGGGACCAACACA	68	96	NM_004557
	Reverse	TCAGGGCCACAGCGGGACAAATC			

JAG1	Forward	GGGCAACACCTTCAATCTCAAG	58.5	122	XM_853730
	Reverse	CATTACTGGAATCCCACGCTTC			
JAG2	Forward	GGGTACGTGCGTGGGC	64		XM_548004
	Reverse	CACCGTTGTAGCAAGGCAG			
HEY1	Forward	CCAGGAAAAGACGAAGAGGC	62.5	226	NM_001002953
	Reverse	CTCCGATAGTCCATAGCAAGGG			

[a] Reference genes

Statistical analysis

Relative gene expression of each gene-product (delta-Cq method) was used as the basis for all comparisons. The non-parametric Mann-Whitney U test was performed to assess statistical differences between normal and diseased tissue, using SPSS software (SPSS Benelux, Gorinchem, the Netherlands). Gene expressions that were not detectable were arbitrarily set to Cq 45 for statistical analysis. p-Values < 0.05 were considered statistically significant.

Immunohistochemistry/-fluorescence

Antibody details for immunohistochemistry/-fluorescence can be found in Table 2.
Whole liver cryosections (6µm) were immunohistochemically stained for Ki67, a marker of active cell proliferation. Slides were air dried for 30 min at RT, fixed in ice-cold aceton:methanol 1:1, and washed in phosphate buffered saline with 0.1% Tween 20 (PBS/T, pH 7.4). Endogenous peroxidase activity was blocked for 30 min at RT in 0.3% H_2O_2 in PBS/T and background staining was blocked with 10% normal goat serum in PBS/T for 30 min at RT. Primary antibody was diluted in blocking serum and incubated for 60 min at RT. The HRP Envision system (Dako) was used. Staining was visualised using diaminobenzidine (DAB; Dako), and counter stained with haematoxylin quickstain (Vector Laboratories) for 5 min. Finally, slides were covered with Aquamount (Vector Laboratories). Canine duodenum served as positive control (data not shown). Immunohistochemistry for vimentin was performed on 4µm thick, paraffin embedded sections essentially as described before [13]. Immunohistochemical pictures were obtained using an Olympus BX41TF Microscope (Olympus Corporation, Tokyo, Japan) with Olympus U-CMAD3 camera and Cellˆ B software (AnalySIS, Olympus).
Immunofluorescent stainings were performed with parallel antibody incubations. The slides were incubated with mixed primary antibodies over night at 4°C, and with mixed secondary antibodies at RT for 60 min. Rinsing steps were performed using TBS with 0.1% Tween 20, and slides were covered with Aquamount (Vector Laboratories). Immunofluorescent double stainings for K7/β-catenin and K7/Notch1-NICD were performed on 15µm ice-cold acetone fixed (normal and LDH) liver-cryosections. Immunofluorescent double stainings against PanCK/Vimentin, HepPar/β-catenin and HepPar/Notch1-NICD were performed on 4 µm paraffin embedded canine LDH liver sections essentially as described previously [13]. For Notch1-NICD incubation in 0.5% Triton for 20 minutes at RT was included for permeabilisation. The nucleus was stained with ToPro3 or DAPI. Slides were analysed using a Leica TCS SPE-II Confocal microscope and Leica software. In all procedures, negative controls were included constituting of a bilateral isotype control.

Table 2. Antibody specifications

	Source/Type	Clone	Company	Antigen retrieval	Dilution
β-Catenin	Rb/po		Abcam	TE pH9	1:2,000
HepPar1	Mu/mo		Dako	TE pH9	1:50
K7	Mu/mo	OV-TL 12/30	Dako		1:50
Ki67	Rb/mo	SP6	LabVision		1:50
PanCK	Rb/po		Dako	TE pH9	1:400
Notch1/NICD	Rb/po	C-20	Santa Cruz	TE pH9	1:100
Vimentin	Mu/mo		Abcam	TE pH9	1:200

Competing interests

The authors declare that they have no competing interests.

Authors' contributions

BA conceived the study, carried out the experiments and wrote the manuscript. HK participated in the design of the study and helped write the manuscript. TI interpreted the stainings. JR and LP participated in the design of the study. BS conceived the study, participated in design and coordination and helped to draft the manuscript. All authors read and approved the final manuscript.

Acknowledgements

The assistance of Anko de Graaf (Centre of Cellular Imaging, Utrecht University, the Netherlands) is greatly appreciated. This work was sponsored by the Dutch Research Counsel NWO ZON/MW (grant-numbers 92003538 and 16004121).

References

1. Center SA: **Diseases of the gallbladder and biliary tree**. *Vet Clin North Am Small Anim Pract* 2009, **39**(3):543-598.
2. Watson PJ, Roulois AJ, Scase TJ, Irvine R, Herrtage ME: **Prevalence of hepatic lesions at post-mortem examination in dogs and association with pancreatitis.** *J Small Anim Pract* 2010, **51**(11):566-572.
3. Poldervaart JH, Favier RP, Penning LC, van den Ingh TS, Rothuizen J: **Primary hepatitis in dogs: a retrospective review (2002-2006).** *J Vet Intern Med* 2009, **23**(1):72-80.
4. Favier RP: **Idiopathic hepatitis and cirrhosis in dogs.** *Vet Clin North Am Small Anim Pract* 2009, **39**(3):481-488.
5. Kapoor A, Simmonds P, Gerold G, Qaisar N, Jain K, Henriquez JA, Firth C, Hirschberg DL, Rice CM, Shields S, Lipkin WI: **Characterization of a canine homolog of hepatitis C virus.** *Proc Natl Acad Sci U S A* 2011, **108**(28):11608-11613.
6. Bexfield NH, Watson PJ, Heaney J, Heeney JL, Tiley L: **Canine hepacivirus is not associated with chronic liver disease in dogs.** *J Viral Hepat* 2014, **21**(3):223-228.

7. van der Laan LJ, de Ruiter PE, van Gils IM, Fieten H, Spee B, Pan Q, Rothuizen J, Penning LC: **Canine hepacivirus and idiopathic hepatitis in dogs from a Dutch cohort.** *J Viral Hepat* 2014, Jun 5. doi: 10.1111/jvh.12268.
8. Riehle KJ, Dan YY, Campbell JS, Fausto N: New concepts in liver regeneration. *J Gastroenterol Hepatol* 2011, **26**(Suppl 1):203-212.
9. Duncan AW, Dorrell C, Grompe M: **Stem cells and liver regeneration.** *Gastroenterology* 2009, **137**(2):466-481.
10. Saxena R, Theise N: **Canals of Hering: recent insights and current knowledge.** *Semin Liver Dis* 2004, **24**:43-48.
11. Ijzer J, Schotanus BA, Vander Borght S, Roskams TA, Kisjes R, Penning LC, Rothuizen J, van den Ingh TS: **Characterisation of the hepatic progenitor cell compartment in normal liver and in hepatitis: an immunohistochemical comparison between dog and man.** *Vet J* 2010, **184**(3):308-314.
12. Schotanus BA, van den Ingh TS, Penning LC, Rothuizen J, Roskams TA, Spee B: **Cross-species immunohistochemical investigation of the activation of the liver progenitor cell niche in different types of liver disease.** *Liver Int* 2009, **29**(8):1241-1252.
13. Kruitwagen HS, Spee B, Viebahn CS, Venema HB, Penning LC, Grinwis GC, Favier RP, van den Ingh TS, Rothuizen J, Schotanus BA: **The canine hepatic progenitor cell niche: Molecular characterisation in health and disease.** *Vet J* 2014, pii: S1090-0233(14)00221-4. doi: 10.1016/j.tvjl.2014.05.024.
14. Ijzer J, Kisjes JR, Penning LC, Rothuizen J, van den Ingh TS: **The progenitor cell compartment in the feline liver: an (immuno)histochemical investigation.** *Vet Pathol* 2009, **46**(4):614-621.
15. Kruitwagen HS, Spee B, Schotanus BA: **Hepatic progenitor cells in canine and feline medicine: potential for regenerative strategies.** *BMC Vet Res* 2014, **10**(1):137.
16. Hu M, Kurobe M, Jeong YJ, Fuerer C, Ghole S, Nusse R, Sylvester KG: **Wnt/beta-catenin signaling in murine hepatic transit amplifying progenitor cells.** *Gastroenterology* 2007, **133**(5):1579-1591.
17. Itoh T, Kamiya Y, Okabe M, Tanaka M, Miyajima A: **Inducible expression of Wnt genes during adult hepatic stem/progenitor cell response.** *FEBS Lett* 2009, **583**(4):777-781.
18. Bi Y, Huang J, He Y, Zhu GH, Su Y, He BC, Luo J, Wang Y, Kang Q, Luo Q, Chen L, Zuo GW, Jiang W, Liu B, Shi Q, Tang M, Zhang BQ, Weng Y, Huang A, Zhou L, Feng T, Luu HH, Haydon RC, He TC, Tang N: **Wnt antagonist SFRP3 inhibits the differentiation of mouse hepatic progenitor cells.** *J Cell Biochem* 2009, **108**(1):295-303.
19. Spee B, Carpino G, Schotanus BA, Katoonizadeh A, Vander Borght S, Gaudio E, Roskams T: **Characterisation of the liver progenitor cell niche in liver diseases: potential involvement of Wnt and Notch signalling.** *Gut* 2010, **59**(2):247-257.
20. Sparks EE, Perrien DS, Huppert KA, Peterson TE, Huppert SS: **Defects in hepatic Notch signaling result in disruption of the communicating intrahepatic bile duct network in mice.** *Dis Model Mech* 2011, **4**(3):359-367.
21. Boulter L, Govaere O, Bird TG, Radulescu S, Ramachandran P, Pellicoro A, Ridgway RA, Seo SS, Spee B, Van Rooijen N, Sansom OJ, Iredale JP, Lowell S, Roskams T, Forbes SJ: **Macrophage-derived Wnt opposes Notch signaling to specify hepatic progenitor cell fate in chronic liver disease.** *Nat Med* 2012, **18**(4):572-579
22. Thompson MD, Monga SP: **WNT/beta-catenin signaling in liver health and disease.** *Hepatology* 2007, **45**(5):1298-1305.
23. Flynn DM, Nijjar S, Hubscher SG, de Goyet Jde V, Kelly DA, Strain AJ, Crosby HA: **The role of Notch receptor expression in bile duct development and disease.** *J Pathol* 2004, **204**(1):55-64.
24. Chiba T, Zheng YW, Kita K, Yokosuka O, Saisho H, Onodera M, Miyoshi H, Nakano M, Zen Y, Nakanuma Y, Nakauchi H, Iwama A, Taniguchi H: **Enhanced self-renewal capability in hepatic stem/progenitor cells drives cancer initiation.** *Gastroenterology* 2007, **133**(3):937-950.
25. Gramantieri L, Giovannini C, Lanzi A, Chieco P, Ravaioli M, Venturi A, Grazi GL, Bolondi L: **Aberrant Notch3 and Notch4 expression in human hepatocellular carcinoma.** *Liver Int* 2007, **27**(7):997-1007.
26. Tan X, Yuan Y, Zeng G, Apte U, Thompson MD, Cieply B, Stolz DB, Michalopoulos GK, Kaestner KH, Monga SP: **Beta-catenin deletion in hepatoblasts disrupts hepatic morphogenesis and survival during mouse development.** *Hepatology* 2008, **47**(5):1667-1679.
27. Köhler C, Bell AW, Bowen WC, Monga SP, Fleig W, Michalopoulos GK: **Expression of Notch-1 and its ligand Jagged-1 in rat liver during liver regeneration.** *Hepatology* 2004, **39**(4):1056-1065.
28. Roskams T: **Different types of liver progenitor cells and their niches.** *J Hepatol* 2006, **45**(1):1-4.
29. Apte U, Thompson MD, Cui S, Liu B, Cieply B, Monga SP: **Wnt/beta-catenin signaling mediates oval cell response in rodents.** *Hepatology* 2008, **47**(1):288-295.
30. Yang W, Yan HX, Chen L, Liu Q, He YQ, Yu LX, Zhang SH, Huang DD, Tang L, Kong XN, Chen C, Liu SQ, Wu MC, Wang HY: **Wnt/beta-catenin signaling contributes to activation of normal and tumorigenic liver progenitor cells.** *Cancer Res* 2008, **68**(11):4287-4295.

31. Jeliazkova P, Jörs S, Lee M, Zimber-Strobl U, Ferrer J, Schmid RM, Siveke JT, Geisler F: **Canonical Notch2 signaling determines biliary cell fates of embryonic hepatoblasts and adult hepatocytes independent of Hes1.** *Hepatology* 2013, **57**(6):2469-2479.
32. Fiorotto R, Raizner A, Morell CM, Torsello B, Scirpo R, Fabris L, Spirli C, Strazzabosco M: **Notch signaling regulates tubular morphogenesis during repair from biliary damage in mice.** *J Hepatol* 2013, **59**(1):124-130.
33. Scholten D, Osterreicher CH, Scholten A, Iwaisako K, Gu G, Brenner DA, Kisseleva T: **Genetic labeling does not detect epithelial-to-mesenchymal transition of cholangiocytes in liver fibrosis in mice.** *Gastroenterology* 2010, **139**:987-998.
34. Swiderska-Syn M, Suzuki A, Guy CD, Schwimmer JB, Abdelmalek MF, Lavine JE, Diehl AM: **Hedgehog pathway and pediatric nonalcoholic fatty liver disease.** *Hepatology* 2013, **57**(5):1814-1825.
35. Syn WK, Jung Y, Omenetti A, Abdelmalek M, Guy CD, Yang L, Wang J, Witek RP, Fearing CM, Pereira TA, Teaberry V, Choi SS, Conde-Vancells J, Karaca GF, Diehl AM: **Hedgehog-mediated epithelial-to-mesenchymal transition and fibrogenic repair in nonalcoholic fatty liver disease.** *Gastroenterology* 2009, **137**:1478-1488.
36. Kalluri R, Weinberg RA: **The basics of epithelial-mesenchymal transition.** J Clin Invest. 2009, **119**(6):1420-148.
37. Lim J, Thiery JP: **Epithelial-mesenchymal transitions: insights from development.** *Development* 2012, **139**(19):3471-3486.
38. Lee JM, Dedhar S, Kalluri R, Thompson EW: **The epithelial-mesenchymal transition: new insights in signaling, development, and disease.** *J Cell Biol* 2006, **172**(7):973-981.
39. Sansom OJ, Reed KR, Hayes AJ, Ireland H, Brinkmann H, Newton IP, Batlle E, Simon-Assmann P, Clevers H, Nathke IS, Clarke AR, Winton DJ: **Loss of Apc in vivo immediately perturbs Wnt signaling, differentiation, and migration.** *Genes Dev*. 2004, **18**(12):1385-1390.
40. Ober EA, Verkade H, Field HA, Stainier DY: **Mesodermal Wnt2b signalling positively regulates liver specification.** *Nature* 2006, **442**(7103):688-691.
41. Hay DC, Fletcher J, Payne C, Terrace JD, Gallagher RC, Snoeys J, Black JR, Wojtacha D, Samuel K, Hannoun Z, Pryde A, Filippi C, Currie IS, Forbes SJ, Ross JA, Newsome PN, Iredale JP: **Stabilization of beta-catenin affects mouse embryonic liver growth and hepatoblast fate.** *Proc Natl Acad Sci U S A* 2008, **105**(34):12301-12306.
42. Decaens T, Godard C, de Reyniès A, Rickman DS, Tronche F, Couty JP, Perret C, Colnot S: **Highly efficient differentiation of hESCs to functional hepatic endoderm requires ActivinA and Wnt3a signaling.** *Hepatology* 2008, **47**(1):247-258.
43. Ishii K, Yoshida Y, Akechi Y, Sakabe T, Nishio R, Ikeda R, Terabayashi K, Matsumi Y, Gonda K, Okamoto H, Takubo K, Tajima F, Tsuchiya H, Hoshikawa Y, Kurimasa A, Umezawa A, Shiota G: **Hepatic differentiation of human bone marrow-derived mesenchymal stem cells by tetracycline-regulated hepatocyte nuclear factor 3beta.** *Hepatology* 2008, **48**(2):597-606.
44. Robrechts C, De Vos R, Van den Heuvel M, Van Cutsem E, Van Damme B, Desmet V, Roskams T: **Primary liver tumour of intermediate (hepatocyte-bile duct cell) phenotype: a progenitor cell tumour?** *Liver* 1998, **18**(4):288-293.
45. Libbrecht L, Desmet V, Van Damme B, Roskams T: **The immunohistochemical phenotype of dysplastic foci in human liver: correlation with putative progenitor cells.** *J Hepatol* 2000, **33**(1):76-84.
46. Alagille D, Estrada A, Hadchouel M, Gautier M, Odievre M, Dommerques JP: **Syndromic paucity of interlobular bile ducts (Alagille syndrome or arteriohepatic dysplasia): review of 80 cases.** *J Pediatr* 1987, **110**:195-200.
47. Li L, Krantz ID, Deng Y, Genin A, Banta AB, Collins CC, Qi M, Traski BJ, Kuo WL, Cochran J, Costa T, Pierpont ME, Rand EB, Piccoli DA, Hood L, Spinner NB: **Alagille syndrome is caused by mutations in human Jagged1, which encodes a ligand for Notch1.** *Nat Genet* 1997, **16**:243-251.
48. Tanimizu N, Miyajima A: **Notch signaling controls hepatoblast differentiation by altering the expression of liver-enriched transcription factors.** *J Cell Sci* 2004, **117**:3165-3174.
49. Nijjar SS, Crosby HA, Wallace L, Hubscher SG, Strain AJ: **Notch receptor expression in adult human liver: a possible role in bile duct formation and hepatic neovascularization.** *Hepatology* 2001, **34**:1184-1192.
50. Nijjar SS, Wallace L, Crosby HA, Hubscher SG, Strain AJ: **Altered Notch ligand expression in human liver disease: further evidence for a role of the Notch signaling pathway in hepatic neovascularization and biliary ductular defects.** *Am J Pathol* 2002, **160**:1695-1703.
51. McCright B, Lozier J, Gridley T. **A mouse model of Alagille syndrome: Notch2 as a genetic modifier of Jag1 haploinsufficiency.** *Development* 2002, **129**;1075-1082.
52. Kodama Y, Hijikata M, Kageyama R, Shimotohno K, Chiba T: **The role of notch signaling in the development of intrahepatic bile ducts.** *Gastroenterology* 2004, **127**:1775-1786.
53. Kuver R, Savard CE, Lee SK, Haigh WG, Lee SP: **Murine gallbladder epithelial cells can differentiate into hepatocyte-like cells in vitro.** *Am J Physiol Gastrointest Liver Physiol* 2007, **293**:G944-G955.

54. Hayward P, Kalmar T, Arias AM: **Wnt/Notch signalling and information processing during development.** *Development* 2008, **135**:411-424.
55. Van den Ingh TSGAM, Van Winkle T, Cullen JM, Charles JA, Desmet VJ: **Morphological classification of parenchymal disorders of the canine and feline liver: 2. Hepatocellular death, hepatitis and cirrhosis.** In: WSAVA Standards for clinical and histological diagnosis of canine and feline liver disease. Edited by Rothuizen J, Bunch SE, Charles JA, et al. Edinburgh, Saunders-Elsevier 2006, 85-102.
56. van Steenbeek FG, Van den Bossche L, Grinwis GC, Kummeling A, van Gils IH, Koeramp MJ, van Leenen D, Holstege FC, Penning LC, Rothuizen J, Leegwater PA, Spee B: **Aberrant gene expression I dog with portosystemic shunts.** *PLoS One* 2013, **8**:e57662.

Chapter 4

Dual specificity tyrosine phosphorylation regulated kinase 1A (DYRK1A) is a regulator of S phase entry in hepatic progenitor cells.

H.S. Kruitwagen, B. Westendorp, C.S. Viebahn, K. Post, M.E. van Wolferen, L.A. Oosterhoff, D.A. Egan, J.M. Delabar, M.J. Toussaint, B.A. Schotanus, A. de Bruin, J. Rothuizen, L.C. Penning* and B. Spee*

Submitted manuscript

*Equal contribution

Abstract

Hepatic progenitor cells (HPCs) are adult liver stem cells that act as second line of defense in liver regeneration. They are normally quiescent, but in case of severe liver damage HPC proliferation is triggered by external activation mechanisms from their niche. Although several important pro-proliferative mechanisms have been described, it is not known which key intracellular regulators govern the switch between HPC quiescence and active cell cycle.
We performed a high throughput kinome siRNA screen in HepaRG cells, a HPC-like cell line, and evaluated the effect on proliferation with a 5-ethynyl-2'-deoxyuridine (EdU) incorporation assay. One hit increased the percentage of EdU-positive cells after knockdown: dual specificity tyrosine phosphorylation regulated kinase 1A (DYRK1A). Although upon DYRK1A silencing the percentage of EdU and phosphorylated histone H3 positive cells was increased, total cell numbers were not increased, possibly through a subsequent delay in cell cycle progression. This phenotype was confirmed with chemical inhibition of DYRK1A using harmine and with primary HPCs cultured as liver organoids. DYRK1A inhibition impaired *D*imerization Partner, *R*B-like, *E*2F and *m*ulti-vulva class B (DREAM) complex formation in HPCs and abolished its transcriptional repression on cell cycle progression. To further analyze DYRK1A function in HPC proliferation, liver organoid cultures were established from mBACtgDyrk1A mice, which harbor one extra copy of the murine *Dyrk1a* gene (*Dyrk+++*). *Dyrk+++* organoids had both a reduced percentage of EdU-positive cells and reduced proliferation compared to wildtype organoids.
This study provides evidence for an essential role of DYRK1A as balanced regulator of quiescence versus S phase entry in HPCs. An exact gene dosage is crucial, as both DYRK1A deficiency and overexpression affect HPC cell cycle progression.

Introduction

The liver is well known for its regenerative capacity, which is primarily based on hepatocyte replication [1, 2]. This first line of defense fails however, in cases of fulminant or chronic liver injury [3-5]. Liver repair then relies on hepatic progenitor cells (HPCs). HPCs are adult liver stem cells that are normally quiescent, but start to proliferate upon severe hepatic damage and can differentiate into mature hepatocytes [6-10]. In practice, this HPC-response is often still insufficient for clinical recovery of liver disease [11].
Adult stem cells require a well-regulated balance between quiescence and cell cycle entry in order to prevent premature exhaustion while maintaining self-renewal capacity [12]. Proliferation is initiated by specific cues from their tissue microenvironment or niche [13]. For HPCs several external activation mechanisms have been described, such as Wnt-signaling, growth factors and cytokines (e.g. hepatocyte growth factor, TWEAK), and specific extracellular matrix components [14-17]. However, it is not known which key intracellular regulators downstream of these external signals govern the switch between quiescence and active cell cycle in HPCs. Identification of these essential determinants of the HPC-response could give greater insight into the biology behind HPC-mediated liver regeneration and could lead to new therapeutic strategies for patients with severe liver disease. In this study we therefore aimed to screen for kinases that are essential in HPC proliferation. Kinases are known for their involvement in the cell cycle and proliferation [18-20]. As a class they are commonly exploited as drug targets, with many (receptor tyrosine) kinase inhibitors already in use in the clinic. To this end, we used a kinase siRNA library in HepaRG cells, a HPC-like cell line, and studied the effect on the cell cycle with a 5-ethynyl-2'-deoxyuridine (EdU) incorporation assay (a detailed screening strategy is summarized in Fig. 1). We hypothesized that silencing a kinase essential for maintaining quiescence should give increased S phase entry and proliferation. The kinome screen generated one hit: dual specificity tyrosine phosphorylation regulated kinase 1A (DYRK1A). To validate our findings, we confirmed the observed phenotype in primary HPCs cultured as liver organoids [21] and also investigated an overexpression model with one extra copy of the DYRK1A gene [22].

Materials and Methods

Culture of HepaRG cell line
Human hepatic progenitor-like cell line HepaRG was obtained from BioPredic International (Rennes, France). Human hepatic stellate cell line LX2 was kindly provided by Scott Friedman (Mount Sinai School of Medicine, New York, USA). Cells were cultured in William's Medium E with 2% v/v fetal calf serum (Life Technologies), 5 µg/ml insulin, 50 µM hydrocortisone hemisuccinate (Sigma-Aldrich), and standard antibiotics at 37°C in 5% CO_2 in air in a humidified incubator.

High throughput siRNA screen, immunofluorescence and image acquisition
A Dharmacon On-Target-Plus siRNA library (Thermo Scientific) targeting 716 kinases in the human genome was used in the primary screen. A transfection protocol was developed that yielded more than 90% transfection efficiency and knockdown without affecting viability or cell loss (<10%). siRNAs were forward transfected in 5,500 HepaRG cells/well (confluency of 30%) in 96-well plates in triplicate at a concentration of 5 nM using 3 µl/ml RNAiMAX transfection reagent (Thermo Scientific)

in antibiotic-free media. As controls, non-targeting (NT) siRNAs and SMARTpool siRNAs against BMI1 proto-oncogene, polycomb ring finger (BMI1) and polo-like kinase 1 (PLK1) were used. Cells were cultured for 48 hours in total after transfection. After 24 hours transfection media was removed and replaced with standard culture medium with antibiotics. After 48 hours cells were pulsed in culture with 10 μM 5-ethynyl-2'-deoxyuridine (EdU) for 3 hours, then washed with phosphate-buffered saline with 0.1% Tween and fixed and permeabilized with 4% paraformaldehyde (PFA) and 0.5% Triton X for 10 minutes at room temperature. Fixative was replaced with PBS and cells were stained for EdU and phosphorylated histone H3 (pH3) using a Sciclone automated workstation (Caliper Life Sciences). EdU staining was performed with 5μM AF488-azide (Thermo Scientific), 1mM $CuSO_4$ and 100mM ascorbic acid according to Salic et al. [23]. For pH3 staining, cells were blocked with 5% v/v normal goat serum (Sigma-Aldrich) and then incubated with rabbit anti-pH3 (1:500, Millipore 06-570, lot number 1957281) for 1 hour. Cells were washed and then incubated with goat anti-rabbit AF568 (1:200, Life Technologies) for 1 hour. Cells were washed and nuclei were counterstained with 4',6-diamidino-2-phenylindole (DAPI, Sigma-Aldrich). Total cell count and the percentage of EdU and pH3 positive cells were calculated with automated image acquisition and data analysis using the Target Activation algorithm of the Cellomics ArrayScan VTI HCS Reader (Thermo Scientific).

Screening strategy, data normalization and hit selection

The screening strategy is summarized in Fig. 1. In a primary screen, all 716 kinases in the library were screened in triplicate in HepaRG cells using a pool of 4 siRNAs per target. After 48 hours the percentage of EdU was determined. Data were normalized with a robust Z score analysis (sample-based normalization) and a significance threshold of 3 was established mathematically by Monte Carlo analysis [24]. Consequently, hits were defined as having a robust Z score of either ≥3 (increased %EdU positive cells after silencing) or ≤-3 (decreased %EdU positive cells after silencing) in at least two out of three replicates. Obtained hits were reanalyzed in a secondary screen with a randomized plate setup and including 10 NT control siRNAs per plate. Transfections were performed in plate triplicates to control for inter-plate variation. In addition, the secondary screen included a second cell line as negative selector to rule out common, non-HPC specific hits. For this purpose the hepatic stellate cell line LX2 was selected, representing liver cells of a different (mesenchymal) lineage. Assuming a biased population in this confirmatory screen, a control-based hit selection was employed using two standard deviations away from the NT controls as cut-off. A target had to be a hit in at least two out of three replicate plates. Remaining hits were technically validated in a deconvolution screen in HepaRG cells, individually transfecting four single siRNAs per target to control for off-target effects. Hit selection was similar as in the secondary screen, with the added requirement that at least two out of four siRNAs had to produce a hit phenotype. In the same transfection experiment RNA was isolated in triplicate to confirm knockdown of the target [25].

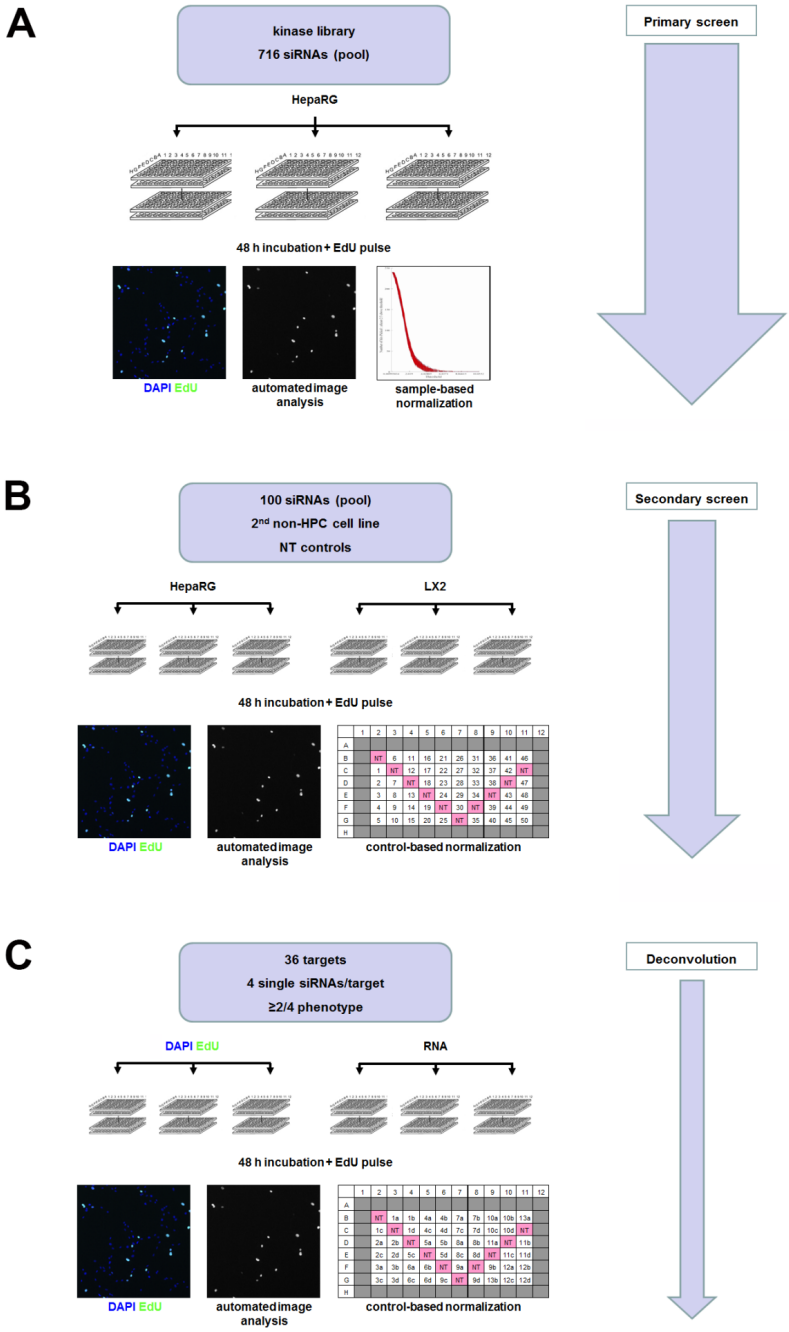

Figure 1. High throughput screen strategy. A. In a primary screen 716 kinases were screened using a pool of 4 siRNAs per target. Transfections were performed in triplicate. After 48 hours cells were pulsed with EdU, stained, and %EdU+ cells was determined with automated image analysis. Hits were selected based on sample-based normalization. B. Secondary screen included a non-HPC cell line (LX2). Transfections were performed in triplicate. Per plate 10 non-targeting (NT) controls distributed at random across the plate were used for control-based hit selection. C. Deconvolution using four single siRNAs per target (at least two had to yield hit phenotype) and control-based hit selection. RNA was isolated to confirm knockdown of the target. Transfections were performed in triplicate for both EdU assay and RNA isolation.

RNA isolation and quantitative reverse transcriptase PCR analysis

RNA was isolated with either sample preparation reagent (Biorad) or an RNeasy kit (Qiagen) from three to six culture replicates. cDNA reaction and qPCR were performed in duplicate essentially as described before [26] on a BioRad CFX thermal cycler (BioRad). Primers were designed for human and mouse *DYRK1A/Dyrk1a*, mouse E2f transcription factor 1 (*E2f1*), cell division cycle 6 (*Cdc6*), proliferating cell nuclear antigen (*Pcna*), cyclin B1 (*Ccnb1*), polo-like kinase 1 (*Plk1*), and epithelial cell transforming 2 (*Ect2*). Gene expression was normalized against reference genes (human: *HPRT* and *RPL19*, mouse: *ß-Actin*, *Rps18* and *Gapdh*). Primers are listed in Table 1.

Table 1. Primer sequences and QPCR conditions

Species	Gene	Direction	Sequence (5' – 3')	Tm (°C)	Product size (bp)
Human	*DYRK1A*	Forward	TTGACTCCTTGATAGGCAAAGGT	60	70
		Reverse	CATTCTTGCTCCACACGATCAT		
	HPRT	Forward	ATAAGCCAGACTTTGTTGGA	60	156
		Reverse	CTCAACTTGAACTCTCATCTTAGG		
	RPL19	Forward	ATGAGTATGCTCAGGCTTCAG	64	150
		Reverse	GATCAGCCCATCTTTGATGAG		
Mouse	*Dyrk1a*	Forward	GTGTCTGCCTTACCATATTCTG	61	83
		Reverse	TGCTGGATCACGGAAGG		
	E2f1	Forward	GCCCTTGACTATCACTTTGGTCTC	64	270
		Reverse	CCTTCCCATTTTGGTCTGCTC		
	Cdc6	Forward	AGTTCTGTGCCCGCAAAGTG	63	289
		Reverse	AGCAGCAAAGAGCAAACCAGG		
	Pcna	Forward	TGAAGATAATGCAGACACCTTAGC	61	124
		Reverse	TGTACTCCTGTTCTGGGATTCC		
	Ccnb1	Forward	AAAGGGAAGCAAAAACGCTAGG	59	130
		Reverse	TGTTCAAGTTCAGGTTCAGGCTC		
	Plk1	Forward	CCAAGCACATCAACCCAGTG	60	147
		Reverse	TGAGGCAGGTAATAGGGAGACG		
	Ect2	Forward	AGAGACGGAGATTGAAAGAGACC	60	110
		Reverse	GTGAGCCAATAGAAAGAGAGTGC		
	ß-Actin	Forward	AGCTCCTTCGTTGCCGGTCCA	57	94
		Reverse	TTTGCACATGCCGGAGCCGTTG		
	Rps18	Forward	GATCCCTGAGAAGTTCCAGCAC	57	120
		Reverse	ACCACATGAGCATATCTCCGC		
	Gapdh	Forward	GAAGGTCGGTGTGAACGG	61	101
		Reverse	TGAAGGGGTCGTTGATGG		

Protein isolation and Western blotting

Total protein was isolated from HepaRG cells cultured in a 6 well plate (165,000 cells/well). Protein isolation and Western blotting were performed essentially as described before [26]. For LIN52 immunoblotting, dephosphorylation of samples (100 µg protein) was performed with 100 U lambda protein phosphatase (λPP, New England Biolabs) in 1x NEBuffer for PMP, supplemented with 1 mM $MnCl_2$ at 30°C for 30 minutes. For DYRK1A immunoblotting, polyclonal antibody against DYRK1A (Sigma-Aldrich HPA015810, lot number A71674) was diluted 1:250 and secondary goat-anti-rabbit antibody (Dako) was diluted 1:5,000. As a loading control β-actin antibody (Thermo Scientific MS1295P1, lot number 1295P1501P) was used in a 1:2,000 dilution. For LIN52 immunoblotting, polyclonal antibody against LIN52 (Sigma-Aldrich HPA000900, lot number A79391) was diluted 1:100 and secondary goat-anti-rabbit antibody (Cell Signaling) was diluted 1:3,000. As a loading control

alpha-tubulin antibody (Sigma-Aldrich T6199, lot number 102M4773V) was used in a 1:1,000 dilution. Omission of the first antibody was used as negative control.

Flow cytometry and cell cycle distribution analysis
HepaRG cells 48 hours after transfection with either NT control or siRNA against DYRK1A were harvested by enzymatic digestion and fixed in 70% ethanol at 4°C overnight. Cells were stained with 5 µg/ml propidium iodide and 250 µg/ml RNase in PBS. For flow cytometry a FACSCalibur (BD Biosciences) was used. Acquired DNA content data were analyzed with FlowJo software for cell cycle distribution (curve fit according to Dean Jett Fox model). DNA content data (DAPI total intensity) from the ArrayScan automated image acquisition were similarly analyzed with FlowJo.

Harmine treatment
Harmine is a specific DYRK1A inhibitor [27, 28]. HepaRG cells and liver organoids were treated with 10 µM harmine (Sigma-Aldrich) or its vehicle (DMSO) control for 48 hours. Medium was refreshed after 24 hours.

Mouse liver organoid culture
Surplus mouse liver samples were obtained from 14-20 weeks old wildtype and mBACtgDyrk1A mice (n=5 transgenic and n=4 wildtype littermates) killed for unrelated research purposes (University 3R-policy). mBACtgDyrk1A mice were generated as described previously and contain one extra copy of the murine dyrk1a gene [22]. Liver samples were processed fresh or immediately frozen in cryopreservative (Life Technologies). Liver was minced and then digested with 125 µg/ml collagenase type XI (Sigma-Aldrich) and 125 µg/ml dispase (Life Technologies) to obtain biliary duct fragments. Ducts were seeded in 3D culture in Matrigel (BD Biosciences) in 48 or 24 well plates and cultured in expansion media as described before [21]. Imaging was performed with an Olympus microscope (CKX41) and a Leica DFC425C camera.

EdU incorporation assay in organoids
Organoids in log phase of growth were pulsed with 10 µM of EdU for 3 hours, fixed in 4% PFA and embedded in paraffin. Organoid sections of 4 µm were routinely dewaxed and rehydrated and stained for EdU as described before and nuclei were counterstained with DAPI. Sections were imaged with an Olympus IMT-2 fluorescence microscope and an Olympus E-330 LCD camera. For at least 2000 cells per condition, total cell number and number of EdU^+ cells were counted.

Organoid growth curves
To quantify liver organoid growth, organoids were cultured in 48 well plates (n=4 wells per condition) and an Alamar blue assay was performed on the same wells on five consecutive days according to the manufacturer's instructions (Life Technologies). Serial fluorescence measurements were made on a Tecan Infinite M200 spectrophotometer and were normalized to day 1.

Organoid γH2AX immunocytochemistry
Paraffin-embedded organoid sections of 4 µm were routinely dewaxed and rehydrated and incubated in 10 mM citrate at 98°C for 30 minutes with an additional 30 minutes cooling down. Endogenous peroxidase activity was blocked with 0.3% H_2O_2 in methanol. Sections were washed with phosphate buffered saline containing 0.1% Tween and incubated with 10% v/v normal goat

serum (Sigma-Aldrich) for 30 minutes at RT. Sections were incubated with rabbit anti-γH2AX (1:500, Millipore MABE205, clone EP854(2)Y, lot number 2452454) at 4°C overnight. Sections were incubated with goat-anti-rabbit (Envision, Dako) for 45 minutes at RT and 3,3'diaminobenzidine was used as chromogen. Haematoxylin was used as counterstain. Imaging was performed with an Olympus microscope (CKX41) and a Leica DFC425C camera, at least 1,000 nuclei were counted per condition.

Statistics

Statistical significance was determined using a non-parametric Mann Whitney U test, $p \leq 0.05$ was considered significant. Analysis was performed in SPSS (IBM SPSS Statistics 22).

Results

RNAi screening of kinase library in HepaRG cell line

In a primary screen 716 kinases were silenced and screened for their effect on EdU incorporation in the HepaRG cell line. After normalization, 100 hits were identified based on a robust Z score of either ≥3 (increased %EdU positive cells after silencing) or ≤-3 (decreased %EdU positive cells after silencing) (Fig. 2*A*). As confirmation that our screen was robust, siRNA's against two essential kinases (BMI1 and PLK1) consistently yielded Z scores of <-3 and non-targeting controls did not yield a hit phenotype. The obtained hits were reanalyzed in a secondary screen in triplicate and, as a biological validation, tested in parallel for their effect in a non-HPC liver cell line (LX2, stellate cell line) to rule out non-HPC specific hits. The secondary screen validated 41 hits, of which 36 were unique for HepaRG cells and did not yield a similar phenotype in LX2 cells. To control for potential off-target effects, a deconvolution screen was performed using single siRNAs and knockdown was confirmed on mRNA level by qPCR (data not shown for all hits). In total 10 hits were confirmed with at least 2 out of 4 siRNAs producing a phenotype (Fig. 2*B*, overview of screen hit confirmation in Fig. 2*C*). Out of these 10 hits, only 1 hit resulted in an increase in %EdU positive cells after silencing. This kinase was identified as dual specificity tyrosine phosphorylation regulated kinase 1A (DYRK1A). DYRK1A is an important regulator of proliferation of neural progenitor cells and pancreatic β cells [29-31]. However, its role in hepatic progenitor cells is unexplored, and was subject of further investigation.

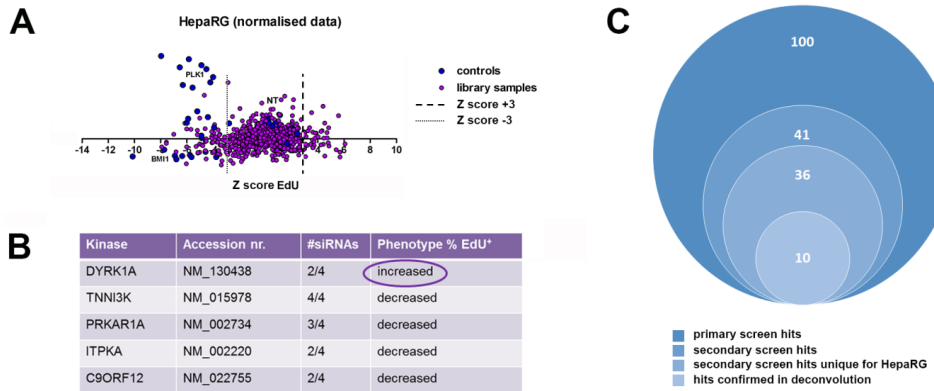

B

Kinase	Accession nr.	#siRNAs	Phenotype % EdU+
DYRK1A	NM_130438	2/4	increased
TNNI3K	NM_015978	4/4	decreased
PRKAR1A	NM_002734	3/4	decreased
ITPKA	NM_002220	2/4	decreased
C9ORF12	NM_022755	2/4	decreased
PIP5K1B	NM_003558	2/4	decreased
PCTK1	NM_006201	2/4	decreased
GCK	NM_033507	2/4	decreased
PIK3CB	NM_006219	2/4	decreased
RPS6KC1	NM_012424	2/4	decreased

Figure 2. RNAi screen hits in HepaRG cell line. A. Scatter plot representing robust Z scores in the primary screen. Out of 716 screened kinases, 100 hits were selected based on a robust Z score of either ≥3 (increased %EdU+ cells after silencing) or ≤-3 (decreased %EdU+ cells after silencing). siRNAs against BMI1 and PLK1 (essential kinases) were used as controls. NT: non targeting control. B. Final hitlist. Deconvolution screening validated 10 hits with ≥2 out of 4 siRNAs producing a phenotype. C. Schematic representation of screen hit confirmation.

Effect of DYRK1A silencing in HepaRG cell line on %EdU$^+$ cells, %pH3$^+$ cells, and proliferation

We first confirmed that siRNA-mediated gene silencing of *DYRK1A* in HepaRG cells resulted in a 97% knockdown on mRNA level and 65% on protein level after 48h (Fig. 3*A*). Consistent with the results from our screen, *DYRK1A* silencing significantly increased the % of EdU$^+$ and phosphorylated histone H3 (pH3)$^+$ cells (Fig. 3, *B* and *C*), suggesting more cells entered S phase and G2/M phase of the cell cycle. However, we did not observe significant changes in total cell numbers after 48 hours of *DYRK1A* silencing (Fig. 3*C*). Cell cycle distribution analysis of Arrayscan DNA content data with FlowJo software showed that upon *DYRK1A* gene silencing the population of cells in S and G2 phase of the cell cycle was increased (Fig. 3*D*). This phenotype was confirmed by flow cytometry (Fig. 3*E*).

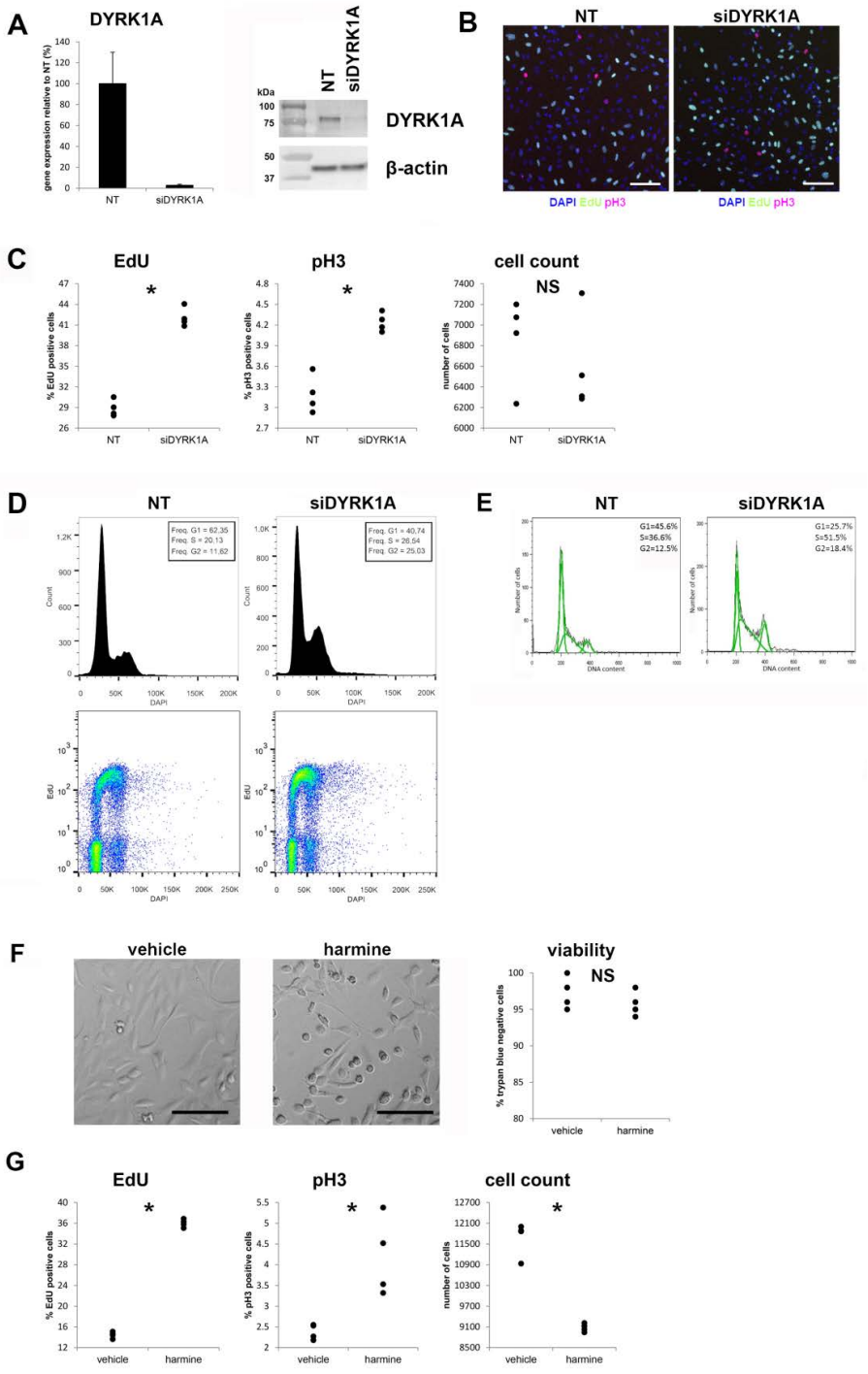

Figure 3. Effects of DYRK1A silencing and chemical inhibition on HepaRG cell cycle. A. Knockdown of DYRK1A after 48 hours on mRNA (97%) and protein level (65%). β-actin served as loading control. B. Representative images of DAPI (blue), EdU (green) and pH3 (red) immunofluorescent staining after either non-targeting control (NT) or siRNA against DYRK1A

(siDYRK1A) transfection. Scale bars indicate 100 µm. C. Dot plots representing percentages of EdU+ and pH3+ cells and total cell count after either NT or siDYRK1A transfection. D. Cell cycle distribution analysis (FlowJo) of total DAPI staining intensity per nucleus and scatterplots of DAPI versus EdU staining intensity per nucleus after either NT or siDYRK1A transfection. E. Flow cytometry analysis of cell cycle distribution using PI as measure of DNA content. F. Representative phase contrast images of HepaRG cells after 48h of treatment with either vehicle or harmine. Scale bars indicate 100 µm. Viability was determined with a trypan blue exclusion assay. G. Dot plots representing percentages of EdU+ and pH3+ cells and total cell count after 48h of treatment with either vehicle or harmine. * indicates $p \leq 0.05$, N.S. not significant.

Validation of phenotype in HepaRG cell line with chemical DYRK1A inhibitor

We tested whether the phenotype could be recapitulated with harmine, a specific chemical inhibitor of DYRK1A [27, 28]. Morphologically, cells had a rounded appearance after incubation with harmine, but viability was not decreased (Fig. 3*F*). Harmine treatment similarly increased the percentage of EdU^+ and $pH3^+$ cells compared to vehicle control, but caused a decrease in cell proliferation (Fig. 3*G*). We concluded that DYRK1A silencing/inhibition enhances progression through the cell cycle but does not enhance cell division. An explanation for these findings could be that DYRK1A enhances S phase entry of cells at the expense of a subsequent delay in G2-M-phase progression. The increased S phase entry upon DYRK1A inhibition is specific for a HPC cell line, because it does not occur in HepG2 or Huh7 cells (hepatocyte cell lines) nor in LX2 cells (hepatic stellate cell line) (data not shown). Although it has many hepatic progenitor features and intact p53, the HepaRG is a tumor cell line. Therefore we asked if DYRK1A would have similar functions in primary HPCs. We utilized organoid technology to evaluate the effects of DYRK1A inhibition on proliferation in primary HPCs, cultured as liver organoids [21].

Effect of DYRK1A inhibition in liver organoids on EdU positivity and proliferation

Liver organoids were treated with either vehicle or harmine and then pulsed with EdU for 6 hours. Also in liver organoids DYRK1A inhibition with harmine resulted in more EdU^+ cells compared to vehicle control (Fig. 4*A*). Again, harmine treatment did not increase overall proliferation of liver organoids over the course of 5 days, as measured by Alamar Blue assay (Fig. 4*B*). Unscheduled entry of cells into S phase may result in replication stress and DNA damage. Therefore we stained cells with the DNA damage marker γH2AX after 72 hours of harmine treatment. However, we did not observe a difference, suggesting that DNA damage cannot explain the cell cycle perturbation of DYRK1A-inhibited cells (Fig. 4*C*).

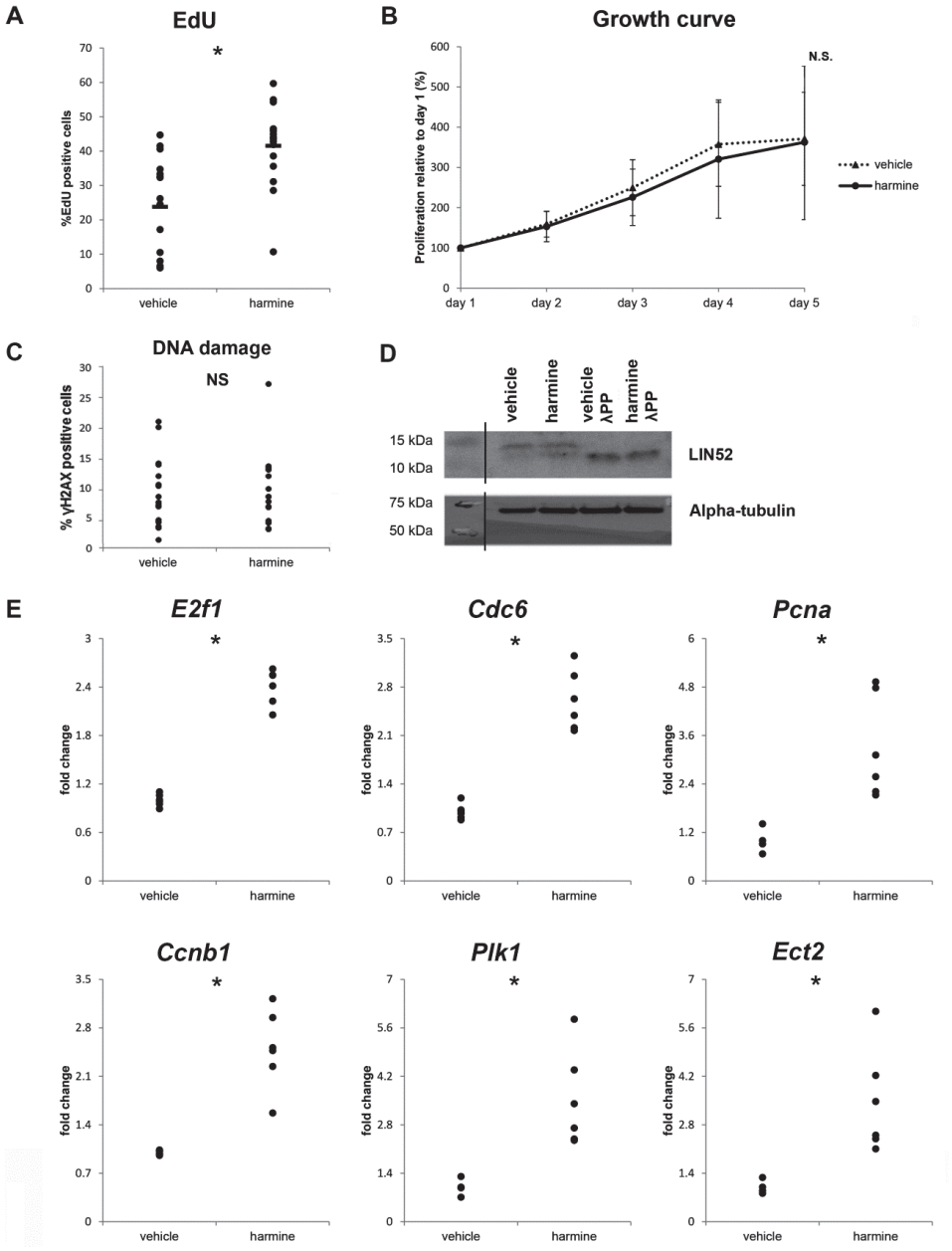

Figure 4. Effects of DYRK1A inhibition on liver organoids. A. Dot plot of percentage of EdU+ cells in liver organoids after 48h of treatment with either vehicle or harmine. Dots represent counted organoid sections (n=16 per condition), at least 2,000 nuclei were counted per condition. B. Growth curve of organoids treated with either vehicle or harmine (n=4 culture replicates per condition) as measured with an Alamar blue assay on the same wells on consecutive days. Serial luminescence measurements were normalized to day 1 (100%). C. Dot plot of percentage γH2AX positive cells indicative of DNA damage in liver organoids after 72h of treatment with either vehicle or harmine. Dots represent counted organoid sections (n=16 per condition), at least 1000 nuclei were counted per condition. D. Western blot for LIN52 (13kDa) in lysates of HepaRG cells treated with harmine or vehicle control and in the same samples after lambda protein phosphatase (λPP)

treatment. The upper band represents the phosphorylated LIN52 protein and the lower band the unphosphorylated protein. Alpha-tubulin served as loading control. E. Dot plots representing relative normalized expression of early (E2f1, Cdc6, Pcna) and late (Ccnb1, Plk1,Ect2) cell cycle progression genes in liver organoids treated with either vehicle or harmine (n=4-6 culture replicates per condition). * indicates $p \leq 0.05$, N.S. not significant.

LIN52 phosphorylation upon DYRK1A inhibition

An earlier study in cell lines by Litovchik et al. demonstrated that DYRK1A-mediated phosphorylation of LIN52 inhibits S phase entry from a quiescent state through assembly of the *D*imerization Partner, *R*B-like, *E*2F and *m*ulti-vulva class B (DREAM) complex [32, 33]. This protein complex represses numerous cell cycle genes [34]. We asked whether this function of DYRK1A would underlie the phenotypes we observed in HPCs, and more specifically, if DYRK1A inhibition would affect LIN52 phosphorylation. We performed a Western blot for LIN52 which yielded two bands, the upper band represents the phosphorylated LIN52 protein and the lower band the unphosphorylated and therefore faster migrating LIN52. Chemical inhibition of DYRK1A in HepaRG cells resulted in less phospho-LIN52 and more unphosphorylated LIN52 (Fig. 4*D*). Impaired DREAM complex formation would facilitate S phase entry and cell cycle progression. Transcriptional analysis of liver organoids showed that DYRK1A inhibition increased the expression of genes associated with G1 and early S phase (*E2f1*, *Cdc6*, *Pcna*) as well as late S, G2 and mitotic progression (*Ccnb1*, *Plk1*, *Ect2*) (Fig. 4*E*). Importantly, these genes are known to be transcriptionally repressed by the DREAM complex (34). Together these data indicate that DYRK1A inhibition decreases LIN52 phosphorylation, resulting in disassembly of the DREAM complex and subsequent upregulation of DREAM target genes and forced S phase entry in hepatic progenitor cells.

Effect of DYRK1A overexpression in liver organoids on EdU positivity and proliferation

Previous work showed that the effects of DYRK1A are highly dependent on gene dosage, as both haploinsufficiency and the presence of an extra copy of the DYRK1A gene have been described to affect proliferation in neural progenitor cells [30, 35]. We hypothesized that an overexpression of DYRK1A in HPCs would impair S phase entry and as a result decrease proliferation. To answer this question liver organoid cultures were established from mBACtgDyrk1A mice, which harbor one extra copy of the murine *Dyrk1a* gene (*Dyrk+++*), and their wildtype (WT) littermates. From both WT and *Dyrk+++* mouse livers biliary duct fragments could be isolated and after two to five days organoids appeared in the cultures. However, the growth of *Dyrk+++* organoids was reduced compared to WT cultures (Fig. 5*A*). Quantitative PCR showed that the liver organoids derived from *Dyrk+++* mice showed a 1.67 fold increase in *Dyrk1a* transcripts consistent with one extra allele of this gene (Fig. 5*B*). Proliferation was quantified with growth curves and was significantly reduced in *Dyrk+++* organoids compared to WT organoids (Fig. 5*C*). To study S phase entry, WT and *Dyrk+++* organoids were pulsed with EdU for 3 hours. *Dyrk+++* organoids had a significantly lower percentage of EdU^+ cells compared to WT organoids (Fig. 5*D*). Thus, one extra allele of Dyrk1a is sufficient to decrease S phase entry and proliferation of primary hepatic progenitor cells.

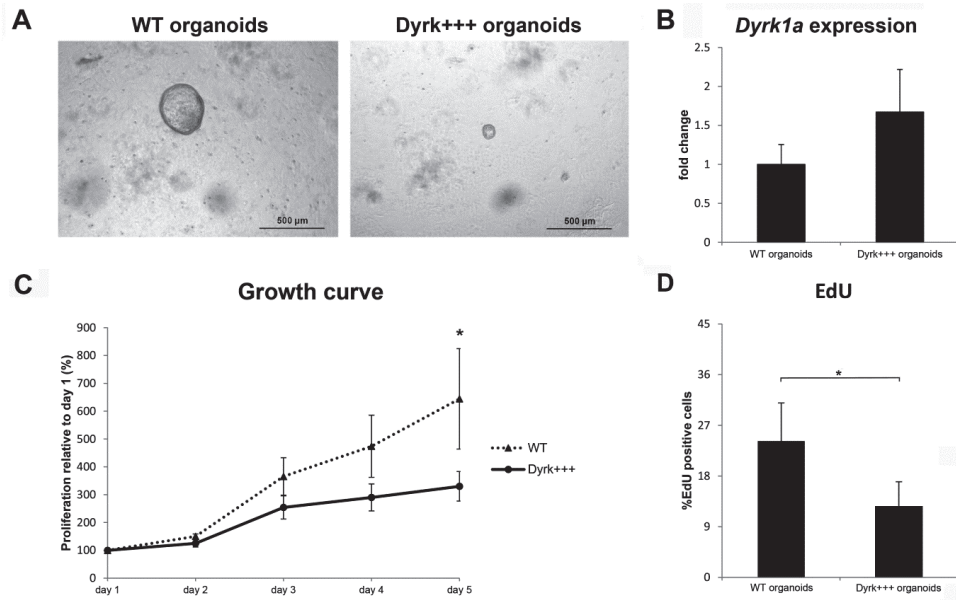

Figure 5. Effects of DYRK1A overexpression in liver organoids on EdU positivity and proliferation. A. Representative phase contrast images of liver organoids cultured from mBACtgDyrk1A mice, which harbor one extra copy of the murine Dyrk1a gene (Dyrk+++), and their wildtype (WT) littermates. Images were taken seven days after duct isolation. B. Relative normalized gene expression of Dyrk1a in liver organoids cultured from WT (n=5 donors) and Dyrk+++ (n=4 donors) mice, showing a 1.67 fold Dyrk1a overexpression. C. Growth curve of WT and Dyrk+++ organoids (n=4 culture replicates per genotype) as measured with an Alamar blue assay on the same wells on consecutive days. Serial luminescence measurements were normalized to day 1 (100%). Representative curve is shown for three WT versus Dyrk+++ donor cultures. D. Percentage of EdU+ cells in WT and Dyrk+++ liver organoids after 48h of treatment with either vehicle or harmine. At least 3500 nuclei were counted per condition (divided over 12 sections per condition). * indicates $p \leq 0.05$, N.S. not significant.

Discussion

Our screen is an unbiased search for intracellular mechanisms in HPC proliferation and reveals DYRK1A as essential kinase in the negative regulation of S phase entry in HPCs. Moreover, an exact gene dosage of DYRK1A proved to be crucial, as both silencing and 1.5 fold overexpression perturbed HPC cell cycle progression.

Our study is in line with previous work showing that DYRK1A plays a particularly important role in tissue-specific stem cells. However the consequences of DYRK1A perturbation seem organ-specific. DYRK1A was initially discovered as the human homolog of the Drosophila minibrain (mnb) gene, involved in neurogenesis [36, 37]. In neural progenitors strict regulation of DYRK1A activity is essential for appropriate function, since both in case of one extra copy and in case of a DYRK1A knockout neurodegenerative and cognitive disorders develop. We found that inhibition of DYRK1A in HPCs increased S phase entry but did not enhance proliferation. *Dyrk1a* haploinsufficiency in mice results in decreased size of certain brain areas [38]. Inactivating *DYRK1A* mutations in humans are associated with mental retardation and microcephaly [39, 40]. Mnb/Dyrk1a loss of function in developing chick spinal cord results in an increased percentage of $BrdU^+$ and mitotic cells but also in increased apoptosis [30]. We also observed an increased percentage of EdU^+ and $pH3^+$ cells, but not

an increased cell number nor decreased cell viability upon DYRK1A inhibition in either HepaRG cells or organoids, which could be explained by a subsequent delay in G2-M-phase progression.
Interestingly, the effect of DYRK1A perturbation are partly similar in pancreatic cells. The DYRK1A inhibitor harmine was discovered in a chemical screen as an activator of rat and human pancreatic β cell replication, a cell type that is predominantly quiescent [31]. Chemical inhibition of DYRK1A increased β cell BrdU and Ki67 labelling both *in vitro* and *in vivo*. This is in agreement with our findings in HPCs. However, the study also described an induction of β cell proliferation, based on increased β cell mass upon partial pancreatectomy and concurrent treatment with harmine in mice. In addition, harmine treatment improved glycemic control in two mouse models after human pancreatic islet transplantation. A confounding factor to this anti-diabetic effect could have been the agonistic effect of harmine on PPARgamma, that was previously shown to improve glucose tolerance and response to insulin in diabetic mice by itself [41]. However, our results strongly suggest that in hepatic progenitor cells DYRK1A inhibition does not enhance proliferation. Its inactivation did not elicit a pro-proliferative effect, despite increased S phase entry and gene expression of various cell cycle markers. Rather, carefully balanced DYRK1A activity appears to play an important role in coordinating S-phase entry of quiescent hepatic progenitor cells.
In line with this, we found that overexpression of DYRK1A in HPCs decreased S phase entry and decreased proliferation. Similarly, in embryonic mouse brain and chick spinal cord *Dyrk1a* overexpression resulted in proliferation arrest of neural progenitors [30, 35]. This was confirmed by Park et al. who found that DYRK1A overexpression resulted in attenuated proliferation of human ES cell-derived neural precursors [29]. DYRK1A is located on the Down Syndrome critical region of chromosome 21 and is considered to contribute to abnormal brain development and mental retardation in human Down Syndrome [29, 42]. To evaluate whether the phenotype we observed is specific for HPCs, we also studied other liver cell lines (stellate cells, hepatocytes) but did not observe the same effect of DYRK1A inhibition on the cell cycle.
Previous publications have reported on a role of DYRK1A in cell cycle progression based on interaction with the DREAM (DP, RB, E2F and MuvB) complex [32, 33, 43]. DYRK1A can phosphorylate LIN52, a subunit of the MuvB core, which is necessary for DREAM complex assembly and entry into a quiescent state. When DYRK1A-mediated phosphorylation of LIN52 is blocked, the MuvB core dissociates from the DREAM complex and binds to MYB (MMB complex) to initiate cell cycle entry. Transcriptional analysis has indicated that the DREAM complex can repress transcription of genes in both early (G1/S) and late (G2/M) cell cycle progression [34]. MMB target genes are transcriptionally activated and are mainly involved in G2/M phase of the cell cycle. We found that chemical inhibition of DYRK1A decreased LIN52 phosphorylation in HPCs, which would impair DREAM and favor MMB complex formation. Indeed, in harmine-treated HPCs expression of early cell cycle DREAM target genes *E2f1*, *Cdc6* and *Pcna* was upregulated as well as expression of late cell cycle MMB target genes *Ccnb1*, *Plk1* and *Ect2*.
There are a few limitations to our study. To reduce variation, the siRNA screen was performed in a cell line, which is naturally transformed and hence may not fully represent HPCs *in vivo*. This limitation could largely be overcome by including primary HPCs as a biological validation of obtained hits. Second, we chose to focus our screen to a kinase library, because kinases are known for their involvement in proliferation and are potential drug targets. Third, we exerted quite a stringent hit validation approach to select only for true positive hits. However, this strategy could have resulted in false negatives.

In conclusion, we found an essential role of DYRK1A as regulator of quiescence versus cell cycle progression in HPCs. A possible mechanism is through interference with DREAM and MMB complex formation, involved in S phase entry from a G0 quiescent state. Future research may focus on upstream regulation of DYRK1A transcription and activity in HPCs and other downstream effector mechanisms of DYRK1A phosphorylation targets. Knowledge gained in these studies can contribute to our understanding of HPC quiescence and activation and may provide tools to enhance HPC-mediated liver regeneration during severe liver disease.

Acknowledgments
This study was funded by the Netherlands Organization for Scientific Research NWO ZON/MW (116004121). The authors would like to thank Daphne Lelieveld and Dr. Sathidpak Nantasanti for technical assistance, Balaji Ramalingam for data analysis, and Prof. Scott Friedman for providing the LX2 cell line.

References

1. Higgins GM and RM Anderson. (1931). Experimental pathology of the liver. I. Restoration of the liver of the white rat following partial surgical removal. Arch Pathol 12:186-202.

2. Riehle KJ, YY Dan, JS Campbell and N Fausto. (2011). New concepts in liver regeneration. J Gastroenterol Hepatol 26: Suppl 1:203-212.

3. Katoonizadeh A, F Nevens, C Verslype, J Pirenne and T Roskams. (2006). Liver regeneration in acute severe liver impairment: a clinicopathological correlation study. Liver Int 26:1225-1233.

4. Lunz JG,3rd, H Tsuji, I Nozaki, N Murase and AJ Demetris. (2005). An inhibitor of cyclin-dependent kinase, stress-induced p21Waf-1/Cip-1, mediates hepatocyte mito-inhibition during the evolution of cirrhosis. Hepatology 41:1262-1271.

5. Liu L, GR Yannam, T Nishikawa, T Yamamoto, H Basma, R Ito, M Nagaya, J Dutta-Moscato, DB Stolz, F Duan, KH Kaestner, Y Vodovotz, A Soto-Gutierrez and IJ Fox. (2012). The microenvironment in hepatocyte regeneration and function in rats with advanced cirrhosis. Hepatology 55:1529–1539.

6. Roskams T, R De Vos, P Van Eyken, H Myazaki, B Van Damme and V Desmet. (1998). Hepatic OV-6 expression in human liver disease and rat experiments: evidence for hepatic progenitor cells in man. J Hepatol 29:455-463.

7. Lowes KN, BA Brennan, GC Yeoh and JK Olynyk. (1999). Oval cell numbers in human chronic liver diseases are directly related to disease severity. Am J Pathol 154:537-541.

8. Libbrecht L, D Cassiman, V Desmet and T Roskams. (2001). Expression of neural cell adhesion molecule in human liver development and in congenital and acquired liver diseases. Histochem Cell Biol 116:233-239.

9. Tan J, P Hytiroglou, R Wieczorek, YN Park, SN Thung, B Arias and ND Theise. (2002). Immunohistochemical evidence for hepatic progenitor cells in liver diseases. Liver 22:365-373.

10. Boulter L, O Govaere, TG Bird, S Radulescu, P Ramachandran, A Pellicoro, RA Ridgway, SS Seo, B Spee, N Van Rooijen, OJ Sansom, JP Iredale, S Lowell, T Roskams and SJ Forbes. (2012). Macrophage-derived Wnt opposes Notch signaling to specify hepatic progenitor cell fate in chronic liver disease. Nat Med 18:572-579.

11. Gouw AS, AD Clouston and ND Theise. (2011). Ductular reactions in human liver: diversity at the interface. Hepatology 54:1853-1863.

12. Orford KW and DT Scadden. (2008). Deconstructing stem cell self-renewal: genetic insights into cell-cycle regulation. Nat Rev Genet 9(2):115-128.

13. Fuchs E and T Chen. (2013). A matter of life and death: self-renewal in stem cells. EMBO Rep 14:39-48.

14. Spee B, G Carpino, BA Schotanus, A Katoonizadeh, S Vander Borght, E Gaudio and T Roskams. (2010). Characterisation of the liver progenitor cell niche in liver diseases: potential involvement of Wnt and Notch signalling. Gut 59:247-257.

15. Ishikawa T, VM Factor, JU Marquardt, C Raggi, D Seo, M Kitade, EA Conner and SS Thorgeirsson. (2012). Hepatocyte growth factor/c-met signaling is required for stem-cell-mediated liver regeneration in mice. Hepatology 55:1215-1226.

16. Tirnitz-Parker JE, CS Viebahn, A Jakubowski, BR Klopcic, JK Olynyk, GC Yeoh and B Knight. (2010). Tumor necrosis factor-like weak inducer of apoptosis is a mitogen for liver progenitor cells. Hepatology 52:291-302.

17. Kallis YN, AJ Robson, JA Fallowfield, HC Thomas, MR Alison, NA Wright, RD Goldin, JP Iredale and SJ Forbes. (2011). Remodelling of extracellular matrix is a requirement for the hepatic progenitor cell response. Gut 60:525-533.

18. Rauch J, N Volinsky, D Romano and W Kolch. (2011). The secret life of kinases: functions beyond catalysis. Cell Commun Signal 9(1):23,811X-9-23.

19. Lindqvist A, V Rodriguez-Bravo and RH Medema. (2009). The decision to enter mitosis: feedback and redundancy in the mitotic entry network. J Cell Biol 185:193-202.

20. Garnier D, P Loyer, C Ribault, C Guguen-Guillouzo and A Corlu. (2009). Cyclin-dependent kinase 1 plays a critical role in DNA replication control during rat liver regeneration. Hepatology 50:1946-1956.

21. Huch M, C Dorrell, SF Boj, JH van Es, VS Li, M van de Wetering, T Sato, K Hamer, N Sasaki, MJ Finegold, A Haft, RG Vries, M Grompe and H Clevers. (2013). In vitro expansion of single Lgr5+ liver stem cells induced by Wnt-driven regeneration. Nature 494:247-250.

22. Guedj F, PL Pereira, S Najas, MJ Barallobre, C Chabert, B Souchet, C Sebrie, C Verney, Y Herault, M Arbones, JM Delabar. (2012). DYRK1A: a master regulatory protein controlling brain growth. Neurobiol Dis 46:190-203.

23. Salic A and TJ Mitchison. (2008). A chemical method for fast and sensitive detection of DNA synthesis in vivo. Proc Natl Acad Sci U S A 105:2415-2420.

24. Birmingham A, LM Selfors, T Forster, D Wrobel, CJ Kennedy, E Shanks, J Santoyo-Lopez, DJ Dunican, A Long, D Kelleher, Q Smith, RL Beijersbergen, P Ghazal, CE Shamu. (2009). Statistical methods for analysis of high-throughput RNA interference screens. Nat Methods 6:569-575.

25. Simpson KJ, LM Selfors, J Bui, A Reynolds, D Leake, A Khvorova and Brugge JS. (2008). Identification of genes that regulate epithelial cell migration using an siRNA screening approach. Nat Cell Biol 10:1027-1038.

26. van Steenbeek FG, L Van den Bossche, GC Grinwis, A Kummeling, IH van Gils, MJ Koerkamp, D van Leenen, FC Holstege, LC Penning, J Rothuizen, PA Leegwater and B Spee. (2013). Aberrant gene expression in dogs with portosystemic shunts. PLoS One 8:e57662.

27. Adayev T, J Wegiel and YW Hwang. (2011). Harmine is an ATP-competitive inhibitor for dual-specificity tyrosine phosphorylation-regulated kinase 1A (Dyrk1A). Arch Biochem Biophys 507:212-218.

28. Gockler N, G Jofre, C Papadopoulos, U Soppa, FJ Tejedor and W Becker. (2009). Harmine specifically inhibits protein kinase DYRK1A and interferes with neurite formation. FEBS J 276:6324-6337.

29. Park J, Y Oh, L Yoo, MS Jung, WJ Song, SH Lee, H Seo and KC Chung. (2010. Dyrk1A phosphorylates p53 and inhibits proliferation of embryonic neuronal cells. J Biol Chem 285):31895-31906.

30. Hammerle B, E Ulin, J Guimera, W Becker, F Guillemot and FJ Tejedor. (2011). Transient expression of Mnb/Dyrk1a couples cell cycle exit and differentiation of neuronal precursors by inducing p27KIP1 expression and suppressing NOTCH signaling. Development 138:2543-2554.

31. Wang P, JC Alvarez-Perez, DP Felsenfeld, H Liu, S Sivendran, A Bender, A Kumar, R Sanchez, DK Scott, A Garcia-Ocaña and AF Stewart. (2015). A high-throughput chemical screen reveals that harmine-mediated inhibition of DYRK1A increases human pancreatic beta cell replication. Nat Med 21:383-388.

32. Litovchick L, S Sadasivam, L Florens, X Zhu, SK Swanson, S Velmurugan, R Chen, MP Washburn, XS Liu and JA DeCaprio. (2007). Evolutionarily conserved multisubunit RBL2/p130 and E2F4 protein complex represses human cell cycle-dependent genes in quiescence. Mol Cell 26:539-551.

33. Litovchick L, LA Florens, SK Swanson, MP Washburn and JA DeCaprio. (2011). DYRK1A protein kinase promotes quiescence and senescence through DREAM complex assembly. Genes Dev 25:801-813.

34. Fischer M, P Grossmann, M Padi and JA DeCaprio. (2016). Integration of TP53, DREAM, MMB-FOXM1 and RB-E2F target gene analyses identifies cell cycle gene regulatory networks. Nucleic Acids Res 44:6070-6086.

35. Yabut O, J Domogauer and G D'Arcangelo. (2010). Dyrk1A overexpression inhibits proliferation and induces premature neuronal differentiation of neural progenitor cells. J Neurosci 30:4004-4014.

36. Tejedor F, XR Zhu, E Kaltenbach, A Ackermann, A Baumann, I Canal, M Heisenberg, KF Fischbach and O Pongs. (1995). minibrain: a new protein kinase family involved in postembryonic neurogenesis in Drosophila. Neuron 14:287-301.

37. Shindoh N, J Kudoh, H Maeda, A Yamaki, S Minoshima, Y Shimizu and N Shimizu. (1996). Cloning of a human homolog of the Drosophila minibrain/rat Dyrk gene from "the Down syndrome critical region" of chromosome 21. Biochem Biophys Res Commun 225:92-99.

38. Fotaki V, M Dierssen, S Alcantara, S Martinez, E Marti, C Casas, J Visa, E Soriano, X Estivill, ML Arbonés. (2002). Dyrk1A haploinsufficiency affects viability and causes developmental delay and abnormal brain morphology in mice. Mol Cell Biol 22:6636-6647.

39. Moller RS, S Kubart, M Hoeltzenbein, B Heye, I Vogel, CP Hansen, C Menzel, R Ullmann, N Tommerup, HH Ropers, Z Tümer and VM Kalscheuer. (2008). Truncation of the Down syndrome candidate gene DYRK1A in two unrelated patients with microcephaly. Am J Hum Genet 82:1165-1170.

40. van Bon BW, A Hoischen, J Hehir-Kwa, AP de Brouwer, C Ruivenkamp, AC Gijsbers, CL Marcelis, N de Leeuw, JA Veltman, HG Brunner and BB de Vries. (2011). Intragenic deletion in DYRK1A leads to mental retardation and primary microcephaly. Clin Genet 79:296-299.

41. Waki H, KW Park, N Mitro, L Pei, R Damoiseaux, DC Wilpitz, K Reue, E Saez, P Tontonoz. (2007). The small molecule harmine is an antidiabetic cell-type-specific regulator of PPARgamma expression. Cell Metab 5:357-370.

42. Kurabayashi N and K Sanada. (2013). Increased dosage of DYRK1A and DSCR1 delays neuronal differentiation in neocortical progenitor cells. Genes Dev 27:2708-2721.

43. Boichuk S, JA Parry, KR Makielski, L Litovchick, JL Baron, JP Zewe, A Wozniak, KR Mehalek, N Korzeniewski, DS Seneviratne, P Schöffski, M Debiec-Rychter, JA DeCaprio and A Duensing. (2013). The DREAM complex mediates GIST cell quiescence and is a novel therapeutic target to enhance imatinib-induced apoptosis. Cancer Res 73:5120-5129.

Part II

Growth factors and hepatic progenitor cells in models of liver disease

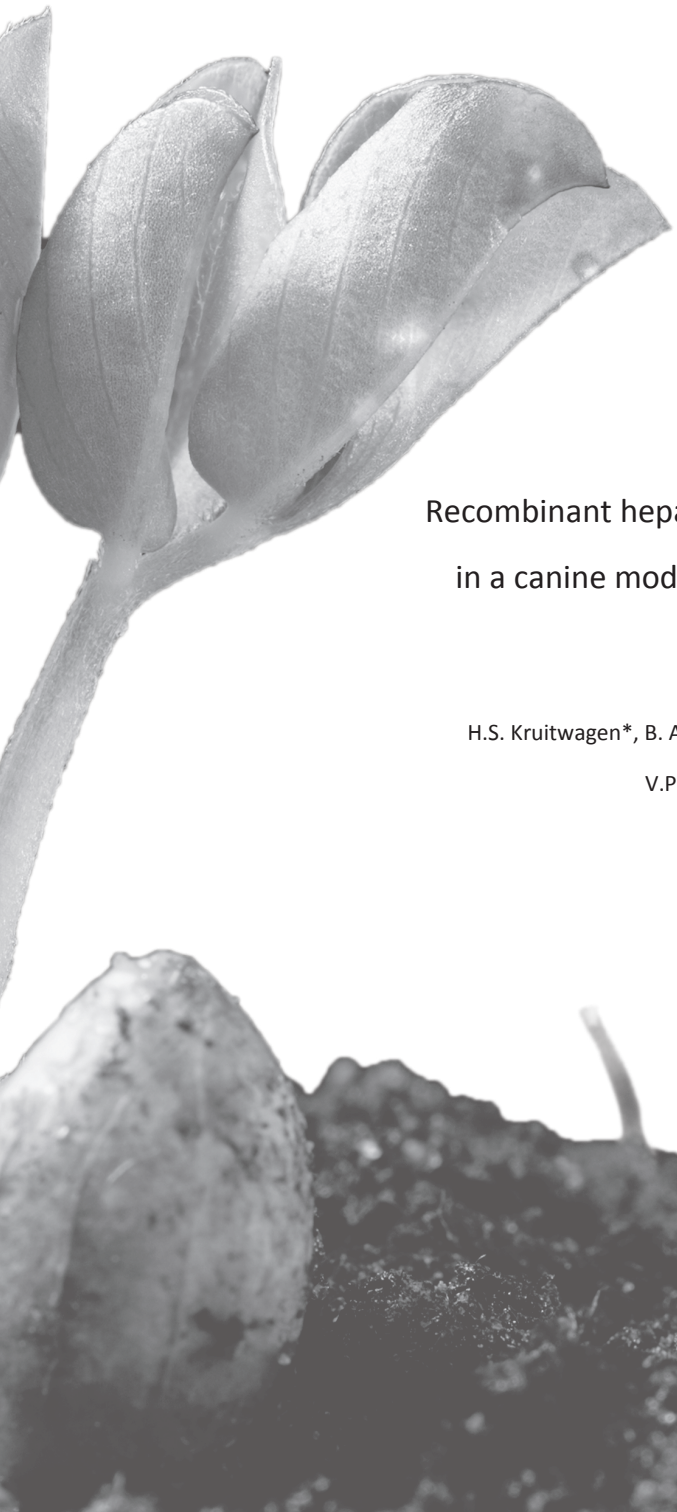

Chapter 5

Recombinant hepatocyte growth factor treatment in a canine model of congenital liver hypoplasia.

H.S. Kruitwagen*, B. Arends*, B. Spee, B. Brinkhof, T.S. van den Ingh,

V.P. Rutten, L.C. Penning, T. Roskams, J. Rothuizen

Liver Int. 2011 Aug;31(7):940-9

*Equal contribution

Abstract

Background: Although the liver has a large regenerative capacity, in many hepatopathies these repair mechanisms fail. The therapeutic potential of Hepatocyte Growth Factor (HGF) has been proven in numerous toxin-induced liver failure models in rodents, but never in spontaneously occurring liver diseases in larger animal models.
Aim: The aim of this study was to induce liver growth in a hypoplastic liver by administration of exogenous recombinant HGF. The natural hypoplastic liver model used is the canine congenital portosystemic shunt (CPSS) characterized by strongly reduced liver growth and function.
Methods: Recombinant HGF (rHGF), 200 μg/kg, was given twice daily during three weeks by intravenous injection in six dogs with CPSS. Liver volumes were determined by computed tomography before and at 1, 2, 3, and 7 weeks after initiation of treatment. Portosystemic shunting was evaluated with an ammonia tolerance test and liver portal perfusion was quantified with scintigraphy. Simultaneously, blood parameters for liver function were assayed and liver biopsies were taken for histology, immunohistochemistry and gene-expression measurements.
Results: During three weeks of HGF treatment, hepatocyte proliferation increased and an increase in liver volume up to 44% was seen, persisting in two dogs up to four weeks after termination of treatment. Ki-67 expression, gene-expression of E2F1 and CDC6, phosphorylated-c-MET and phosphorylated-ERK1/2 protein levels confirmed increased hepatocyte proliferation and HGF signaling. The aberrant portal perfusion did not change during treatment.
Conclusions: Transient *in vivo* liver growth is shown using CPPS as naturally occurring large animal model, indicating therapeutic potential of HGF in liver disease.

Introduction

The growing incidence of chronic liver diseases and limited availability of donor organs reflect the need for new therapeutic strategies (1). Growth factors have a huge potential to elicit liver regeneration and to improve the management and outcome of both acute and chronic liver disease (2, 3). A promising candidate to stimulate liver growth is Hepatocyte Growth Factor (HGF). HGF was discovered in regenerating canine liver tissue as a growth factor that could reverse liver atrophy (4). Besides this mitogenic potential, HGF has motogenic and morphogenic effects in many tissue types including the liver (5). The therapeutic potential of HGF is proven in numerous toxin-induced acute and chronic liver failure models in rodents (6-8). To our knowledge no studies have investigated the use of HGF in clinical patients or large animal models with spontaneous liver disease. Therefore longitudinal molecular changes during HGF treatment and post-treatment effects are unknown. Dogs with liver diseases referred to veterinary academic centers are gaining increased attention as a bridge from rodent models to human medicine (9), because they show a high homology with human liver diseases (10-12). Dogs with hampered liver growth and function were advocated to study the effect of HGF treatment, since their hypoplastic livers lack confounders such as severe fibrosis and active inflammation (13). The hampered liver growth is caused by a congenital portosystemic shunt (CPSS) of the liver, which is an abnormal vascular communication between the hepatic portal vein and the caudal vena cava, or the vena azygos (14, 15). Consequently, portal blood flow from the gastrointestinal tract is diverted past the liver. Dogs with CPSS have a reduced hepatic volume (16, 17). CPSS offers a unique large animal model to investigate liver growth and give proof of principle, as it is a simple model of liver hypoplasia without concurrent pathology. On a molecular level, the presence of the receptor of HGF (c-MET), and functional downstream regulators indicate that dogs with CPSS are excellent candidates for treatment with HGF (13).
The aim of the present study is to examine the effect of recombinant HGF treatment on liver size and function in a canine model of liver hypoplasia. To achieve this, a clinical study was devised in which privately-owned dogs with a congenital portosystemic shunt were treated with recombinant HGF. We hypothesized that HGF could have a hepatotrophic effect in clinical liver hypoplasia, resulting in an increase in liver size upon three weeks of HGF administration. Since post-treatment effects are rarely measured in rodent models, we included a follow-up measurement at four weeks after the last HGF administration. Results showed a significant increase in liver volume indicating that recombinant HGF could be an effective treatment for hypoplastic liver diseases.

Materials and methods

Materials.
Recombinant feline HGF (rHGF 150 µg/ml dissolved in 0.3 M NaCl, 100 mM sodium citrate, and 0.01% Tween 80) was provided by Zenoaq (Fukushima, Japan) and was stored at -20°C until use. Feline HGF has a high homology in amino acid sequence with canine HGF (97.5 %). Furthermore, mitogenic activity of recombinant feline HGF is similar to recombinant human HGF and recombinant canine HGF in canine liver cells *in vitro* (supplemental file 1) (18).

Dogs, rHGF treatment and sampling.
This experiment was approved by and performed to the standards of the local ethics committee as required under Dutch legislation. Written informed consent from the owners was obtained for all

dogs. Six dogs entered in the study with a mean age of 2.0 years (range 0.5-5.7 years) and a body weight of less than 7 kilograms. Breeds included Yorkshire terrier (n=2), Jack Russel terrier (n=2), West Highland White terrier (n=1) and Miniature Poodle (n=1). By means of ultrasonography, all dogs were diagnosed with an extrahepatic congenital portosystemic shunt at the University Clinic for Companion Animals, Utrecht University (19). The dogs were hospitalized and received treatment with rHGF (200 µg/kg; two times a day) for a period of 3 weeks through a central venous catheter (Cavafix®Certo®, B.Braun, Oss, the Netherlands) in the jugular vein. Liver volume measurements, liver biopsies for molecular and histopathological analysis, and blood and urine analysis were performed before (week 0) during (weeks 1, 2, and 3) and 7 weeks (week 7) after starting rHGF treatment (Fig. 1). Ultrasound guided liver biopsies were taken with a 14G tru-cut needle (ACN™, Medicor, Nieuwegein, the Netherlands). One week in advance and during the study the dogs were fed the Royal Canin hepatic diet (Veghel, the Netherlands).

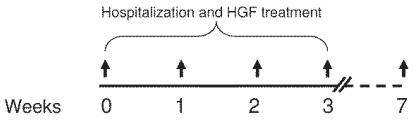

Figure 1. Schedule of hospitalization and rHGF treatment. Numbers 0-7 on the X-axis indicate weeks of treatment. HGF treatment is daily for three weeks. Measurements were performed before rHGF administration (week 0), during rHGF treatment (week 1, 2, and 3) and dogs returned to the clinic for a follow-up measurement four weeks after the last rHGF administration (week 7). Arrows indicate an examination point of blood and urine analysis, CT scan, perfusion scintigraphy, and liver biopsy (exception: no liver biopsy in week 2).

Blood and urine analysis.
Blood was sampled through the jugular catheter and plasma was analyzed with routine clinical laboratory methods for the following parameters; activity of alanine aminotransferase (ALT), aspartate aminotransferase (AST), alkaline phosphatase (AP), and concentration of ammonia, (fasting) bile acids concentration, total protein, albumin, urea, creatinin, and fibrinogen. Coagulation was further measured by assessing prothrombin time (PT) and activated partial thromboplastin time (APTT). Urine was sampled by ultrasound-guided cystocenthesis and analyzed for total proteins and creatinine. All clinical chemistry parameters were assessed under standardized conditions.

Anaesthesia.
General anaesthesia was required for computed tomography, perfusion scintigraphy, and sampling of liver biopsies. For premedication, 0.3 mg/kg methadone IV (Eurovet, Bladel, the Netherlands) and 0.02 mg/kg atropine IM (Eurovet) were used. For induction, 1-5 mg/kg propofol IV (PropoVet™, AST Farma, Oudewater, the Netherlands) was given. For maintenance of anaesthesia isoflurane (IsoFlo, AST Farma) was given via an endotracheal tube (0.5-2% Et). During recovery 10-20 µg/kg buprenorphine was given intramuscularly (Temgesic®, Schering-Plough, Utrecht, the Netherlands).

Determination of liver volume using computed tomography (*CT)*.
CT was performed in the anaesthetized dogs with a single slice spiral CT scanner (Secura, Philips NV, Eindhoven, the Netherlands). CT of the liver was performed using 120 kV, 280 mA, 0.7 s scan time, with a pediatric filter and contrast enhanced (Xenetix®, Brussels, Belgium). Section thickness was 3

mm, with a 1 mm pitch and a reconstructed section thickness of 2 mm. Liver volume was calculated using EasyVision software (Philips Healthcare, Eindhoven, the Netherlands) with a window width of 200 and a window level of 50. Determination of the Region of Interest and liver volume calculation was performed as described before (20).

Liver histology and Ki-67 immunohistochemistry.
For (immuno)histochemistry, liver biopsies were fixed in 4% formaldehyde which was replaced by 70% EtOH after 4 hours, embedded in paraffin, and stored at 4°C until use. For histological evaluation, tissue sections were stained with H&E and were examined by one board-certified veterinary pathologist (TvdI). Tissue sections were mounted on poly-L-lysine coated slides and used directly for immunohistochemistry. An immunohistochemistry protocol was used as described before, however for the washing steps PBS-Tween 0.1% was used (21). As a negative control, the primary antibody was omitted. For all sections the total number of Ki-67 positive hepatocyte nuclei was counted at 200x original magnification in the parenchyma, excluding portal triads and cells of non-hepatic origin. For each section, the total parenchymal area was calculated with ImageTool software (University of Texas Health Science Center, San Antonio, USA) and a spatial calibration using standardized magnification settings. Scoring was performed blindly.

Perfusion scintigraphy.
Perfusion scintigraphy was performed as described previously (22). A shunt index (SI) was calculated, describing the fraction of portal blood that bypasses the liver.

Ammonia tolerance test.
The validated ammonia tolerance test was used to measure the metabolic effect of portosystemic shunting. A dose of 2 ml/kg NH_4Cl (5%) was administered rectally to the colon via a 2.0 mm Arnolds® catheter (AUV, Cuijk, the Netherlands). The amount of ammonia in the blood was measured at 0, 20, and 40 minutes after the injection using the Ammonia Test Kit II (Arkray, Amstelveen, the Netherlands) combined with the Ammonia Checker II (Menarini, Florence, Italy) (23).

RNA isolation, reverse transcriptase reaction and real-time quantitative PCR (QPCR).
For RNA isolation and real-time quantitative PCR measurements, liver biopsies were fixed in RNAlater (Applied Biosystems, Nieuwerkerk a/d IJssel, the Netherlands) for 24 hours and then stored at -70°C until use. RNA isolation and QPCR were performed as described previously (18). Gene-expressions were normalized with the average gene-expressions of the endogenous references *Beta-2-microglobulin* (*B2M)*, *Hypoxanthine Guanine Phosphoribosyl Transferase-1* (*HPRT1)*, *Ribosomal Protein S5* (*RPS5)*, and *Ribosomal Protein S19 (RPS19)* (24, 24). Primer sequences and characteristics are indicated in Table 1. Statistical analysis was performed using R software (The R Foundation for Statistical Computing, Vienna, Austria) and consisted of a general linear model on the log normalized relative gene expression with random dog liver sample effects and fixed time effects. Changes were considered significant when $p \leq 0.05$.

Table 1. Nucleotide sequences of dog-specific primers for real-time quantitative PCR

Gene	F/R	Sequence (5' → 3')	Tm (°C)	Product size (bp)	Accession number
albumin	F	TGTTCCTGGGCACGTTTTTGTA	63.8	92	AB090854
	R	GGCTTCATATTCCTTGGCGAGTCT			
ASL	F	CTAGAGGTACAGAAGCGG	58	125	XM_536832
	R	TGCTGTTGAGAGTGATGG			
HGFA	F	AAACTGGAGCGGATGGCACAG	66	128	AY458142
	R	ACACAGACGTTTGGCATCGAGAAGTAT			
c-MET	F	TGTGCTGTGAAATCCCTGAATAGAATC	56	112	AB118945
	R	CCAAGAGTGAGAGTACGTTTGGATGAC			
E2F1	F	GCCCCATTGACGTTTTCC	62	179	XM_542963.2
	R	GAGCAGGGACTGGCTGG			
CDC6	F	CAGTTCTGTGCCCGAAAAGTC	63.5	291	XM_537648
	R	GAGGAGCAAAGAGCAGACCAAG			
B2M	F	TCCTCATCCTCCTCGCT	61.2	85	XM_535458
	R	TTCTCTGCTGGGTGTCG			
HPRT	F	AGCTTGCTGGTGAAAAGGAC	56	100	NM_001003357
	R	TTATAGTCAAGGGCATATCC			
RPS5	F	TCACTGGTGAGAACCCCCT	62.5	141	XM_533568
	R	CCTGATTCACACGGCGTAG			
RPS19	F	CCTTCCTCAAAAAGTCTGGG	61	95	XM_533657
	R	GTTCTCATCGTAGGGAGCAAG			

Western blot analysis.

For Western blot analysis, liver biopsies were snap frozen in liquid nitrogen and stored at -70°C until use. Western blotting was performed as described previously (13). Densitometric analysis of immunoreactive bands was performed with a ChemiDoc™ XRS System (Bio-Rad Laboratories, Veenendaal, the Netherlands) with Quantity One 4.6.5 software. Used antibodies are listed in Table 2.

Table 2. Antibodies used in Western blotting

Antigen	Manufacturer	Product size (kDa)	Dilution	Secondary antibody	Dilution
c-MET	Sigma (H97861)	169	1:750	Anti-goat	1:20,000
p-c-MET	Abcam (Ab5662)	169	1:750	Anti-rabbit	1:20,000
ERK1/2	Cell Signalling (9102)	44/42	1:1,000	Anti-rabbit	1:20,000
p-ERK1/2	Cell Signalling (9101)	44/42	1:500	Anti-rabbit	1:20,000
Actin	Lab Vision	42	1:2,000	Anti-mouse	1:20,000

Results

Clinical course of the HGF treatment.

During and after HGF treatment no sign of hepatic encephalopathy was noted in any of the patients, except for one dog that showed sopor and ataxia in the first week. No other direct adverse effect of the HGF administration was observed. After three weeks of treatment, one dog was renounced from the study due to haemolytic anemia and thrombocytopenia in week two and nephrotic syndrome in week three.

Blood and urine analysis.

Liver enzymes ALT and AP did not change during rHGF treatment. Low urea values were measured, varying from 0 to 2.0 mmol/L (ref: 3.0 to 12.5 mmol/L) reflecting hyperammonemia in dogs with CPSS. Low albumin values were measured, varying from 15 to 26 g/L (ref: 26 to 37 g/L), reflecting

insufficient liver function in dogs with CPSS. Overall, blood and urine parameters did not change considerably during and after rHGF treatment (data not shown).

Liver histology and proliferation index.

No recognizable portal veins were observed in the portal areas. Proliferation of arterioles and bile ducts, representing the usual pathological reaction of portal vein hypoperfusion, was observed (25). In addition, in most tissue sections lipogranulomas were present. Overall, a mild degree of non-specific inflammation was present with an increased amount of neutrophilic granulocytes in the hepatic sinusoids, a pronounced reticulohistiocytic system, and Kupffer cell proliferation. During and after rHGF treatment liver histology did not change. Binucleated hepatocytes (Table 3) were counted in the periportal parenchyma and expressed as the mean number per portal area. 1.31 Binuclear cells were present in week 0. During rHGF treatment the number increased to 1.77 in week 1 and 1.88 in week 3, and decreased to 1.02 in week 7. Immunohistochemical determinations of Ki-67 positive hepatocytes are provided in Fig. 2. At week 0, the number of Ki-67 positive hepatocyte nuclei ranged from 0.6-6.4 per mm^2, reflecting the liver's low proliferative state. At week 1, the number of Ki-67 positive hepatocytes ranged from 5.2 to 97.2 per mm^2, and at week 3 from 2.8-24.3 per mm^2. At week 7, the number of Ki-67 positive hepatocytes decreased to pretreatment levels in all dogs, except in dog number 3 (23.4 positive nuclei per mm^2). Examples of bi-nucleated hepatocytes and Ki-67 positive cells are provided in supplemental file 2.

Table 3. Proliferation index. Number of binucleated hepatocytes per portal area before rHGF administration (week 0), during rHGF treatment (week 1 and 3) and four weeks after rHGF treatment (week 7).

Weeks	Dog 1	Dog 2	Dog 3	Dog 4	Dog 5
0	1.3	1.8	2.0	1.0	0.5
1	2.1	2.4	2.2	1.4	0.75
3	1.6	2.0	3.7	1.0	1.1
7	0.6	1.5	1.7	0.9	0.4

Liver volume.

Liver volume was calculated from CT scans and increase is expressed as percentage of volume in week 0 (Fig. 2). During rHGF treatment all dogs showed an increase in liver volume, ranging from 13% to 44% within three weeks time. The progression and persistence of liver growth varied between dogs. Dog number 1 showed the largest increase in liver volume (44%), with most liver growth occurring in the last week of treatment (33%) (Fig.2). Dog number 2 reached a 27% increase after three weeks of treatment. At week 7, the increase in liver volume was sustained in two dogs at 16% and 13% (dog 2 and 3, respectively). Liver volume had decreased to pretreatment values in three dogs (dogs number 1, 4, and 5).

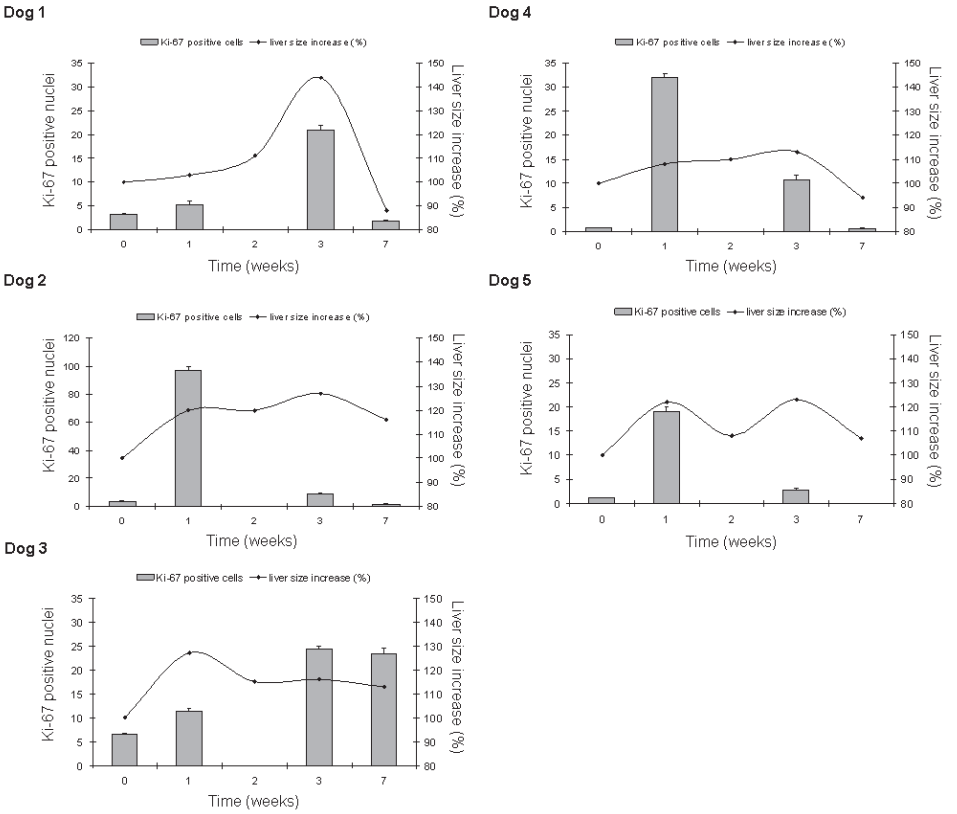

Figure 2. Liver volumes for each dog during and after rHGF treatment. Numbers 0-7 on the X-axis indicate weeks of treatment. Volume measurements were performed before rHGF administration (week 0), during rHGF treatment (week 1, 2, and 3) and dogs returned to the clinic for a follow-up measurement four weeks after the last rHGF administration (week 7). Liver volume is expressed as percentage of liver volume in week 0. Ki-67 positivity is expressed as number of positive hepatocyte nuclei per mm2 of hepatic parenchyma including standard deviation.

Portosystemic shunting.

Fasting blood ammonia levels were elevated in most dogs, varying from 34 to 135 µmol/L (reference: 24 to 45 µmol/L). Perfusion scintigraphy showed a shunt index that ranged from 96 to 100% in all dogs at entrance of the study. Portal perfusion of the liver did not change during and after rHGF treatment (supplemental file 4). Accordingly, results of the ammonia tolerance tests were and remained abnormal in all dogs. Blood ammonia levels consistently increased after rectal ammonia administration.

Gene expression of proliferation and liver function markers.

The mRNA levels of genes involved in hepatocyte function and HGF signalling are depicted in Fig. 3. Hepatocyte function was evaluated by measuring expression of *albumin (ALB)* and *argininosuccinate lyase* (*ASL*). *ALB* expression did not change during rHGF treatment, however *ASL* expression was down regulated in week 1 and 3 (all dogs) and normalized in week 7. HGF signalling showed a stable expression of *HGF activator (HGFA)* and *c-MET* during rHGF treatment. The expression of the

proliferation markers *E2F1* and its downstream effector *CDC6* increased significantly in week 1 and returned to basal levels in week 3 and 7.

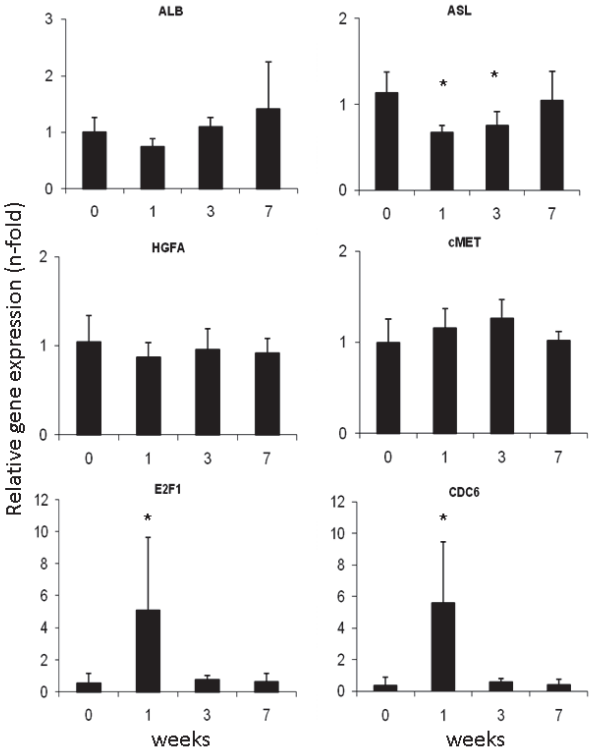

Figure 3. Gene-expression. The mRNA levels of several target genes were measured in liver tissue before rHGF treatment (week 0), during rHGF treatment (week 1 and 3) and four weeks after rHGF treatment (week 7). Bars represent average gene-expression and standard deviation of five dogs. * indicates significant change with $p \leq 0.05$

Activation of the HGF pathway.

During and after rHGF treatment, the presence and activation of key regulators of the HGF pathway were investigated with Western blotting (Fig. 4). In all dogs an equal amount of c-MET protein was detected throughout the study, confirming susceptibility of the liver to the administered rHGF. In the dogs c-MET phosphorylation upon rHGF treatment was increased in week 1 and 3, however in week 7 phosphorylated c-MET protein levels returned to pre-treatment control levels (Fig. 4 A, and Fig. 4B). Activation of ERK1/2, one of the main MAP kinases in HGF signalling, was measured with an anti-phospho-ERK1/2 antibody. The quantity varied between dogs, but an upregulation of activated ERK1/2 was found in all dogs during rHGF treatment (Fig. 4 A, and Fig. 4C).

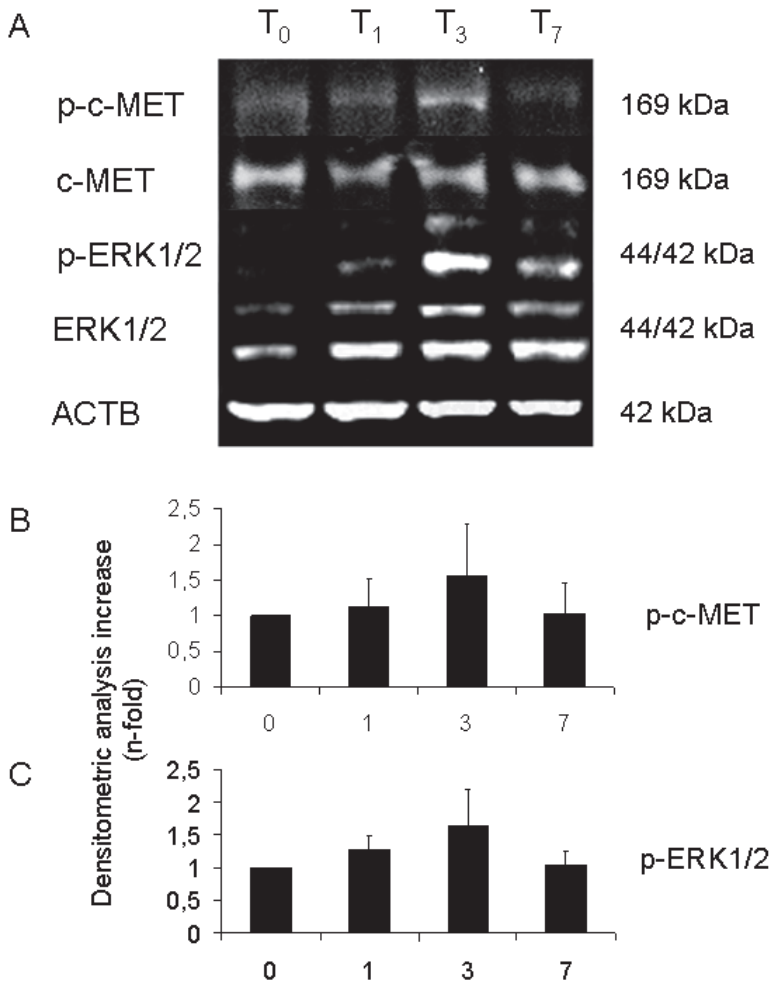

Figure 4. Activation of the HGF pathway. Western blot analysis on (phosphorylated) c-MET, (phosphorylated) ERK1/2 in liver samples for each dog before rHGF treatment (week 0), during rHGF treatment (week 1 and 3) and four weeks after rHGF treatment (week 7). Beta-actin (ACTB) was used as a loading control. Representative Western blot samples of dog 2 are shown in (A); Densitometric analysis of the expression of proteins of interest normalised to the densitometry of the loading control beta-actin is shown for phosphorylated c-MET (B) and phosphorylated ERK1/2 (C). Average increase (n-fold) is compared to week 0. Standard errors are based on normalised densitometric analysis of all individual dogs (n=5).

Discussion

To our knowledge this is the first study to describe the clinical application of rHGF. Both at an organ level and a biomolecular level, insight was gained on the action of HGF as an organotrophic factor in this naturally occurring hypoplastic liver disease. Three weeks treatment with rHGF resulted in a transient increase in liver volume.

HGF is well known as an organotrophic factor and has therefore been suggested as potential therapy to stimulate tissue regeneration in a wide variety of diseases, including liver diseases. However,

successful HGF application in rodent models should be followed by experiments in suitable large animal models to prove the clinical potential. The dog liver has been shown to activate specific pathways in liver disease that closely resemble those in man. HGF treatment was recently suggested for dogs with CPSS (13). This inherited disease is due to the presence of a large congenital portosystemic shunt, which causes poor perfusion of the liver by portal blood, resulting in hypoplasia of the liver and intrahepatic portal tree. In the absence of inflammation and fibrosis, this disease represents an uncomplicated model to test the proposed growth stimulation by HGF for the liver parenchyma and portal vasculature (26-28).

Our findings correlate with many experimental studies that have demonstrated HGF-induced hepatocyte proliferation and liver regeneration after experimentally induced acute or chronic liver failure in small animal model experiments (6-8, 29, 30). Dogs with CPSS represent the first clinical large animal model that confirms a proliferative activity of exogenous recombinant HGF and the capacity to partially regenerate a growth-stunted liver. Previous studies implicated insulin as a key factor for restoring liver size in a comparable model. The present model may indeed be considered insulin-deprived, since the liver receives virtually no portal blood and hence only systemic instead of portal insulin levels. However, our data show that HGF can induce liver growth without co-administration of insulin (31). Although providing proof of principle, this study also showed that longer treatment than three weeks is needed to obtain sustained clinical effects. The short term treatment did not result in long term recovery of liver volume in these dogs. Such findings are crucial to bridge fundamental rodent models with clinical human therapies. Although the response to HGF varied quantitatively, the liver growth was consistent over all dogs that completed the study. A comparable effect can also be seen after surgical ligation of a portosystemic shunt where the increase in liver volume ranges from 43 to 63% after two to four months (20). In the present study, liver volume (and hepatocyte proliferation) was increased after three weeks of HGF treatment. However, a remission of liver volume was seen at four weeks after cessation of HGF treatment in three out of five dogs (Fig. 2). This remission could be explained by the unaltered portal blood flow to the liver. The portal blood flow plays an important role in liver size and regeneration, due to both the delivery of hepatotrophic factors (derived from the intestine, pancreas, and spleen) by the portal vein and portal blood pressure (32-34). The importance of the portal blood flow is illustrated by several experimental models. For instance, an obstruction of the portal blood flow in one part of the liver (portal vein embolization) induces atrophy of the affected part and hypertrophy of the other unaffected part. Conversely, a reduction of the portal flow weakens hepatocyte proliferation and delays regeneration of the liver after partial hepatectomy (35, 36). This physiology is also apparent when surgical ligation of a portosystemic shunt is performed in this canine model, after which liver volume increases within weeks (37). Considering these studies, an HGF-induced increase in liver volume in our dogs with CPSS was not accompanied by a parallel growth of the portal vein branches. Portal perfusion was very low in all dogs and did not improve during or after HGF administration. On the other hand, in absence of portal blood pressure in this study a significant increase in liver volume could be achieved, which subsided after the HGF administration was stopped.

Generally, in liver regeneration there is a clear correlation between liver size and function. Liver size is steered by the need for hepatic capacity, which is determined by body weight. This is a well known phenomenon in transplantation medicine, where a liver graft either grows or decreases in size when the acceptor is relatively higher or lower in body weight, respectively. Moreover, when residual liver volume of the donor is too low after transplantation, the ‘small for size syndrome’ develops, characterized by hepatic insufficiency (38). In case of CPSS there is an obvious lack of liver function,

as these dogs develop hepatic encephalopathy, hypoalbuminemia and often have prolonged coagulation times. However these symptoms do not arise immediately after birth, although CPSS is a congenital defect. When the dog reaches maturity, its body weight increases but liver size remains low. When the discrepancy between increasing metabolic demands and hampered liver growth becomes too high, the dog will develop clinical signs of hepatic insufficiency. In our study, an increase in liver size with HGF treatment did not result in an improved liver function as all dogs remained hypoalbuminemic. It is very likely that this restriction on the size-versus-function equilibrium is caused by the aberrant portal perfusion in CPSS.

As HGF has biological effects in multiple tissue types, safety of HGF administration in dogs was assessed in a previous study (18). After one week of HGF administration, histopathology was performed on heart, lung, spleen, kidneys, pancreas, duodenum, jejunum, colon, ovaries, uterus, adrenal gland, and brain of six dogs. No abnormalities could be detected in any of the tissue samples (unpublished data).

The availability of large amounts of recombinant feline HGF and the high homology with canine HGF prompted the use of feline HGF in this clinical study (39). Despite high protein homology (97.5 %), an immunological reaction was triggered in all dogs receiving feline rHGF. Anti-feline HGF antibodies were detected with an ELISA after two weeks of treatment (data supplemental file 3). However they did not completely block biological activity of rHGF, as liver growth and receptor activation could still be noted in week 3 (Fig. 4).

The dog which was renounced from the study showed signs of nephrotic syndrome in week 3 and died in week 5. Post-mortem sections of the kidneys revealed an immune-mediated membranous glomerulonephritis, which was confirmed by immunofluorescence showing IgM and IgG deposits in the glomerular membranes (data not shown). In future applications the use of homologous HGF would be preferred.

In conclusion, considerable liver growth was seen upon rHGF treatment in dogs with CPSS. The clinical model presented here supports data acquired in rodent model studies. In contrast to rodent studies which are often terminated at the end of treatment, this large animal model allowed us to perform *in vivo* follow up measurements. Within four weeks after cessation of the treatment, in three out of five dogs liver volume returned to pre-treatment levels. This emphasizes the need to investigate the effects of long-term HGF administration to achieve permanent restoration of liver size. More importantly it stresses the need to include more and diverse models to investigate treatment effects prior to application in clinical human research. Recombinant HGF treatment resulted in increased liver growth in a large animal model of liver hypoplasia (CPSS), indicating potential applicability of HGF treatment in hepatic abnormalities.

Acknowledgments

The authors would like to acknowledge the technical assistance of Yvonne Pollak and Vivian van Essen. The biostatistical assistance by Jan van den Broek (Centre for Biostatistics, Utrecht University) is highly appreciated. The contribution of Yasuyuki Suzuta and Masato Fukui for delivery of the recombinant HGF is highly valued. We also thank Cornelia Viebahn for thoroughly reading the manuscript.

References

1. Iredale JP. Cirrhosis: New research provides a basis for rational and targeted treatments. *BMJ* 2003; **327**: 143-7.

2. Mizuno S, Nakamura T. Hepatocyte growth factor: A regenerative drug for acute hepatitis and liver cirrhosis. *Regen Med* 2007; **2**: 161-70.

3. Mizuno S, Matsumoto K, Nakamura T. Hepatocyte growth factor suppresses interstitial fibrosis in a mouse model of obstructive nephropathy. *Kidney Int* 2001; **59**: 1304-14.

4. Starzl TE, Jones AF, Terblanche J*, et al*. Growth-stimulating factor in regenerating canine liver. *Lancet* 1979; **1**: 127-30.

5. Matsumoto K, Nakamura T. Emerging multipotent aspects of hepatocyte growth factor. *J Biochem* 1996; **119**: 591-600.

6. Kosai K, Matsumoto K, Funakoshi H, Nakamura T. Hepatocyte growth factor prevents endotoxin-induced lethal hepatic failure in mice. *Hepatology* 1999; **30**: 151-9.

7. Matsuda Y, Matsumoto K, Yamada A*, et al*. Preventive and therapeutic effects in rats of hepatocyte growth factor infusion on liver fibrosis/cirrhosis. *Hepatology* 1997; **26**: 81-9.

8. Kanemura H, Iimuro Y, Takeuchi M*, et al*. Hepatocyte growth factor gene transfer with naked plasmid DNA ameliorates dimethylnitrosamine-induced liver fibrosis in rats. *Hepatol Res* 2008; **38**: 930-9.

9. Neff MW, Rine J. A fetching model organism. *Cell* 2006; **124**: 229-31.

10. Foster JR. Spontaneous and drug-induced hepatic pathology of the laboratory beagle dog, the cynomolgus macaque and the marmoset. *Toxicol Pathol* 2005; **33**: 63-74.

11. Spee B, Arends B, van den Ingh TS*, et al*. Transforming growth factor beta-1 signalling in canine hepatic diseases: New models for human fibrotic liver pathologies. *Liver Int* 2006; **26**: 716-25.

12. Spee B, Arends B, van den Ingh TS*, et al*. Major HGF-mediated regenerative pathways are similarly affected in human and canine cirrhosis. *Comp Hepatol* 2007; **6**: 8.

13. Spee B, Penning LC, van den Ingh TS*, et al*. Regenerative and fibrotic pathways in canine hepatic portosystemic shunt and portal vein hypoplasia, new models for clinical hepatocyte growth factor treatment. *Comp Hepatol* 2005; **4**: 7.

14. van den Ingh TS, Rothuizen J, Meyer HP. Circulatory disorders of the liver in dogs and cats. *Vet Q* 1995; **17**: 70-6.

15. Stringer MD. The clinical anatomy of congenital portosystemic venous shunts. *Clin Anat* 2008; **21**: 147-57.

16. Santilli RA, Gerboni G. Diagnostic imaging of congenital porto-systemic shunts in dogs and cats: A review. *Vet J* 2003; **166**: 7-18.

17. Lamb CR. Ultrasonography of portosystemic shunts in dogs and cats. *Vet Clin North Am Small Anim Pract* 1998; **28**: 725-53.

18. Arends B, Spee B, Hoffmann G*, et al*. In vitro and in vivo bioactivity of recombinant canine hepatocyte growth factor. *Vet J* 2008; **178**: 70-7.

19. Szatmari V, Rothuizen J, van den Ingh TS, van Sluijs FJ, Voorhout G. Ultrasonographic findings in dogs with hyperammonemia: 90 cases (2000-2002). *J Am Vet Med Assoc* 2004; **224**: 717-27.

20. Stieger SM, Zwingenberger A, Pollard RE, Kyles AE, Wisner ER. Hepatic volume estimation using quantitative computed tomography in dogs with portosystemic shunts. *Vet Radiol Ultrasound* 2007; **48**: 409-13.

21. van Rijn SJ, Grinwis GC, Penning LC, Meij BP. Expression of ki-67, PCNA, and p27kip1 in canine pituitary corticotroph adenomas. *Domest Anim Endocrinol* 2010; **38**: 244-52.

22. Meyer HP, Rothuizen J, van den Brom WE*, et al*. Quantitation of portosystemic shunting in dogs by ultrasound-guided injection of 99MTc-macroaggregates into a splenic vein. *Res Vet Sci* 1994; **57**: 58-62.

23. Rothuizen J, van den Ingh TS. Rectal ammonia tolerance test in the evaluation of portal circulation in dogs with liver disease. *Res Vet Sci* 1982; **33**: 22-5.

24. Brinkhof B, Spee B, Rothuizen J, Penning LC. Development and evaluation of canine reference genes for accurate quantification of gene expression. *Anal Biochem* 2006; **356**: 36-43.

25. Baade S, Aupperle H, Grevel V, Schoon HA. Histopathological and immunohistochemical investigations of hepatic lesions associated with congenital portosystemic shunt in dogs. *J Comp Pathol* 2006; **134**: 80-90.

26. Sengupta S, Gherardi E, Sellers LA*, et al*. Hepatocyte growth factor/scatter factor can induce angiogenesis independently of vascular endothelial growth factor. *Arterioscler Thromb Vasc Biol* 2003; **23**: 69-75.

27. Taniyama Y, Morishita R, Hiraoka K*, et al*. Therapeutic angiogenesis induced by human hepatocyte growth factor gene in rat diabetic hind limb ischemia model: Molecular mechanisms of delayed angiogenesis in diabetes. *Circulation* 2001; **104**: 2344-50.

28. Suzuki H, Toyoda M, Horiguchi N*, et al*. Hepatocyte growth factor protects against fas-mediated liver apoptosis in transgenic mice. *Liver Int* 2009; **29**: 1562-8.

29. Ueki T, Kaneda Y, Tsutsui H*, et al*. Hepatocyte growth factor gene therapy of liver cirrhosis in rats. *Nat Med* 1999; **5**: 226-30.

30. Ueno S, Aikou T, Tanabe G*, et al*. Exogenous hepatocyte growth factor markedly stimulates liver regeneration following portal branch ligation in dogs. *Cancer Chemother Pharmacol* 1996; **38**: 233-7.

31. Starzl TE, Watanabe K, Porter KA, Putnam CW. Effects of insulin, glucagon, and insuling/glucagon infusions on liver morphology and cell division after complete portacaval shunt in dogs. *Lancet* 1976; **1**: 821-5.

32. Braet F, Shleper M, Paizi M*, et al*. Liver sinusoidal endothelial cell modulation upon resection and shear stress in vitro. *Comp Hepatol* 2004; **3**: 7.

33. Sato Y, Koyama S, Tsukada K, Hatakeyama K. Acute portal hypertension reflecting shear stress as a trigger of liver regeneration following partial hepatectomy. *Surg Today* 1997; **27**: 518-26.

34. Pouyet M, Mechet I, Paquet C, Scoazec JY. Liver regeneration and hemodynamics in pigs with mesocaval shunt. *J Surg Res* 2007; **138**: 128-34.

35. Uemura T, Miyazaki M, Hirai R*, et al*. Different expression of positive and negative regulators of hepatocyte growth in growing and shrinking hepatic lobes after portal vein branch ligation in rats. *Int J Mol Med* 2000; **5**: 173-9.

36. Nobuoka T, Mizuguchi T, Oshima H*, et al*. Portal blood flow regulates volume recovery of the rat liver after partial hepatectomy: Molecular evaluation. *Eur Surg Res* 2006; **38**: 522-32.

37. Kummeling A, Teske E, Rothuizen J, Van Sluijs FJ. Coagulation profiles in dogs with congenital portosystemic shunts before and after surgical attenuation. *J Vet Intern Med* 2006; **20**: 1319-26.

38. Clavien PA, Petrowsky H, DeOliveira ML, Graf R. Strategies for safer liver surgery and partial liver transplantation. *N Engl J Med* 2007; **356**: 1545-59.

39. Miyake M, Saze K, Yaguchi T*, et al*. Canine hepatocyte growth factor: Molecular cloning and characterization of the recombinant protein. *Vet Immunol Immunopathol* 2003; **95**: 135-43.

Supplemental information

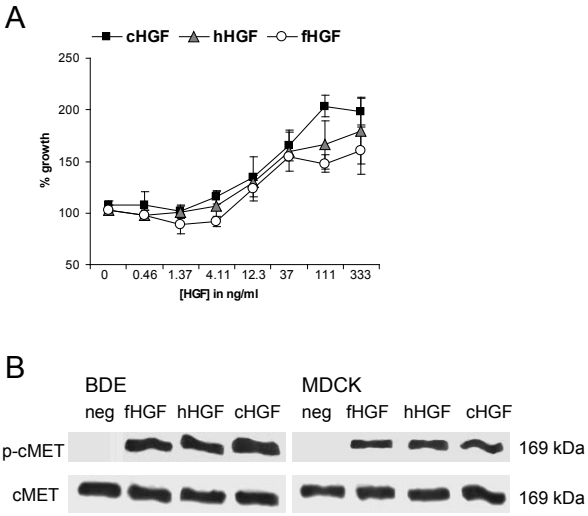

Supplemental file 1. *In vitro* activity of recombinant HGF. Two canine cell lines were treated with recombinant canine HGF (Intervet, Boxmeer, the Netherlands, cHGF), recombinant human HGF (R&D Systems Europe, Oxon, UK, hHGF), and recombinant feline HGF (Zenoaq, Fukushima, Japan, fHGF). (A) Line graph representing the mean percentage growth of bile-duct epithelial cells (BDE) after 48 hours recombinant HGF treatment, as measured by the MTT assay. Cellular proliferation was induced at a concentration of 11 ng/mL HGF and a maximal proliferative activity was seen around 100 ng/mL HGF. No differences were seen in proliferative activity between recombinant fHGF, cHGF, and hHGF. (B) Effect of recombinant HGF treatment on the c-MET protein in BDE or Madin-Darby Canine Kidney cells (MDCK) after 5 minutes of treatment with HGF. Phosphorylation of c-MET was observed in both cell lines after 5 minutes of incubation with HGF. No differences were seen in c-MET phosphorylation after recombinant fHGF, cHGF, or hHGF treatment.

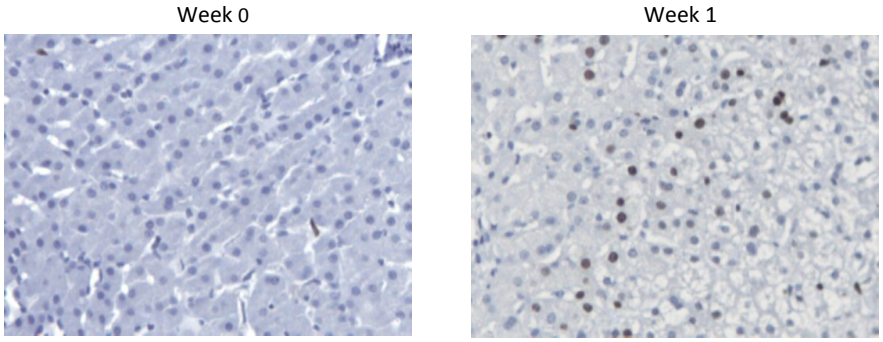

Supplemental file 2. Examples of Ki-67 positive hepatocytes. Immunohistochemical staining of Ki-67 (proliferation index) positive nuclei in hepatocytes of untreated (week 0) and after one week of recombinant HGF treatment are shown in (B). Original magnification 200x.

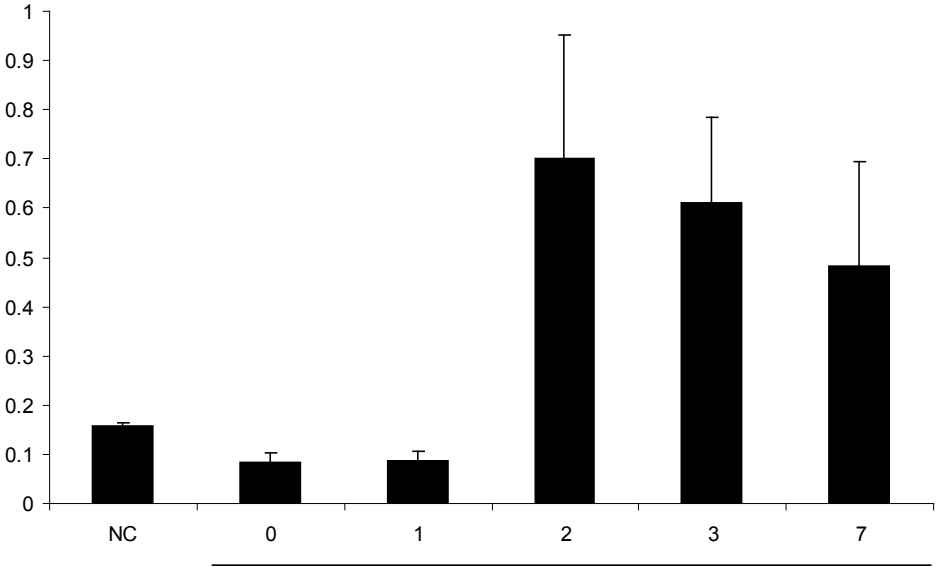

Supplemental file 3. ELISA measuring dog anti-fHGF IgG formation during and after HGF treatment compared to control. As no standardized concentration of dog anti-fHGF IgG was available, antibody formation was quantified as sample absorbance with subtraction of background signal. As a negative control, normal non-HGF treated dogs were used (NC). Sample absorbance retained basal levels in week 0 and 1, comparable to the negative control. However, in all dogs a clear increase in signal can be detected in week 2, 3, and 7 indicating anti-fHGF IgG formation during HGF treatment and persistence of circulating antibodies four weeks after treatment.

Week	Dog 1	Dog 2	Dog 3	Dog 4	Dog 5
0	100	97	97	98	96
1	100	97	97	99	99
2	99	97	98	98	97
3	99	98	94	98	99
7	96	98	94	98	98

Supplemental file 4. Shunt index (%) calculated by perfusion scintigraphy before rHGF administration (week 0), during rHGF treatment (week 1 and 3) and four weeks after rHGF treatment (week 7).

Chapter 6

Canine liver organoid transplantation in a COMMD1 deficient dog model of metabolic liver disease.

H.S. Kruitwagen, L.A. Oosterhoff, M.E. van Wolferen, C. Chen, F.G. van Steenbeek, S. Nantasanti, C.R. Vinke, A. Kummeling, G. van Straten, L.C. Akkerdaas, L.W.L. van Bruggen, J. Wolfswinkel, G.C.M. Grinwis, S.A. Fuchs, H. Gehart, N. Geijsen, J. Rothuizen, B.A. Schotanus, L.C. Penning, B. Spee

Manuscript in preparation

Abstract

Metabolic liver disease can be treated with liver transplantation, but liver cell transplantation is considered as an attractive alternative. However, human hepatocyte transplantations still require a donor liver. We investigated the recently developed liver organoid culture technique to robustly expand adult liver stem cells *in vitro* and evaluated their potential for autologous cell transplantation in a large animal model of metabolic liver disease.

COMMD1 deficient dogs with hepatic copper storage disease similar to human Wilsons disease were subjected to a transplantation protocol that could be adopted for future human clinical application. Autologous liver stem cells were isolated from a Tru-cut liver biopsy and expanded as organoids *in vitro*. Liver organoids were genetically modified with the full length canine COMMD1 gene (gene correction) together with a fluorescent marker gene, and were differentiated towards hepatocyte-like cells. In three dogs a left lateral liver lobectomy was performed to induce liver regeneration and a permanent intravenous catheter was placed in the portal vein and connected to a subcutaneous port. On three consecutive days, a total of 4.5-7.3x10^8 autologous gene-corrected organoid-derived liver cells were infused in the portal vein of two dogs. The third dog received vehicle and served as control. Dogs received cyclosporine for the first three months after transplantation. A one year longitudinal follow-up consisted of repeated blood analysis, liver biopsies for cell tracking and biliary ^{64}Cu excretion studies. After one year one dog was retransplanted by means of intrahepatic injections with organoid fragments and liver was harvested after seven days.

In dogs transplanted via the portal vein, no evidence of significant engraftment or repopulation of the liver was found and biliary ^{64}Cu excretion did not improve. Upon intrahepatic injections, transplanted liver organoids engrafted in the liver and showed evidence of *in vivo* proliferation.

In conclusion, liver organoids can be used for autologous cell transplantation purposes. Canine liver organoid transplantations can serve as translational model for human clinical application. More research is needed to define the best route of administration and pretreatment to ensure engraftment, selective repopulation and functional recovery of the liver over time.

Introduction

Liver transplantation is a curative treatment for many liver diseases. However, important drawbacks such as donor organ shortage, the invasiveness of the procedure, and the need for life-long immunosuppression have urged the search for alternative treatment options (Jorns et al., 2012; Forbes et al., 2015). In metabolic liver disease a genetic defect impairs a specific metabolic function leading to clinical disease and cell transplantation with healthy donor hepatocytes that repopulate (part of) the organ is a viable alternative to whole-organ transplantation. Human hepatocyte transplantations have been successfully performed in Crigler-Najjar syndrome, phenylketonuria, and urea cycle defects (Fox et al., 1998; Puppi et al., 2008; Stéphenne et al., 2006, 2012). However, transplanted hepatocytes were sourced from a donor liver and recipients still required immunosuppression to avoid rejection of allogenic hepatocytes. Moreover, hepatocytes isolated from a human liver cannot be expanded *in vitro* and also and have a short-lived clinical effect, which necessitates repeated cell transplantations (Puppi et al., 2012; Forbes et al., 2015). The lack of follow up biopsies prevents insight into the efficacy of human hepatocyte transplantation.
Recently a three-dimensional primary culture system was developed from LGR5 positive adult liver stem cells based on R-spondin-mediated proliferation (Huch et al., 2013a). Cultured as liver organoids, these cells retain a progenitor phenotype during *in vitro* expansion and can be differentiated towards hepatocyte-like cells by changing the culture medium composition. First established for mouse, a liver organoid culture was subsequently developed for human and rat (Huch et al., 2015; Kuijk et al., 2016). Transplantation potential of liver organoid-derived cells was tested in experimental rodent models of metabolic liver disease and successful hepatic engraftment and repopulation was reported for mouse, rat and human liver organoids. This prompted the question whether human liver organoids could be a new expandable cell source for transplantation in human metabolic liver disease (Huch et al., 2013b).
Before human liver organoids can be applied in a first-in-man transplantation study, it is imperative to test several important aspects in an appropriate large animal model (Volk et al., 2013; Kruitwagen et al., 2014). A large animal model permits (1) evaluation of the optimal route of cell administration (e.g. in mouse and rat intraportal infusions are not feasible), (2) autologous transplantation when hepatic progenitor cells are procured from a liver biopsy, cultured as organoids and genetically modified, and (3) longitudinal follow-up in the same animal with both functional readouts and liver biopsies for cell tracking and safety evaluation. Furthermore, clinical efficacy should ideally be investigated in a spontaneous liver disease more closely resembling the human clinical situation than experimental rodent models.
Dogs have naturally occurring liver diseases and mechanisms of canine liver disease and regeneration show striking similarities with humans on both a molecular and cellular level (Spee et al., 2007; Schotanus et al., 2009; Ijzer et al., 2010). Copper toxicosis is a canine metabolic liver disease that is encountered in one third of all canine chronic hepatitis cases (Poldervaart et al., 2009). Various genetic and environmental causes for copper toxicosis have been described for different dog breeds (Fieten et al., 2012, 2016). Canine copper storage disease based on a deletion of exon 2 of the copper metabolism domain containing 1 (*COMMD1*) gene is both the earliest and most extensively described etiology and results in high hepatic copper levels (van de Sluis et al., 2002). COMMD1 deficiency (-/-, autosomal recessive inheritance) results in impaired copper excretion from hepatocytes into the bile (Su et al., 1982; Klomp et al., 2003) and COMMD1 deficient dogs develop hepatic copper storage disease and chronic hepatitis similar to human Wilson's disease

(Favier et al., 2012). In mouse and rat models of copper toxicosis, hepatocyte transplantations showed positive effects on lowering liver copper levels and improving biliary copper excretion (Malhi et al., 2002; Allen et al., 2004; Sauer et al., 2012). We hypothesized that canine COMMD1$^{-/-}$-linked copper toxicosis could be a valuable disease model to study liver organoid transplantation in order to translate these findings to human metabolic liver disease, such as Wilsons disease. A canine liver organoid culture system has been established and extensively characterized and COMMD1$^{-/-}$ organoids could be genetically corrected to restore the copper excretion phenotype (Nantasanti et al., 2015). Our study objective was to transplant cells from autologous gene-corrected canine liver organoids in COMMD1 deficient dogs with a methodology that could be easily extrapolated to human clinical application. We aimed to investigate the potential of canine organoid-derived liver cells for engraftment, repopulation and functional recovery of liver disease in time. In this report, we describe the results of the first in dog transplantations of autologous liver organoids in copper storage disease.

Materials and methods

Study design

A schematic representation of the study design can be found in Figure 1. Three months before transplantation a biliary ^{64}Cu excretion study was performed and liver biopsies were taken to obtain autologous liver stem cells residing in biliary duct fragments. Ducts were cultured as three-dimensional liver organoids and lentivirally transduced with a construct containing the full length canine *COMMD1* gene. Organoids were expanded and differentiated towards hepatocyte-like cells. Organoids were dissociated and transplanted on three consecutive days via the portal vein. To provide a regenerative stimulus, a partial hepatectomy was performed on the first day of transplantation as this is known to promote proliferation of transplanted cells (Guha et al., 2001). Follow up measurements consisting of blood analysis, liver biopsies and biliary ^{64}Cu excretion studies were performed one week, one month, three months, six months, nine months, and one year after transplantation. One dog (dog nr. 1) was retransplanted two years after the beginning of the study by means of intrahepatic injections. Seven days after intrahepatic transplantation, the dog was euthanized and the liver was harvested.

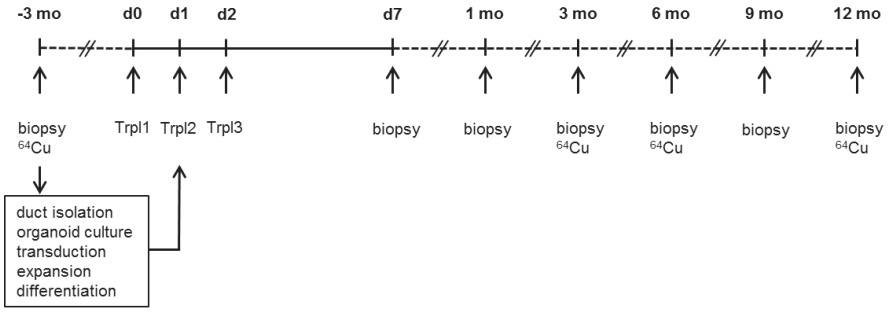

Figure 1. Study design. Liver biopsies were performed three months before transplantation (for establishment of autologous liver organoid culture) and one week, one month, three months, six months, nine months, and one year after transplantation. Biliary ^{64}Cu excretion studies were performed three months before transplantation and three months, six months, and one year after transplantation.

Microbead perfusion of canine liver

To investigate feasibility of organoid-derived liver cell transplantation via the portal vein in the dog, a pilot experiment was performed to determine minimum cell size for portal delivery. In canine hepatic scintigraphy, ^{99}Tc-labeled macro aggregated albumin particles of 10-90 µm in size are used to quantify portal blood flow. In a normal dog all particles lodge in the hepatic vasculature after intraportal delivery (Meyer et al., 1994). To verify if indeed 10 µm would constitute the minimum cell size to prevent systemic flow through, a heparinized cadaveric canine liver (right lateral lobe, approximately 14% of liver mass) was infused with 21x10^6 10 µm red fluorescent microbeads (1 ml/min, Life Technologies) in HBSS (10 ml/min, Gibco). Infusion was given via the portal vein branch using an inflated balloon catheter (MILA) to prevent backflow to the other lobes. The inferior vena cava was ligated caudal to the liver and cannulated cranial to the liver to collect all flow-through. Infusion with HBSS was continued for an additional 15 minutes after microbead infusion. Flow through was centrifuged at 250 g for 5 minutes.

Liver was sampled using wedge biopsies and 14G Tru-cut biopsies. Fresh 1 mm thick slices were cut from the wedge biopsies for direct evaluation of native fluorescence using an Olympus IMT-2 microscope. Tru-cut biopsies were frozen in TissueTek (Sakura), cryosections were prepared and immediately microscopically evaluated for the presence of microbeads.

COMMD1 deficient dogs

All studies were approved by the Utrecht University's ethical committee, as required under Dutch legislation (study numbers 2014.III.04.039 and 2014.III.12.112). For the duration of the studies, dogs were hospitalized in the Utrecht University Clinic for Companion Animals and all interventions were executed and/or supervised by board-certified veterinary specialists. Three COMMD1-/- Beagle – Bedlington terrier crossbreed dogs (details in Table 1) were used from a breeding colony harboring a deletion in exon 2 of the *COMMD1* gene (van de Sluis et al., 2002). Dogs were genotyped using 25 ng DNA isolated from an EDTA blood sample or buccal swab. PCR was performed in a 25 µl reaction volume containing 2 mM $MgCl_2$, 200 µM dNTPs, 2.5 units platinum Taq polymerase and 0.5 µM of each primer (sequences in Table 3). Deletion-specific primers were designed to span the 39.7-kb deletion in the canine COMMD1 gene, generating an amplicon of 238 basepairs in case of an affected genotype (Forman et al., 2005). Control primers were located within the deletion, generating an amplicon of 508 basepairs in case of a wildtype genotype. Thermal cycling was performed using a 59°C annealing temperature on a GeneAmp PCR system (Applied Biosystems) and reaction products were separated using agarose gel electrophoresis (Fig. 2).

Normal dog liver samples were obtained from fresh cadavers from dogs used in non-liver related research (surplus material, Utrecht University 3R-policy).

Table 1. Details of COMMD1-/- dogs at the start of the study.

Dog	Age	Sex	Weight (kg)	Liver copper (µg/g dwl)
1	5 y	male	15.0	3797
2	8 mo	male	15.5	1442
3	8 mo	female	10.6	3086

y: years; *mo:* months; *dwl*: dry weight liver (liver copper ref. <400 µg/g dwl)

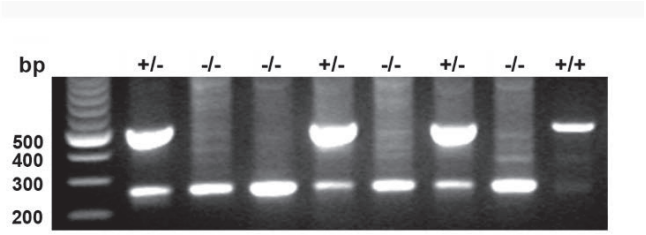

Figure 2. COMMD1-/- dog genotyping. Gel electrophoresis of COMMD1 PCR products indicating the genotype of wildtype, carrier and affected dogs. In wildtype dogs with a full length COMMD1 gene (+/+) only the control amplicon of 508 bp (basepairs) is generated. In COMMD1 deficient dogs (-/-) a deletion-specific amplicon of 238 bp is generated. Heterozygous dogs (+/-) carry both alleles, hence both amplicons are formed.

Biliary duct isolation, autologous liver organoid culture, lentiviral transduction, and differentiation
Canine liver organoid culture and lentiviral transduction was performed essentially as described before (Nantasanti et al., 2015). Briefly, two 14G Tru-cut liver biopsies were minced and digested in DMEM with 1% v/v FCS containing 0.3 mg/ml collagenase type II and 0.3 mg/ml dispase (all from Gibco) at 37°C. Biliary duct fragments appeared in the supernatant after two to four hours. Ducts were plated in Matrigel (BD Biosciences) and expansion medium was added to the wells after gelation. Organoids were passaged by mechanical disruption once a week at a 1:6 split ratio.
At passage two, organoids were enzymatically dissociated and lentiviral (LV) transduction with a pHAGE2-EF1a-COMMD1-DsRed-PuroR or a pHAGE2-EF1a-COMMD1-eGFP-PuroR construct was performed using spinoculation as described earlier (Nantasanti et al., 2015). Culture was continued with puromycin to select for transduced cells. Transduction efficiency was confirmed (>90%) using flow cytometry using a FACSCalibur (Becton Dickinson) (data not shown). Autologous gene-corrected liver organoids were expanded for transplantation in 12 well plates (Greiner) in 100 µl Matrigel droplets per well and a total of 324 wells were cultured for each dog.
To induce differentiation towards hepatocyte-like cells 25 ng/ml BMP7 (Peprotech) was added to the expansion medium after the last passage. Four days after the last passage, Wnt-conditioned medium, ROCK inhibitor and Noggin were withdrawn from the medium and BMP7 treatment was continued. Six days after the last passage, nicotinamide, R-spondin-1-conditioned medium and FGF10 were also withdrawn from the medium, BMP7 was continued and 100 ng/ml FGF19 (R&D Systems), 10 µM DAPT (Selleckchem) and 30 µM dexamethasone (Sigma-Aldrich) were added (differentiation medium, DM). Culture in DM was continued for eight to nine days.

Harvest of liver organoids for intraportal transplantation
On each consecutive transplantation day (day 0, day 1, day 2) 108 wells of differentiated autologous pHAGE2-EF1a-COMMD1-DsRed-PuroR-transduced liver organoids were harvested just prior to transplantation. Organoids were isolated from Matrigel using cold advanced DMEM/F12 (Gibco), mechanically dissociated and digested with TrypLE select enzyme (Gibco). Digestion was stopped when the majority of organoid fragments had reached a size of 10 cells or less (Fig. 3A). The cell suspension was passed through a 70 µm cell strainer and aliquots were taken for cell counting and a 0.4% trypan blue viability assay (Bio-rad). The cells were resuspended in Sterofundin ISO (B. Braun) and transferred to a 20 ml syringe precoated with autologous serum (Fig. 3B). Cells were kept on ice until transplantation.

To evaluate the differentiation level of transplanted liver organoids, extra wells were harvested from the same experiment for gene expression analysis and for liver enzyme measurements as previously described (Nantasanti et al., 2015; Kruitwagen et al., 2017).

Partial hepatectomy and implantation of permanent Port-A-Cath system in the portal vein
On the first day of transplantation (day 0) dogs were anesthetized for a partial hepatectomy and placement of a vascular access system in the portal vein. Dogs received glycopyrrolate (0.01 mg/kg IM), methadone (0.5 mg/kg IV), and cefazolin (20 mg/kg IV) pre-operatively and propofol (1-4 mg/kg IV) to induce anesthesia. Anesthesia was maintained with fentanyl (10-20 µg/kg/h IV) or remifentanil (0.20 µg/kg/min IV) and isoflurane in O_2 and air (1:1) via an endotracheal tube (Matsumoto et al., 1999). Using a midline celiotomy approach, a left lateral hepatic lobectomy was performed resulting in approximately 20% reduction in liver mass (based on previous experiments) (Fig. 3C). The resected lobe was sampled for quantitative copper measurement (by instrumental neutron activation analysis, Bode 1990), RNA isolation and histology. A permanent Port-A-Cath (PAC) system was then implanted in the portal vein to provide non-invasive access for repeated intraportal delivery of cells (Darwish et al., 2004) (Fig. 3D). A PORT-A-CATH II POWER PAC (Smiths Medical) was used, consisting of a 1.9 mm polyurethane catheter and a polysulfone and titanium portal. The catheter was inserted in either a jejunal or splenic vein using an open vein technique. The catheter tip was advanced into the portal vein and placed 1-2 cm caudal to the liver hilum. The catheter was fixed to the vein proximal to the venotomy site using a polypropylene Chinese finger trap suture. The portal was placed in a subcutaneous pocket on the abdominal wall and connected to the catheter. PAC patency was confirmed by the ability to withdraw portal blood and flushing with heparinized saline. A gripper needle was placed percutaneously into the portal and was removed again on day 5. The first cell fraction (day 0) was transplanted via the PAC intraoperatively. The abdomen was routinely closed and postoperatively dogs were admitted to the intensive care unit for monitoring and analgesia (fentanyl 3-5 µg/kg/h IV and ketamine 3-5 µg/kg/min IV). After several days dogs were switched to oral tramadol (3-5 mg/kg q6h) for an additional three to five days.

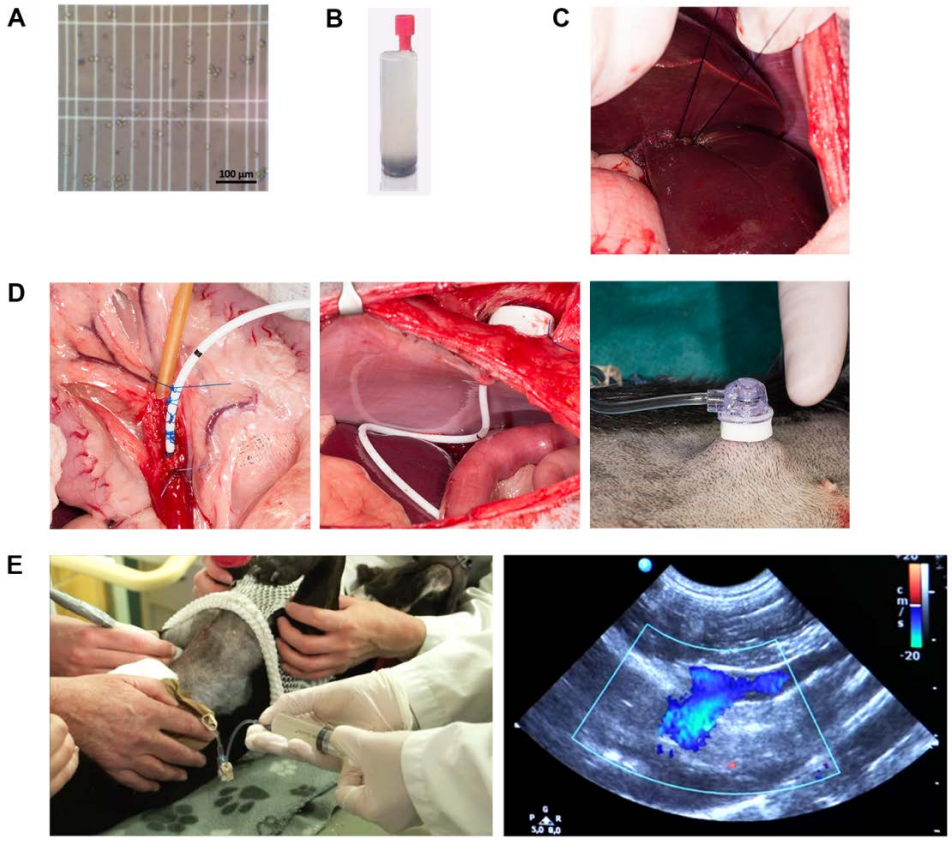

Figure 3. Intraportal transplantation of organoid-derived liver cells. A. Representative picture of cell suspension after organoid digestion, yielding both single cells and small fragments. B. Cell suspension in Sterofundin ISO prior to transplantation. C. Left lateral lobectomy of the liver. D. Port-A-Cath (PAC) implantation. The catheter was inserted in either a jejunal (image) or splenic vein and connected to the subcutaneous portal. A gripper needle was placed into the portal, allowing non-invasive access to the portal vein. E. Transplantation of organoid-derived liver cells on day 1 and 2 via the PAC under abdominal Doppler ultrasound guidance. Images under C-E courtesy of Multimedia Department.

Transplantation of organoid-derived liver cells by intraportal delivery

On day 0, organoid-derived liver cell transplantation was performed intraoperatively to enable visual monitoring of infusion via the PAC and possible effects on abdominal organs in case of portal hypertension. Additional monitoring consisted of invasive arterial blood pressure measurements, electrocardiography (ECG) and oxygen saturation measurements. Before and after transplantation, portal pressure was measured via the PAC using a water column method (dog 2, dog 3). Cell suspension was infused via the gripper needle of the PAC into the portal vein, not exceeding a flow velocity of 2 ml/min (Meyburg et al., 2009). On day 1 and 2, the second and third fraction of organoid-derived liver cells were transplanted without sedation under abdominal Doppler ultrasound guidance (Philips HD11) (Fig. 3E).

Transplantation of organoid-derived liver cells by intrahepatic injection

One dog (dog nr. 1) was retransplanted two years after the beginning of the study by means of intrahepatic injections during a celiotomy. The same anesthesia protocol and cyclosporine regimen

were used as during the first intraportal transplantation, but the second celiotomy did not include a hepatic lobectomy. For intrahepatic transplantation, pHAGE2-EF1a-COMMD1-eGFP-PuroR transduced autologous liver organoids were cultured under undifferentiated (EM, n=24 wells of a 24 well plate) and differentiated (DM, n=6 wells of a 24 well plate) conditions. Organoids were isolated from Matrigel using cold advanced DMEM/F12 (Gibco) and mechanically dissociated into small fragments (Fig. 4A). Fragments were not enzymatically digested. Fragments were resuspended in 0.9% NaCl with 10% autologous serum and transferred to serum-precoated Eppendorf tubes. Immediately before injection, fragments were transferred to a serum-precoated syringe with a 12 mm 29G needle (Kruuse). Two injection sites were established with EM organoids and one site with DM organoids. Per injection site, 5-9 injections of 50 µl each spaced 2 mm apart were administered slowly into the liver at a depth of 10-12 mm. Injection sites were marked with electrocautery and polypropylene sutures (Fig. 4B). As a control, one injection site received vehicle injections. The abdomen was routinely closed and post-operative analgesia was provided with ketamine (3-5 µg/kg/min IV) and methadone (0.5 mg/kg q6h IV), which was changed to sufentanyl (0.2 µg/kg/h IV) after two days. Seven days after intrahepatic transplantation, the dog was euthanized with pentobarbital IV and the liver was harvested. As positive control, one extra liver organoid injection site was established post-mortem. All injection sites were sampled by resecting a 1x1 cm piece of liver between the polypropylene sutures, cutting 2 cm deep into the parenchyma. The 1x1x2 cm rectangular liver specimen was then cut into four pieces to create section levels at 0.5, 1, 1.5 and 2 cm liver depth. At the 1 cm section level, three 2x2 mm specimens were removed for RNAisolation. Liver tissue was fixed in 10% neutral buffered formalin for 24h, transferred to 70% ethanol and embedded in paraffin.

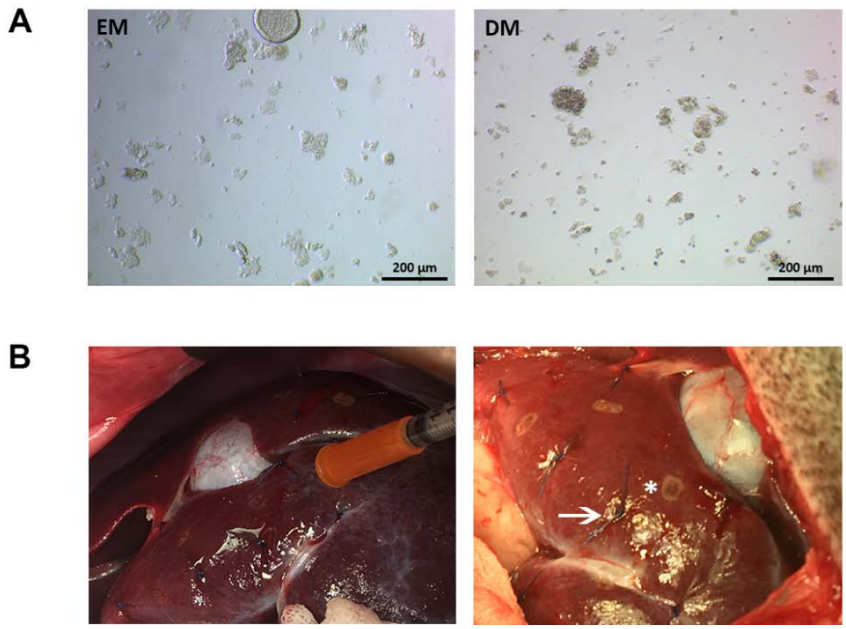

Figure 4. Intrahepatic transplantation of organoid-derived liver cells. A. Representative images of organoid fragments in undifferentiated (EM) and differentiated (DM) conditions before injection. B. Injections were made with a 29G needle and injection sites marked with polypropylene sutures (arrow) and electrocautery (asterisk).

Immune suppression

Dogs were treated with cyclosporine (ASTfarma) to prevent potential rejection of genetically modified autologous cells (Fang et al., 1995; Kocken et al., 1996; Benedetti et al., 1997; Arruda et al., 2009). Dosage was readjusted based on weekly cyclosporine plasma levels as measured 2 hours after oral administration (peak plasma concentration) (Archer et al., 2014). Treatment was initiated the day before transplantation and continued for 1 month at 6.25 mg/kg q12h (0.6-1.0 mg/L peak plasma concentration). Dosage was then lowered to 3.13 mg/kg q12h (0.3-0.6 mg/L peak plasma concentration) and treatment continued for an additional two months.

Liver biopsies and blood analysis

For post-transplantation cell tracking the liver was biopsied with a 14G or 16G Tru-cut automatic biopsy instrument (Angiotech) in the sedated dog (methadone 0.5 mg/kg IM, propofol 1-4 mg/kg IV, lidocaine local abdominal block). At each time point (Figure 1) four biopsies were taken, when possible two each from two separate lobes. From each 19 mm biopsy sample a 2 mm piece was removed, submerged in RNAlater for 24h at 4°C and subsequently stored at -70°C. The remaining biopsy samples were fixed in 10% neutral buffered formalin for 4h, transferred to 70% ethanol and embedded in paraffin. Blood analysis was performed prior to each liver biopsy and consisted of complete blood counts, serum/plasma biochemistry (including liver enzymes, albumin and fibrinogen concentrations), and coagulation tests (prothrombin time (PT) and activated partial thromboplastin time (APTT)).

RNA isolation and quantitative reverse transcriptase PCR analysis

RNA was isolated from organoids and liver tissue using a RNeasykit (Qiagen) and converted to cDNA using an iScript kit (Bio-rad) according to the manufacturers' instructions. QPCR was performed in duplicate on a MyiQ thermal cycler using SYBRgreen supermix (both Bio-rad). Expression was measured of leucine-rich repeat-containing G protein-coupled receptor 5 (*LGR5)*, SRY-box 9 (*SOX9)*, albumin (*ALB*), cytochrome 3A12 (*CYP3A12*), arginase 1 (*ARG1*), *COMMD1* exon 2, *DsRed*, and *eGFP*. Glyceraldehyde-3-phosphate dehydrogenase (*GAPDH*), hypoxanthine phosphoribosyltransferase 1 (*HPRT1*), and ribosomal protein S5 (*RPS5*) were measured as reference genes to calculate relative gene expression using a delta Cq method. Primer sequences can be found in Table 2.

Table 2 Primer sequences for quantitative reverse transcription PCR

Gene	Direction	Sequence (5' – 3')	Tm (°C)	Product size (bp)
LGR5	Forward	CTCAGCGTCTTCACCTCCT	66	130
	Reverse	TGGGAATGTATGTCAAAGCGT		
SOX9	Forward	CGCTCGCAGTACGACTACAC	63	105
	Reverse	GGGGTTCATGTAGGTGAAGG		
ALB	Forward	TGTTCCTGGGCACGTTTTTGTA	64	92
	Reverse	GGCTTCATATTCCTTGGCGAGTCT		
CYP3A12	Forward	AGTATGGAGATGTGTTGGTG	58	133
	Reverse	TCTTGTGGGTTGTTGAGG		
ARG1	Forward	CAACCTGTGTCTTTCCTCCT	62	200
	Reverse	GCCAATTCCCAGTTTATCCAC		
COMMD1 exon 2	Forward	GACCAAGCTGCTGTCATTTCCAA	60	122

	Reverse	TTGCCGTCAACTCTCCAACTCA		
DsRed	Forward	GAAGAAGACTATGGGCTGGG	65.5	134
	Reverse	ATGTAGATGGACTTGAACTCCAC		
eGFP	Forward	ATCTGCACCACCGGCAAGCT	62.5	129
	Reverse	GGGCATGGCGGACTTGAAGA		
GAPDH	Forward	TGTCCCCACCCCAATGTATC	58	100
	Reverse	CTCCGATGCCTGCTTCACTACCTT		
HPRT1	Forward	AGCTTGCTGGTGAAAAGGAC	58	104
	Reverse	TTATAGTCAAGGGCATATCC		
RPS5	Forward	TCACTGGTGAGAACCCCCT	62.5	141
	Reverse	CCTGATTCACACGGCGTAG		

DNA isolation from liver biopsies and genomic PCR analysis

DNA was isolated from three sections (10 µm) each of paraffin embedded liver biopsies using a DNeasykit (Qiagen). Samples were digested overnight at 56°C with proteinase K and DNA was isolated according to the manufacturer's instructions. Primers were developed for *GAPDH* (control) and *DsRed* (sequences in Table 3). Thermal cycling was performed with a GeneAmp PCR system (Applied Biosystems) and reaction products were separated using agarose gel electrophoresis. DNA from DsRed-transduced organoids was used as positive control.

Table 3 Primer sequences genomic DNA PCR

Gene	Direction	Sequence (5' – 3')	Tm (°C)	Product size (bp)
COMMD1 - deletion	Forward	CCTGCTTATGGTCTTTCCTTTG	59	236
	Reverse	GTACAACAAAGGGATCCCTG		
COMMD1 - control	Forward	GAGCCCCACGAAACAGACTA	59	508
	Reverse	TGGTCCACATCTTCCAATCA		
GAPDH	Forward	TGTCCCCACCCCAATGTATC	58	100
	Reverse	CTCCGATGCCTGCTTCACTACCTT		
DsRed	Forward	GAAGAAGACTATGGGCTGGG	68.5	134
	Reverse	ATGTAGATGGACTTGAACTCCAC		

Immunocyto-/histochemical staining

Sections of paraffin-embedded liver samples and organoids were dewaxed and rehydrated using a graded ethanol series. Immunocyto-/histochemical staining (ICC/IHC) for COMMD1, DsRed, eGFP, and Ki67 was performed essentially as described before (Kruitwagen et al., 2017). Details are provided in Table 4. Normal dog liver and normal dog liver post-mortem injected with DsRed-transduced organoids were used as positive control for respectively COMMD1 and DsRed immunohistochemistry. Van Gieson-elastica histochemical staining was performed routinely. Images were obtained with an Olympus microscope (CKX41) combined with a Leica DFC425C camera.

Table 4. Antibodies, antigen retrieval methods and chromogens used in ICC/IHC

Antigen	Antibody Cat. No.	Source	Clone	Company	Dilution	Antigen retrieval	Chromogen
COMMD1	NBP2-03755	mouse	1F2	Novus Biologicals	1:100	TE	DAB
DsRed	OARA01891	rabbit		Aviva Systems Biology	1:500	TE	DAB
eGFP	2555	rabbit		Cell Signaling	1:200	Ci	AEC
Ki67	RM-9106-S	rabbit	SP6	Thermo Fischer Scientific	1:50	Ci	DAB+nickel

Cat. No.: catalog number; *TE*: 10mM Tris 1mM EDTA pH 9.0 30 minutes 98°C; *Ci*: 10mM citrate pH 6.0 30 minutes 98°C; *DAB*: 3,3'-diaminobenzidine; *AEC* : 3-amino-9-ethylcarbazole; DAB+nickel: DAB + 0.3% (w/v) di-ammonium nickel (II) 6-hydrate

Biliary ^{64}Cu excretion measurements

Excretion of exogenously administered ^{64}Cu into the bile was investigated as described previously (Mandigers et al., 2007). Dogs were kept in a metabolic cage for the duration of the study. A 1.5 mg copper wire was irradiated for ten hours in a reactor, providing an activity of approximately 45 MBq/mg. Copper was dissolved in 50 µl concentrated HNO_3 (10.3M) and neutralized with 1.3 ml NaOH (0.5M). A dose of 0.003 mg/kg copper was prepared in 2.5 ml of autologous heparinized plasma, corresponding to 10% of the copper plasma pool. Dogs received methadone (0.3 mg/kg IM, repeated dose after three hours) to close the sphincter of Oddi and ^{64}Cu was administered into the cephalic vein. After six hours dogs were sedated with methadone (0.5 mg/kg IM) and propofol (1-4 mg/kg IV). Under ultrasound guidance the gallbladder was punctured and emptied by aspiration. Activity of ^{64}Cu in bile was measured with a gamma counter and corrected for decay between administration of the IV dose and measurement of the bile.

Results

Minimum cell size for canine intraportal cell transplantation

After 10 µm microbead perfusion, sections of liver were microscopically evaluated for the presence of red fluorescent beads. In 1 mm thick liver sections microbeads could be observed arranged as branching strings, indicative of a position lodged in the intrahepatic vasculature (Fig. 5A). Microbeads could also be found in cryosections of Tru-cut liver biopsies (Fig. 5B). Approximately 50% of the biopsy sections (15/25) contained one or more beads. In the vena cava flow-through 140 microbeads out of a total infused $21x10^6$ microbeads were found, indicating that over 99.9% of the microbeads were trapped in the liver. Bead size was microscopically compared with canine liver organoids after trypsin digestion, yielding single cells and small fragments. Both in EM (undifferentiated) and DM (differentiated) conditions, organoid-derived single cells were larger than the microbeads (Fig. 5C). We concluded that based on size, organoid-derived single cells and fragments should lodge in the canine hepatic vasculature after intraportal delivery.

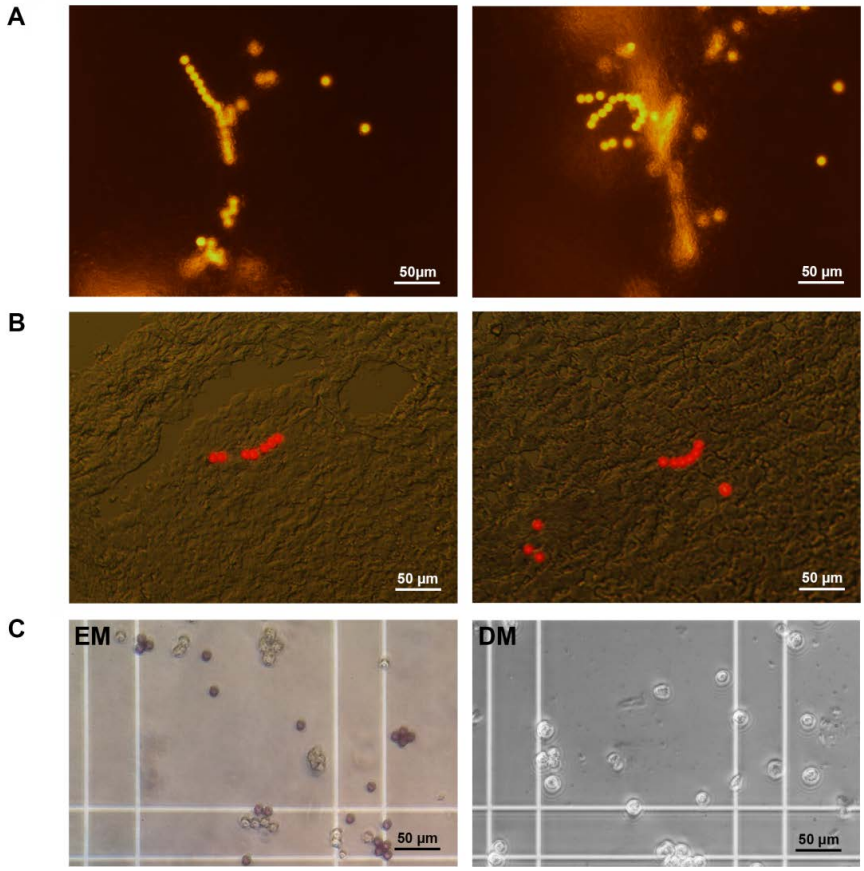

Figure 5. Determining minimum cell size for canine intraportal cell transplantation. Red fluorescent 10 µm microbeads were infused in a cadaveric canine liver lobe via the portal vein. A. Microbeads were arranged as branching strings in 1 mm thick liver sections. B. Cryosections of liver biopsies indicating the presence of microbeads in the liver after perfusion. Beads were found in approximately 50% of all biopsy sections. C. Cell size of canine liver organoids after trypsin digestion, resulting in single cells and small organoid fragments. Undifferentiated (EM) organoid-derived liver cells were mixed with red 10 µm microbeads and size was microscopically evaluated in a Bürker-Türk counting chamber. Size was compared to differentiated (DM) organoid-derived liver cells.

Establishment and differentiation of LV-corrected autologous liver organoid cultures

Patient-specific organoids were successfully cultured from liver biopsies (Fig. 6A). After lentiviral (LV) transduction followed by puromycin selection, all organoids in culture acquired a red (DsRed) or green (eGFP) fluorescent phenotype (Fig. 6B). Presence of the COMMD1 protein in liver organoids after transduction was confirmed by immunocytochemistry (Fig. 6C). After expansion, organoid differentiation was induced by changing medium composition from EM (expansion medium) to DM (differentiation medium). Differentiation level was evaluated on transcriptional and protein level. Gene expression of liver stem/progenitor cell markers *LGR5* and *SOX9* decreased upon differentiation, whereas expression of hepatocyte markers *MRP2*, *CYP3A12*, and *ARG1* increased (Fig. 6D). However, we did not detect an increase in intracellular liver enzymes after differentiation (data not shown).

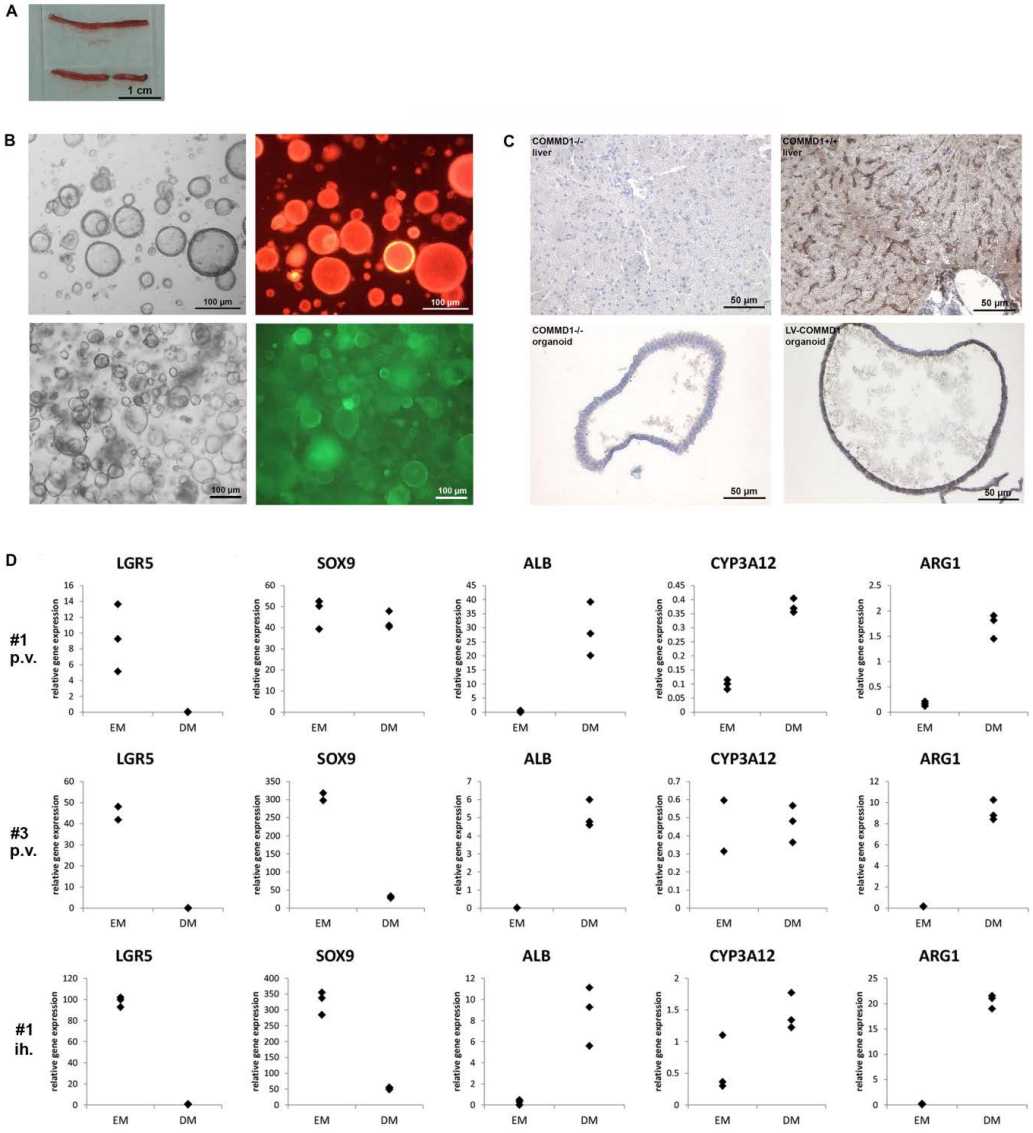

Figure 6. Establishment and differentiation of LV-corrected autologous liver organoid cultures. A. Two 14G liver biopsies were used to isolate patient-specific liver progenitor cells. B. Phase-contrast and fluorescent images of autologous liver organoid cultures after lentiviral transduction with pHAGE2-EF1a-COMMD1-DsRed-PuroR (red) or pHAGE2-EF1a-COMMD1-eGFP-PuroR (green). C. Representative images of immunohisto-/cytological staining for COMMD1 in canine COMMD1-/- liver, COMMD1+/+ (wildtype) liver, COMMD1-/- organoids and in COMMD1-/- organoids after lentiviral (LV) transduction. D. Relative gene expression of liver progenitor and hepatocyte markers of liver organoids cultured in expansion medium (EM) and differentiation medium (DM). Transcriptional profiles are shown for individual dogs, prior to transplantation in either the portal vein (p.v., dog 1, dog 3) or intrahepatic (ih., dog 1) transplantation.

Intraportal transplantation: clinical course, complications and follow up

In total, dog 1 received $4.5x10^8$ and dog 3 received $7.3x10^8$ organoid-derived liver cells. The total dosage was divided over three days. Viability before transplantation ranged from 92 to 99% (Fig. 7A). Infusion of the cell suspension in dog 3 resulted in a slight increase in portal pressure from 13 mm H_2O pre- to 17 mm H_2O post infusion, which normalized to 12 mm H_2O within two hours (Fig. 7B). Vehicle injection in dog 2 did not increase portal pressure (13 mm H_2O pre- and 14 mm H_2O post infusion). In both dog 1, 2, and 3 portal infusions of either vehicle or cells were not associated with changes in heart rate or mean arterial blood pressure or any other adverse events.

Dog 1 and dog 2 developed a hemoabdomen 24 hours post-operatively, necessitating a second surgical intervention to secure hemostasis. In dog 3 the surgical approach for the lobectomy was modified to a finger fracture technique and the total heparin dose used for catheter flushing was reduced. Dog 3 had an unremarkable recovery.

All dogs had gastrointestinal side effects from the oral cyclosporine treatment, such as anorexia, vomiting and diarrhea. This was managed with antiemetic (metoclopramide, ondansetron) and antacid (omeprazole) treatment.

Long term complications of the PAC occurred in all dogs. In dog 1 the catheter had dislocated after two months, in dogs 2 and 3 thrombus formation was observed at the tip of the catheter in the portal vein after one to three months. PACs were surgically removed in all three dogs, and in dog 2 and dog 3 liver wedge biopsies were taken during the surgery (5 months post-transplantation). Plasma activity levels for liver enzymes alkaline phosphatase (ALP) and alanine aminotransferase (ALT) were within reference range or minimally elevated before transplantation and increased in all three dogs on the days after liver lobectomy (Fig. 7C). Values decreased to pre-transplantation levels within one month and remained stable during the twelve months follow up. Blood analysis showed a decrease in hematocrit, total protein and albumin on the days after surgery in all three dogs, indicative of blood loss. Fibrinogen levels were elevated post-operatively in dog 1 and dog 3. APTT and PT were prolonged in dog 1 and dog 2 in the days after surgery, coinciding with hemoabdomen development in these dogs.

Biliary ^{64}Cu excretion after six hours was ≤1% of the total injected dose in all dogs at the start of the study (Fig. 7D). This is consistent with hepatic copper storage disease (Mandigers et al., 2007). Biliary copper excretion did not improve post-transplantation.

A

	Total cell count	Viability
Dog 1	$4.5x10^8$	92-95%
Dog 3	$7.3x10^8$	95-99%

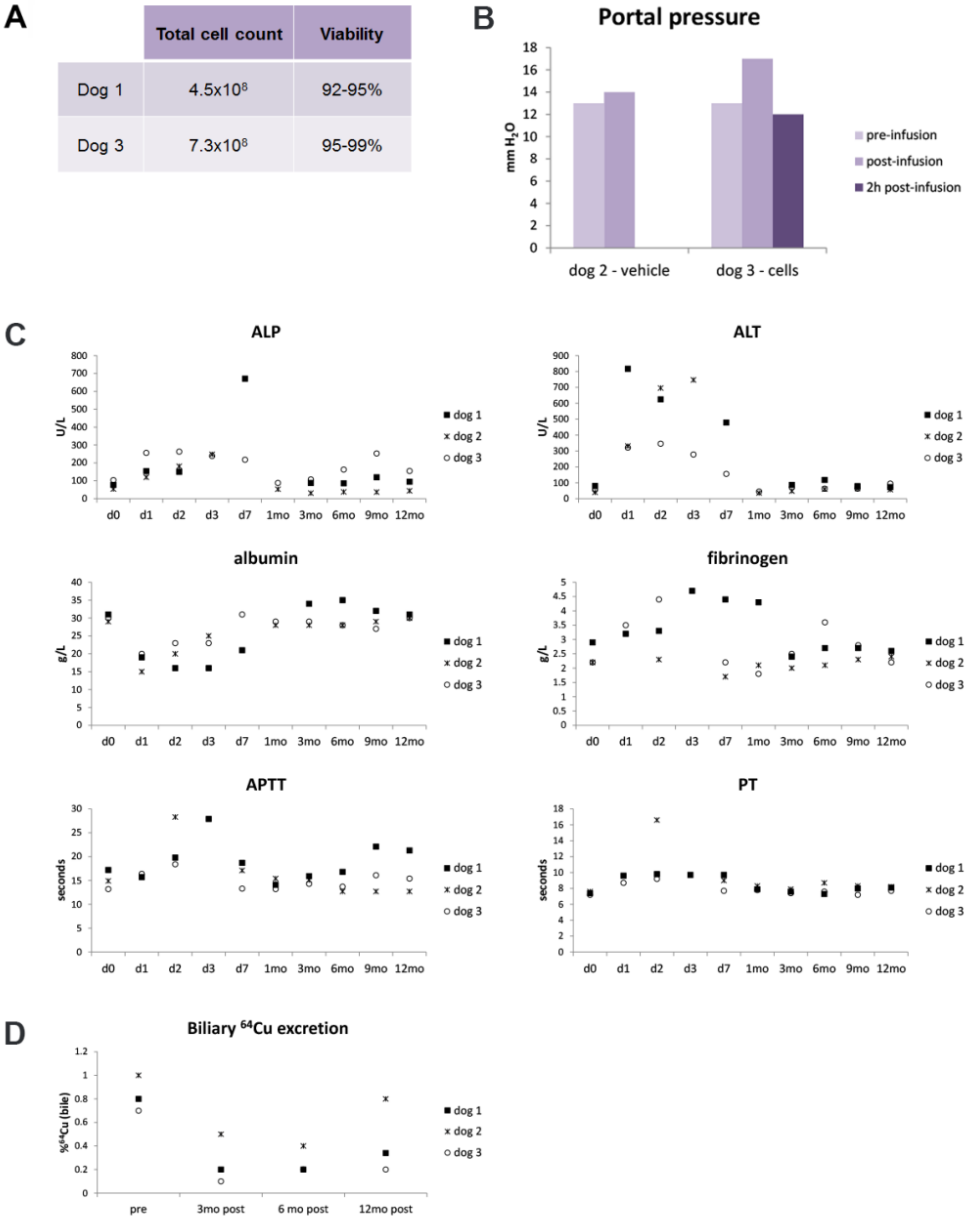

Figure 7. Clinical evaluation of intraportal transplantation. A. Viability and number of cells transplanted in dog 1 and dog 3. B. Portal pressure in mm H_2O before and after vehicle (dog 2) or cell transplantation (dog 3) via the Port-A-Cath. C. Blood analysis of liver enzymes (alkaline phosphatase: ALP, ref. <89 U/L); alanine aminotransferase: ALT, ref. <70 U/L), albumin (ref. 26-37 g/L), fibrinogen (ref. 1.0-2.7 g/L), and coagulation (prothrombin time: PT, ref. 7.2-9.9 seconds; activated partial thromboplastin time: APTT, ref. 13.2-18.2 seconds). d0: day 0; 1mo: 1 month post-transplantation D. Biliary copper excretion was calculated as percentage of total injected ^{64}Cu dose measured in the bile after 6 hours.

Hepatic engraftment after intraportal transplantation

Per sampling time point (Fig. 1) four liver biopsies were evaluated for the presence of transplanted cells on RNA, DNA and cell/tissue level based on the expression of full length COMMD1 and/or DsRed. Quantitative reverse transcriptase PCR analysis failed to detect transcripts of COMMD1 exon 2 or DsRed in liver samples post-transplantation (data not shown). PCR on DNA isolated from biopsies after transplantation was negative for the presence of the DsRed gene on all sampling time points from all three dogs (Fig. 8A). Immunohistochemical staining for COMMD1 resulted in a sinusoidal staining pattern in normal dog liver (Fig. 8B). Post-transplantation biopsies (dog 1: 112 sections; dog 3: 240 sections) were all negative for COMMD1 immunoreactivity. Immunohistochemical staining for DsRed similarly failed to show the presence of engrafted cells, although very sporadically a single or several positive cells could be observed in biopsies of dog 1 and dog 3.

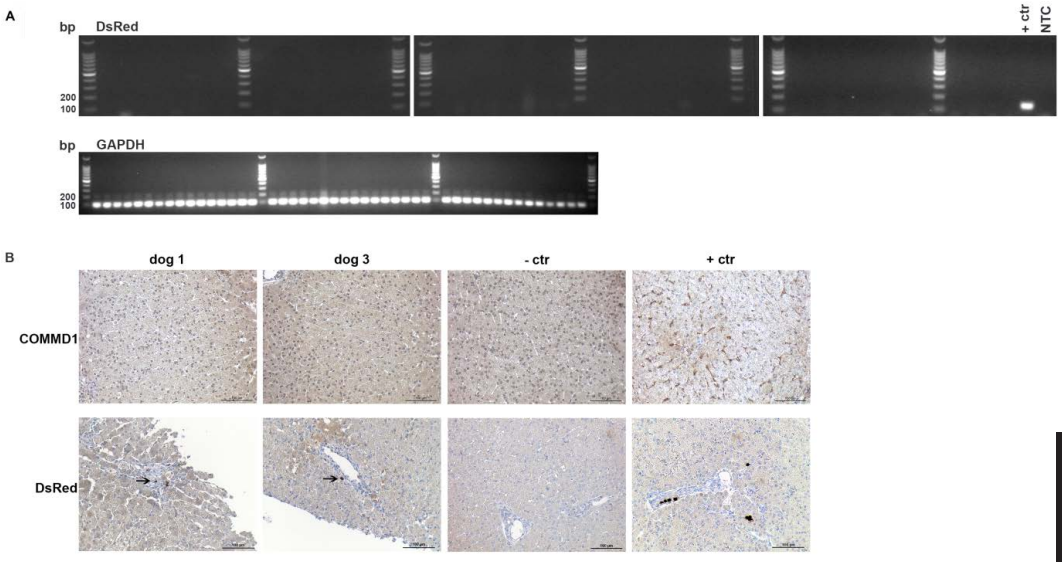

Figure 8. Cell tracking after intraportal transplantation. A. Agarose gel with DsRed PCR products of DNA isolated from post-transplantation liver biopsies. DNA from DsRed-transduced organoids was used as positive control (+ ctr). NTC: no template control. B. Representative images of immunohistochemical (IHC) stainings for COMMD1 and DsRed in liver biopsy sections of dog 1 and dog 3 one month post-transplantation. Arrows indicate DsRed positive cells, which were sporadically found in biopsies post-transplantation. Dog 2 received vehicle injection and served as negative control (- ctr). For COMMD1 IHC normal dog liver was used as positive control (+ctr), for DsRed IHC normal dog liver post-mortem injected with DsRed-transduced organoids was used as positive control.

Engraftment after intrahepatic injection

Because of lack of significant engraftment after intraportal transplantation, dog 1 was retransplanted two years after the beginning of the study by intrahepatic injections with pHAGE2-EF1a-COMMD1-eGFP-PuroR transduced autologous liver organoids. Undifferentiated (cultured in EM) and differentiated (cultured in DM) organoids were transplanted in separate injection sites and liver was harvested after seven days. Post-mortem, one extra injection site was established to serve as positive control. Engraftment was evaluated on RNA and cell/tissue level based on the expression

of full length COMMD1 and/or eGFP. Upon QPCR analysis both COMMD1 exon 2 and eGFP transcripts were detected in tissue from the post-mortem established injection site, with an expression level 20 to 40-fold lower compared to organoid lysates. COMMD1 exon 2 and eGFP mRNA levels were undetectable in samples from the EM and DM organoid intrahepatic injection sites harvested after seven days (Fig. 9A). On tissue level, eGFP immunohistochemical staining showed organoid engraftment in all injection sites harvested after seven days (Fig. 9B). We observed eGFP positive cell clusters and organoid-like structures with a multifocal distribution in the majority of the liver sections. Preliminary data suggest engraftment efficiency did not differ between EM and DM conditions (organoid counts per section, data not shown). To investigate proliferative status of organoids, Ki67 staining was performed. Cultured organoids in EM conditions showed positive nuclear staining, whereas organoids in DM conditions were mainly Ki67 negative (Fig. 9C). Serial staining for eGFP and Ki67 on sections of hepatic injection sites revealed positive nuclei in organoids in EM conditions seven days after intrahepatic injection, indicative of organoid proliferation *in vivo*. DM organoids remained mainly Ki67 negative after intrahepatic injection. Injected organoids in the liver were consistently embedded in newly formed fibrous tissue in all conditions except in the post-mortem injected liver samples. Van Gieson-elastica staining indicated a (sometimes circular) deposition of loosely arranged, non-birefringent collagen fibrils around the engrafted organoids in the liver (Fig. 9D). Elastin fibers were absent. In non-injected, vehicle injected and post-mortem injected liver samples stromal deposition was mainly confined to large portal areas and was characterized by a higher staining intensity and the presence of small amounts of elastin fibers.

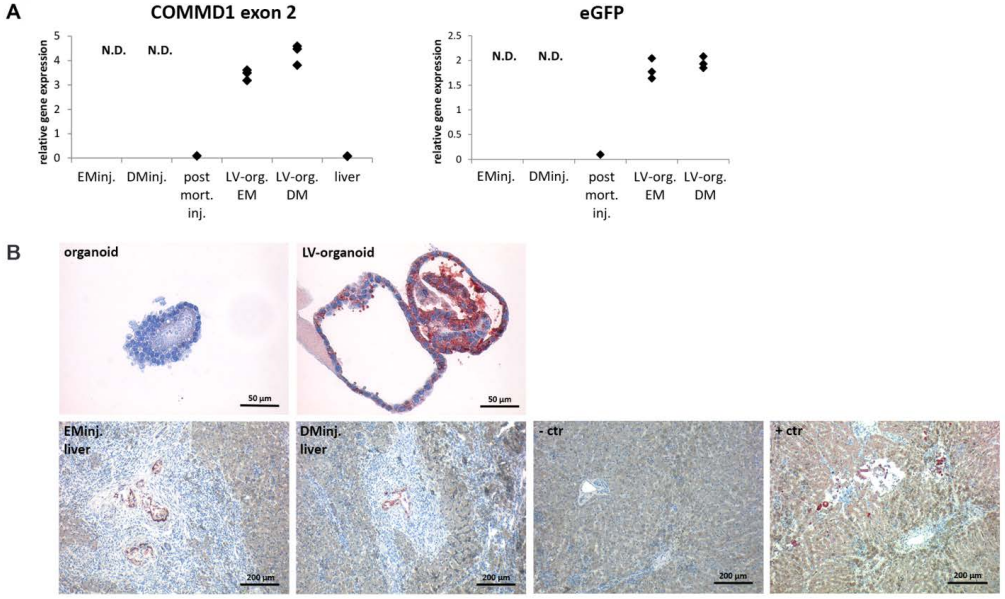

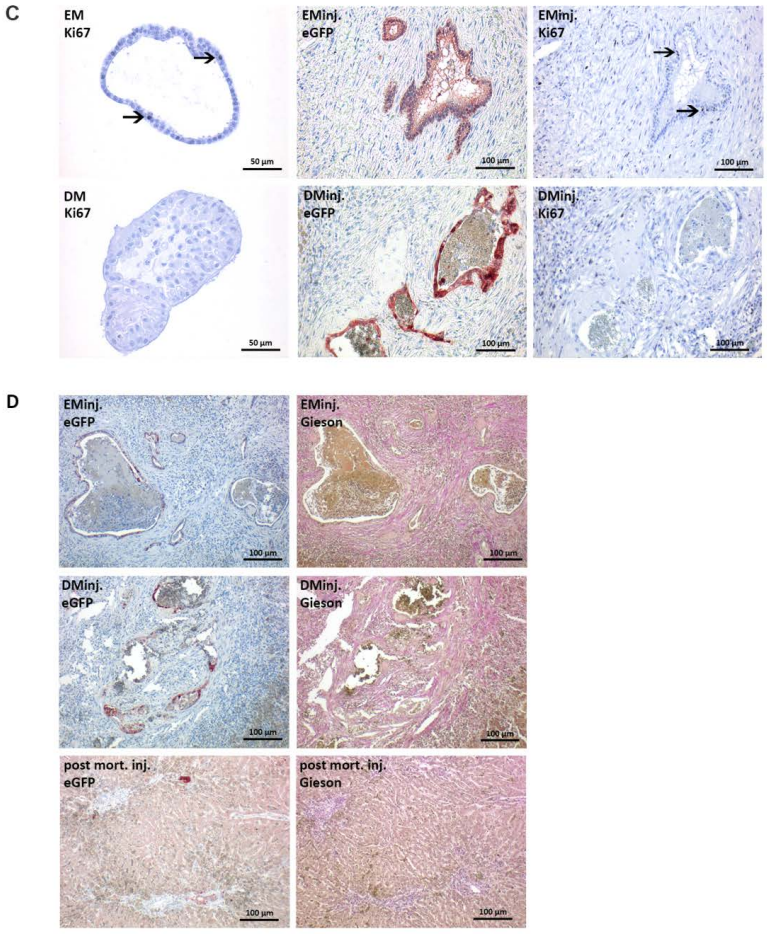

Figure 9. Cell tracking after transplantation by intrahepatic injection. A. Relative gene expression of COMMD1 exon 2 and eGFP in liver injections sites of undifferentiated (EMinj.) and differentiated (DMinj.) organoids. A post-mortem established injection site (post mort. inj.), normal liver and/or lentivirally (LV) transduced organoids in EM and DM served as positive control. B. Representative images of immunocyto-/histochemical (IHC) stainings for eGFP (red chromogen) in dog 1 liver organoids, organoids transduced with pHAGE2-EF1a-COMMD1-eGFP-PuroR (LV-organoid), and EM and DM organoid liver injection sites, showing eGFP positive structures in the recipient liver. Vehicle injected liver served as negative control (- ctr); post-mortem injected liver served as positive control (+ ctr). C. Representative images of serial IHC stainings for eGFP (red chromogen) and Ki67 (brown/black chromogen). Organoids in EM conditions show nuclear staining for Ki67 (arrows) both *in vitro* (EM) and seven days after intrahepatic injection (EMinj.). Organoids in DM conditions were mainly negative for Ki67 *in vitro* (DM) and remained negative *in vivo* (DMinj.). D. Representative images of serial IHC stainings for eGFP (red chromogen) and van Gieson-elastica stainings of liver injected with EM en DM organoids and post-mortem injected control liver. Extracellular matrix deposition can be seen surrounding the engrafted organoids, which is absent in post-mortem injected liver.

Discussion

In the present study, autologous canine liver organoids were transplanted in a COMMD1 deficient model of copper storage disease. Preliminary data indicate engraftment and proliferation in the liver after intrahepatic injection of organoid fragments.

Organoids were cultured from liver biopsies and could be massively expanded in culture for cell transplantation. In metabolic liver disease an estimated 2-5% repopulation of the liver with normal hepatocytes would suffice for clinical recovery of liver disease (Sancho-Bru et al., 2009). With an estimated liver mass of 300 to 350 gram (Marchioro et al., 1967) and taking the hepatocellularity of a dogs' liver into account (Sohlenius-Sternbeck 2006), the total cell dose we transplanted in dog 1 and dog 3 would constitute 0.6-1.2% repopulation. This number of cells was reached after 10-12 weeks of autologous liver organoid culture from two 14G Tru-cut biopsies.

In reported human and canine (pre)clinical hepatocyte transplantations, the preferred route of administration was via the portal vein (Kocken et al., 1996; Fox et al., 1998; Puppi et al., 2008; Stéphenne et al., 2006, 2012) although some studies report on cell transplantation via the hepatic artery (Khan et al., 2010; Cardinale et al., 2014). Experimental mouse, rat and human liver organoid transplantations in rodents were performed by intrasplenic injection, also resulting in cellular engraftment into the liver via the portal vein (Huch et al., 2013, 2015; Kuijk et al., 2016). This prompted us to develop a transplantation technique in dogs using a permanent catheter (PAC) in the portal vein, providing a low-invasive option for repeated intraportal delivery of cells. Moreover, this approach could be easily translated to human clinical application (Darwish et al., 2004).

Intraportal transplantation in two dogs of canine organoid-derived liver cells via the PAC was feasible and did not result in adverse events such as portal hypertension, as reported in human hepatocyte transplantation (Jorns et al., 2012). However, both on short (one week) and long term (one year) intraportal transplantation did not result in significant engraftment. Only sporadically were individual cells positive for the DsRed transgene found in liver biopsies after transplantation. Mouse organoid transplantation has a reported efficiency of 5/15 successfully transplanted mice with a 0.1-1% repopulation percentage (Huch et al., 2013). Rat organoid transplantation was successful in 3 out of 7 transplanted animals (Kuijk et al., 2016). Conceivably, unsuccessful transplantation in a rodent could be the result of the intrasplenic injection route which requires the cells to leave the splenic pulp to reach the portal bloodstream (Cheng et al., 2009). In our dogs, we have transplanted cells directly into the portal vein. In human and experimental rodent hepatocyte transplantations, transplanted cells are known to embolize in the sinusoids, cross the fenestrae in the endothelium, and integrate in the hepatic parenchyma. Any cells remaining in the vascular lumen will be cleared by phagocytosis within 24-48 hours (Gupta et al., 1995, 1999; Jorns et al., 2012). In human hepatocyte transplantation engraftment efficiency is low and often repeated infusions of cells are provided (Jorns et al., 2012; Puppi et al., 2012). Therefore we divided the total transplanted cell dose over three infusions on consecutive days, which is known to promote hepatic engraftment (Ira Fox, personal communication).

Successful engraftment was accomplished with intrahepatic injections of canine autologous liver organoid fragments. Organoid differentiation status did not affect engraftment efficiency, but only undifferentiated organoids showed active proliferation *in vivo* seven days post-transplantation. Interestingly, when human hepatocytes are transplanted the clinical effect is generally short-lived and little is known about the behavior of transplanted hepatocytes within the recipient's liver. One study described the presence of donor cells in liver biopsies one year after transplantation which suggests long-term persistence (Stéphenne et al., 2006), but evidence of *in vivo* proliferation is lacking. This phenomenon has precluded the clinical application of human hepatocyte transplantation for permanent recovery of metabolic liver disease and hence its use is currently limited to bridging a patient to orthotopic liver transplantation (Jorns et al., 2012; Forbes et al., 2015). The fact that canine organoids survive and proliferate in the recipient liver after intrahepatic

injection as fragments but not after intraportal administration as single cells can be explained by a number of factors. For instance it could stem from a lack of extravasation capacity of canine organoid-derived single cells, which would constitute a species-difference as mouse and rat organoid-derived single cells were able to engraft via the portal route (Huch et al., 2013; Kuijk et al., 2016). Also, the extravasation itself is largely a process resulting from embolization in the sinusoids and a secondary sinusoidal disruption (Gupta et al., 1999), although integrin-mediated ECM interactions are also suggested to play a role (Kumaran et al., 2005). A second reason could be a difference in survival or engraftment capacity between organoid-derived single cells and organoid fragments. In dissociated human pluripotent stem cells, loss of intercellular contact primes for apoptosis (Ohgushi et al., 2010). This could be investigated by comparing engraftment after intrahepatic injections of both organoid-derived single cells and organoid fragments. A third option would be translocation of the cells to the pulmonary or systemic circulation after intraportal administration. However, canine cadaveric liver perfusion with 10 µm sized microbeads smaller than organoid-derived single cells resulted in entrapment of all of the beads within the liver.
Likewise, ^{99}Tc labeled macroaggregated albumin aggregates of 10-90 µm lodge in the canine liver after intraportal injection (Meyer et al., 1994). In human hepatocyte and liver progenitor cell transplantations, intraportal administration of radioactively labeled cells also yielded exclusive hepatic and no pulmonary entrapment (Bohnen et al., 2000; Cheng et al., 2009; Defresne et al., 2014). Similar radiotracer studies would need to be performed in dogs after canine organoid-derived liver cell transplantations to conclusively determine hepatic biodistribution.
An unexpected finding was the fibrous tissue that surrounded the engrafted organoids in the liver after intrahepatic injection. Histochemical analysis of injected and control liver tissue was more suggestive for *de novo* synthesis rather than pre-existence of the stroma, based on the lower staining intensity and non-birefringence of the fibrils. This can be interpreted as a tissue reaction towards the injected organoid fragments, but another possibility is that the organoids themselves produce extracellular matrix components. Hepatic progenitor cells have been proposed to be able to contribute to hepatic fibrosis (Knight et al., 2007; Kuramitsu et al., 2013). An *in vivo* profibrogenic phenotype of transplanted liver organoids would be highly undesirable and further research is needed to study the etiology of the fibrous tissue development, for example whether it depends on the administration route, cell/fragment size, and/or differentiation status.
Although the number of transplanted dogs was low, we were able to perform a longitudinal study with pre-transplantation control measurements for each dog. This is an advantage over rodent models, in which repeated liver biopsies for cell tracking and safety evaluation are not feasible.
Another limitation could be the relatively low level of organoid differentiation towards hepatocyte-like cells that was achieved. Currently, the level of maturation that can be achieved or maintained *in vitro* is also suboptimal for liver organoids from other species, for iPS-derived liver cells and even for primary hepatocytes (Huch et al., 2013, 2015; Kuijk et al., 2016; Ochiya et al., 2010; Frazcek et al., 2013). If hepatocytes can be successfully transplanted, then perhaps the low level of maturation could explain the lack of engraftment of canine liver organoids after intraportal delivery. Conversely, after intrahepatic injection undifferentiated organoids were not only able to engraft but also to proliferate *in vivo*, which is an important requirement for repopulation of the recipient liver with healthy cells.
In conclusion, canine liver organoids can be used for cell transplantation. After intraportal transplantation no significant engraftment was observed, but upon intrahepatic injections organoids engrafted in the canine liver and proliferated *in vivo*. An important focus for future research should

be the improvement of liver organoid differentiation to evaluate the effect on cellular engraftment and repopulation potential. In future transplantations, intraportal and intrahepatic administration routes should be compared within the same procedure. Engraftment and subsequent contribution of organoid-derived liver cells to functional recovery of liver disease should be evaluated both on short- and long-term. These studies are pivotal for the translation of liver organoid transplantations from an experimental setting to human clinical application.

Acknowledgements

The authors would like to thank Ivo Sullot (Smiths Medical), Manon Vos, Ronald Kisjes, and Lotte Janssen for technical assistance, and colleagues from the Utrecht University clinic for companion animals (especially Jeffrey de Gier, Inge van Duiven, Ronald Jan Corbee, and Intensive Care Unit staff) for clinical assistance.

References

Allen KJ, Cheah DM, Wright PF, Gazeas S, Pettigrew-Buck NE, Deal YH, Mercer JF, Williamson R. Liver cell transplantation leads to repopulation and functional correction in a mouse model of Wilson's disease. J Gastroenterol Hepatol. 2004;19(11):1283-90.

Archer TM, Boothe DM, Langston VC, Fellman CL, Lunsford KV, Mackin AJ.
Oral cyclosporine treatment in dogs: a review of the literature. J Vet Intern Med. 2014;28(1):1-20.

Arruda VR, Favaro P, Finn JD. Strategies to modulate immune responses: a new frontier for gene therapy. Mol Ther. 2009;17(9):1492-503.

Benedetti E, Kirby JP, Asolati M, Blanchard J, Ward MG, Williams R, Hewett TA, Fontaine M, Pollak R. Intrasplenic hepatocyte allotransplantation in dalmation dogs with and without cyclosporine immunosuppression. Transplantation. 1997;63(9):1206-9.

Bode P. Instrumental neutron activation analysis in a routine way. J Trace Microprobe Tech. 1990;8: 139-54.

Bohnen NI, Charron M, Reyes J, Rubinstein W, Strom SC, Swanson D, Towbin R. Use of indium-111-labeled hepatocytes to determine the biodistribution of transplanted hepatocytes through portal vein infusion. Clin Nucl Med. 2000;25(6):447-50.

Cardinale V, Carpino G, Gentile R, Napoletano C, Rahimi H, Franchitto A, Semeraro R, Nuti M, Onori P, Berloco PB, Rossi M, Bosco D, Brunelli R, Fraveto A, Napoli C, Torrice A, Gatto M, Venere R, Bastianelli C, Aliberti C, Salvatori FM, Bresadola L, Bezzi M, Attili AF, Reid L, Gaudio E, Alvaro D. Transplantation of human fetal biliary tree stem/progenitor cells into two patients with advanced liver cirrhosis. BMC Gastroenterol. 2014;14:204.

Cheng K, Benten D, Bhargava K, Inada M, Joseph B, Palestro C, Gupta S. Hepatic targeting and biodistribution of human fetal liver stem/progenitor cells and adult hepatocytes in mice. Hepatology. 2009;50(4):1194-203.

Darwish AA, Sokal E, Stephenne X, Najimi M, de Goyet Jde V, Reding R. Permanent access to the portal system for cellular transplantation using an implantable port device. Liver Transpl. 2004;10(9):1213-5.

Defresne F, Tondreau T, Stéphenne X, Smets F, Bourgois A, Najimi M, Jamar F, Sokal EM. Biodistribution of adult derived human liver stem cells following intraportal infusion in a 17-year-old patient with glycogenosis type 1A. Nucl Med Biol. 2014;41(4):371-5.

Fang B, Eisensmith RC, Wang H, Kay MA, Cross RE, Landen CN, Gordon G, Bellinger DA, Read MS, Hu PC, et al. Gene therapy for hemophilia B: host immunosuppression prolongs the therapeutic effect of adenovirus-mediated factor IX expression. Hum Gene Ther. 1995;6(8):1039-44.

Favier RP, Spee B, Schotanus BA, van den Ingh TS, Fieten H, Brinkhof B, Viebahn CS, Penning LC, Rothuizen J. COMMD1-deficient dogs accumulate copper in hepatocytes and provide a good model for chronic hepatitis and fibrosis. PLoS One. 2012;7(8):e42158.

Fieten H, Leegwater PA, Watson AL, Rothuizen J. Canine models of copper toxicosis for understanding mammalian copper metabolism. Mamm Genome. 2012;23(1-2):62-75.

Fieten H, Gill Y, Martin AJ, Concilli M, Dirksen K, van Steenbeek FG, Spee B, van den Ingh TS, Martens EC, Festa P, Chesi G, van de Sluis B, Houwen RH, Watson AL, Aulchenko YS, Hodgkinson VL, Zhu S, Petris MJ, Polishchuk RS, Leegwater PA, Rothuizen J. The Menkes and Wilson disease genes counteract in copper toxicosis in Labrador retrievers: a new canine model for copper-metabolism disorders. Dis Model Mech. 2016;9(1):25-38.

Forbes SJ, Gupta S, Dhawan A. Cell therapy for liver disease: From liver transplantation to cell factory. J Hepatol. 2015;62(1 Suppl):S157-69.

Forman OP, Boursnell ME, Dunmore BJ, Stendall N, van den Sluis B, Fretwell N, Jones C, Wijmenga C, Rothuizen J, van Oost BA, Holmes NG, Binns MM, Jones P. Characterization of the COMMD1 (MURR1) mutation causing copper toxicosis in Bedlington terriers. Anim Genet. 2005;36(6):497-501.

Fox IJ, Chowdhury JR, Kaufman SS, Goertzen TC, Chowdhury NR, Warkentin PI, Dorko K, Sauter BV, Strom SC. Treatment of the Crigler-Najjar syndrome type I with hepatocyte transplantation. N Engl J Med. 1998;338(20):1422-6.

Fraczek J, Bolleyn J, Vanhaecke T, Rogiers V, Vinken M. Primary hepatocyte cultures for pharmaco-toxicological studies: at the busy crossroad of various anti-dedifferentiation strategies. Arch Toxicol. 2013;87(4):577-610.

Guha C, Deb NJ, Sappal BS, Ghosh SS, Roy-Chowdhury N, Roy-Chowdhury J. Amplification of engrafted hepatocytes by preparative manipulation of the host liver. Artif Organs. 2001;25(7):522-8.

Gupta S, Rajvanshi P, Lee CD. Integration of transplanted hepatocytes into host liver plates demonstrated with dipeptidyl peptidase IV-deficient rats. Proc Natl Acad Sci U S A. 1995;92(13):5860-4.

Gupta S, Rajvanshi P, Sokhi R, Slehria S, Yam A, Kerr A, Novikoff PM. Entry and integration of transplanted hepatocytes in rat liver plates occur by disruption of hepatic sinusoidal endothelium. Hepatology. 1999;29(2):509-19.

Huch M, Dorrell C, Boj SF, van Es JH, Li VS, van de Wetering M, Sato T, Hamer K, Sasaki N, Finegold MJ, Haft A, Vries RG, Grompe M, Clevers H. In vitro expansion of single Lgr5+ liver stem cells induced by Wnt-driven regeneration. Nature. 2013a;494(7436):247-50.

Huch M, Boj SF, Clevers H. Lgr5(+) liver stem cells, hepatic organoids and regenerative medicine. Regen Med. 2013b;8(4):385-7.

Huch M, Gehart H, van Boxtel R, Hamer K, Blokzijl F, Verstegen MM, Ellis E, van Wenum M, Fuchs SA, de Ligt J, van de Wetering M, Sasaki N, Boers SJ, Kemperman H, de Jonge J, Ijzermans JN, Nieuwenhuis EE, Hoekstra R, Strom S, Vries RR, van der Laan LJ, Cuppen E, Clevers H. Long-term culture of genome-stable bipotent stem cells from adult human liver. Cell. 2015;160(1-2):299-312.

Ijzer J, Schotanus BA, Vander Borght S, Roskams TA, Kisjes R, Penning LC, Rothuizen J, van den Ingh TS. Characterisation of the hepatic progenitor cell compartment in normal liver and in hepatitis: an immunohistochemical comparison between dog and man. Vet J. 2010;184(3):308-14.

Jorns C, Ellis EC, Nowak G, Fischler B, Nemeth A, Strom SC, Ericzon BG. Hepatocyte transplantation for inherited metabolic diseases of the liver. J Intern Med. 2012;272(3):201-23.

Khan AA, Shaik MV, Parveen N, Rajendraprasad A, Aleem MA, Habeeb MA, Srinivas G, Raj TA, Tiwari SK, Kumaresan K, Venkateswarlu J, Pande G, Habibullah CM. Human fetal liver-derived stem cell transplantation as supportive modality in the management of end-stage decompensated liver cirrhosis. Cell Transplant. 2010;19(4):409-18.

Klomp AE, van de Sluis B, Klomp LW, Wijmenga C. The ubiquitously expressed MURR1 protein is absent in canine copper toxicosis. J Hepatol. 2003;39(5):703-9.

Knight B, Lim R, Yeoh GC, Olynyk JK. Interferon-gamma exacerbates liver damage, the hepatic progenitor cell response and fibrosis in a mouse model of chronic liver injury. J Hepatol. 2007;47(6):826-33.

Kocken JM, Borel Rinkes IH, Bijma AM, de Roos WK, Bouwman E, Terpstra OT, Sinaasappel M. Correction of an inborn error of metabolism by intraportal hepatocyte transplantation in a dog model. Transplantation. 1996;62(3):358-64.

Kruitwagen HS, Spee B, Schotanus BA. Hepatic progenitor cells in canine and feline medicine: potential for regenerative strategies. BMC Vet Res. 2014;10:137.

Kruitwagen HS, Oosterhoff LA, Vernooij IGWH, Schrall IM, van Wolferen ME, Bannink F, Roesch C, van Uden L, Molenaar MR, Helms JB, Grinwis GCM, Verstegen MMA, van der Laan LJW, Huch M, Geijsen N, Vries RG, Clevers H, Rothuizen J, Schotanus BA, Penning LC, Spee B. Long-Term Adult Feline Liver Organoid Cultures for Disease Modeling of Hepatic Steatosis. Stem Cell Reports. 2017;8(4):822-830.

Kuijk EW, Rasmussen S, Blokzijl F, Huch M, Gehart H, Toonen P, Begthel H, Clevers H, Geurts AM, Cuppen E. Generation and characterization of rat liver stem cell lines and their engraftment in a rat model of liver failure. Sci Rep. 2016;6:22154.

Kumaran V, Joseph B, Benten D, Gupta S. Integrin and extracellular matrix interactions regulate engraftment of transplanted hepatocytes in the rat liver. Gastroenterology. 2005;129(5):1643-53.

Kuramitsu K, Sverdlov DY, Liu SB, Csizmadia E, Burkly L, Schuppan D, Hanto DW, Otterbein LE, Popov Y. Failure of fibrotic liver regeneration in mice is linked to a severe fibrogenic response driven by hepatic progenitor cell activation. Am J Pathol. 2013;183(1):182-94.

Malhi H, Irani AN, Volenberg I, Schilsky ML, Gupta S. Early cell transplantation in LEC rats modeling Wilson's disease eliminates hepatic copper with reversal of liver disease. Gastroenterology. 2002;122(2):438-47.

Mandigers PJ, Bode P, van Wees AM, van den Brom WE, van den Ingh TS, Rothuizen J. Hepatic (64)Cu excretion in Dobermanns with subclinical hepatitis. Res Vet Sci. 2007;83(2):204-9.

Marchioro TL, Porter KA, Brown BI, Otte JB, Starzl TE. The effect of partial portacaval transposition on the canine liver. Surgery. 1967;61(5):723-32.

Matsumoto N, Koizumi M, Sugai M. Hepatolobectomy-induced depression of hepatic circulation and metabolism in the dog is counteracted by isoflurane, but not by halothane. Acta Anaesthesiol Scand. 1999;43(8):850-4.

Meyburg J, Alexandrova K, Barthold M, Kafert-Kasting S, Schneider AS, Attaran M, Hoerster F, Schmidt J, Hoffmann GF, Ott M. Liver cell transplantation: basic investigations for safe application in infants and small children. Cell Transplant. 2009;18(7):777-86.

Meyer HP, Rothuizen J, van den Brom WE, Voorhout G, van Sluijs FJ, How KL, Pollak YW. Quantitation of portosystemic shunting in dogs by ultrasound-guided injection of 99MTc-macroaggregates into a splenic vein. Res Vet Sci. 1994;57(1):58-62.

Nantasanti S, Spee B, Kruitwagen HS, Chen C, Geijsen N, Oosterhoff LA, van Wolferen ME, Pelaez N, Fieten H, Wubbolts RW, Grinwis GC, Chan J, Huch M, Vries RR, Clevers H, de Bruin A, Rothuizen J, Penning LC, Schotanus BA. Disease Modeling and Gene Therapy of Copper Storage Disease in Canine Hepatic Organoids. Stem Cell Reports. 2015;5(5):895-907.

Nussler A, Konig S, Ott M, Sokal E, Christ B, Thasler W, Brulport M, Gabelein G, Schormann W, Schulze M, Ellis E, Kraemer M, Nocken F, Fleig W, Manns M, Strom SC, Hengstler JG. Present status and perspectives of cell-based therapies for liver diseases. J Hepatol. 2006;45(1):144-59.

Ochiya T, Yamamoto Y, Banas A. Commitment of stem cells into functional hepatocytes. Differentiation. 2010;79(2):65-73.

Ohgushi M, Matsumura M, Eiraku M, Murakami K, Aramaki T, Nishiyama A, Muguruma K, Nakano T, Suga H, Ueno M, Ishizaki T, Suemori H, Narumiya S, Niwa H, Sasai Y. Molecular pathway and cell state responsible for dissociation-induced apoptosis in human pluripotent stem cells. Cell Stem Cell. 2010;7(2):225-39.

Poldervaart JH, Favier RP, Penning LC, van den Ingh TS, Rothuizen J. Primary hepatitis in dogs: a retrospective review (2002-2006). J Vet Intern Med. 2009;23(1):72-80.

Puppi J, Tan N, Mitry RR, Hughes RD, Lehec S, Mieli-Vergani G, Karani J, Champion MP, Heaton N, Mohamed R, Dhawan A. Hepatocyte transplantation followed by auxiliary liver transplantation--a novel treatment for ornithine transcarbamylase deficiency. Am J Transplant. 2008;8(2):452-7.

Puppi J, Strom SC, Hughes RD, Bansal S, Castell JV, Dagher I, Ellis EC, Nowak G, Ericzon BG, Fox IJ, Gómez-Lechón MJ, Guha C, Gupta S, Mitry RR, Ohashi K, Ott M, Reid LM, Roy-Chowdhury J, Sokal E, Weber A, Dhawan A. Improving the techniques for human hepatocyte transplantation: report from a consensus meeting in London. Cell Transplant. 2012;21(1):1-10.

Sancho-Bru P, Najimi M, Caruso M, Pauwelyn K, Cantz T, Forbes S, Roskams T, Ott M, Gehling U, Sokal E, Verfaillie CM, Muraca M. Stem and progenitor cells for liver repopulation: can we standardise the process from bench to bedside? Gut. 2009;58(4):594-603.

Sauer V, Siaj R, Stöppeler S, Bahde R, Spiegel HU, Köhler G, Zibert A, Schmidt HH. Repeated transplantation of hepatocytes prevents fulminant hepatitis in a rat model of Wilson's disease. Liver Transpl. 2012;18(2):248-59.

Schotanus BA, van den Ingh TS, Penning LC, Rothuizen J, Roskams TA, Spee B. Cross-species immunohistochemical investigation of the activation of the liver progenitor cell niche in different types of liver disease. Liver Int. 2009;29(8):1241-52

van de Sluis B, Rothuizen J, Pearson PL, van Oost BA, Wijmenga C. Identification of a new copper metabolism gene by positional cloning in a purebred dog population. Hum Mol Genet. 2002;11(2):165-73.

Sohlenius-Sternbeck AK. Determination of the hepatocellularity number for human, dog, rabbit, rat and mouse livers from protein concentration measurements. Toxicol In Vitro. 2006;20(8):1582-6.

Spee B, Arends B, van den Ingh TS, Roskams T, Rothuizen J, Penning LC. Major HGF-mediated regenerative pathways are similarly affected in human and canine cirrhosis. Comp Hepatol. 2007;6:8.

Stéphenne X, Najimi M, Sibille C, Nassogne MC, Smets F, Sokal EM. Sustained engraftment and tissue enzyme activity after liver cell transplantation for argininosuccinate lyase deficiency. Gastroenterology. 2006;130(4):1317-23.

Stéphenne X, Debray FG, Smets F, Jazouli N, Sana G, Tondreau T, Menten R, Goffette P, Boemer F, Schoos R, Gersting SW, Najimi M, Muntau AC, Goyens P, Sokal EM. Hepatocyte transplantation using the domino concept in a child with tetrabiopterin nonresponsive phenylketonuria. Cell Transplant. 2012;21(12):2765-70.

Su L, Owen C, Zollman PE, Hardy RM. A defect of biliary excretion of copper in copper-laden Bedlington terriers. Am J Physiol Gastrointest Liver Physiol. 1982; 243(3):G231-G236.

Volk SW, Theoret C. Translating stem cell therapies: the role of companion animals in regenerative medicine. Wound Repair Regen. 2013;21(3):382-94.

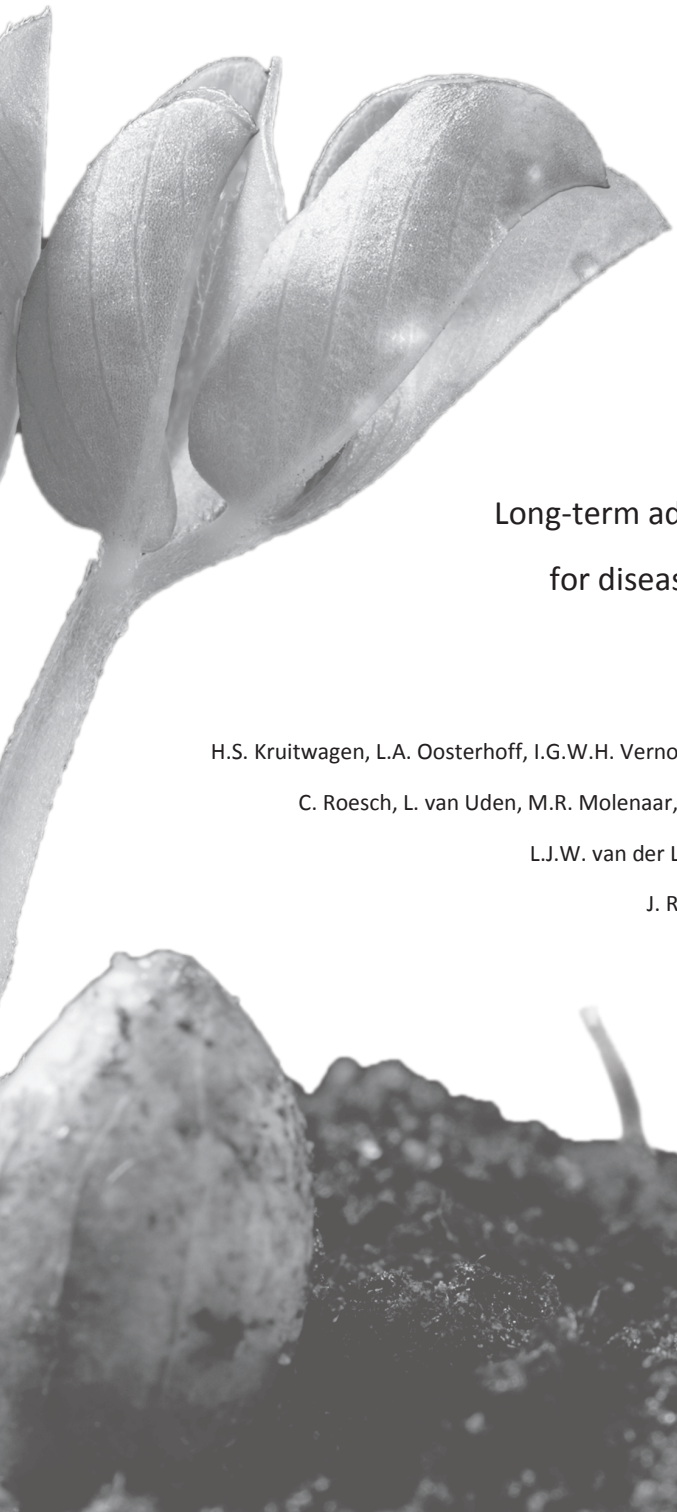

Chapter 7

Long-term adult feline liver organoid cultures for disease modeling of hepatic steatosis.

H.S. Kruitwagen, L.A. Oosterhoff, I.G.W.H. Vernooij, I.M. Schrall, M.E. van Wolferen, F. Bannink, C. Roesch, L. van Uden, M.R. Molenaar, J.B. Helms, G.C.M. Grinwis, M.M.A. Verstegen, L.J.W. van der Laan, M. Huch, N. Geijsen, R.G Vries, H. Clevers, J. Rothuizen, B.A. Schotanus, L.C. Penning, B. Spee

Stem Cell Reports. 2017;8(4):822-83

Summary

Hepatic steatosis is a highly prevalent liver disease, yet research is hampered by the lack of tractable cellular and animal models. Steatosis also occurs in cats, where it can cause severe hepatic failure. Previous studies demonstrate the potential of liver organoids for modeling genetic diseases. To examine the possibility of using organoids to model steatosis, we established a long-term feline liver organoid culture with adult liver stem cell characteristics and differentiation potential towards hepatocyte-like cells. Next, organoids from mouse, human, dog, and cat liver were provided with fatty acids. Lipid accumulation was observed in all organoids and interestingly, feline liver organoids accumulated more lipid droplets than human organoids. Finally, we demonstrate effects of interference with β-oxidation on lipid accumulation in feline liver organoids. In conclusion, feline liver organoids can be successfully cultured and display a predisposition for lipid accumulation, making them an interesting model in hepatic steatosis research.

Introduction

A specific adult liver stem cell population acting as second line of defense in liver regeneration has been described in several species, including rodents, humans, canines and felines (Wang et al., 2003; Roskams et al., 2003; Kruitwagen et al., 2014; Ijzer et al., 2009). Recently, a three-dimensional and highly proliferative organoid culture system was developed for mouse, human and dog liver stem cells (Huch et al., 2013; Huch et al., 2015; Nantasanti et al., 2015). Liver organoids have been proposed as *in vitro* disease modeling tool for several genetic liver diseases, such as α1-antitrypsin deficiency, Alagille syndrome, and canine copper storage disease (Huch et al., 2013; Huch et al., 2015; Nantasanti et al., 2015). However, many liver diseases do not have monogenetic etiology and have a more complex pathophysiology. We aimed to explore the potential of liver organoids to model non-genetic metabolic liver disease.
One of the most common metabolic liver diseases in human is liver steatosis, also known as non-alcoholic fatty liver disease (NAFLD) (Younossi et al., 2016). Interestingly, a severe type of hepatic steatosis also occurs in cats (feline hepatic lipidosis, FHL) (Center et al., 1993). Both in human and feline steatosis, hepatocyte lipid overload arises from an increased amount of free fatty acids (FFA) that are offered to the liver and obesity and insulin-resistance are known risk factors for its development (Center, 2005, Cohen et al., 2011). NAFLD can result in hepatocyte degeneration and inflammation (non-alcoholic steatohepatitis, NASH), and ultimately in excessive liver fibrosis and hepatocellular carcinoma (Cohen et al., 2011).
We asked whether liver organoids could be used to model hepatic steatosis and if so, whether there would be species differences in hepatocyte lipid-handling capacity. We hypothesized that liver cells from cats could have pronounced lipid accumulation properties. For this purpose, a culture system of feline liver progenitor cells as three dimensional organoids was established from cat liver samples. First, we describe the isolation, long-term culture and characterization of feline liver organoids. Second, we investigate the potential of liver organoids to model hepatic steatosis and compare lipid accumulation capacity between organoids of mouse, human, dog and cat liver. Third, as proof-of-principle we show the effects of interference with β oxidation on lipid accumulation and viability in feline liver organoids.

Results

Establishment of the feline liver organoid culture
Organoids were successfully cultured from cat liver samples of different origin (i.e. fresh, frozen, and fine needle aspirate (FNA)) (Fig. 1A). Biliary duct fragments were observed in the supernatant after digestion (Fig. 1B). After 3-6 days in culture, spherical structures appeared with occasional folding and budding. Morphology and passage rate were similar between donors and tissue sources. It was even possible to culture organoids from an undigested FNA plated straight into Matrigel; organoids appeared after five days, emerging from the remnant liver tissue fragments (Fig. 1C). Organoid morphology remained similar between passages (p1 to p25, Fig. 1D). Feline liver organoids could be cultured in expansion media as published for mouse, dog and human liver organoids with varying success rate on short and long-term culture (Figure S1) (Huch et al., 2013; Nantasanti et al., 2015; Huch et al., 2015). However, a hybrid medium (hereafter named cat expansion medium, cEM),

performed best and allowed for a high split ratio (1:11) in long-term culture. It was possible to cryopreserve feline liver organoids as fragments, which formed organoids again upon thawing.

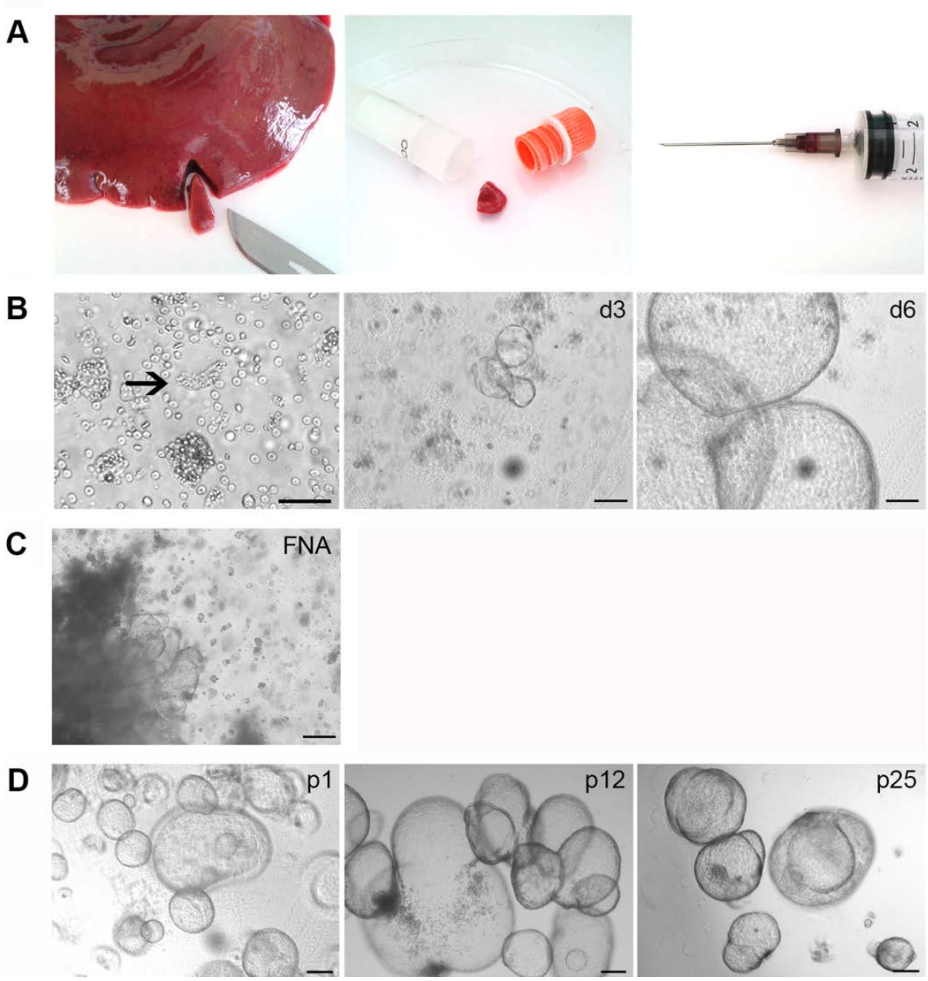

Figure 1. Establishment of an organoid culture from feline liver samples. (A) Fresh and snap frozen liver samples (wedge biopsies of 5 mm3) could be used with equal success rate to establish an organoid culture. It was also possible to start a feline liver organoid culture from a fine needle aspirate (aspirate visible in the conus of the needle). (B)Representative phase contrast images of duct isolation and organoid culture. After enzymatic digestion of feline liver samples, biliary duct fragments (arrow) were observed (scalebar represents 50 µm). Ducts were cultured in Matrigel and defined medium. After approximately three days in culture (d3) spherical structures appeared that rapidly grew out to large organoids within six days (d6) (scalebars represent 100 µm). (C) Representative phase contrast image of an undigested fine needle aspirate (FNA) plated straight into Matrigel. After five days, organoids emerged from the remnant liver tissue fragments (scalebar represents 100 µm). (D) Representative phase contrast images of feline liver organoids in early, medium and late passages (p1, p12 and p25, scalebars represent 100 µm). Morphology remained similar during long-term culture. See also Figure S1.

Characterization of feline liver organoids

We observed feline liver organoids microscopically as spherical structures with occasional folding and intraluminal epithelial projections (Fig. 2A). They were composed of single-layered cubical epithelium and stained positive for epithelial marker E-cadherin (Fig. 2A). When pulsed with EdU for six hours, 16.4±8.1% of organoid nuclei had incorporated the thymidine analogue (S phase of cell cycle, representative image shown in Fig. 2A). Gene expression analysis indicated that feline liver organoids expressed adult stem cell markers *LGR5*, *PROM1* and *BMI1* (Fig. 2B). Feline liver organoids expressed hepatic progenitor cell/biliary markers *KRT7* (Ijzer et al., 2009), *KRT19* and *HNF1β*, as well as early hepatocyte specification markers *HNF4α* and *TBX3* and very low levels of *ALB*. Genes of mature hepatocyte markers *PROX1*, *PC*, *HMGCL*, *TTR*, *FAH* and *CYP3A132* were expressed but at low levels compared to normal cat liver. Gene expression patterns remained stable throughout the culture. At protein level, feline liver organoids were 100% positive for K19 (strong cytoplasmic staining), HNF1β (moderate-strong nuclear staining) and self-renewal marker BMI1 (moderate-strong nuclear staining) (Fig. 2C). Feline liver organoids were mainly negative for albumin immunoreactivity, but in many organoids a weak cytoplasmic staining was observed in small clusters of cells within single organoids. All organoids were negative for mature hepatocyte marker HepPar-1. Feline liver organoids were mainly negative for ZO1, but in some organoids a weak membranous staining was observed in small clusters of cells within single organoids. Metaphase spread analysis showed a normal chromosome count in low and high passages, indicating long-term genetic stability of the cells similar to liver organoids from other species (Fig. 2D) (Huch et al., 2013; Huch et al., 2015; Nantasanti et al., 2015).

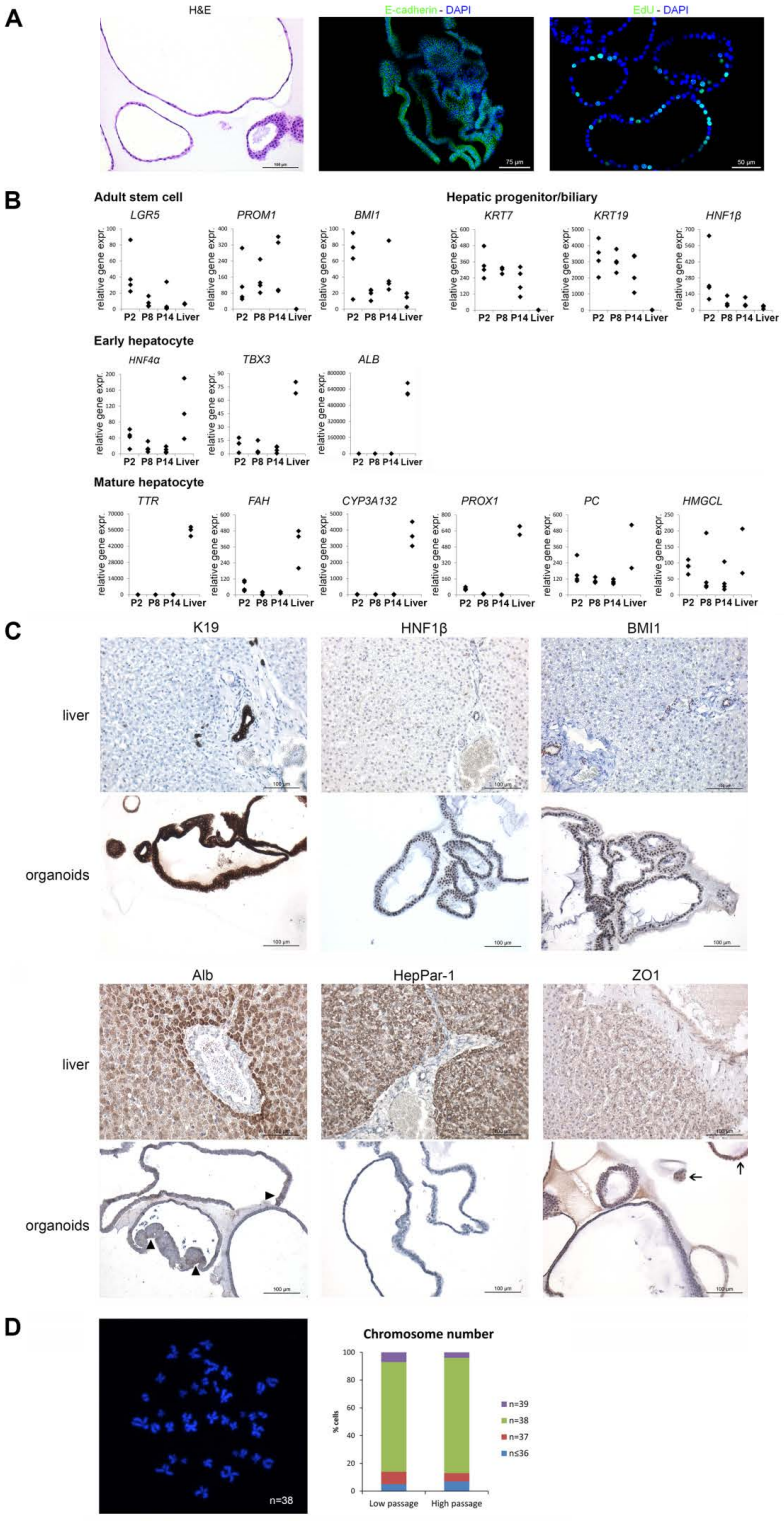
A
H&E
E-cadherin - DAPI
EdU - DAPI
B
Adult stem cell
LGR5
PROM1
BMI1
Hepatic progenitor/biliary
KRT7
KRT19
HNF1β
Early hepatocyte
HNF4α
TBX3
ALB
Mature hepatocyte
TTR
FAH
CYP3A132
PROX1
PC
HMGCL
relative gene expr.
P2 P8 P14 Liver
C
K19
HNF1β
BMI1
liver
organoids
Alb
HepPar-1
ZO1
D
n=38
Chromosome number
% cells
n=39
n=38
n=37
n≤36
Low passage
High passage

Figure 2. Characterization of feline liver organoids (A) Representative cytological and immunofluorescent images of feline liver organoids. Haematoxylin and eosin (H&E) staining showed organoids consisted of single-layered cubical epithelium. They stained positive for epithelial marker E-cadherin (green) and were highly proliferative in culture as shown with an EdU staining (green, marks S phase of the cell cycle). DAPI (blue) was used as nuclear counterstain. (B) Gene expression analysis of feline liver organoids (n=4 donors) in different passages (p2, p8, p14) and normal cat liver. Relative gene expression (expr.) is shown of adult stem cell, progenitor/biliary, and early and mature hepatocyte markers. (C) Representative images of immunocyto-/histochemical stainings of feline liver organoids and normal cat liver. Organoids stained positive for progenitor/biliary markers K19, HNF1β and BMI1. They stained negative for hepatocyte marker HepPar-1 but for albumin and ZO1 small clusters of cells within single organoids stained positive (indicated with arrowheads and arrows, respectively). (D) Karyotyping of feline liver organoids. A representative metaphase spread is shown of a cell with a normal chromosome number (n=38). Chromosome counts were compared between low and high passage number cultures (p3-7 vs. p16-23, n=4 donors per category) and plotted as percentage of cells with a normal chromosome number (n=38), 1 gain (n=39), 1 loss (n=37) or 2 or more loss (n≤36).

Differentiation of organoids towards hepatocyte-like cells

Upon culture in differentiation medium (DM), gene expression of mature hepatocyte markers *FAH*, *CYP3A132* and *TTR* increased compared to EM conditions, while expression of adult stem cell marker *LGR5* decreased (Fig. 3A). Keratin 19 immunoreactivity changed from a strong cytoplasmic to a moderate membranous staining, indicative of an 'intermediate hepatocyte' phenotype (Roskams et al., 2004) (Fig. 3B). BMI1 immunoreactivity changed from a moderate-strong nuclear staining in EM conditions to a weak nuclear staining in DM conditions. ZO1 staining increased in differentiated feline liver organoids, as more cells were positive in DM compared to EM conditions. Organoids in DM but not in EM accumulated glycogen as indicated by positive PAS staining. HepPar1 staining was not observed upon differentiation (data not shown). Proliferation ceased abruptly after switching organoids from EM to DM (Fig. 3C). Hepatocyte function testing revealed increased aspartate aminotransferase levels, albumin secretion into the medium and CYP450 activity in organoids in DM conditions compared to EM conditions (Fig. 3D).

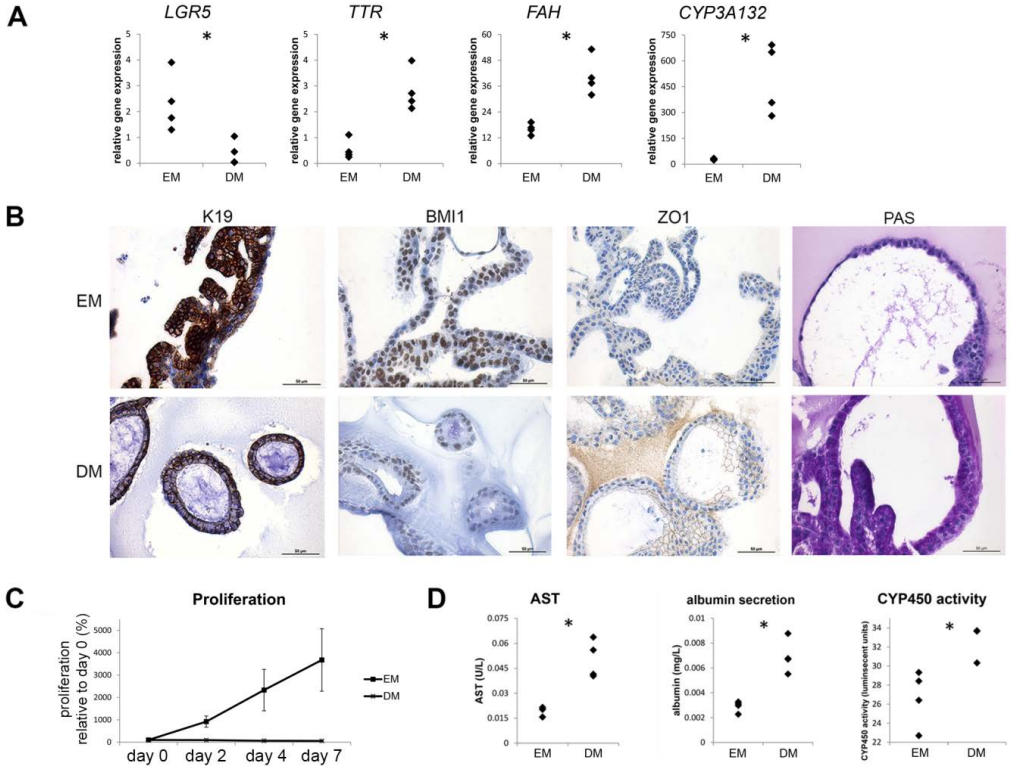

Figure 3. Differentiation of feline liver organoids towards hepatocyte-like cells. (A) Relative gene expression of feline liver organoids cultured in expansion medium (EM) and differentiation medium (DM) (n=4 donors). * indicates significance ($p<0.05$, Mann Whitney U test). (B) Representative images of immunocytochemical stainings for K19, BMI1 and ZO1 and PAS staining (indicating glycogen accumulation) of feline liver organoids cultured in EM and DM. (C) Growth curve derived from an Alamar blue assay of feline liver organoids cultured in EM and in DM for seven days (n=4 donors). Proliferation is presented as percentage relative to day 0 measurement. (D) Hepatocyte function tests of feline liver organoids cultured in EM and DM (n=4 donors). Aspartate aminotransferase (AST) levels, albumin secretion in the medium, and CYP450 activity were corrected for cell input with Alamar blue. * indicates significance ($p<0.05$, Mann Whitney U test).

Feline liver organoids for disease modeling of hepatic steatosis

To investigate liver organoids as potential *in vitro* model for steatosis, we mimicked circumstances of excess free fatty acid (FFA) concentrations and measured intracellular lipid accumulation with lipophilic dye LD540 using flow cytometry (Fig. S2). We compared organoids from mouse, human, dog and cat liver (four donors each) to assess species differences in lipid accumulation capacity. Median fluorescence intensity of LD540 was quantified in liver organoid cells after either control (BSA) or FFA treatment. For all four species, an increase in LD540 median fluorescence intensity was observed after FFA treatment compared to control, indicating intracellular lipid accumulation (Fig. 4A). When this increase was compared between species, cat liver organoids showed more lipid accumulation than human liver organoids after FFA treatment (192±104 vs. 61±36, $p=0.029$). LD540 positive intracellular lipid droplets were visualized in whole mount immunofluorescent stainings of mouse, human, dog and cat liver organoids after FFA treatment (representative images shown in Fig. 4B). Transcriptional analysis of human and cat liver organoids treated with FFA indicated that in both

species *PLIN2* was upregulated, consistent with increased lipid droplet formation (Fig. 4C, Fig. S3). *SREBF1*, a transcription factor that induces *de novo* lipogenesis, was decreased in human and feline organoids. FFA treated feline organoids increased their expression of *CPT1A* (a key enzyme in β-oxidation) and *PPARG*, a transcription factor known to enhance β-oxidation. Both genes were unchanged in human organoids. In human organoids, FFA treatment decreased expression of *PPARA* and its downstream targets *ACADSB* and *AGPAT2*. Next, we studied the effects of either etomoxir or L-carnitine supplementation compared to FFA treatment alone on lipid accumulation and viability in feline liver organoids. Etomoxir, a carnitine palmitoyltransferase-1 inhibitor, blocks the transfer of FFA over the mitochondrial membrane (carnitine shuttle), preventing them from entering β-oxidation. Conversely, L-carnitine is an essential co-factor for the carnitine shuttle. In feline liver organoids, FFA treatment decreased viability of the cells compared to BSA control (86±2% vs. 96±2%, p=0.034) (Fig. 4D); morphologically, the organoids gained a dark appearance (Fig. 4E). Lipid accumulation increased with the FFA+etomoxir combination compared with FFA treatment alone (253±69 vs. 176±56, p=0.034), and organoid viability decreased (82±3% vs. 86±2% p=0.034). On the other hand, lipid accumulation decreased with FFA+carnitine supplementation compared with FFA treatment alone (146±39 vs. 176±56, p=0.034), with an increase in organoid viability (90±3% vs. 86±2% p=0.034). The morphology of the organoids treated with FFA+carnitine was more comparable to the BSA control than to the FFA treated organoids, indicating that L-carnitine may help alleviate the surplus.

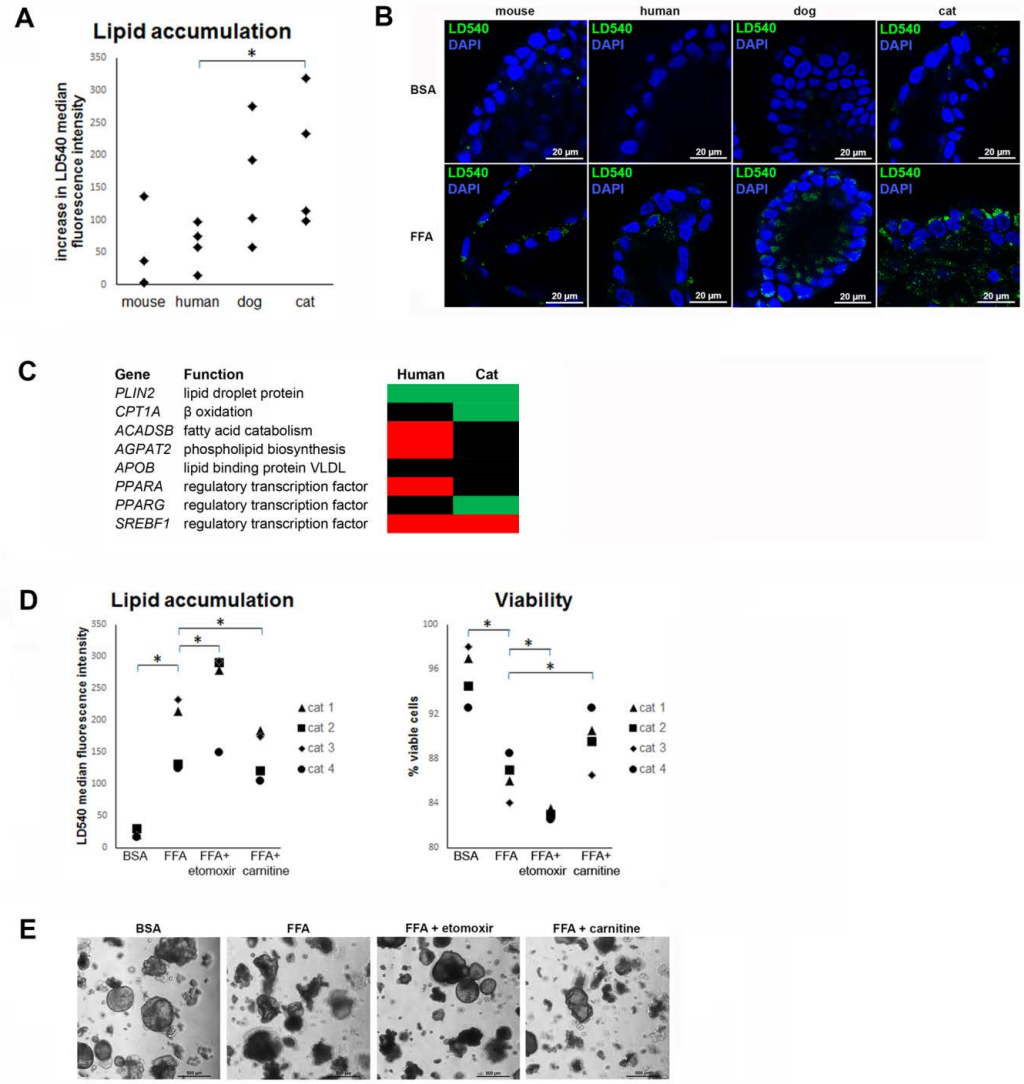

Figure 4. Liver organoids for disease modeling of hepatic steatosis. (A) Lipid accumulation in liver organoids from mouse, human, dog and cat (n=4 donors per species). Intracellular lipids were stained with LD540 and fluorescence was quantified using flow cytometry (see also Figure S2). Data are presented as dot plot and indicate the increase in LD540 median fluorescence intensity after free fatty acid (FFA) treatment compared to control treatment with BSA. * indicates significance ($p<0.05$ Mann Whitney U test). (B) Representative immunofluorescent images of LD540 stainings of mouse, human, dog and cat liver organoids after control treatment (BSA) and FFA treatment. Intracellular lipid droplets stain green, nuclei are counterstained with DAPI (blue). (C) Heatmap representing the transcriptional analysis of human and cat liver organoids treated with FFA compared to control treatment (BSA). Red: decreased gene expression. Black: unchanged gene expression. Green: increased gene expression. See also Figure S3. (D) Lipid accumulation in feline liver organoids treated with control (BSA), FFA, FFA plus etomoxir, and FFA plus L-carnitine. Intracellular lipid was quantified with flow cytometry and plotted as LD540 median fluorescence intensity for each individual donor (cat 1, 2, 3, 4). * indicates significance ($p<0.05$ Wilcoxon signed rank test). Cellular viability after treatment was measured using a trypan blue assay. * indicates significance ($p<0.05$ Wilcoxon signed rank test). (E) Representative phase contrast images of feline liver organoids treated with control (BSA), FFA, FFA plus etomoxir, and FFA plus L-carnitine.

Discussion

In the present study, long-term genetically stable feline liver organoid cultures were established and extensively characterized. To our knowledge, the liver organoids described in this study are the only available primary non-transformed long-term cell culture system from cats.
Feline liver organoids retain characteristics similar to liver organoids of other species, including massive proliferation capacity, an epithelial nature and their gene expression pattern (Huch et al., 2013; Huch et al., 2015; Nantasanti et al., 2015). Feline liver organoids were positive for progenitor/biliary markers as well as early hepatocyte specification markers, indicative of a hepatic progenitor cell (HPC) phenotype (Roskams et al, 2003). Additionally, in some parts or cell clusters within single organoids, albumin or ZO1 was expressed, whereas the rest of the structure was negative, indicating that there are different maturation levels within an organoid. This has also been described for mouse small intestinal organoids, which harbor a crypt and villus domain representative of a stem cell pool and a more mature progeny, respectively (Sato et al., 2009).
Feline liver organoid differentiation was associated with an abrupt cease in proliferation, a phenomenon also observed in cultures of primary hepatocytes, which cannot be expanded and rapidly dedifferentiate *in vitro* (Fraczek et al., 2013). Although feline liver organoids showed a higher expression of liver specific genes and had increased albumin secretion and AST and CYP3A activity upon differentiation, they did not reach full maturation (e.g. they remained negative for HepPar-1). Until now it has not been possible to accomplish full hepatocyte maturation *in vitro* from an immature cell type, such as ES or iPS cells (Ochiya et al., 2010; Zhang et al., 2013), nor to maintain maturation status of primary hepatocytes in culture (Fraczek et al., 2013). Future research is needed to elucidate pathways that are important for terminal differentiation of hepatocytes.
We compared several liver organoid species (mouse, human, dog and cat) and in all observed lipid accumulation when liver organoids were provided with free fatty acids. Oleate and palmitate represent the most abundant FA species in healthy and steatotic human and cat liver (Araya et al., 2004; Fujiwara et al., 2015). Hence, oleate and palmitate are widely used in lipidomics research and are considered physiologically relevant for modeling hepatic lipid accumulation (Gómez-Lechón et al. 2007). Hepatocytes have three major routes to handle FFA. They can (i) enter β oxidation to provide energy or a substrate for ketogenesis, or they can be re-esterified to triglycerides and either (ii) become excreted in very-low-density lipoproteins (VLDL) or (iii) stored as intracellular lipid droplets. There were marked species differences in the extent of lipid accumulation on a cellular level: feline liver organoids accumulated more lipids compared to human liver organoids. This exaggerated phenotype of lipid overload in feline liver cells complies with the fact that steatosis in cats often leads to liver failure and severe disease (Center, 2005). We can speculate that the other metabolic pathways handling excess FFA (β oxidation, VLDL secretion) are quickly saturated in feline hepatocytes, leading to extensive lipid droplet formation. Both human and feline organoids upregulated *PLIN2* expression after FFA treatment, an essential machinery protein in lipid accumulation in lipid droplets. However, we also observed differences in transcriptional activation between human and feline organoids after FFA treatment which could be explained by differences in activation of essential lipid regulatory pathways (mainly via PPARA and PPARG). Future research might focus on species differences in PPARA and PPARG signaling in response to excess FFA and their effects on hepatocellular lipid catabolism and storage.

To further explore the value of feline liver organoids as a research model for steatosis, we tested the effect of small molecules on lipid metabolism. Lipid accumulation was enhanced in the presence of etomoxir, indicating that β oxidation is an important metabolic pathway handling excess fatty acids in feline liver cells. Conversely, supplementation of L-carnitine of feline liver organoids attenuated lipid accumulation in high fat conditions and improved cellular viability. This is in concordance with the finding that exogenous L-carnitine supplementation can ameliorate FFA oxidation in cats with FHL (Center et al., 2012). The possibility to interfere *in vitro* with organoid lipid accumulation offers opportunities to test new drugs that enhance β oxidation or promote VLDL secretion, with the aim to eliminate superfluous triglycerides from hepatocytes *in vivo*.
In conclusion, we describe a long-term 3D primary culture of feline liver organoids and demonstrate that they retain characteristics of adult liver stem cells and are highly similar to liver organoids of other species. The pronounced phenotype of lipid accumulation in feline liver organoids compared to organoids from other species reveals remarkable species differences in cellular lipid-handling capacity. Hence, feline liver organoids represent an *in vitro* magnifying glass to investigate the molecular underpinnings of fatty liver disease and can be a valuable research tool to explore new therapeutic strategies for hepatic steatosis.

Experimental Procedures

Liver samples
Surplus liver samples were obtained postmortem from five cats (two female, three male); no animals were harmed or killed for the purpose of this study. Sample handling is further described in the Supplemental Experimental Procedures.
Mouse (n=4 donors) and dog (n=4 donors) liver organoid cultures were generated as described earlier from surplus liver material harvested from animals in non-liver related research (experiments approved by the Utrecht University's ethical committee) (Huch et al., 2013; Nantasanti et al., 2015). Human (n=4 donors) liver organoid cultures were generated as described earlier from surplus material of donor livers used for liver transplantations performed at the Erasmus Medical Center, Rotterdam, the Netherlands (approved by the Medical Ethical Council of the Erasmus MC, Rotterdam) (Huch et al., 2015).

Isolation of biliary ducts and feline liver organoid culture
Liver wedge biopsies were minced with scalpel blades and washed in DMEM medium with 1% v/v fetal calf serum (FCS) and 1% v/v penicillin-streptomycin (all from Gibco). Samples were enzymatically digested with 0.3 mg/ml type II collagenase (Gibco) and 0.3 mg/ml dispase (Gibco) at 37°C for 2-3 hours and triturated every 20 minutes. Supernatant was checked for biliary duct fragments. Supernatant was centrifuged at 80g for 5 minutes at 4°C and pelleted ducts were mixed with cold Matrigel (BD Biosciences). The FNA material was washed, but not minced nor digested before mixing with Matrigel. Matrigel suspension was seeded as droplets in 48 or 24 well plates and allowed to solidify at 37°C before overlaying with culture medium. Expansion medium as published for mouse, dog and human liver organoids was tested on feline liver organoids (Huch et al., 2013; Nantasanti et al., 2015; Huch et al., 2015). Medium effects on organoid proliferation were evaluated on short term (1 week growth curve) with an Alamar blue assay according to the manufacturer's instructions (Life Technologies). Medium effects on organoid expansion in long term culture were

derived from weekly split ratios. Based on the obtained results (see also Fig. S1), a new medium composition was developed (cat expansion medium, cEM), which was a hybrid between dog and human expansion media. cEM consisted of Advanced DMEM/F12, supplemented with 1% v/v penicillin-streptomycin, 1% v/v GlutaMax, 10 mM Hepes (all Gibco), 2% v/v B27 minus vitamin A (Invitrogen), 1% N2 (Invitrogen), 10 mM nicotinamide (Sigma-Aldrich), 1.25 mM N-acetylcysteine (Sigma-Aldrich), 5% v/v R-spondin-1 conditioned medium (the Rspo1-Fc-expressing cell line was a kind gift from Calvin J. Kuo, Stanford, USA), 10 µM forskolin (Sigma-Aldrich), 10 µM Y-27632 (ROCK inhibitor, Selleckchem), 0.5 µM A83-01 (TGFβ inhibitor, Tocris Bioscience), 50 ng/ml EGF (Invitrogen), 25 ng/ml HGF (Peprotech), 0.1 µg/ml FGF10 (Peprotech), 1 nM gastrin (Sigma-Aldrich), and 0.1 µg/ml Noggin (Peprotech). Medium was changed every 2-3 days. Organoids were passaged by mechanical disruption once a week at an average split rate of 1:11. Imaging of the organoids was performed using an Olympus CKX41 microscope in combination with a Leica DFC425C camera.

Feline liver organoid differentiation

Feline liver organoids of four donors in similar passage number (p5-7) were cultured in EM for five days and then medium composition was changed. In differentiation medium (DM), nicotinamide, R-spondin-1, forskolin, and Y27632 were withdrawn and 25 ng/ml BMP7 (Peprotech), 10 µM DAPT (γ-secretase inhibitor, Selleckchem), and 30 µM dexamethasone (Sigma-Aldrich) were added. DM was replaced every other day until the end of differentiation (day 7).

Measuring lipid accumulation in liver organoids with flow cytometry

Liver organoids of mouse, human, dog and cat (four donors per species) were treated with either 0.4 mM oleate (C18:1) and 0.2 mM palmitate (C16:0) coupled to 12% w/v fatty acid-free BSA (all from Sigma-Aldrich) or with fatty acid-free BSA as vehicle control for 24h (details provided in the Supplemental Experimental Procedures) and then dissociated to single cells with TrypLE select enzyme (Gibco). Cell suspensions were washed and an aliquot was mixed with 0.4% trypan blue and counted on an automated cell counter (Biorad). Cells were incubated with 0.025 µg/mL LD450 (lipophilic dye, kindly provided by Christoph Thiele, Bonn, Germany) for 30 min at 37°C. Incubations without LD540 served as a negative control. Cells were washed and resuspended in HBSS with 5nM Sytox Red (Gibco). Cells were analyzed by flow cytometry on a FACSAria II SORP (BD Biosciences) (Fig. S1). A 635 nm laser with an emission detection of 670/30 nm was used to detect Sytox red; dead cells were excluded from analysis. To detect lipid accumulation in cells using LD540, a 532 nm laser with emission detection at 610/20 nm was used. The voltage was either 619 mV (Sytox red) or 300 mV (LD540).

Supplemental Information

Supplemental Information includes three Supplemental Figures and Supplemental Experimental Procedures.

Author contributions

Conceptualization, H.S.K., L.C.P., and B.S.; Methodology/experiments, H.S.K., L.A.O., I.G.W.H.V., I.M.S., M.E.V.W., F.B., C.R., L.V.U., and M.R.M.; Data analysis/interpretation: H.S.K., M.R.M., J.B.H., G.C.M.G., and B.S.; Writing, H.S.K., L.C.P., and B.S.; Funding acquisition, H.S.K and B.S.; Resources, M.M.A.V., L.J.W.V.D.L., M.H., N.G., R.G.V., H.C., J.R., B.A.S., and L.C.P.

Acknowledgements

The authors would like to thank the Utrecht University Center for Cell Imaging for technical assistance with imaging, Stefan van der Elst from the Hubrecht Institute for technical assistance with flow cytometry experiments, dr. Sathidpak Nantasanti for technical advice, dr. Hilda Toussaint for providing surplus mouse liver samples, and Sarah Opitz for editing the manuscript. This study was sponsored by the Winn Feline Foundation (grant nr. W15-037). Parts of this work were funded by the Dutch Research Council NWO ZON/MW (116004121).

References

Araya, J., Rodrigo, R., Videla, L.A., Thielemann, L., Orellana, M., Pettinelli, P., and Poniachik, J. (2004). Increase in long-chain polyunsaturated fatty acid n - 6/n - 3 ratio in relation to hepatic steatosis in patients with non-alcoholic fatty liver disease. Clin. Sci. (Lond). *106*, 635-643.

Center, S.A., Crawford, M.A., Guida, L., Erb, H.N., and King, J. (1993). A retrospective study of 77 cats with severe hepatic lipidosis: 1975-1990. J. Vet. Intern. Med. *7*, 349-359.

Center, S.A. (2005). Feline hepatic lipidosis. Vet. Clin. North Am. Small Anim. Pract. *35*, 225-269.

Center, S.A., Warner, K.L., Randolph, J.F., Sunvold, G.D., and Vickers, J.R. (2012). Influence of dietary supplementation with (L)-carnitine on metabolic rate, fatty acid oxidation, body condition, and weight loss in overweight cats. Am. J. Vet. Res. *73*, 1002-1015.

Cohen, J.C., Horton, J.D., and Hobbs, H.H. (2011). Human fatty liver disease: old questions and new insights. Science *332*, 1519-1523.

Fraczek, J., Bolleyn, J., Vanhaecke, T., Rogiers, V., and Vinken, M. (2013). Primary hepatocyte cultures for pharmaco-toxicological studies: at the busy crossroad of various anti-dedifferentiation strategies. Arch. Toxicol. *87*, 577-610.

Fujiwara, M., Mori, N., Sato, T., Tazaki, H., Ishikawa, S., Yamamoto, I., and Arai, T. (2015). Changes in fatty acid composition in tissue and serum of obese cats fed a high fat diet. BMC Vet. Res. *11*, 200.

Gómez-Lechón, M.J., Donato, M.T., Martínez-Romero, A., Jiménez, N., Castell, J.V., and O'Connor J.E. (2007). A human hepatocellular in vitro model to investigate steatosis. Chem. Biol. Interact. *165*, 106-116.

Huch, M., Dorrell, C., Boj, S.F., Van Es, J.H., Li, V.S., Van De Wetering, M., Sato, T., Hamer, K., Sasaki, N., Finegold, M.J., et al. (2013). In vitro expansion of single Lgr5+ liver stem cells induced by Wnt-driven regeneration. Nature *494*, 247-250.

Huch, M., Gehart, H., Van Boxtel, R., Hamer, K., Blokzijl, F., Verstegen, M.M., Ellis, E., Van Wenum M., Fuchs, S.A., De Ligt, J., et al. (2015). Long-term culture of genome-stable bipotent stem cells from adult human liver. Cell *160*, 299-312.

Ijzer, J., Kisjes, J.R., Penning, L.C., Rothuizen, J., and Van Den Ingh, T.S.G.A.M. (2009). The progenitor cell compartment in the feline liver: an (immuno)histochemical investigation. Vet. Pathol. *46*, 614-621.

Kruitwagen, H.S., Spee, B., Viebahn, C.S., Venema, H.B., Penning, L.C., Grinwis, G.C., Favier, R.P., van den Ingh, T.S.G.A.M., Rothuizen, J., and Schotanus, B.A. (2014). The canine hepatic progenitor cell niche: molecular characterisation in health and disease. Vet. J. *201*, 345-352.

Nantasanti, S., Spee, B., Kruitwagen, H.S., Chen, C., Geijsen, N., Oosterhoff, L.A., Van Wolferen, M.E., Pelaez, N., Fieten, H., Wubbolts, R.W., et al. (2015). Disease modeling and gene therapy of copper storage disease in canine hepatic organoids. Stem Cell Reports *5*, 895-907.

Ochiya, T., Yamamoto, Y., and Banas, A.(2010). Commitment of stem cells into functional hepatocytes.

Roskams, T.A., Libbrecht, L., and Desmet, V.J. (2003). Progenitor cells in diseased human liver. Semin. Liv. Dis. *23*, 385-396.

Roskams, T.A., Theise, N.D., Balabaud, C., Bhagat, G., Bhathal, P.S., Bioulac-Sage, P,, Brunt, E.M., Crawford, J.M., Crosby, H.A., and Desmet, V. (2004). Nomenclature of the finer branches of the biliary tree: canals, ductules, and ductular reactions in human livers. Hepatology *39*, 1739-1745.

Sato, T., Vries, R.G., Snippert, H.J., Van De Wetering, M., Barker, N., Stange, D.E., Van Es, J.H., Abo, A., Kujala, P., Peters, P.J. et al. (2009). Single Lgr5 stem cells build crypt-villus structures in vitro without a mesenchymal niche. Nature *459*, 262-265.

Wang, X., Foster, M., Al-Dhalimy, M., Lagasse, E., Finegold, M., and Grompe, M. (2003). The origin and liver repopulating capacity of murine oval cells. Proc. Natl. Acad. Sci. USA *100*, 11881-11888.

Younossi, Z.M., Koenig, A.B., Abdelatif, D., Fazel, Y., Henry, L., and Wymer, M. (2016). Global epidemiology of nonalcoholic fatty liver disease-Meta-analytic assessment of prevalence, incidence, and outcomes. Hepatology *64*, 73-84.

Zhang, Z., Liu, J., Liu, Y., Li, Z., Gao, W.Q., and He, Z. (2013). Generation, characterization and potential therapeutic applications of mature and functional hepatocytes from stem cells. J. Cell. Physiol. *228*, 298-305.

Supplemental Figures

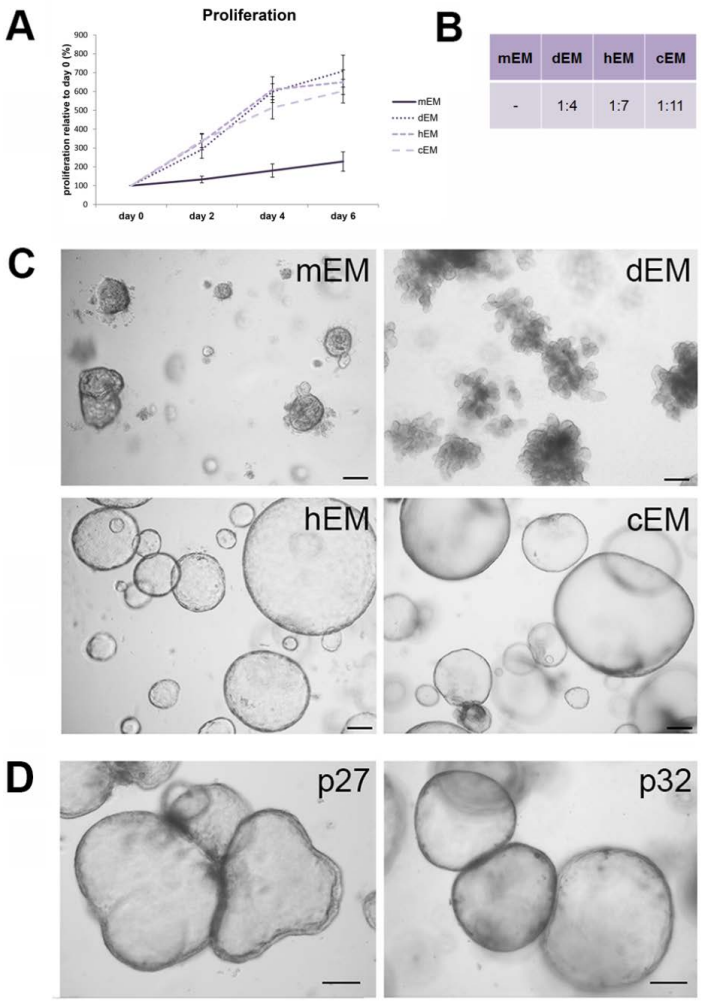

Figure S1. Performance of different expansion media in short and long-term feline liver organoid culture. Related to Figure 1 and Experimental Procedures. A. Short term proliferation as indicated by an Alamar blue growth curve of feline liver organoids cultured in mouse, dog, human and cat expansion medium (mEM, dEM, hEM, and cEM, respectively). Organoids showed significantly less proliferation on mEM than on the other expansion media within one week of culturing. n=4 donors per culture condition. B. Long term expansion potential of feline liver organoids cultured in mEM, dEM, hEM, and cEM as indicated by weekly split rates from passage 11 to passage 26. Mouse EM failed to support feline liver organoid growth for more than five passages for two donors, with a maximum of 15 passages for other donors. C. Representative phase contrast images of feline liver organoids cultured in mEM, dEM, hEM, and cEM. In mEM feline organoids remained small and were surrounded by cellular debris. Feline organoids cultured in dEM were heavily folded, and had a round appearance in hEM and cEM. cEM performed best and allowed for a high split ratio (1:11) in long-term culture. Scalebars represent 100 µm. D. Representative phase contrast images of feline liver organoids in cEM in long-term culture. Growth slowed down after passage 27 (p27) but cultures could be continuously expanded until at least passage 32 (p32). Scalebars represent 100 µm.

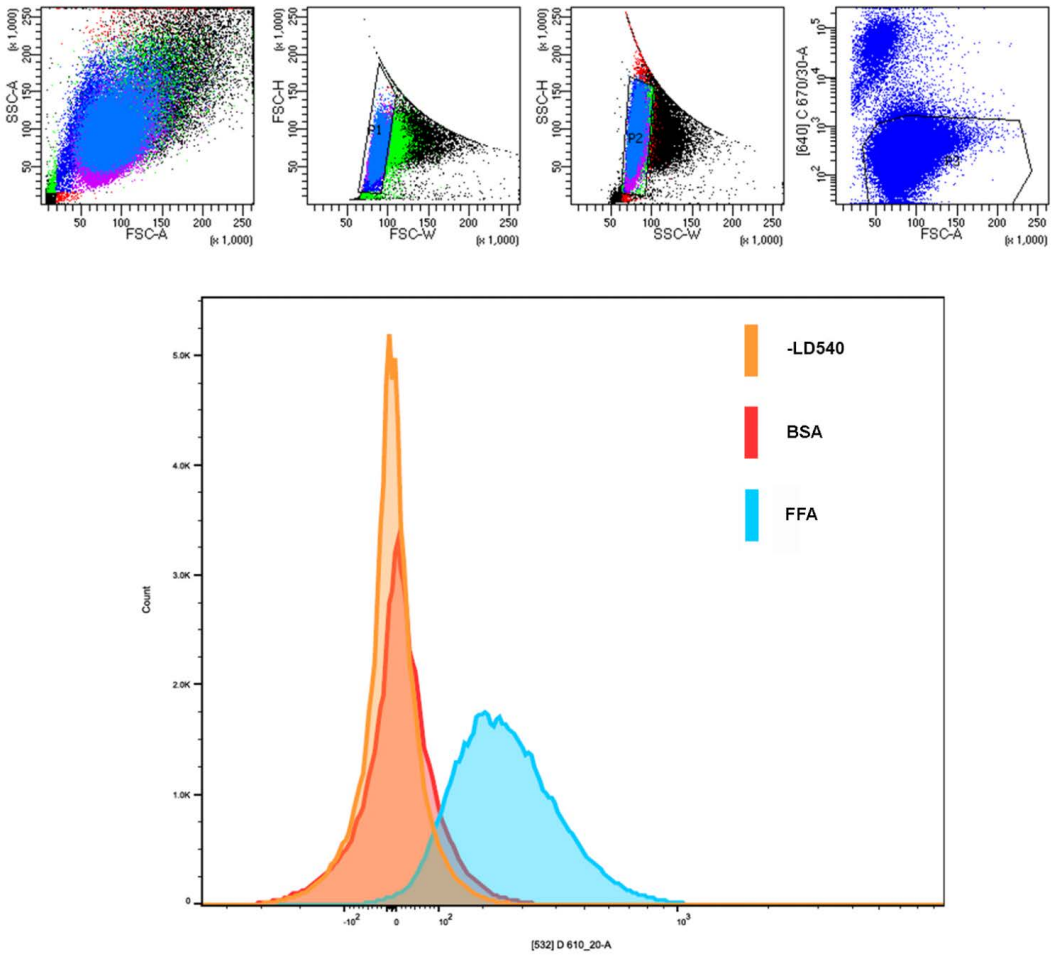

Figure S2. Flow cytometry analysis of LD540 in liver organoids. Related to Figure 4. Representative plots are shown of a liver organoid flow cytometry experiment to illustrate workflow and data analysis. Single cells were selected in gate P1 and P2 based on forward scatter (FSC) and side scatter (SSC). Next, live cells were selected in gate P3 based on Sytox red exclusion (670/30 emission). To detect lipid accumulation in cells using LD540 a 532 nm laser with emission detection at 610/20 nm was used. LD540 median fluorescence intensity of the population was calculated and compared between cells treated with BSA (control) and cells treated with free fatty acids (FFA). Cells treated with FFA but not stained with LD540 served as a technical negative control to rule out autofluorescence.

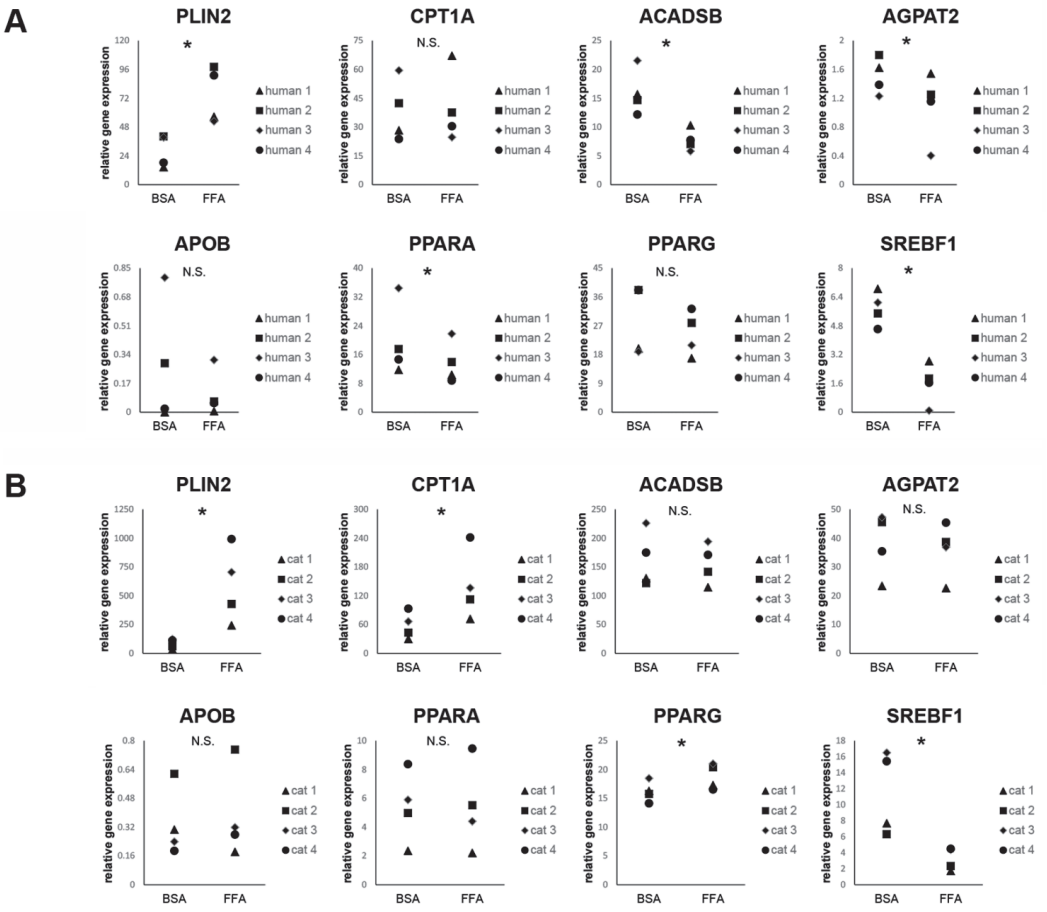

Figure S3. Gene expression analysis of human and feline liver organoids after treatment with free fatty acids. Related to Figure 4. A. Relative gene expression of human liver organoids treated with free fatty acids (FFA) compared to control treatment (BSA). n=4 donors per experimental condition. N.S.: not significant; * indicates significance ($p<0.05$, Wilcoxon signed rank test). B. Relative gene expression of feline liver organoids treated with free fatty acids (FFA) compared to control treatment (BSA). n=4 donors per experimental condition. N.S.: not significant; * indicates significance ($p<0.05$, Wilcoxon signed rank test).

Supplemental Experimental Procedures

Liver samples
Surplus liver samples (wedge biopsies of 5 mm^3) were obtained postmortem from five cats. From one cat, both a wedge biopsy and a fine needle aspirate (FNA, 22G) from the liver were taken. Liver was sampled fresh and processed immediately or frozen in freezing medium (Gibco). Three out of five samples originated from a frozen biobank, were snap frozen upon sampling and had been stored for seven years at -70°C prior to use in this study (surplus material of cats used in non-liver related research, approved by the Utrecht University's ethical committee as required under Dutch legislation).

RNA isolation, cDNA synthesis and quantitative reverse transcription PCR
RNA from organoids (n=4 donors per species) and normal cat liver (n=3 donors) was isolated and converted to cDNA as described previously (Nantasanti et al., 2015). QPCR was performed in duplicate on three culture replicates per donor on a BioRad MyiQ thermal cycler using SYBRgreen supermix (BioRad). Species specific primers were developed for leucine-rich repeat-containing G protein-coupled receptor 5 (*LGR5*); prominin 1/CD133 (*PROM1*); B cell-specific Moloney murine leukaemia virus integration site 1 (*BMI1*); keratin 7 (*KRT7*); keratin 19 (*KRT19*); hepatic nuclear factor 1 homeobox β (*HNF1β*); hepatic nuclear factor 4 homeobox α (*HNF4α*); T-box 3 (*TBX3*); albumin (*ALB*); prospero homeobox 1 (*PROX1*); pyruvate carboxylase (*PC*); 3-hydroxymethyl-3-methylglutaryl-CoA lyase (*HMGCL*); transthyretin (*TTR*); fumarylacetoacetate hydrolase (*FAH*); cytochrome 3A132 (*CYP3A132*); perilipin 2 (*PLIN2*); carnitine palmitoyltransferase 1A (*CPT1A*); acyl-CoA dehydrogenase, short/branched chain (*ACADSB*); 1-acylglycerol-3-phosphate O-acyltransferase 2 (*AGPAT2*); apolipoprotein B (*APOB*); peroxisome proliferator activated receptor alpha (*PPARA*); peroxisome proliferator activated receptor gamma (*PPARG*); and sterol regulatory element binding transcription factor 1 (*SREBF1*) (lipid metabolism genes were derived from Wruck et al., 2015, and Graffmann et al., 2016). For feline cells, tyrosine 3-monooxygenase/ tryptophan 5-monooxygenase activation protein, zeta (*YWHAZ*), ribosomal protein S5 (*RPS5*) and hypoxanthine phosphoribosyltransferase (*HPRT-1*) were used as reference genes to calculate relative gene expression (delta Cq method). For human cells beta-2-microglobulin (*B2M*), *HPRT-1* and ribosomal protein L19 (*RPL19*) were used as reference genes. Expression levels that were undetectable were arbitrarily set to a Cq value of 45. Primer details are listed in Table S1.

Immunocyto-/histochemical and whole mount immunofluorescent staining
Organoids were fixed in 10% neutral buffered formalin, embedded in paraffin and sections of 4 µm were cut. H&E staining was routinely performed. For immunocyto-/histochemical staining of K19, HNF1β, BMI1, albumin, HepPar-1, and tight junction protein 1 (ZO1), sections were dewaxed and rehydrated and antigen retrieval was performed (methods listed in Table S2). Sections were blocked with 10% normal goat serum (NGS, Sigma-Aldrich) and primary antibody was incubated at 4°C overnight (antibody dilutions listed in Table S2). As negative control, isotype antibodies were used or primary antibody was omitted. Secondary antibody was incubated for 45 minutes at room

temperature (EnVision, Dako), signal was visualized with 3,3'-diaminobenzidine and sections were counterstained with haematoxylin. Imaging was performed using an Olympus microscope (CKX41) in combination with a Leica DFC425C camera. PAS staining was performed routinely.
For whole mount immunofluorescent staining feline liver organoids were carefully harvested from Matrigel and fixed in 10% neutral buffered formalin for 45 minutes on ice. Organoids were permeabilized and blocked with 0.5% v/v Triton X100, 1% v/v DMSO, 1% w/v BSA, and 10% v/v NGS in PBS. Mouse anti-E-cadherin (BD Biosciences) was diluted 1:500 and incubated at 4°C over two nights. Secondary goat anti-mouse AF488 antibody (Life Technologies) was diluted 1:100 and incubated for 2 hours at room temperature. Nuclei were stained with 4',6-Diamidine-2'-phenylindole (DAPI, Sigma-Aldrich). Organoids were mounted using ProLong Diamond Antifade mounting medium (Life Technologies) and imaged using a confocal microscope (Leica). An EdU incorporation assay and whole mount imaging was performed as described previously (Nantasanti et al., 2015). Briefly, organoids in log-phase of growth were pulsed with 10 µM 5-ethynyl-2´-deoxyuridine (EdU, thymidine analogue) for six hours, fixed and stained with 5 µM AF488 azide, 100 mM ascorbic acid, and 1mM $CuSO_4$ in a click reaction. Nuclei were stained with DAPI. For LD540 whole mount staining, fixed organoids were incubated in 0.025 µg/mL LD450 in PBS for 1 hour at room temperature. After washing, nuclei were stained with DAPI and organoids were mounted with ProLong Diamond Antifade mounting medium (Life Technologies) and imaged using a confocal microscope (Leica).

Karyotyping
Feline liver organoids of four donors in low (p3-7) and high (p16-23) passage numbers in log-phase of growth were arrested in metaphase with 15 µg/ml colchicine (KaryoMax, Gibco) overnight. Organoids were trypsinized to single cell level, incubated with hypotonic buffer (0.075 M KCl) for 10 minutes and then fixed with methanol-acetic acid (3:1). Chromosome spreads were routinely prepared and imaged using an Olympus fluorescence microscope. At least 100 spreads were counted for both low and high passages numbers; a chromosome count of n=38 is normal for feline cells.

Hepatic function tests after feline liver organoid differentiation
Feline liver organoids of four donors were incubated with DM for seven days. DM was replaced every other day. As control, culture was continued in parallel with EM for all four donors until day 7. Proliferation was measured on days 0, 2, 4, and 7 of differentiation with an Alamar blue assay according to the manufacturer's instructions (Life Technologies). Wells were washed and organoid culture was continued with EM/DM, allowing for serial measurements on the same wells throughout the experiment (growth curve). On day 7, medium was harvested for albumin measurement and organoids were harvested for immunocytochemistry, gene expression analysis, liver enzyme measurement, and CYP450 assay (n=3 wells per donor). Albumin detection in the medium and liver-specific enzyme aspartate aminotransferase (AST) detection in organoid lysates were performed as described previously (Nantasanti et al., 2015). Cytochrome P450 activity was measured according to the manufacturer's instructions with the P450-Glo™ assay (Promega) specific for CYP3A4. CYP3A is one of the major cytochromes active in feline liver (Van Beusekom et al., 2010). All values were corrected for cell input with Alamar blue.

Fatty acid treatment of liver organoids

Liver organoids in similar passage number (p5-7) of mouse, human, dog and cat were cultured in 12 well plates in their specific EM for three days (four donors per species). For free fatty acid (FFA) treatment, a generic organoid expansion medium was designed for all species to accommodate for differences in lipid content of the medium (*e.g.* dog EM contains serum), which consisted of Advanced DMEM/F12, supplemented with 1% v/v penicillin-streptomycin, 1% v/v GlutaMax, 10 mM Hepes (all Gibco), 2% v/v B27 minus vitamin A (Invitrogen), 1% v/v N2 (Invitrogen), 10 mM nicotinamide (Sigma-Aldrich), 1.25 mM N-acetylcysteine (Sigma-Aldrich), 5% v/v R-spondin-1 conditioned medium, 25 ng/ml HGF (Peprotech), 0.1 µg/ml FGF10 (Peprotech), and 10 nM gastrin (Sigma-Aldrich). Either 0.4 mM oleate (C18:1) and 0.2 mM palmitate (C16:0) coupled to 12% w/v fatty acid-free BSA were added (all from Sigma-Aldrich) or only fatty acid-free BSA as vehicle control. FFA concentrations were based on pilot experiments (data not shown) and literature (Gómez-Lechón et al., 2007). Organoids were cultured with either free fatty acids (FFA) or BSA for 24 hours and were then harvested for RNA isolation, whole mount staining with LD540 and flow cytometry.
For feline organoids the β oxidation of excess FFA was studied by culturing them with either fatty acid-free BSA (control), FFA (0.4 mM oleate and 0.2 mM palmitate), FFA plus 50 µM etomoxir (carnitine palmitoyltransferase-1 inhibitor, Cayman), or FFA plus 1 mM L-carnitine (Selleckchem). DMSO was used as solvent for etomoxir and was therefore added as vehicle control to the other treatment media. Concentration of etomoxir was based on pilot experiments (data not shown); concentration of L-carnitine was based on literature (Odle et al., 1995). Pictures before and after 24 hours of treatment were taken with a Olympus microscope in combination with a Leica camera. Feline liver organoids were then harvested for flow cytometry.

Statistical tests

Data are presented as mean ± SD. Statistical analysis was performed in SPSS (IBM SPSS Statistics 22). All statistical tests were performed on four biological replicates. A Kruskall Wallis test was performed in cases of multiple group testing. A nonparametric Mann Whitney U test was performed on independent samples. A nonparametric 1-tailed Wilcoxon signed rank test was used for related samples. $P<0.05$ was considered significant.

Table S1. Primer sequences and QPCR conditions

Species	Gene	Direction	Sequence (5' – 3')	Tm (°C)	Product size (bp)
Cat	*LGR5*	Forward	GGAAAGTTTGACTTTAACTGGA	58	101
		Reverse	GCAGGTTGTAAGATAGATCTAGCA		
	PROM1	Forward	TGAGCCAGTACACCACCA	61	150
		Reverse	GTCTCTTTGATTGCTTCTGCC		
	BMI1	Forward	CAATGGCTCTAACGAAGATAGAG	60	120
		Reverse	TACTTTCCGATCCAATCTGTTCTG		

	KRT7	Forward	CCAGACCAAGTTTGAGACC	58	131
		Reverse	TCTTAATGCTGTCGATCTCAG		
	KRT19	Forward	AATCACGAGGAGGAAGTCAG	58	106
		Reverse	CGTCACTCAGGATCTTGG		
	HNF1β	Forward	GTCACAGGTCTGAACCAG	61	130
		Reverse	GGTTGAATTGTCGGAGGA		
	HNF4α	Forward	TGTACTCCTGCAGATTTAGTC	58	88
		Reverse	CGGAAGCACTTCTTGAGC		
	TBX3	Forward	GAAGAAGAGGTGGAGGATGAC	63	115
		Reverse	GAAACATTCGCCTTCCCG		
	ALB	Forward	CGAGAAGCACATCAGAGTG	58	84
		Reverse	AAAGGCAACCAGTACCAG		
	PROX1	Forward	GCAGGAAGGATTGTCACC	58	118
		Reverse	GCATCTGTTGAACTTTACATCG		
	PC	Forward	TCAATACCCGCCTCTTCC	61	109
		Reverse	GTTCAGGTCACTTATAGCCAG		
	HMGCL	Forward	GGGCATCAGGAAACTTGG	65	83
		Reverse	GCTTCTGGAGGTTCACAC		
	TTR	Forward	CAAAGTGGAAATAGACACCAAGTC	58	81
		Reverse	GTGAACACCACCTCTGCA		
	FAH	Forward	GAGTCCTTGCGGAATCTG	58	129
		Reverse	CGTGTAGTCACCTATGGC		
	CYP3A132	Forward	GGTGCTCCTCTATCTATATGGGA	60	201
		Reverse	TCTGTGATCGCCAACACTG		
	PLIN2	Forward	TCGCAGTTAATCCACAACC	64	127
		Reverse	CACGGACTTCAAGCAAGG		
	CPT1A	Forward	CCGAACATTCCGTATCCCA	63	150
		Reverse	TGATGAGTCCTTTGCCGA		
	ACADSB	Forward	TTTGCCCAGGAACAGATTGC	62	109
		Reverse	TTTCAATACCCATCAACCCTTGC		
	AGPAT2	Forward	GTCTTCTTCATCAACCGGCAG	61	95
		Reverse	ACCCACACCTTGAGATTCTCC		
	APOB	Forward	ACTCGATTCAAGCACCTCC	66	123
		Reverse	GCACCTCCAGTTCAACCT		

	PPARA	Forward	GACAAATGTGACCGTAGCTG	60	109
		Reverse	AAACGAATTGCGTTATGGGA		
	PPARG	Forward	TGTGACCTTAACTGTCGTATCC	66	134
		Reverse	CTTCTCTTTCTCCGCCTGTG		
	SREBF1	Forward	CGTTTCTTCGTGGATGGG	63	140
		Reverse	ACAATTCAGTGCTCGCTC		
	YWHAZ	Forward	GAAGAGTCCTACAAAGACAGCACGC	65	115
		Reverse	AATTTTCCCCTCCTTCTCCTGC		
	RPS5	Forward	CAGGTCTTGGTGAATGCG	58	129
		Reverse	CCAGATGGCCTGATTCAC		
	HPRT-1	Forward	TTATGGACAGGACCGAGC	60	107
		Reverse	GTCAGCAAAGAATTTATAGCCC		
Human	*PLIN2*	Forward	GCTGAGCACATTGAGTCACG	58	102
		Reverse	TGGTACACCTTGGATGTTGG		
	CPT1A	Forward	CCTACCACGGGTGGATGTTC	61	101
		Reverse	CAACATGGGTTTTCGGCCTG		
	ACADSB	Forward	CACCATTGCAAAGCATATCG	65	117
		Reverse	GCAAGGCACTTACTCCCAAC		
	AGPAT2	Forward	CCGAGTTCTACGCCAAGGTC	61	121
		Reverse	CCGATGATGCTCATGTTCTCC		
	APOB	Forward	ATCTTCAACATGGCGAGGGA	61	81
		Reverse	TGTCTTATGATAGTTGTTGACCGC		
	PPARA	Forward	AACATCCAAGAGATTTCGCAATCC	60	121
		Reverse	AAAGCGTGTCCGTGATGACC		
	PPARG	Forward	GATGTCTCATAATGCCATCAGGT	65	108
		Reverse	TCAGCGGACTCTGGATTCAG		
	SREBF1	Forward	CCAGGTGACTCAGCTATTCC	61	110
		Reverse	CATCCGAGAATTCCTTGTCCC		
	B2M	Forward	CTTTGTCACAGCCCAAGATAG	58	83
		Reverse	CAATCCAAATGCGGCATCTTC		
	HPRT-1	Forward	TATTGTAATGACCAGTCAACAG	60	192
		Reverse	GGTCCTTTTCACCAGCAAG		
	RPL19	Forward	ATGAGTATGCTCAGGCTTCAG	64	150
		Reverse	GATCAGCCCATCTTTGATGAG		

Table S2. Antibody specifications and antigen retrieval methods

Antibody	Source	Clone	Company	Dilution	Antigen retrieval
K19	mouse	b170	Novocastra	1:300	10 mM citrate pH 6.0 98°C
HNF1β	rabbit		Sigma	1:400	10 mM citrate pH 6.0 98°C
BMI1	mouse	F6	Millipore	1:300	10mM Tris 1mM EDTA pH 9.0 98°C
albumin	mouse	HSA-11	Sigma	1:2500	10mM Tris 1mM EDTA pH 9.0 98°C
HepPar-1	mouse	OCH1E5	Dako	1:50	10mM Tris 1mM EDTA pH 9.0 98°C
ZO1	rabbit		Invitrogen	1:250	0.8% pepsin 37°C

Supplemental References

Van Beusekom, C.D., Schipper, L., and Fink-Gremmels, J. (2010). Cytochrome P450-mediated hepatic metabolism of new fluorescent substrates in cats and dogs. J. Vet. Pharmacol. Ther. *33*, 519-527.

Gómez-Lechón, M.J., Donato, M.T., Martínez-Romero, A., Jiménez, N., Castell, J.V., and O'Connor J.E. (2007). A human hepatocellular in vitro model to investigate steatosis. Chem. Biol. Interact. *165*, 106-116.

Graffmann, N., Ring, S., Kawala, M.A., Wruck, W., Ncube, A., Trompeter, H.I., and Adjaye J. (2016). Modeling Nonalcoholic Fatty Liver Disease with Human Pluripotent Stem Cell-Derived Immature Hepatocyte-Like Cells Reveals Activation of PLIN2 and Confirms Regulatory Functions of Peroxisome Proliferator-Activated Receptor Alpha. Stem Cells Dev. *25*, 1119-33.

Nantasanti, S., Spee, B., Kruitwagen, H.S., Chen, C., Geijsen, N., Oosterhoff, L.A., Van Wolferen, M.E., Pelaez, N., Fieten, H., Wubbolts, R.W., et al. (2015). Disease modeling and gene therapy of copper storage disease in canine hepatic organoids. Stem Cell Reports *5*, 895-907.

Odle, J., Lin, X., Van Kempen, T.A., Drackley, J.K., and Adams, S.H. (1995). Carnitine palmitoyltransferase modulation of hepatic fatty acid metabolism and radio-HPLC evidence for low ketogenesis in neonatal pigs. J. Nutr. *125*, 2541-2549.

Wruck, W., Kashofer, K., Rehman, S., Daskalaki, A., Berg, D., Gralka, E., Jozefczuk, J., Drews, K., Pandey, V., Regenbrecht, C., et al. (2015). Multi-omic profiles of human non-alcoholic fatty liver disease tissue highlight heterogenic phenotypes. Sci Data *2*, 150068.

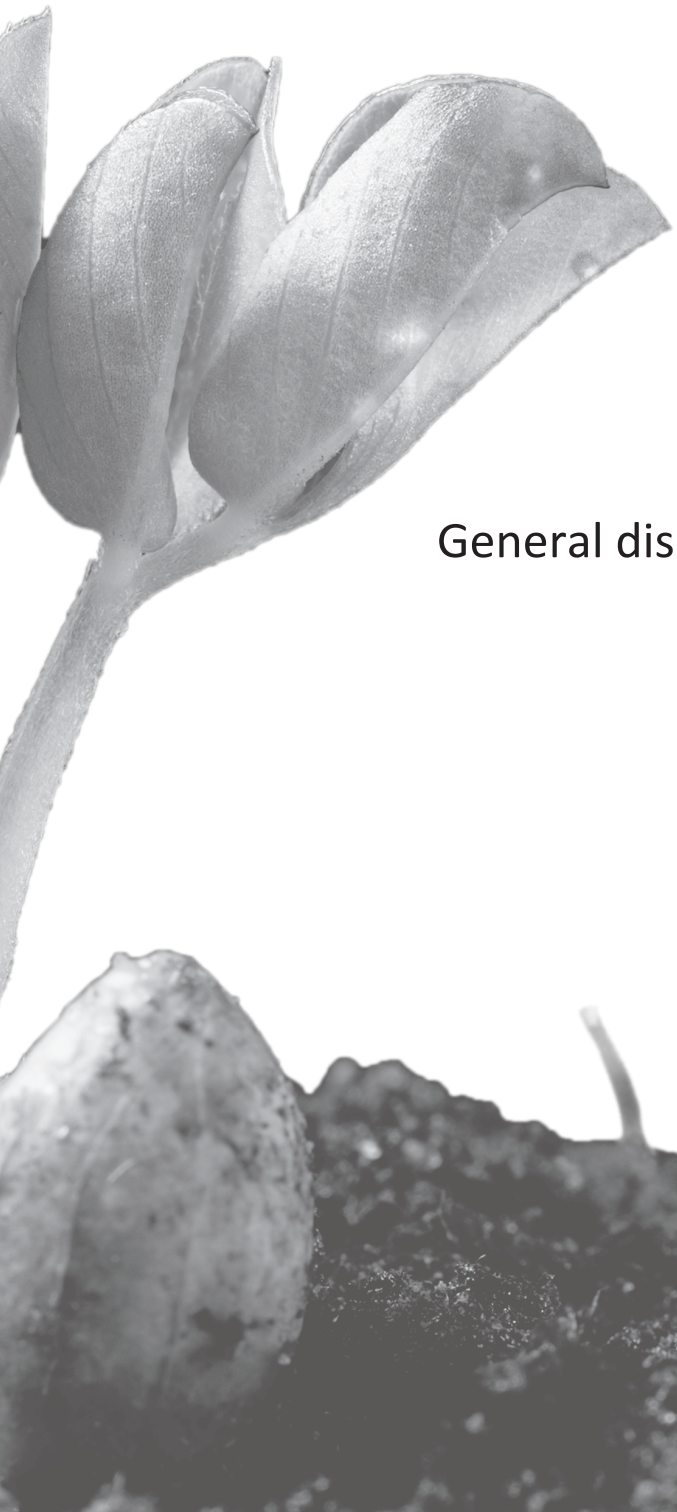

Chapter 8

General discussion and summary

Introduction

The liver is famous for its regenerative capacity, but in many liver diseases these repair mechanisms fall short and clinical signs of hepatic dysfunction develop. Liver regeneration requires a complex interplay of cells and stimulatory substances, such as growth factors, in order to restore liver size and function (Fausto et al., 2006). Most of the insight into the fundamental biology behind this process is derived from experimental rodent studies, but also from canine studies (Higgins et al., 1931; Marchioro et al., 1967). Key findings were then investigated in human liver pathology, which has given clinical relevance to pathways of liver regeneration (Roskams et al., 1998; Marshall et al., 2005; Apte et al., 2009; Truant et al., 2013). For veterinary medicine and more specifically in canine and feline hepatology, much less is known about the functional involvement of different cell types and pathways during liver disease and regeneration. In the last decade, considerable steps were taken to gain fundamental understanding of the molecular biology of canine and feline liver disease (Spee et al., 2007; Arends et al., 2009; Schotanus et al., 2009; Ijzer et al., 2010). In this thesis fundamental studies are presented that add to this basis (**part I**) and applied studies that build on gained knowledge to benefit both the veterinary and human liver patient (**part II**).

Translating bench to bedside

In biomedical research focusing on the advancement of medicine, the 'bench to bedside' concept is widely used to describe the translation of experimental findings from the lab bench to human clinical application. In this process several steps are required to bridge the gap between petri dish and human patient. Each step in the development of a new innovative therapeutic intervention is associated with specific research questions and requires an appropriate model to answer them. Fundamental drug target discovery can be done with cell lines that are highly standardized and stable (**chapter 4**). Findings then need to be validated and/or scrutinized for clinical relevance with *ex vivo* descriptive pathology studies (**chapter 2**, **chapter 3**) or primary cell culture systems (**chapter 4**, **chapter 7**). In the next phase, animal experiments are needed to evaluate both efficacy and safety of the new therapy. Experimental rodent studies are a valuable first step to establish proof of concept. However, mice and rats are highly standardized in genetic background, food, and housing which makes them fundamentally different from a human clinical situation. Moreover, an experimentally induced model generally does not fully mimic human disease in all its heterogeneity. Large animal models offer the advantage of naturally occurring diseases that are more similar to their human counterpart on a clinical, pathological, and biochemical level (Volk et al., 2013; Hoffman et al., 2016). Based on their size large animals also permit more diagnostic and therapeutic interventions compared to rodents. Hence, large animal experiments are a valuable tool to test new therapeutic strategies in a preclinical setting (**chapter 5**, **chapter 6**). Some specific diseases similarly affect humans and domesticated animals, which offers a translational research opportunity on another level. Investigating differences and similarities in disease patho(physio)logy between species can aid in our understanding of liver disease in both human and veterinary patients (**chapter 7**).

Part I: Hepatic progenitor cell activation mechanisms

Depending on the species and type of liver injury, several hepatic stem cell niches have been described from a periportal location (Kuwahara et al., 2008; Turner et al., 2011), to a biliary (Furuyama et al., 2011; Semeraro et al., 2012; Raven et al., 2017), and a pericentral origin (Wang et al., 2015). Hepatic progenitor cells (HPCs) are adult stem cells of the liver that are normally quiescent, but start to proliferate during certain types of liver disease and can differentiate to adult hepatocytes or cholangiocytes (Roskams et al., 2003; Wang et al., 2003; Boulter et al., 2012). They are considered a second line of defense in liver regeneration when hepatocyte replication fails or is exhausted but activation is generally too little or too late (Lowes et al., 1999; Katoonizadeh et al., 2006). Therefore, insights into specific activation mechanisms could provide new therapeutic strategies to induce liver regeneration in severe liver disease in both veterinary and human hepatology.

In **Chapter 1**, we reviewed the current body of knowledge on HPCs in dogs and cats and compared it to data from rodent studies and human pathology. HPCs are characterized morphologically by marker expression and histological appearance and on a functional level by proliferation/self-renewal and differentiation capacity. Marker expression is quite similar between rodent, canine and human HPCs as they share markers such as BCRP1, CD29, CD133, K7 (also published for cat), K19, OPN, and SOX9. In liver histology, proliferated HPCs generate a ductular structure and are hence described as a 'ductular reaction'. This is also a shared feature between species and the extent of the ductular reaction is correlated with the type and severity of liver disease. As the prevalence of specific liver diseases differs between dogs and cats, this is reflected in the published studies investigating tissue reaction patterns during liver disease. In dogs, HPC activation has been seen in liver sections of patients with acute and chronic hepatitis and cirrhosis. In cats, HPC activation has been described in acute hepatitis and feline hepatic lipidosis (also known as fatty liver disease or steatosis). In both species, an association was found between hepatocellular carcinoma malignancy grade and HPC marker expression. Activation of HPCs is driven by external factors that originate from neighboring cells and stroma, together constituting the HPC niche or micro-environment. Functional studies in rodents and descriptive pathology studies in human have identified hepatic stellate cells, macrophages and laminin as important niche components. Also in dogs a spatial relationship has been observed between activated HPCs, stellate cells and macrophages during liver disease, suggesting similar niche composition. Knowledge acquired on fundamental HPC biology in different species and reaction patterns to disease are important parameters when evaluating valuable large animal models for human clinical translation. We proposed the dog as relevant animal model to study preclinical HPC transplantations and the cat as translational model for human fatty liver disease and cholangiopathies.

Chapter 2 describes the characteristics of the canine HPC and its niche in the normal liver, in different forms of hepatitis, and in biliary disease. We used laser-microdissection to harvest and compare the HPC niche in quiescent (normal liver) and activated (lobular dissecting hepatitis, LDH) states. Transcriptional profiles were established and differentially expressed markers were further studied on protein level with immunohistochemistry in acute hepatitis, chronic hepatitis, LDH, and extrahepatic cholestasis. Marker expression varied depending on the type of disease, but in all diseases activated HPCs were positive for CD29, CD44, BMI1, HNF4α, SOX9, and HNF1β.

Immunofluorescent double stainings showed that the ductular reaction was consistently surrounded by laminin, an extracellular matrix component and ligand for CD29, activated hepatic stellate cells and macrophages.

Wnt/β-catenin and Notch signaling have been reported as important pathways in rodent and human HPC activation (Spee et al., 2010). To study whether these pathways are also important for canine HPC activation, efforts were made in **chapter 3** to study Wnt and Notch downstream signaling targets in quiescent and activated canine HPCs. A canine liver disease that is characterized by massive HPC activation is lobular dissecting hepatitis (LDH), a severe liver disease with a rapid clinical course and extensive fibrosis. Wnt/β-catenin and Notch target gene expression was increased in the activated HPC niche from LDH samples. HPCs in LDH were Ki67 (proliferation marker) and vimentin (mesenchymal marker) positive. Immunofluorescent double stainings showed nuclear presence of β-catenin and cytoplasmic and/or nuclear presence of Notch1/NICD in HPCs, indicating active Wnt and Notch signaling. This staining was not present in intermediate and mature hepatocytes. Together these results indicate that Wnt/β-catenin and Notch signaling are activated in proliferating canine HPCs and inactive in mature hepatocytes. Manipulation of these pathways *in vitro* in cultured canine HPCs might be used to enhance either expansion or differentiation towards a hepatocyte-like cell type.

Although several activation mechanisms have been described for HPCs from various species, it is not known which essential intracellular signals determine the switch from a quiescent to a proliferative state. In **chapter 4**, we performed a high-throughput RNAi screening experiment to search for kinases that affect the decision to enter S phase of the cell cycle in HPCs. A human HPC-like cell line, HepaRG, was used in the screen and findings were subsequently validated in primary HPCs cultured as liver organoids. One hit resulted in an increase in the percentage of cells in S phase (EdU^+) after knockdown, however without increasing the total number of cells. This hit was dual specificity tyrosine phosphorylation regulated kinase 1A (DYRK1A), a kinase known to affect proliferation of neural progenitor cells (Park et al., 2010; Hämmerle et al., 2011). RNAi screen findings were confirmed with different readouts (flow cytometry), with a chemical inhibitor of DYRK1A (harmine), and with liver organoids. Increased percentage of cells in S phase (EdU+) and in G2/M phase (pH3) without increased proliferation was seen in all conditions, possibly explained by a delay in cell cycle progression. A possible mechanism of DYRK1A-mediated enhanced S phase entry was the impairment of DREAM complex formation, as suggested by decreased LIN52 phosphorylation and associated changes in transcription of cell cycle progression genes after DYRK1A inhibition in HPCs. Conversely, liver organoids cultured from mice expressing one extra allele of the murine Dyrk1a gene (mBACtgDyrk1A) had both a decreased percentage of cells in S phase and decreased proliferation when compared with organoids from wild type controls. In conclusion, an exact dosage of DYRK1A seems essential for the regulation of S phase entry and proliferation of HPCs.
Our RNAi screen resulted in a total of 10 kinase hits which significantly increased or decreased the proliferation rate of HPC-like cells *in vitro*. We have pursued detailed studies into the mechanism of action of DYRK1A being the only factor which influenced the cell cycle positively. The other signals identified in the RNAi screen had a negative effect on HPC proliferation after knockdown. These signals were not investigated as they are out of scope for the present project. However, they may be highly relevant as potential targets to exogenously inhibit HPC proliferation. This could be a desirable new interventional strategy for liver tumors (e.g. hepatocellular carcinomas) with hepatic

progenitor cell characteristics. Both in man and dog, liver tumors with a HPC marker signature have a more malignant phenotype and lack effective treatment options (Uenishi et al., 2003; van Sprundel et al., 2010, Govaere et al., 2014).

From **part I** the following can be concluded:

- Both marker expression and niche composition of canine hepatic progenitor cells resemble their human counterpart.
- Wnt/β-catenin and Notch signaling are activated in proliferating canine HPCs.
- Dogs are a relevant large animal model to study hepatic progenitor cell transplantations for human clinical translation.
- High throughput screening revealed DYRK1A as balanced regulator of hepatic progenitor cell S phase entry and proliferation.

Part II: Growth factors and hepatic progenitor cells in models of liver disease

In the second part of this thesis, we applied knowledge gained from *in vitro* experiments to *in vivo* disease models to study liver regeneration (**chapter 5**) and transplantation (**chapter 6**). In 2015 a liver organoid culture system was developed for dog primary HPCs, based on expansion with Wnt agonists and differentiation with Notch inhibitors (Nantasanti et al., 2015). Transplantation potential was suggested based on successful transplantations of mouse, rat, and human liver organoids (Huch et al, 2013; Kuijk et al., 2016; Huch et al., 2015). Additionally, a role was proposed for organoids in disease modeling research for genetic diseases such as cystic fibrosis and Alagille syndrome (Dekkers et al., 2013; Huch et al., 2015). This prompted us to further investigate this option for liver organoids and we developed a new *in vitro* research model in **chapter 7**.

Hepatocyte growth factor (HGF) is an important mitogen for hepatocytes and is essential for liver regeneration. In **chapter 5**, we tested the therapeutic potential of exogenous HGF supplementation in dogs with a hypoplastic liver secondary to a congenital portosystemic shunt (CPSS). In portosystemic shunting, portal blood carrying trophic factors is diverted past the liver circumventing the hepatic parenchyma. As a result the liver is reduced in size, but can grow out to normal proportions after surgical attenuation of the shunt. We hypothesized that HGF therapy in CPSS dogs could similarly induce hepatocyte proliferation and liver regeneration, with a secondary effect of enhancing portal perfusion. Six CPSS dogs were treated with intravenous recombinant HGF for three weeks and effects on liver size were determined by computed tomography before, during and after treatment. Liver growth could be induced by exogenous HGF therapy and was supported on a molecular level by increased Ki67 labeling in the liver, increased gene expression of proliferation markers E2F1 and CDC6 and downstream signaling targets of HGF in liver biopsies. However, liver size decreased again after cessation of HGF therapy and portal perfusion did not improve throughout the study period. We concluded that HGF therapy is feasible to induce liver regeneration in absence of portal perfusion in CPSS dogs, but that the effects are transient and increased liver size is not maintained when treatment is discontinued.

In **chapter 6** we investigated the possibility of using HPCs cultured as liver organoids for cell

transplantation purposes in a dog model of metabolic liver disease. Human patients with various metabolic liver diseases have already been successfully transplanted with allogenic hepatocytes (Jorns et al., 2012). Our objective was to test autologous transplantation of gene-corrected organoid-derived liver cells in a COMMD1-deficient dog model of copper storage disease. This large animal model closely resembles human Wilson's disease. Autologous hepatic progenitor cells were isolated from 14G Tru-cut liver biopsies and cultured as three-dimensional liver organoids. A gene correction was performed and organoids were differentiated towards hepatocyte-like cells. Organoids were dissociated and transplanted either via the portal vein on three consecutive days or via intrahepatic injections. Intraportal transplantation of autologous organoid-derived liver cells did not result in engraftment of the cells and biliary copper excretion did not improve. Intrahepatic injections were successful and after seven days transplanted cells were found engrafted in the injection sites. Furthermore, engrafted undifferentiated organoids were Ki67 positive indicating proliferation *in vivo*. Organoids in the liver were surrounded by fibrous tissue, most likely originating from *de novo* synthesis. Further research in appropriate animal models is needed to determine optimal route of administration, organoid pretreatment, and evaluate tissue reactions to transplanted organoid-derived liver cells. Only then can liver organoid transplantations safely be translated to human clinical application in metabolic liver disease.

Primary hepatic progenitor cells cultured as liver organoids can not only be used for transplantation, they have proved to be a valuable tool in disease modeling research as well. We asked whether liver organoids could be used to model metabolic liver disease and whether we could investigate species differences in metabolic processes using liver organoids. Hepatic steatosis is a disease characterized by excessive lipid accumulation in liver cells and occurs in both human and cat, albeit with a different etiology. **In chapter 7**, we developed a robust culture system for feline liver organoids from cat liver wedge biopsies and from fine needle aspirates (all surplus material). Cultures could be expanded for months and showed both phenotypic and genetic stability. Feline liver organoids could be differentiated to a more mature hepatocyte-like state. Next, we created a disease model of steatosis by providing organoids with excess free fatty acids and measuring intracellular lipid accumulation. We compared liver organoids from mouse, human, dog, and cat liver for their lipid handling capacity and learned that feline liver organoids accumulated more lipid than human liver organoids. This was further investigated on a transcriptional level, which further substantiated the differential regulation of lipid metabolism between species and can lead to new insights on potential therapeutic targets for human and feline steatosis. In fact, we were able to interfere with the steatotic phenotype in feline liver organoids by either blocking or enhancing beta oxidation of exogenous fatty acids. Therefore, feline liver organoids are a new primary *in vitro* research model that may partly replace animal experiments and have potential for drug development for feline hepatic lipidosis.

From **part II** the following can be concluded:

- HGF therapy induces liver growth in the absence of portal perfusion, but does not improve liver perfusion; increased liver size lasts only for the duration of the treatment.
- Canine HPCs can be isolated from a biopsy, cultured as liver organoids, genetically corrected, and highly expanded to be used for autologous cell transplantation.
- Feline liver organoids can be cultured and are a new research model for hepatic steatosis.

Conclusions and recommendations for future research

In this thesis new activation mechanisms for canine and human HPCs are presented that can be important targets in liver regenerative medicine. A screening approach has identified a regulatory kinase previously unknown to affect HPC proliferation and nine other signals that can be targeted to decrease HPC proliferation. Future research could focus on expression of these signals and pathways during (absence of) HPC-mediated liver regeneration and liver cancer, and investigate *in vitro* and *in vivo* manipulation options to either enhance or inhibit HPC proliferation.

Although liver diseases in humans and dogs differ in etiology and prevalence, essential pathways and cells that contribute to regeneration are quite similar. Dogs with naturally occurring liver disease are the ideal animal species for preclinical evaluation of hepatic progenitor cell transplantations. The obstacles that were encountered and overcome in the first in dog HPC transplantations can now be anticipated and appropriately dealt with for the first in human transplantations. Future research needs to focus on the best pretreatment of the cells, the recipient and route of administration in order to define an optimal protocol suitable for human application. The recently published availability of humanized mouse (and perhaps in the near future also pig) livers (Azuma et al., 2007; Hasegawa et al., 2011; Washburn et al., 2011; Hickey et al., 2016) to test human liver cell transplantations is a promising development which allows the evaluation of human liver cell behavior after transplantation in a humanized liver. However, it is important to recognize that although there is an obvious advantage of studying human cells for human clinical application, humanized livers are a xenograft model and human donor cells will encounter species differences in reactions with host cells, stromal interactions, and even basic physiological aspects (e.g. body temperature, hormones, metabolism). Hence, autologous canine liver organoid transplantation in a relevant canine disease model might have more predictive value for the efficacy of autologous human liver organoid transplantations in a human disease setting.

Both in hepatology and in other physiological aspects cats cannot be considered small dogs. Feline liver diseases such as hepatic lipidosis and cholangitis are infrequently encountered in dogs but have human counterparts in non-alcoholic fatty liver disease and primary sclerosing cholangitis (Center, 2005; Otte et al., 2017; Cohen et al., 2011; Boonstra et al., 2013). More research into the pathophysiology and molecular biology of feline liver disease is needed to design new therapeutic strategies. The availability of feline liver organoids as a primary cell culture can advance this development. Organoid cultures can be established from diseased and control liver tissues, urging the need for prospective biobanking of surplus liver samples. Liver organoids also offer the possibility of *in vitro* drug testing for either toxicity studies or as new therapeutic intervention for feline hepatic lipidosis, reducing the need for animal experiments. Innovation in drugs that lower triglyceride content in feline liver organoids could then be extrapolated to liver organoids from other species, including human.

Advances in both the understanding and treatment of liver diseases rely on evidence-based translation of *in vitro* findings to clinical application. Similarly, fundamental aspects of liver regeneration and hepatic progenitor cell biology need to be investigated and compared between species in order to obtain insight in appropriate animal models and to enable researchers to learn from the differences. The ability to discern and interpret essential species differences is deeply embedded in the veterinary profession, which makes veterinary academic researchers valuable partners in translational medical research to benefit both veterinary and human patients.

References

Apte U, Singh S, Zeng G, Cieply B, Virji MA, Wu T, Monga SP. Beta-catenin activation promotes liver regeneration after acetaminophen-induced injury. Am J Pathol. 2009;175(3):1056-65.

Arends B, Vankelecom H, Vander Borght S, Roskams T, Penning LC, Rothuizen J, Spee B. The dog liver contains a "side population" of cells with hepatic progenitor-like characteristics. Stem Cells Dev. 2009;18(2):343-50.

Azuma H, Paulk N, Ranade A, Dorrell C, Al-Dhalimy M, Ellis E, Strom S, Kay MA, Finegold M, Grompe M. Robust expansion of human hepatocytes in Fah-/-/Rag2-/-/Il2rg-/- mice. Nat Biotechnol. 2007;25(8):903-10.

Boonstra K, Weersma RK, van Erpecum KJ, Rauws EA, Spanier BW, Poen AC, van Nieuwkerk KM, Drenth JP, Witteman BJ, Tuynman HA, Naber AH, Kingma PJ, van Buuren HR, van Hoek B, Vleggaar FP, van Geloven N, Beuers U, Ponsioen CY; EpiPSCPBC Study Group. Population-based epidemiology, malignancy risk, and outcome of primary sclerosing cholangitis. Hepatology. 2013;58(6):2045-55.

Boulter L, Govaere O, Bird TG, Radulescu S, Ramachandran P, Pellicoro A, Ridgway RA, Seo SS, Spee B, Van Rooijen N, Sansom OJ, Iredale JP, Lowell S, Roskams T, Forbes SJ. Macrophage-derived Wnt opposes Notch signaling to specify hepatic progenitor cell fate in chronic liver disease. Nat Med. 2012;18(4):572-9.

Center SA. Feline hepatic lipidosis. Vet Clin North Am Small Anim Pract. 2005;35(1):225-69.

Cohen JC, Horton JD, Hobbs HH. Human fatty liver disease: old questions and new insights. Science. 2011;332(6037):1519-23.

Dekkers JF, Wiegerinck CL, de Jonge HR, Bronsveld I, Janssens HM, de Winter-de Groot KM, Brandsma AM, de Jong NW, Bijvelds MJ, Scholte BJ, Nieuwenhuis EE, van den Brink S, Clevers H, van der Ent CK, Middendorp S, Beekman JM. A functional CFTR assay using primary cystic fibrosis intestinal organoids. Nat Med. 2013;19(7):939-45.

Fausto N, Campbell JS, Riehle KJ. Liver regeneration. Hepatology. 2006;43(2 Suppl 1):S45-53.

Furuyama K, Kawaguchi Y, Akiyama H, Horiguchi M, Kodama S, Kuhara T, Hosokawa S, Elbahrawy A, Soeda T, Koizumi M, Masui T, Kawaguchi M, Takaori K, Doi R, Nishi E, Kakinoki R, Deng JM, Behringer RR, Nakamura T, Uemoto S. Continuous cell supply from a Sox9-expressing progenitor zone in adult liver, exocrine pancreas and intestine. Nat Genet. 2011;43(1):34-41.

Govaere O, Komuta M, Berkers J, Spee B, Janssen C, de Luca F, Katoonizadeh A, Wouters J, van Kempen LC, Durnez A, Verslype C, De Kock J, Rogiers V, van Grunsven LA, Topal B, Pirenne J, Vankelecom H, Nevens F, van den Oord J, Pinzani M, Roskams T. Keratin 19: a key role player in the invasion of human hepatocellular carcinomas. Gut. 2014;63(4):674-85.

Hämmerle B, Ulin E, Guimera J, Becker W, Guillemot F, Tejedor FJ. Transient expression of Mnb/Dyrk1a couples cell cycle exit and differentiation of neuronal precursors by inducing p27KIP1 expression and suppressing NOTCH signaling. Development. 2011;138(12):2543-54.

Hasegawa M, Kawai K, Mitsui T, Taniguchi K, Monnai M, Wakui M, Ito M, Suematsu M, Peltz G, Nakamura M, Suemizu H. The reconstituted 'humanized liver' in TK-NOG mice is mature and functional. Biochem Biophys Res Commun. 2011;405(3):405-10.

Hickey RD, Mao SA, Glorioso J, Elgilani F, Amiot B, Chen H, Rinaldo P, Marler R, Jiang H, DeGrado TR, Suksanpaisan L, O'Connor MK, Freeman BL, Ibrahim SH, Peng KW, Harding CO, Ho CS, Grompe M, Ikeda Y, Lillegard JB, Russell SJ, Nyberg SL. Curative ex vivo liver-directed gene therapy in a pig model of hereditary tyrosinemia type 1. Sci Transl Med. 2016;8(349):349ra99.

Higgins GM, Anderson RM. Experimental pathology of the liver – Restoration of the liver of the white rat following partial surgical removal. Arch Pathol. 1931;12:186-202.

Hoffman AM, Dow SW. Concise Review: Stem Cell Trials Using Companion Animal Disease Models. Stem Cells. 2016;34(7):1709-29.

Huch M, Dorrell C, Boj SF, van Es JH, Li VS, van de Wetering M, Sato T, Hamer K, Sasaki N, Finegold MJ, Haft A, Vries RG, Grompe M, Clevers H. In vitro expansion of single Lgr5+ liver stem cells induced by Wnt-driven regeneration. Nature. 2013;494(7436):247-50.

Huch M, Gehart H, van Boxtel R, Hamer K, Blokzijl F, Verstegen MM, Ellis E, van Wenum M, Fuchs SA, de Ligt J, van de Wetering M, Sasaki N, Boers SJ, Kemperman H, de Jonge J, Ijzermans JN, Nieuwenhuis EE, Hoekstra R, Strom S, Vries RR, van der Laan LJ, Cuppen E, Clevers H. Long-term culture of genome-stable bipotent stem cells from adult human liver. Cell. 2015;160(1-2):299-312.

Ijzer J, Schotanus BA, Vander Borght S, Roskams TA, Kisjes R, Penning LC, Rothuizen J, van den Ingh TS. Characterisation of the hepatic progenitor cell compartment in normal liver and in hepatitis: an immunohistochemical comparison between dog and man. Vet J. 2010;184(3):308-14.

Jorns C, Ellis EC, Nowak G, Fischler B, Nemeth A, Strom SC, Ericzon BG. Hepatocyte transplantation for inherited metabolic diseases of the liver. J Intern Med. 2012;272(3):201-23.

Katoonizadeh A, Nevens F, Verslype C, Pirenne J, Roskams T. Liver regeneration in acute severe liver impairment: a clinicopathological correlation study. Liver Int. 2006;26(10):1225-33.

Kuijk EW, Rasmussen S, Blokzijl F, Huch M, Gehart H, Toonen P, Begthel H, Clevers H, Geurts AM, Cuppen E. Generation and characterization of rat liver stem cell lines and their engraftment in a rat model of liver failure. Sci Rep. 2016;6:22154.

Kuwahara R, Kofman AV, Landis CS, Swenson ES, Barendswaard E, Theise ND. The hepatic stem cell niche: identification by label-retaining cell assay. Hepatology. 2008;47(6):1994-2002.

Lowes KN, Brennan BA, Yeoh GC, Olynyk JK. Oval cell numbers in human chronic liver diseases are directly related to disease severity. Am J Pathol. 1999;154(2):537-41.

Marchioro TL, Porter KA, Brown BI, Otte JB, Starzl TE. The effect of partial portacaval transposition on the canine liver. Surgery. 1967;61(5):723-32.

Marshall A, Rushbrook S, Davies SE, Morris LS, Scott IS, Vowler SL, Coleman N, Alexander G. Relation between hepatocyte G1 arrest, impaired hepatic regeneration, and fibrosis in chronic hepatitis C virus infection. Gastroenterology. 2005;128(1):33-42.

Nantasanti S, Spee B, Kruitwagen HS, Chen C, Geijsen N, Oosterhoff LA, van Wolferen ME, Pelaez N, Fieten H, Wubbolts RW, Grinwis GC, Chan J, Huch M, Vries RR, Clevers H, de Bruin A, Rothuizen J, Penning LC, Schotanus BA. Disease Modeling and Gene Therapy of Copper Storage Disease in Canine Hepatic Organoids. Stem Cell Reports. 2015;5(5):895-907.

Otte CM, Penning LC, Rothuizen J. Feline biliary tree and gallbladder disease. J Feline Med Surg. 2017;19(5):514-528

Park J, Oh Y, Yoo L, Jung MS, Song WJ, Lee SH, Seo H, Chung KC. Dyrk1A phosphorylates p53 and inhibits proliferation of embryonic neuronal cells. J Biol Chem. 2010;285(41):31895-906.

Raven A, Lu WY, Man TY, Ferreira-Gonzalez S, O'Duibhir E, Dwyer BJ, Thomson JP, Meehan RR, Bogorad R, Koteliansky V, Kotelevtsev Y, Ffrench-Constant C, Boulter L, Forbes SJ. Cholangiocytes act as facultative liver stem cells during impaired hepatocyte regeneration. Nature. 2017;547(7663):350-354.

Roskams T, De Vos R, Van Eyken P, Myazaki H, Van Damme B, Desmet V. Hepatic OV-6 expression in human liver disease and rat experiments: evidence for hepatic progenitor cells in man. J Hepatol. 1998;29(3):455-63.

Roskams TA, Libbrecht L, Desmet VJ. Progenitor cells in diseased human liver. Semin Liver Dis. 2003;23(4):385-96.

Schotanus BA, van den Ingh TS, Penning LC, Rothuizen J, Roskams TA, Spee B. Cross-species immunohistochemical investigation of the activation of the liver progenitor cell niche in different types of liver disease. Liver Int. 2009;29(8):1241-52.

Semeraro R, Carpino G, Cardinale V, Onori P, Gentile R, Cantafora A, Franchitto A, Napoli C, Anceschi M, Brunelli R, Bosco D, Torrice A, Reid L, Gaudio E, Alvaro D. Multipotent stem/progenitor cells in the human foetal biliary tree. J Hepatol. 2012;57(5):987-94.

Spee B, Arends B, van den Ingh TS, Roskams T, Rothuizen J, Penning LC. Major HGF-mediated regenerative pathways are similarly affected in human and canine cirrhosis. Comp Hepatol. 2007;6:8.

Spee B, Carpino G, Schotanus BA, Katoonizadeh A, Vander Borght S, Gaudio E, Roskams T. Characterisation of the liver progenitor cell niche in liver diseases: potential involvement of Wnt and Notch signalling. Gut. 2010;59(2):247-57.

van Sprundel RG, van den Ingh TS, Desmet VJ, Katoonizadeh A, Penning LC, Rothuizen J, Roskams T, Spee B. Keratin 19 marks poor differentiation and a more aggressive behaviour in canine and human hepatocellular tumours. Comp Hepatol. 2010;9(1):4.

Truant S, Bouras AF, Petrovai G, Buob D, Ernst O, Boleslawski E, Hebbar M, Pruvot FR. Volumetric gain of the liver after major hepatectomy in obese patients: a case-matched study in 84 patients. Ann Surg. 2013;258(5):696-702.

Turner R, Lozoya O, Wang Y, Cardinale V, Gaudio E, Alpini G, Mendel G, Wauthier E, Barbier C, Alvaro D, Reid LM. Human hepatic stem cell and maturational liver lineage biology. Hepatology. 2011;53(3):1035-45.

Uenishi T, Kubo S, Yamamoto T, Shuto T, Ogawa M, Tanaka H, Tanaka S, Kaneda K, Hirohashi K. Cytokeratin 19 expression in hepatocellular carcinoma predicts early postoperative recurrence. Cancer Sci. 2003;94(10):851-7.

Volk SW, Theoret C. Translating stem cell therapies: the role of companion animals in regenerative medicine. Wound Repair Regen. 2013;21(3):382-94.

Wang X, Foster M, Al-Dhalimy M, Lagasse E, Finegold M, Grompe M. The origin and liver repopulating capacity of murine oval cells. Proc Natl Acad Sci U S A. 2003;100:11881-8.

Wang B, Zhao L, Fish M, Logan CY, Nusse R. Self-renewing diploid Axin2(+) cells fuel homeostatic renewal of the liver. Nature. 2015;524(7564):180-5.

Washburn ML, Bility MT, Zhang L, Kovalev GI, Buntzman A, Frelinger JA, Barry W, Ploss A, Rice CM, Su L. A humanized mouse model to study hepatitis C virus infection, immune response, and liver disease. Gastroenterology. 2011;140(4):1334-44.

Nederlandse samenvatting voor niet-ingewijden

Inleiding

De lever is van oudsher al bekend om zijn indrukwekkende vermogen tot regeneratie. Echter, in veel leverziekten schiet deze herstelcapaciteit tekort en ontstaan symptomen van klinisch leverfalen. Leverregeneratie komt tot stand door een complex samenspel van cellen en groeifactoren dat erop gericht is de grootte en functie van de lever op peil te houden. De meeste kennis over de biologie achter dit proces komt voort uit experimentele studies met muizen en ratten, maar ook uit studies in honden. Deze kennis is vervolgens getoetst op klinische relevantie in pathologische monsters van humane leverziekten, wat tot diepgaand inzicht in de mechanismen achter leverziekten en –herstel heeft geleid. Net als bij mensen komen ook bij honden en katten spontaan optredende leverziekten voor met een vergelijkbaar verloop, maar kennis over de cellen en moleculaire signaalroutes die bijdragen aan leverziekte en leverregeneratie bij deze diersoorten is pas recent tot stand gekomen. In dit proefschrift wordt een bijdrage geleverd aan de basale kennis over stamcel-gemedieerde leverregeneratie bij meerdere diersoorten (**deel I**) en worden diverse toegepaste studies beschreven die gebruik maken van de verkregen kennis om tot nieuwe therapieën te komen voor zowel veterinaire als humane leverpatiënten (**deel II**).

Translatie tussen laboratorium en patiënt

In het biomedisch onderzoek wordt het 'bench-to-bedside' concept gebruikt in de translationale geneeskunde, die erop gericht is om bevindingen vanuit het laboratorium (de labtafel of 'bench') tot klinische toepassing te brengen ('bedside'). Wat werkt in het laboratorium in een kweekschaaltje (*in vitro*) kan in een daadwerkelijke patiënt (*in vivo*) heel anders uitpakken. De vele stappen die nodig zijn voor het ontwikkelen van nieuwe behandelmethoden voor een bepaalde ziekte vereisen elk een juist onderzoeksmodel om de specifieke vraag te kunnen beantwoorden. Fundamentele vraagstukken over processen in de cel kunnen het beste worden benaderd met studies in cellijnen, die zeer gestandaardiseerd zijn (**hoofdstuk 4**). Vervolgens moeten deze bevindingen worden getoetst op klinische relevantie in weefselmonsters van leverpatiënten (**hoofdstuk 2**, **hoofdstuk 3**) of in primaire celkweken direct vanuit leverweefsel (**hoofdstuk 4**, **hoofdstuk 7**). Een volgende fase in de ontwikkeling van nieuwe therapeutische interventies is het testen van zowel werking als veiligheid in een levend organisme met dierproeven. Knaagdierstudies zijn een belangrijke eerste stap om het therapeutische concept *in vivo* te bewijzen. Muizen en ratten zijn geüniformeerd in afkomst, voeding en huisvesting om de proeven zo veel mogelijk gestandaardiseerd te kunnen uitvoeren. Hierin zijn ze echter fundamenteel verschillend van humane patiënten in al hun diversiteit. Bovendien zijn ziektemodellen in knaagdieren kunstmatig opgewekt en lijken daarmee lang niet altijd op humaan voorkomende ziektebeelden die sterk wisselend kunnen zijn in hun verschijningsvorm en reactie op behandelingen. Zogeheten grote diermodellen met van nature optredende ziektes bieden het voordeel dat ze veel meer op de humane situatie lijken wat betreft hun klinische, pathologische en biochemische eigenschappen. Een belangrijk bijkomend voordeel is dat in grote diersoorten diverse diagnostische technieken en behandelmethoden kunnen worden toegepast waar een muis of rat te klein voor is, maar die in de humane geneeskunde routinematig worden uitgevoerd. Daarom zijn experimenten in grote diermodellen zeer waardevol om onder preklinische omstandigheden nieuwe behandelingen te testen (**hoofdstuk 5**, **hoofdstuk 6**). Translationeel biomedisch onderzoek kan ook op fundamenteel mechanistisch niveau plaatsvinden, omdat bepaalde specifieke ziekten zowel bij mensen als dieren voorkomen. Kennis van verschillen en overeenkomsten in hoe het ziekteproces zich in mens en dier ontwikkelt, kan leiden tot nieuwe inzichten in behandeling van zowel humane als veterinaire patiënten (**hoofdstuk 7**).

Deel I: Activatiemechanismen van lever progenitor cellen

Lever progenitor cellen zijn volwassen stamcellen in de lever, die als reservepopulatie dienen en bijdragen aan leverregeneratie tijdens zeer ernstige of chronische leverschade. Deze cellen zijn aangetroffen in levers van knaagdieren en mensen, maar ook in levers van honden en katten. Helaas is de stamcel-gemedieerde bijdrage aan leverregeneratie vaak onvoldoende om tot klinisch herstel te leiden. Inzicht in de signalen die deze regeneratie op gang brengen kan leiden tot aangrijpingspunten voor nieuwe behandelmethodes, zogeheten regeneratieve geneeskunde.

In **hoofdstuk 1** wordt de wetenschappelijke literatuur over lever progenitor cellen in diverse diersoorten samengevat. Er wordt een vergelijking gemaakt tussen de lever progenitor cel zoals deze is beschreven voor muis, rat, hond, kat en mens. De meeste kenmerkende eiwitten (markers) voor deze cellen komen overeen tussen de verschillende diersoorten en ook de reactie in het weefsel ten tijde van leverziekte is vergelijkbaar bij deze diersoorten. Als lever progenitor cellen geactiveerd worden vormen ze buisvormige structuren, de zogeheten ductulaire reactie, die in uitgebreidheid correleert met de ernst van de leverziekte. Honden en katten verschillen in de typen leverziekten die van nature voorkomen. Logischerwijs is de beschikbare literatuur over lever progenitor cel activatie tijdens specifieke leverziektes bij de hond en de kat hiervan een afspiegeling. Bij de hond zien we veelal leverontsteking (hepatitis) die op termijn kan leiden tot ernstige verbindweefseling van de lever (cirrhose). Dit gaat gepaard met uitgebreide ductulaire reacties. In katten is leververvetting een prominent ziektebeeld, alsmede ziekte van de galwegen (galwegontstekingen). In katten met vervette levers werd ook een lever progenitor cel respons beschreven. In zowel honden als katten met leverkanker werd bovendien een associatie gevonden tussen kwaadaardigheid van de tumor en de lever progenitor cel markers die in de tumor worden aangetroffen. Activatie van lever progenitor cellen wordt voornamelijk aangestuurd door cellen en moleculen uit hun omgeving, de zogeheten niche. Bij honden en katten werd gevonden dat deze niche voornamelijk bestaat uit macrofagen (afweercellen), stellaatcellen en laminine, zoals ook eerder beschreven voor lever progenitor cellen van knaagdieren en mensen. Op basis van de verschillen en overeenkomsten in voorkomen van leverziekten en de geassocieerde lever progenitor cel respons wordt de hond voorgesteld als interessante diersoort voor lever progenitor cel transplantatiestudies en de kat als translationeel diermodel voor leververvetting en galwegziekten.

In **hoofdstuk 2** wordt een onderzoek beschreven naar de kenmerken en de niche van lever progenitor cellen in levers van honden met diverse vormen van leverontsteking (hepatitis) en galwegziekte. Dit werd vergeleken met levers van gezonde honden. Met een speciale techniek (laser microdissectie) werden de cellen verzameld uit weefselcoupes en werd onderzocht welke markergenen er tot expressie werden gebracht. De bevindingen werden vervolgens op eiwitniveau bevestigd door immunohistochemische kleuringen in weefselcoupes van honden met leverziekten. De markers die de geactiveerde lever progenitor cellen kenmerkten waren CD29, CD44, BMI1, HNF4α, SOX9, en HNF1β. Met immunofluorescente dubbelkleuringen werd vervolgens aangetoond dat de niche van geactiveerde lever progenitor cellen bestond uit laminine, geactiveerde stellaatcellen en macrofagen.

In **hoofdstuk 3** zijn twee belangrijke beschreven signaalroutes (Wnt/β-catenine en Notch) voor lever progenitor cel activatie onderzocht in leverweefsel van gezonde honden en honden met lobular dissecting

hepatitis (LDH). LDH is een zeer ernstige leverziekte bij de hond die acuut ontstaat, snel progressief verloopt en gekenmerkt wordt door uitgebreide bindweefselvorming in de lever. Opvallend is de sterke mate van lever progenitor cel activatie in deze patiënten. Met behulp van laser microdissectie zijn de geactiveerde lever progenitor cellen van weefselcoupes van LDH patiënten verzameld en is genexpressie van onderdelen van de Wnt/β-catenine en Notch signaalroutes gemeten. Deze bleek te zijn verhoogd in vergelijking met niet-geactiveerde lever progenitor cellen uit levers van gezonde honden. Met immunohistochemische kleuringen werd vervolgens aangetoond dat de Wnt/β-catenine en Notch signaalroutes ook op eiwitniveau geactiveerd waren in geactiveerde en delende lever progenitor cellen van honden met LDH. De omliggende volwassen levercellen (hepatocyten) waren negatief voor Wnt/β-catenine en Notch eiwitten. Dit betekent dat Wnt/β-catenine en Notch signaalroutes mogelijk zouden kunnen worden gemanipuleerd *in vitro* om gekweekte lever progenitor cellen te vermenigvuldigen of zich juist te laten specialiseren tot hepatocyt.

Er zijn reeds diverse activatiemechanismen van lever progenitor cellen beschreven die afkomstig zijn van externe stimuli aan de cel vanuit zijn omgeving. Maar het is niet bekend welke signalen in de cel uiteindelijk bepalen of een lever progenitor cel in rustende toestand blijft, danwel de omschakeling maakt naar een actieve celcyclus met celdeling tot gevolg. In **hoofdstuk 4** hebben we een screeningsexperiment gedaan om te onderzoeken welke kinases (signaaleiwitten verantwoordelijk voor een snelle aan/uitschakeling van een doeleiwit) hiervoor essentieel zijn door ze allemaal afzonderlijk uit te schakelen met siRNA's en het resulterende effect op de celcyclus te onderzoeken. De screen is gedaan in een cellijn met lever progenitor cel eigenschappen en de resultaten zijn daarna gevalideerd in primaire lever progenitor celkweken direct vanuit leverweefsel, zogeheten lever organoïden. Onze screen leverde één hit op waarbij na uitschakeling een toegenomen celcyclus activiteit werd gezien. Deze hit was 'dual specificity tyrosine phosphorylation regulated kinase 1A' (DYRK1A), een kinase waarvan bekend is dat het de celdeling van progenitor cellen in de hersenen en van bèta-cellen in de alvleesklier beïnvloedt. Opvallend resultaat was dat in lever progenitor cellen met geïnactiveerd DYRK1A de celcyclus werd geactiveerd, maar dat dit niet leidde tot meer celdeling, wat wel is beschreven voor de andere celtypen. Mogelijk spelen er compensatoire of feedback mechanismen die verdere voortgang door de celcyclus afremmen, waardoor uiteindelijk niet het aantal cellen toeneemt als DYRK1A wordt geïnactiveerd. DYRK1A is betrokken bij de vorming van een eiwitcomplex (het DREAMcomplex) wat belangrijk is voor de beslissing van cellen om in rustende toestand te blijven, danwel een actieve celcyclus in te gaan. We vonden aanwijzingen dat DREAMcomplex vorming in lever progenitor cellen die waren behandeld met een DYRK1A-remmer inderdaad was afgenomen en dat de expressie van genen die betrokken zijn bij de voortgang door de celcyclus overeenkomstig was veranderd. Vervolgens hebben we onderzocht wat er gebeurt als er één extra kopie van het DYRK1A gen in lever progenitor cellen aanwezig is. Hiervoor zijn lever organoïden gekweekt van mBACtgDyrk1A transgene muizen met een extra kopie van het gen, waarin bleek dat hierin een tegenovergesteld fenotype aanwezig was. Een extra DYRK1A kopie leidde tot een afname van celcyclus activiteit en celdeling. Concluderend kunnen we stellen dat DYRK1A activiteit in een exacte 'dosering' essentieel is voor de regulatie van de celcyclus en celdeling in lever progenitor cellen.
In de screen werden naast DYRK1A nog negen andere hits gevonden, die allen betrokken lijken te zijn bij de celdeling van lever progenitor cellen. Toekomstig onderzoek kan zich richten op deze signalen die wellicht te manipuleren zijn, waarmee mogelijk nieuwe therapieën voor levertumoren met lever progenitor cel markers kunnen worden ontwikkeld.

Uit **deel I** kan het volgende worden geconcludeerd:

- Lever progenitor cellen van de hond lijken op die van de mens wat betreft marker expressie en niche.
- Wnt/β-catenine en Notch signaalroutes zijn geactiveerd in delende lever progenitor cellen van de hond.

- Honden zijn een relevant groot diermodel voor humaan translationeel onderzoek naar lever progenitor cel transplantaties.
- Uit een groot screeningsonderzoek kwam naar voren dat DYRK1A een uitgebalanceerde regulator is van de celcyclus van lever progenitor cellen.

Deel II: Groeifactoren en lever progenitor cellen in modellen voor leverziekten

In het tweede deel van dit proefschrift zijn toegepaste studies uitgevoerd naar lever regeneratie (**hoofdstuk 5**) en transplantatie (**hoofdstuk 6**) die voortbouwen op reeds bestaande fundamentele kennis. Eerdere wetenschappelijke publicaties beschreven een primair (direct uit leverweefsel afkomstig) kweeksysteem voor lever progenitor cellen van muis, rat, hond en mens als lever organoïden. Lever organoïden konden worden gebruikt als *in vitro* onderzoeksmodel voor erfelijke leverziektes en experimentele transplantaties in muizen. In **hoofdstuk 7** beschrijven we een nieuw organoïden onderzoeksmodel voor niet-erfelijke leverziekte en de ontwikkeling van dit lever organoïden kweeksysteem voor de kat.

Een belangrijke groeifactor voor volwassen levercellen is HGF ('hepatocyte growth factor'). In **hoofdstuk 5** wordt een studie beschreven waarin werd gekeken of HGF als behandeling kan worden gegeven aan honden met een onderontwikkelde lever ten gevolge van een aangeboren levershunt (congenitale portosystemische shunt), een afwijkend bloedvat dat bloed om de lever heen leidt. Als een levershunt chirurgisch wordt gesloten, groeit de lever uit tot normale proporties. Onze hypothese was dat HGF therapie de lever zou laten uitgroeien en dat de doorbloeding als gevolg daarvan zou verbeteren. Zes honden met een levershunt werden drie weken behandeld met HGF via de bloedbaan. Leveromvang werd gemeten met CT scans voor, tijdens en na behandeling. HGF behandeling leidde inderdaad tot groei van de lever, wat ook op moleculair niveau in leverbiopten werd gezien middels toename van celdelingen en veranderde genexpressies. Het effect bleek echter slechts tijdelijk, want na stoppen van de HGF gift keerde de leveromvang weer terug naar het uitgangsniveau. De doorbloeding bleef gedurende de studie afwijkend en verbeterde niet na het uitgroeien van de lever. We kunnen hieruit concluderen dat met HGF-behandeling levergroei kan worden geïnduceerd onder omstandigheden van vrijwel afwezige portale doorbloeding. De effecten zijn echter tijdelijk en het toegenomen levervolume wordt na stoppen van de behandeling niet op peil gehouden.

In **hoofdstuk 6** wordt een transplantatiestudie beschreven met lever organoïden in honden met een erfelijke metabole leverziekte (stofwisselingsziekte die zijn oorsprong vindt in de lever). Mensen met metabole leverziekten krijgen vaak een nieuwe lever middels transplantatie, maar dergelijke leverziekten kunnen mogelijk ook met celtransplantatie worden behandeld. Hiervoor is in knaagdierstudies en in enkele humane studies bewijs gevonden. Dit zijn wel allogene (lichaamsvreemde) celtransplantaties geweest. Wij onderzochten of we cellen uit lever organoïden konden gebruiken voor een autologe (lichaamseigen) transplantatie in combinatie met gentherapie. Dit is gedaan in honden met een mutatie in het COMMD1 gen, waardoor koperstapelingshepatitis ontstaat. Een vergelijkbaar ziektebeeld bestaat ook bij de mens en heet daar de ziekte van Wilson. We isoleerden lichaamseigen lever progenitor cellen uit leverbiopten van deze honden en corrigeerden het gendefect in het laboratorium. Vervolgens werden deze cellen sterk vermenigvuldigd in kweek en gaven we de cellen terug aan dezelfde hond middels een transplantatie via de poortader of via injecties in de lever. Als de cellen via de poortader werden getransplanteerd sloegen ze niet aan, maar als ze via injecties in de lever werden toegediend konden ze zeven dagen later nog in de lever worden teruggevonden. Onder specifieke omstandigheden bleken ze zich zelfs in het leverweefsel te

vermenigvuldigen. Een belangrijke ongewenste bevinding was dat de organoïden die werden teruggevonden in het leverweefsel bleken te worden omgeven door bindweefsel. Verder onderzoek in een relevant groot diermodel is nodig om te bepalen wat de juiste transplantatieroute is en de juiste kweekomstandigheden voor de organoïden en om te voorkomen dat er bindweefsel ontstaat in het weefsel. Pas als aan deze voorwaarden is voldaan, kan de stap naar humane toepassing in (pediatrische) metabole leverziekten worden gemaakt.

In **hoofdstuk 7** is onderzocht of lever organoïden ook als onderzoeksmodel voor niet-erfelijke leverziekte kunnen worden gebruikt. Een belangrijke niet-erfelijke leverziekte bij mensen en katten is leververvetting, waarbij overmatige vetopslag in levercellen optreedt als ze worden blootgesteld aan hoge toevoer van vetzuren. De vetzuren zijn afkomstig uit een te vet dieet (bij mensen) of uit afbraak van vetweefsel (bij vastende katten). We wilden ook weten of er diersoortverschillen zijn in de manier waarop levercellen met overmatig vet omgaan. Daartoe ontwikkelden we een lever organoïden kweeksysteem voor de kat en voerden uitgebreide karakterisatiestudies uit. De organoïden konden worden opgekweekt uit lever progenitor cellen afkomstig uit grote leverbiopten en uit naaldbiopten, welke bij katten met leverziekten vaak toegepast worden. Vervolgens boden we lever organoïden van muizen, mensen, honden en katten een overmaat aan vetzuren aan en werd de vetopslag in de cel gemeten en vergeleken tussen de verschillende diersoorten. Katten lever organoïden bleken de meest uitgesproken vetopslag te laten zien en verschilden hiermee van humane organoïden, ook op vetstofwisselings-genexpressie niveau. Inzicht in dergelijke verschillen kan mogelijk leiden tot nieuwe aangrijpingspunten voor medicijnen die de vetstofwisseling beïnvloeden. Om dit als concept verder te onderzoeken hebben we een onderdeel van de vetstofwisseling (de bèta-oxidatie) gestimuleerd of geremd. Dit leidde inderdaad tot een meetbare verandering van vetopslag. Hiermee kunnen we stellen dat lever organoïden van de kat een nieuw en interessant onderzoeksmodel zijn voor zowel katten als mensen met leververvetting, waarbij *in vitro* experimenten deels dierproeven kunnen vervangen.

Uit **deel II** kan het volgende worden geconcludeerd:

- HGF behandeling kan een onderontwikkelde lever laten uitgroeien onder omstandigheden van minimale portale doorbloeding, maar dit effect verdwijnt zodra de behandeling stopt.
- Honden lever progenitor cellen kunnen worden verzameld uit een biopt, sterk vermenigvuldigd in kweek als lever organoïden, genetisch gecorrigeerd en worden gebruikt voor autologe celtransplantatie.
- Ook van de kat kunnen lever organoïden worden gekweekt, die op basis van hun opvallende vetstapelingscapaciteit een nieuw onderzoeksmodel zijn voor leververvetting.

Conclusies en aanbevelingen voor toekomstig onderzoek

In dit proefschrift worden nieuwe activatiemechanismen beschreven voor lever progenitor cellen van hond en mens, die aanknopingspunten vormen voor het ontwikkelen van nieuwe behandelingen binnen de regeneratieve geneeskunde van de lever. Volgende stappen in dit onderzoek zijn het bestuderen van deze mechanismen tijdens progenitor cel gemedieerde leverregeneratie (of het gebrek hieraan in sommige ziektebeelden) en in levertumoren. Ook kunnen de activatiemechanismen mogelijk *in vitro* en *in vivo* worden gestuurd met medicijnen om lever progenitor cellen te stimuleren tot celdeling of juist hierin te remmen.

Mensen en honden krijgen te maken met verschillende soorten leverziekten, maar op weefselniveau zijn er duidelijke overeenkomsten in de signaalroutes en cellen die bijdragen aan het herstel van de lever. Daarom zijn honden met natuurlijk optredende leverziekten in al hun verscheidenheid een zeer interessant groot diermodel voor preklinische studies naar lever progenitor cel transplantaties. Op de problemen die werden gezien tijdens de eerste transplantaties in honden kan nu worden geanticipeerd tijdens de eerste transplantaties in mensen, wat de kans van slagen doet toenemen. Toekomstig onderzoek naar de beste kweekomstandigheden en transplantatieroute is erg belangrijk om tot een volwaardig humaan klinisch toepasbaar protocol te komen. De onderzoeker heeft inmiddels naast honden ook andere translationele diermodellen tot zijn beschikking, namelijk muizen met een lever die grotendeels uit menselijke volwassen levercellen bestaat ('humanized mouse liver'). Dit model is zeer interessant, omdat het de mogelijkheid biedt om transplantatie van humane levercellen in een grotendeels 'humane' lever te testen zonder van een daadwerkelijk humaan testobject gebruik te hoeven maken. Er zijn echter een aantal essentiële nadelen aan dit model die niet zo makkelijk op te lossen zijn. De lever bestaat uit meer dan alleen levercellen, er zijn immers ook stellaatcellen en cellen die de bloedvaten bekleden die in dit model van muizenherkomst blijven. Juist deze cellen alsook het aanwezige bindweefsel spelen een belangrijke rol bij de reactie op getransplanteerde humane donorcellen. Daarnaast verschilt de muis op basale aspecten zoals lichaamstemperatuur, hormonale en metabole status danig van de mens. Dit maakt dat autologe transplantatie van honden lever organoïden in een relevant honden ziektemodel meer voorspellende waarde kan hebben voor het welslagen van autologe humane lever organoïden transplantatie in een humane leverziekte.

Katten verschillen van honden in vele fysiologische opzichten, maar ook in de mate waarin bepaalde leverziekten bij deze diersoorten worden gezien. Veel meer dan bij honden zien we bij katten ziekten als leververvetting en galgangontsteking, wat vergelijkbare ziektebeelden zijn met niet-alcoholische leververvetting en primaire scleroserende cholangitis bij de mens. Bij katten staat de kennis over het ontstaan en verloop van deze ziekten op moleculair niveau nog in de kinderschoenen en dit zal moeten worden uitgediept om tot nieuwe behandelmogelijkheden voor zieke katten te komen. Met de komst van lever organoïden als primair celkweeksysteem voor katten levercellen komt deze onderzoeksmogelijkheid binnen handbereik. Door levermonsters van katten met leverziekten te verzamelen kan een zogeheten biobank worden opgezet, waaruit toekomstig onderzoeksmateriaal kan worden verkregen. Andere mogelijkheden zijn om zonder gebruik van dierproeven *in vitro* toxiciteitstesten van nieuwe medicijnen op lever organoïden van de kat uit te voeren of om medicijnen die vetstapeling kunnen verlagen te testen. Dit biedt perspectieven voor zowel de kat als de mens met leververvetting.

Inzicht in het verloop van leverziekten is erg belangrijk om tot nieuwe behandelingen te komen. Bevindingen die in het laboratorium worden gedaan zullen na degelijk wetenschappelijk onderzoek moeten worden toegepast in de kliniek. Kennis over de fundamentele aspecten van lever regeneratie en de rol van lever stamcellen hierin moet worden opgedaan bij verschillende diersoorten om de juiste diermodellen te kunnen selecteren voor specifieke onderzoeksvragen en om te kunnen leren van eventuele verschillen. Diersoort-overschrijdend inzicht behoort bij uitstek tot het vakgebied van de dierenarts. Dierenartsen hebben niet alleen oog voor de vele fysiologische verschillen tussen diersoorten, waaronder de mens, maar weten deze ook te interpreteren en extrapoleren. Dit maakt veterinaire wetenschappelijk onderzoekers waardevolle partners bij translationeel medisch onderzoek tot heil van mens en dier.

Acknowledgements

(Dankwoord)

Promoveren doe je weliswaar alleen, de weg ernaar toe leg je af in een team. De afgelopen jaren heb ik het grote voorrecht gehad om onderzoek te mogen doen bij de ‘levergroep’ van het Departement Geneeskunde van Gezelschapsdieren. Een zeer hecht team waarin de neuzen allemaal van een andere kant komen, maar zonder uitzondering dezelfde kant op staan.

Ik wil allereerst mijn promotor prof. Jan Rothuizen bedanken, de geestelijk vader van onze onderzoeksgroep. Toen je mij benaderde voor deze functie heb ik na lang aarzelen geweigerd, waarna ik diezelfde dag nog een voicemail bericht van jou kreeg met de vraag ‘of we hier toch niet nog even over konden praten’. Dat kon, dat deden we nog diezelfde week en de rest is geschiedenis. Ik heb er geen moment spijt van gehad. Jouw tomeloze inzet, je enthousiasme voor de wetenschap en enorme schat aan kennis van verbazingwekkend veel vakgebieden is aanstekelijk en sterk motiverend. Je stond altijd achter me, maar steeds met een scherpe blik, kritische vragen en een prikkende opmerking paraat. Hoe druk je het ook had, je maakte tijd voor het lezen van manuscripten, overleg, emails of een praatje over hoe het ging. Dank voor deze kans, dank voor je vertrouwen, ik ben er een betere onderzoeker van geworden.

Mijn tweede promotor prof. Jan Willem Hesselink wil ik ook heel graag bedanken voor alle steun, ook al raakte je pas laat bij mijn promotie betrokken. Dank ook voor je support bij onze transplantatiestudie, waarbij we heel wat obstakels hebben moeten overwinnen. Je bleef vertrouwen houden in onze keuzes en strategie, waarvoor veel dank.

Mijn copromotor dr. Bart Spee, wat een topper ben je toch. Als trekker van de groep ben je niet alleen kundig maar ook zeer betrokken, zowel op inhoudelijk als persoonlijk vlak. Ik kon altijd bij je binnenlopen, voor een vraag, een grapje, of het lenen van je speelgoedpistooltje om Frank mee te bestoken. Menig discussie werd gevoerd over QPCR/Western blot/isotype controle, emails werden (mits kort en bondig) altijd per ommegaande beantwoord en refworks-sores ten tijde van paper submissies werden op afstand op vrijdagavond opgelost. Je verzet bergen werk en het is tijd dat je daar de credits voor krijgt: bedankt voor alles!

Mijn tweede copromotor dr. Louis Penning, een rol die je op het lijf geschreven is maar die je officieel ook pas in het laatste jaar van mijn promotietraject officieel ging bekleden. Je steun is niet aflatend geweest, altijd was je oprecht geïnteresseerd en stelde je de meest uiteenlopende vragen die me telkens weer aan het denken zetten. Je emails zijn soms wat cryptisch, maar de geoefende lezer haalt de essentie er wel uit. Bedankt voor al je hulp, je opbeurende spirit en je eerlijke attitude. Wat fijn dat je er altijd voor me was.

Mijn paranimfen, Loes Oosterhoff en Emilie Kruitwagen, wil ik ook bedanken dat zij vandaag achter mij staan. Loes, je kwam als student bij me stage lopen en we hebben je nooit meer laten gaan. Je staat niet voor niks bekend als ‘Queen Organoid’: je kweek skills zijn onovertroffen en je hebt van het begin af aan me bijgestaan in de transplantatiestudie en bij de ontwikkeling van de katten lever organoiden kweek. Je inzet is zeer groot en van onschatbare waarde geweest voor een belangrijk deel van dit boekje, het is dus niet alleen fijn maar ook logisch dat je vandaag mijn paranimf bent. Emilie, dierbaar zussie, we delen onze liefde voor dieren en je hebt van dichtbij al die jaren meegemaakt hoe ik mijn werk met veel plezier deed, maar ook de offers die het vergde en de hoofdbrekens die ermee gepaard gingen. Dank voor je steun ook vandaag!

Dank aan alle leden van de levergroep, essentieel onderdeel van mijn dagelijkse werkplezier en voorbeeld van teamspirit. Dr. Hille Fieten, jarenlang mijn favoriete kamergenootje, steun en toeverlaat. Wat ben ik blij dat het 'vloekenpotje' toen nog niet op onze kamer stond… Dank voor al je support op leuke en minder leuke momenten, je bent een kanjer! Dr. Frank van Steenbeek, je bent een gedegen en gedreven onderzoeker en we hebben veel lol samen, niet in de laatste plaats over onze 'sokmethode' om primair honden endotheel te isoleren. Voor jou sta ik altijd paraat om 's avonds laat een portocavale shunt uit een puppy ter grootte van een cavia te prepareren. Dr. Kerstin Schneeberger, onze nieuwe biofabricatie postdoc en nu al ben je onmisbaar. Met je droge humor en je geweldige spinner flask kweken heb je al snel een welverdiende plek in ons team veroverd. Chen Chen, fellow PhD candidate and room mate, thank you very much for our discussions, for creating the eGFP/DsRed-COMMD1 lentiviral construct, and for your unique sense of humor. All the best in finishing your own PhD, you'll do more than great! Emily Wu, thank you for our nice chats and good luck finishing your own thesis. Ing. Monique van Wolferen, jou ben ik zeer veel dank verschuldigd voor ontelbare QPCR platen, kleuringen, kweekwerk en een zekere Western blot die ons nog lang in onze nachtmerries zal blijven achtervolgen. Je bent een hele lieve en fijne collega en ik kon altijd bij je terecht, bedankt voor alles!

Een grote reeks voormalig collega's ben ik dank verschuldigd voor hun steun. Allereerst dr. Cornelia Viebahn, de eerste postdoc op ons NWO-project. Ik heb veel van je geleerd, je was een goede supervisor maar je koos voor een gezin, een droom die uitkwam. Dr. Baukje Schotanus, de derde postdoc op ons NWO-project, collega-dierenarts en zeer fijne sparring partner. Ook van jou heb ik veel geleerd, niet alleen inhoudelijk over stamcelbiologie maar ook over lastige loopbaankeuzes tussen onderzoek en kliniek. Bedankt voor al jullie hulp! Thanks also to my former colleagues in the group: Ermanno Malagola, dr. Hideyuki Kanemoto, dr. Sathidpak ('Ja') Nantasanti, dr. Andre Conceição Meneses, dr. Manabu Sakai, and prof. Iwan Burgener. Dear Ja, thank you for all your help and your expertise in liver organoid cultures, I'm glad you were there for the first in dog transplantations! Andre and Iwan, thank you for our collaboration and all the best in finishing our canine intestinal organoid project. Dr. Brigitte Arends, veel dank voor je kundige begeleiding van mijn Honours Program, het heeft ons een mooie (en mijn allereerste) paper opgeleverd! Dr. Ted van den Ingh, dank voor de discussies en accurate analyses van de pathologische levermonsters die ik je mocht sturen, je had altijd een toegevoegd perspectief.

Samenwerking met collega's van andere departementen en instituten is essentieel onderdeel van het uitvoeren van modern wetenschappelijk onderzoek. In willekeurige volgorde wil ik dan ook de volgende onderzoekers hartelijk danken voor hun bijdrage en hulp aan onze projecten en delen van dit proefschrift. Binnen onze faculteit wil ik prof. Alain de Bruin, dr. Bart Westendorp en dr. Hilda Toussaint van het departement Pathobiologie bedanken voor onze gezamenlijke experimenten en discussies in het DYRK1A-project. Jullie kennis van zaken en grote toewijding was zeer waardevol! Ook dr. Guy Grinwis wil ik ontzettend bedanken voor intelligente input op vele projecten en pathologische interpretaties en expertise. Overbezet en/of ziek, je stond altijd voor me klaar. Emails waren zelden zonder een grapje, wat maar bewijst dat humor tot de essentiële arbeidsvitaminen behoort. Van het departement Biochemie en Celbiologie wil ik prof. Bernd Helms en ing. Martijn Molenaar bedanken voor onze samenwerking in het onderzoek naar lipidenstapeling in lever organoiden. Het leverde een 'vette' paper op en een tweede grant is binnengehaald om hier vervolg aan te geven. Dit kan ik niet zonder jullie, dank daarvoor! I would like to express my sincere gratitude

towards our collaborators from the Hubrecht Institute: prof. Hans Clevers, prof. Niels Geijsen, dr. Rob Vries, dr. Meritxell Huch, dr. Helmuth Gehart and ing. Stefan van der Elst. Thank you for your valuable input, for sharing your expertise and many fruitful discussions. Thank you to dr. David Egan from the Utrecht Cell Screening Center for your advice. Thank you to dr. Delabar for sending your Dyrk1A transgenic mouse liver samples to us. Translatie naar humane toepassingen is gedaan in samenwerking met diverse medische centra. Want hoewel onze patiënten vier pootjes hebben in plaats van twee, uiteindelijk zijn er meer overeenkomsten dan verschillen tussen de veterinaire en humane geneeskunde. Ik bedank prof. Roderick Houwen, prof. Edward Nieuwenhuis en dr. Sabine Fuchs van het Wilhelmina Kinderziekenhuis voor hun input om de lever organoiden transplantaties bij honden van preklinische waarde voor humaan (pediatrische) toepassing te maken. Ik ben ervan overtuigd dat deze samenwerking essentieel is om de stap naar metabole leverziekten bij kinderen te gaan maken. Dr. Ira Fox from the University of Pittsburgh and expert in hepatocyte transplantation in pediatric metabolic liver disease: thank you very much for your valuable input on our liver organoid transplantations in dogs with copper toxicosis. Your institute is not only famous for pioneering work in liver transplantations, but also on the use of dogs as translational animal model. Thank you for flying over to participate in our annual progress meetings and your long-distance assistance via email. Ook bedank ik dr. Luc van der Laan en dr. Monique Verstegen van het Erasmus Medisch Centrum voor onze fijne samenwerking op het lever organoiden lipidenstapelingsproject. Ik heb jullie proactieve houding en alle hulp enorm gewaardeerd. Furthermore I would like to thank the Winn Feline Foundation for sponsoring our feline liver organoid projects.

Veel dank ben ik verschuldigd aan alle klinische collega's van ons departement Geneeskunde van Gezelschapsdieren. Voor met name de HGF studie en het transplantatieproject heb ik veel met jullie samengewerkt en altijd met ontzettend veel genoegen. Ik bedank alle betrokken disciplines voor steun door de jaren heen, uiteraard dr. Robert Favier van de hepatologie en mijn collega's van de interne geneeskunde, maar ook de chirurgie, anesthesie, diagnostische beeldvorming, IZA/ZPA, dierverpleging en het diagnostisch laboratorium. Van leverbiopten, perfusie scintigrafie en cyclosporinespiegel bepalingen tot sectio's bij nacht en ontij: ik heb jullie allemaal zeer vaak lastig moeten vallen en altijd was ik welkom, dank daarvoor! Speciaal wil ik bedanken dr. Giora van Straten (die met een telefoon aan zijn oor nog een galpunctie kan doen), dr. Anne Kummeling (zeer kundig lever- en poortaderchirurg en de rust zelve), Ies Akkerdaas (al jaren betrokken als onze onderzoeksdieren ergens voor moeten slapen) en Leonie van Bruggen (als radioloog betrokken bij de scans en echo's van onze transplantatiestudie). Bedankt voor jullie enthousiasme, tomeloze inzet en hulp! Een bijzonder woord van dank voor dr. Jeffrey de Gier en zijn collega's van de afdeling voortplanting. Toen we begonnen met de transplantatiestudie moesten de honden ervoor zelfs nog worden gefokt. Zonder jouw hulp (natuurlijk altijd buiten kantooruren) bij de fertiliteitsbegeleiding en kraamzorg was dit nooit gelukt, dank voor alles. Ook dr. Ronald Jan Corbee en Inge van Duiven wil ik danken voor hun steun en kundige begeleiding rondom alles wat met onze dierproeven te maken had.

Ook wil ik al mijn onderzoekscollega's uit het JDV-gebouw bedanken, de tweede verdieping is dankzij jullie een tweede thuis voor me geweest. Bedankt voor jullie gezelligheid, hulp, expertise, discussies en natuurlijk de 'echte' koffie. Een speciaal woord van dank voor Jeannette Wolfswinkel voor alle last-minute bestellingen, het feit dat we het ML-1 weer eens bezet mochten houden op transplantatiedag en voor alle hulp door de jaren heen.

Dank aan alle studenten die ik mocht begeleiden en die betrokken waren bij mijn onderzoek. Honours Program studenten Krista Post (tevens super taartenbakker) en Christel Vinke (tevens captain van het puppy kraamzorgteam), jullie waren geweldig! De twee 'Ingrids' (master studenten op het katten lever organoiden project): Ingrid Vernooij en Ingrid Schrall, beide afkomstig van een boerderij en geen katten-fan, maar toch met grote inzet gewerkt voor het project, bedankt! Verder bedank ik Hanne Venema, Farah Bannink, Camille Roesch, Lisa van Uden, Ruby Lieshout, Hannah Versteegh en alle andere studenten door de jaren heen voor hun hulp.

Lieve vrienden en (oud-)buren, wat hebben jullie al die jaren meegeleefd! Ik kon bij jullie altijd mijn ei (of de hond/kat/kippen, of de kinderen…) kwijt en een en ander leren relativeren. Het voert te ver om jullie allemaal bij naam te noemen, maar een speciaal woord van dank aan mijn Excellent Tracé vriendinnetjes (uit de steentijd toen het nog geen HP heette): dr. Renée van Sprundel, Heleen ter Borg, dr. Sarah van Rijn en dr. Floryne Buishand voor alle gezellige ETentjes door de jaren heen. Met of zonder kids, het is altijd fijn om bij te praten! Een extra speciaal woord van dank aan Astrid Pulles, voor onze vriendschap die al begon in de brugklas, een studie diergeneeskunde c.q. geneeskunde overleefde en nu floreert ten tijde van een PhD track, inmiddels met lieve man en liefste kinderen erbij. Fijn om elkaar te kunnen bellen (al gaat het dan meestal over de kinderen), met zijn allen een weekend weg te gaan of op een zomerdag met een koud biertje in het zwembad te zitten. Ik koester dit en kijk nu al uit naar jouw verdediging!

Lieve Rob en Gea, heel veel dank voor al die jaren van steun en meeleven, veel gezelligheid en natuurlijk het oppassen op de kinderen. Wat fijn om zulke lieve schoonouders te hebben! Lieve Justin en Maartje, ook jullie wil ik bedanken voor alle steun de afgelopen jaren en de gezellige avondjes, altijd met een luisterend oor. Laten we dit vaker doen.

Lieve papa en Marion, wat fijn om regelmatig bij jullie aan te kunnen schuiven aan een rijk gedekte tafel en samen een goed glas wijn van eigen 'Heerlijkckheid' te kunnen drinken. Bedankt voor alle steun, hulp en gezelligheid de afgelopen jaren, we komen graag weer helpen plukken. Dank ook aan Victor en Sabrina, Barbara en Egon, David en Juliette voor alle gezelligheid en goede gesprekken, inmiddels vieren we kerst met een steeds grotere groep!

Lieve mam, jij hebt met papa de basis gelegd voor mijn huidige loopbaan door me van jongs af aan te stimuleren het beste uit mezelf te halen, kritisch te zijn en met een open blik en oog voor detail naar de wereld te kijken. Pas dan zie je alles. Dank voor je hulp en steun, dank ook voor je zorg voor onze kinderen aan wie je nu de wonderen van de natuur laat zien. Lieve Emilie en Stefan, ik had me geen lievere zus en zwager kunnen wensen! Bedankt voor jullie steun, de dagjes uit naar Artis (dat bootje varen komt heus nog wel…) en alle gezelligheid door de jaren heen.

Promoveren is verre van trouwen in je eentje. Onderzoek doe je samen, trouwen ook. Lieve Thom, als echtgenoot ben je steunpilaar, klankbord en bliksemafleider geweest de afgelopen jaren, maar vooral de liefde van mijn leven. Je laat me vrij om mijn dromen en ambities te volgen. Ik ga niet beloven dat het rustiger wordt vanaf nu, je kent me beter dan dat. Ik had dit niet zonder jou gekund, dankjewel. Liefste Emma en Thijs, dit boekje is opgedragen aan ons gezin wat met jullie komst zo verrijkt is. Ook al gaat mama heel vaak werken, mama komt ook altijd weer thuis. Het is belangrijk om te houden van wat je doet, maar het meest hou ik van jullie.

Curriculum vitae

Hedwig Kruitwagen was born on November 23, 1983 in Nijmegen. She obtained her high school diploma with honors in 2002 and moved to Utrecht to study veterinary medicine at the Faculty of Veterinary Medicine, Utrecht University. Upon finishing her doctoral phase (with honors), she was selected to participate in the Honors Program of the Faculty. This enabled her to gain research experience for an extended period of time and she joined the hepatology research group at the Department of Clinical Sciences of Companion Animals. She performed an experimental study in liver regenerative medicine, in which dogs with an inborn liver shunt were treated with hepatocyte growth factor therapy. During this study she mastered various molecular biology techniques. Hedwig started her clinical rotations in 2008 and obtained her DVM degree in 2010. After a brief period working in private practice, she started her PhD study under supervision of prof. Jan Rothuizen. She worked on a Translational Adult Stem cell research project entitled 'Liver progenitor cells for functional recovery of liver disease', funded by a grant from the Dutch Research Council. The aim of the project was to translate fundamental findings to clinical application of adult stem cells, in collaboration with human medical centers. It is within this project that Hedwig did her PhD and part of a postdoc study. She did fundamental research into stem cell-mediated liver regeneration and was involved in the development of liver organoid cultures from dogs and cats and intestinal organoid cultures from dogs. Furthermore, she performed liver organoid transplantations and used organoids for disease modeling research of hepatic steatosis. In 2016 she worked part-time as veterinarian in the internal medicine section of the Utrecht University Clinic for Companion Animals. Hedwig is married to Thom Argante and together they have two children, Emma and Thijs.

Hedwig Kruitwagen werd geboren op 23 november 1983 in Nijmegen en groeide daar op. Ze ging naar het Stedelijk Gymnasium waar ze in 2002 haar diploma (cum laude) haalde. Vervolgens ging ze diergeneeskunde studeren in Utrecht, waar ze aansluitend aan haar doctoraal (cum laude) werd geselecteerd om deel te nemen aan het facultaire Honours Program. Dit stelde haar in de gelegenheid om tijdens haar studie gedurende langere tijd onderzoekservaring op te doen, wat ze deed bij de hepatologie van het departement Geneeskunde van Gezelschapsdieren. Ze onderzocht of honden met een aangeboren levershunt behandeld konden worden met een groeifactor (HGF), waarmee ze in aanraking kwam met de regeneratieve geneeskunde en ervaring opdeed met diverse moleculair biologische analysetechnieken. In 2008 begon ze aan haar coschappen en in de zomer van 2010 studeerde ze af als dierenarts, differentiatie gezelschapsdieren. Na een korte tijd als waarnemend dierenarts te hebben gewerkt, begon ze in 2010 als PhD student bij prof. Jan Rothuizen op het door NWO gesubsidieerde Translationeel Adult Stamcel-onderzoeksproject 'Liver progenitor cells for functional recovery of liver disease'. Dit project moest binnen de looptijd stamcelonderzoek van fundamentele vraagstukken naar klinische toepassing brengen in samenwerking met humane medische centra. Ze deed haar promotieonderzoek en deel van een postdoc in dit project. Ze deed fundamenteel onderzoek naar leverregeneratie en was betrokken bij de ontwikkeling van een lever organoiden kweeksysteem van hond en kat en van darm organoiden van de hond. Tevens onderzocht ze toepassingen voor transplantatie en ziektemodellen voor steatose. Daarnaast was ze in 2016 deels werkzaam als dierenarts bij de afdeling interne geneeskunde van de Universiteitskliniek voor Gezelschapsdieren. Hedwig is getrouwd met Thom Argante en samen hebben ze twee kinderen, Emma en Thijs.

List of publications

Kruitwagen HS, Oosterhoff LA, Vernooij IGWH, Schrall IM, van Wolferen ME, Bannink F, Roesch C, van Uden L, Molenaar MR, Helms JB, Grinwis GCM, Verstegen MMA, van der Laan LJW, Huch M, Geijsen N, Vries RG, Clevers H, Rothuizen J, Schotanus BA, Penning LC, Spee B. Long-Term Adult Feline Liver Organoid Cultures for Disease Modeling of Hepatic Steatosis. Stem Cell Reports. 2017;8(4):822-830.

Conceicao Meneses A, Schneeberger K, **Kruitwagen HS**, Penning LC, van Steenbeek FG, Burgener IA, Spee B. Intestinal organoids – current and future applications. Veterinary Sciences. 2016;3(4):31.

Dirksen K, Roelen YS, van Wolferen ME, **Kruitwagen HS**, Penning LC, Burgener IA, Spee B, Fieten H. Erythrocyte copper chaperone for superoxide dismutase and superoxide dismutase as biomarkers for hepatic copper concentrations in Labrador retrievers. Vet J. 2016;218:1-6.

Oosterhoff LA, **Kruitwagen HS**, Spee B, van Steenbeek FG. Isolation and Culture of Primary Endothelial Cells from Canine Arteries and Veins. J Vis Exp. 2016;(117).

Nantasanti S, Spee B, **Kruitwagen HS**, Chen C, Geijsen N, Oosterhoff LA, van Wolferen ME, Pelaez N, Fieten H, Wubbolts RW, Grinwis GC, Chan J, Huch M, Vries RR, Clevers H, de Bruin A, Rothuizen J, Penning LC, Schotanus BA. Disease Modeling and Gene Therapy of Copper Storage Disease in Canine Hepatic Organoids. Stem Cell Reports. 2015;5(5):895-907.

Schotanus BA, **Kruitwagen HS**, van den Ingh TS, van Wolferen ME, Rothuizen J, Penning LC, Spee B. Enhanced Wnt/β-catenin and Notch signalling in the activated canine hepatic progenitor cell niche. BMC Vet Res. 2014;10:309.

Tuohetahuntila M, Spee B, **Kruitwagen HS**, Wubbolts R, Brouwers JF, van de Lest CH, Molenaar MR, Houweling M, Helms JB, Vaandrager AB. Role of long-chain acyl-CoA synthetase 4 in formation of polyunsaturated lipid species in hepatic stellate cells. Biochim Biophys Acta. 2015;1851(2):220-30.

Kruitwagen HS, Spee B, Fieten H, van Steenbeek FG, Schotanus BA, Penning LC. Translation From Mice to Men: Are Dogs a Dodgy Intermediate? EMJ Hepatol. 2014;1:48-54.

Kruitwagen HS, Spee B, Schotanus BA. Hepatic progenitor cells in canine and feline medicine: potential for regenerative strategies. BMC Vet Res. 2014;10:137.

Kruitwagen HS, Spee B, Viebahn CS, Venema HB, Penning LC, Grinwis GC, Favier RP, van den Ingh TS, Rothuizen J, Schotanus BA. The canine hepatic progenitor cell niche: molecular characterisation in health and disease. Vet J. 2014;201(3):345-52.

Kruitwagen HS, Arends B, Spee B, Brinkhof B, van den Ingh TS, Rutten VP, Penning LC, Roskams T, Rothuizen J. Recombinant hepatocyte growth factor treatment in a canine model of congenital liver hypoplasia. Liver Int. 2011;31(7):940-9.

Manuscripts in preparation

van den Bossche L, Schoonenberg VAC, Burgener IA, Penning LC, Schrall IM, **Kruitwagen HS**, van Wolferen ME, Grinwis GCM, Kummeling A, Rothuizen J, van Velzen JF, Stathonikos N, Molenaar MR, Helms JB, Brouwers JFHM, Spee B, van Steenbeek FG. Aberrant hepatic lipid storage and metabolism in canine portosystemic shunts. accepted for publication in PLOS ONE

Kruitwagen HS, Westendorp B, Viebahn CS, Post K, van Wolferen ME, Oosterhoff LA, Egan DA, Delabar JM, Toussaint MJ, Schotanus BA, de Bruin A, Rothuizen J, Penning LC, Spee B. Dual specificity tyrosine phosphorylation regulated kinase 1A (DYRK1A) is a regulator of S phase entry in hepatic progenitor cells. submitted manuscript

Kruitwagen HS, Oosterhoff LA, van Wolferen ME, Chen C, van Steenbeek FG, Nantasanti S, Vinke CR, Kummeling A, van Straten G, Akkerdaas LC, van Bruggen LWL, Wolfswinkel J, Grinwis GCM, Fuchs SA, Gehart H, Geijsen N, Rothuizen J, Schotanus BA, Penning LC, Spee B. Canine liver organoid transplantation in a COMMD1 deficient dog model of metabolic liver disease. manuscript in preparation

Conceicao Meneses A, Schneeberger K, **Kruitwagen HS**, Oosterhoff LA, van Wolferen ME, Vries RG, Clevers H, Penning LC, Burgener IA, Spee B. Establishment and characterization of canine intestinal organoid cultures. manuscript in preparation

Wu X, Chie H, van Wolferen ME, **Kruitwagen HS**, Spee B, Fieten H, Penning LC. Reduced FXR-activity in copper-laden COMMD1-deficient canine livers. manuscript in preparation

De Nies KS*, **Kruitwagen HS***, van Straten G, van Bruggen LWL, Robben JH, Schotanus BA, Akkerdaas LC, Kummeling A. Innovative approach and usability of implantable venous access system in the portal vein: technique, results and complications in three dogs. manuscript in preparation

*equal contribution